

Pumping when the wind blows

Demand response in the
Dutch delta

MSc. thesis
T.J.T. van der Heijden
4138236



On the cover

The cover image shows an old windmill and new wind turbines, depicting the old and new method of powering pumping through wind energy. The image was retrieved from <http://www.wattisduurzaam.nl>.

Pumping when the wind blows

Demand Response in the Dutch delta

T.J.T. van der Heijden

to obtain the degree of Master of Science in Civil Engineering
at the Delft University of Technology,
to be defended publicly on February 8, 2019 at 15:00 PM

Student number: 4138236
Project duration: June, 2018 – January, 2019
Thesis committee: Dr. ir. E. Abraham, TU Delft, supervisor
Ir. D. Lugt, HKV, supervisor
Dr. R. R. P. van Nooyen, TU Delft
Prof. dr. P. Palensky, TU Delft

An electronic version of this thesis is available at <http://repository.tudelft.nl/>.

Preface

*Ties van der Heijden
Delft, December 2018*

This document is my final thesis for my MSc. Civil Engineering, at Watermanagement, TU Delft. With Edo Abraham and Dorien Lugt as personal supervisors. This thesis was done in cooperation with HKV, under supervision of Dorien Lugt and Durk Klopstra.

I would like to thank Edo, Ronald, Peter and Dorien for their interest and close involvement with this thesis. Without their advice and corrections this thesis would not have been possible. I would also like to thank Tian for his personal involvement and interest in my research. For helping me whenever I asked for help and supporting every presentation I gave at TU Delft. And Saket, for pointing me towards the SARIMA model.

Furthermore I would like to thank my parents, Heddy and Alfons, for their seemingly forever (financial) support during my whole education and life so far. I would also like to thank Kim, my sister, for a listening ear whenever I needed it and her interest and enthusiasm for my work. And Daniël, for cheering with me the first time IPOPT did not crash.

I'd also like everyone who has occupied "Hokje 1" (A.K.A. CiTG 4.84) with me: Stijn, Martijn, Lisa, Wouter, Emilie, Jasper, Ilse, Niek, Maud, Manuel and Nicael. Thanks for keeping the oxygen levels up and caffeine levels high. And off course, I'll always remember the karaoke nights at Koperen Kat. Working through the summer holidays was not the best part of writing this thesis, but you guys got me through it with pleasure!

In my thesis I searched for a connection with the energy transition. Climate change is the biggest and most complex challenge we are facing in modern history. Habits need to change, money has to be spent, jobs will be lost. And all under a deadline, and with possible catastrophic consequences in case of failure. Making the energy transition work is key to tackling this challenge. In my opinion, it is a tough but exciting problem. The energy transition can't be done through one sector; the energy sector. I believe a multidisciplinary approach is key to making the transition successful, where everybody has to look at what he or she can do with the knowledge and tools they possess.

My time studying at TU Delft gave me general tools and specific knowledge. My time working for Vandebroun inspired me to be more active in a problem the world is facing. My time at TU Delft Energy Club (under the Delft Energy Initiative) gave me the knowledge about the "world of energy", that I will finally put into something tangible. This thesis will be my first scientific, hopefully successful, contribution to making the energy transition work.

Abstract

This thesis investigates the potential of a large pumping station in IJmuiden, the Netherlands, for participating in Demand Response. Due to climate change, renewable energy is on the rise. The intermittency of energy, together with its unpredictable supply, are a big hurdle for the energy transition. Two methods are promising solutions to this problem; large scale energy storage and demand response. Since large scale energy storage is not yet economically feasible, demand response has an important role to play in the early days of the energy transition.

Using energy when it is generated requires a data-stream from the generation facilities on production, which is not (yet) widely available. The market price, however, is an indication of the scarcity of energy, since it is based on the ratio between supply and demand. Besides that, there is a correlation between a low energy price and sustainable energy production since marginal costs of sustainable energy production are lower than fossil energy production. This makes using sustainable energy cheaper than fossil energy, and gives Demand Response a business case.

In this thesis, a Model Predictive Control is created that uses energy market data to minimize energy costs. Multiple energy markets are analyzed with respect to their suitability for the pumping station in IJmuiden to act on them. The day ahead market is called the APX in the Netherlands, and this is where energy is bought and sold the day before consumption. The intraday market, also called the flexibility market, is where energy can be bought and sold up to 5 minutes before consumption. A strategy combining these two markets will be evaluated. This is done by using a predicted day ahead price, generated by a SARIMA model, to create a plan. This plan will then be followed, but deviations from the plan are allowed against intraday market price.

Due to imperfections of the market (mismatch between supply and demand), imbalances are occurring. These imbalances result in frequency deviations of the grid, and voltage deviations. Tenner, the Dutch TSO (Transmission system operator), is responsible for minimizing these imbalances. In order to minimize the imbalance, TenneT gives a real-time indication of the imbalance on the grid, and positive contributions are rewarded while negative contributions are punished. This is done through the use of the imbalance price; a price per volume of imbalance caused or solved. The imbalance price is based on the aFRR market, where bids can be done on possible activation. Since the imbalance market is a fast-acting market, it is not suitable for a large pumping station like IJmuiden. However, the aFRR market will be analyzed in this thesis.

The effects of expected future development, like sea level rise and energy market changes, will be analyzed and simulated as well. A higher sea level would result in more pumping, and less discharging under gravity. Which causes the pump schedule to become less flexible. The results show that it is possible to apply demand response to a pumping station, and the intraday market makes it possible for the MPC to adjust its energy use during the day.

The aFRR market analysis shows a lot of potential for the pumping station, possibly making up for all energy costs made through the spot markets.

The conclusion of this thesis is that Rijkswaterstaat can possibly save energy costs on pumping, based on the fixed energy price, provided by Rijkswaterstaat, they pay now. Based on a reference scenario where the MPC only minimizes energy use, and a fixed ENDEX energy price, the proposed MPC makes about 10% less costs in the German market scenario. The Dutch market scenario does not show cost savings. In the Netherlands there is not much correlation between low energy prices and renewable energy yet, since renewable energy is not a big part of the energy mix in the Netherlands. This correlation is expected to become more present when the Dutch energy mix becomes more sustainable. This is expected to result in lower CO₂ emission through the energy use of the pumping station. However, more research is needed to confirm this.

Contents

Abstract	v
List of Figures	xi
List of Tables	xv
1 Introduction	1
1.1 Demand response	1
1.2 The Dutch delta.	3
1.3 A new role for Rijkswaterstaat	4
1.4 This research	5
2 Case study for Demand Response	7
2.1 Amsterdam-Rijnkanaal & Noordzeekanaal	7
2.2 Markermeer & IJsselmeer	8
3 Electricity markets	11
3.1 The day ahead market	12
3.2 Intraday market.	12
3.3 ENDEX	13
3.4 Imbalance market	13
3.5 aFRR/mFRR	14
3.6 Correlation price and carbon intensity.	16
3.7 Future developments.	17
4 Methodology	19
4.1 Model predictive control	19
4.2 Solver	20
4.2.1 Theory.	20
4.3 Simulation.	21
4.3.1 Model	21
4.3.2 Energy use	21
4.3.3 Energy cost	21
4.3.4 CO ₂ emission.	21
4.3.5 Regulating volume	21
4.3.6 Model runs	21
4.4 SARIMA model	22
4.4.1 Theory.	22
4.4.2 Market analysis	23
4.4.3 Extracting model parameters	24
4.4.4 Model training.	24
4.4.5 Model verification.	25
5 Internal Model	27
5.1 Flow model	27
5.2 Structures.	29
5.2.1 Undershot gates	29
5.2.2 Pumping station	30
5.3 Wind effects.	31

6	Data	33
6.1	Energy data	33
6.1.1	Dutch data	33
6.1.2	German market data	35
6.2	Discharge data	35
6.3	Water level data	36
6.4	Wind data	36
6.5	Day Ahead market data	36
6.6	Intraday market data	36
7	Optimization problem	37
7.1	Constraints	37
7.1.1	Mass balance	37
7.1.2	Gates	39
7.1.3	Pumping station IJmuiden	41
7.1.4	Scaling of constraints and variables	42
7.1.5	Time	42
7.2	Objectives	43
7.2.1	Day ahead market	43
7.2.2	Day ahead + intraday market	44
7.2.3	aFRR	45
7.2.4	Penalty functions	47
7.2.5	Full optimization problem	48
8	Results and Discussion	51
8.1	Verification of MPC	51
8.2	Sensitivity analysis	53
8.2.1	Prediction horizon	53
8.2.2	Price prediction	57
8.2.3	Measurement error	58
8.3	Reference	59
8.4	Long simulation with optimal settings	62
8.5	Future scenario	64
8.5.1	German market	64
8.5.2	Sea level rise	68
8.6	Possibilities for the aFRR	70
8.7	Study limitations	73
8.7.1	Optimal parameter choices	73
8.7.2	Data limitations	73
8.7.3	Market assumptions	74
8.7.4	Model limitations	75
8.7.5	Simulation limitations	76
9	Conclusion	77
9.1	Electricity markets	77
9.2	Controller sensitivity	77
9.3	Benefits	78
9.4	Markermeer and IJsselmeer	78
9.5	Final	79
10	Recommendations	81
10.1	Optimization	81
10.1.1	Bucket model	81
10.1.2	Pump configuration	82
10.1.3	Optimization process	82
10.1.4	Fish migration/maximum discharge	82

10.2 Simulation	82
10.2.1 Non-linear estimator of state	82
10.2.2 Energy use	82
10.3 Strategy	83
10.3.1 Markets	83
10.3.2 Clustering energy use	83
10.3.3 Optimizing on sustainable energy generation	83
10.4 Data availability	84
10.4.1 Electricity generation data	84
10.4.2 Water system data	84
10.4.3 Intraday market data	84
10.5 Further research	84
10.5.1 Discharge uncertainty	84
10.5.2 System's sensitivity to waterboard discharge	84
10.5.3 Day ahead market deadline	85
10.5.4 Prediction horizon MPC currently applied	85
10.5.5 Price prediction	85
10.5.6 Upscaling	85
10.5.7 Penalty on setpoint deviation	85
10.5.8 Scaling of the objective function	86
10.5.9 Uncertainty of data	86
10.6 Personal recommendations	86
10.6.1 Extending pumping capacity	86
Bibliography	87
A Appendix A	91
A.1 Energy production data correction	91
A.1.1 Biomass	91
A.1.2 Coal	91
A.1.3 Gas	92
A.1.4 Nuclear	92
A.1.5 Solar	92
A.1.6 Wind	92
B Appendix B	101
B.1 aFRR market analysis	101
B.1.1 Downward regulating bids, activations and price	101
B.1.2 Activation time and probability	104
B.1.2.1 $P = \text{€}84,-/\text{MWh}$	104
B.1.2.2 $P = \text{€}63,-/\text{MWh}$	107
B.1.2.3 $P = \text{€}42,-/\text{MWh}$	110
B.1.2.4 $P = \text{€}31,50/\text{MWh}$	113
B.1.2.5 $P = \text{€}29,-/\text{MWh}$	116
B.1.2.6 $P = \text{€}21,-/\text{MWh}$	119
B.1.2.7 $P = \text{€}0,-/\text{MWh}$	122
B.1.2.8 Conclusion	124
C Appendix C	125
C.1 Piecewise linearization gate equations	125
C.1.1 Optimization	125
C.2 Power curve optimization	129
C.2.1 Q-dH & P-dH curves	129
C.2.2 Optimization	130
C.2.3 Results	131

D Appendix D	133
D.1 Wind effects	133
D.1.1 Markermeer and IJsselmeer	133
D.1.2 Noordzeekanaal	134
E Appendix E	135
E.1 Optimize on CO ₂ /sustainable energy use	135
F Appendix F	137

List of Figures

1.1	Load shape adjustments due to demand response [17]	2
1.2	The study area	4
2.1	Amsterdam IJ-front [source: Waternet]	7
2.2	Oranjesluizen-complex [source: Google Maps]	8
3.1	Timeline of energy markets [source: Norwegian Water Resources and Energy Directorate]	11
3.2	Day ahead price 10-02-2016 [source: ENTSO-E]	12
3.3	Imbalance 10-02-2016 [source: ENTSO-E]	13
3.4	Forecasted REG over total imbalance [source: ENTSO-E]	14
3.5	Feasible workspace pumping station IJmuiden for participating on the aFRR market	15
3.6	Carbon intensity and day ahead price - Dutch market	16
3.7	Carbon intensity and day ahead price - German market	16
3.8	Carbon intensity over day ahead price	16
4.1	Model Predictive Control schematization	19
4.2	Depiction of receding horizon control	20
4.3	Stationarity testing	24
4.4	Market price timeseries autocorrelation	25
4.5	Receding horizon 1-Day ahead predicted and actual day ahead price, Dutch market	25
4.6	Size of daily minimum, maximum and average 95%-confidence interval of April 1st 2017, over prediction length, Dutch market	26
4.7	Receding horizon 1-Day ahead predicted and actual day ahead price, German market	26
4.8	Size of daily minimum, maximum and average 95%-confidence interval of April 1st 2017, over prediction length, German market	26
5.1	Concept bucket model	27
5.2	Allowable water level ranges and setpoint level of IJsselmeer and Markermeer per month	28
5.3	Internal model schematic	28
5.4	Explained equation for gates	30
5.5	Wind effects explained	31
6.1	Energy production by source	34
6.2	Day ahead and intraday market prices 10-02-2016 - 17-02-2016	36
7.1	Linearization gate discharge equation Den Oever	40
7.2	Power curve fit with gurobi	42
7.3	Day ahead plan and intraday phase	44
8.1	Optimized fluxes of the North Sea canal	52
8.2	Optimized pump energy and energy prices	52
8.3	Simulated water level of the North Sea canal for different prediction horizons	54
8.4	Relative performance for different prediction horizons	54
8.5	Cumulative cost for different prediction horizons	54
8.6	Cumulative energy use for different prediction horizons	55

8.7	Cumulative gate discharge in IJmuiden for different prediction horizons	55
8.8	Cumulative carbon emission for different prediction horizons	56
8.9	Cumulative regulating volume for different prediction horizons	56
8.10	Cumulative cost comparison predicted and actual day ahead price	57
8.11	Relative performance of MPC with different measurement errors	58
8.12	Cumulative costs with N=1.5 and measurement errors	58
8.13	Cumulative costs for different prediction horizons, including reference	59
8.14	Cumulative energy use for different prediction horizons, including reference	60
8.15	Cumulative CO ₂ emission for different prediction horizons, including reference	60
8.16	Cumulative gate discharge for different prediction horizons, including reference	61
8.17	Relative performance of different prediction horizons with reference scenario's	61
8.18	Cumulative cost for long run, N=2, including reference	62
8.19	Cumulative energy use for long run, N=2, including reference	63
8.20	Cumulative carbon emission for long run, N=2, including reference	63
8.21	Cumulative regulating volume for long run, N=2, including reference	63
8.22	Cumulative costs with N=2, German market scenario	64
8.23	Cumulative energy use with N=2, German market scenario	65
8.24	Cumulative carbon emission with N=2, German market scenario	65
8.25	Cumulative cost with N=2, Dutch and German market scenario	66
8.26	Cumulative regulating volume with N=2, Dutch and German market scenario	66
8.27	Fluxes NZK 07-04-2017 - 09-04-2017, German market scenario	67
8.28	Energy use and energy price 07-04-2017 - 09-04-2017, German market scenario	67
8.29	Energy use and carbon intensity 07-04-2017 - 09-04-2017, German market scenario	67
8.30	Cumulative cost N1.5, +0.5m sea level	68
8.31	Cumulative energy use N=1.5, +0.5m sea level	68
8.32	Cumulative carbon emission N=1.5, +0.5m sea level	69
8.33	Cumulative pumped volume N=1.5, +0.5m sea level	69
8.34	Maximum possible extra energy use per timestep, while downward activation occurred	70
8.35	Maximum cost per timestep due to downward activation	71
8.36	Cumulative maximum regulating volume without costs	71
8.37	Cumulative maximum profit through downward activation	72
8.38	Cumulative total cost for being active on day ahead, intraday and aFRR market	72
8.39	Decrease in discharge per step-wave time and height	76
10.1	10-bucket model Noordzeekanaal	81
A.1	Electricity generation with biomass, raw data. [ENTSO-E]	93
A.2	Electricity generation with biomass, corrected data.	93
A.3	Electricity generation with coal, raw data. [ENTSO-E]	94
A.4	Electricity generation with coal, corrected data.	94
A.5	Electricity generation with gas, raw data. [ENTSO-E]	95
A.6	Electricity generation with gas, corrected data.	95
A.7	Electricity generation by nuclear energy, raw data. [ENTSO-E]	96
A.8	Electricity generation by nuclear energy, corrected data.	96
A.9	Electricity generation with solar energy, raw data. [ENTSO-E]	97
A.10	Electricity generation with solar energy, corrected data.	97
A.11	Electricity generation with onshore wind energy, raw data. [ENTSO-E]	98
A.12	Electricity generation with offshore wind energy, raw data. [ENTSO-E]	98
A.13	Electricity generation with onshore wind energy, corrected data.	99
A.14	Electricity generation with offshore wind energy, corrected data.	99
B.1	Downward regulating bids	102
B.2	Activated downward regulating volume	102
B.3	Downward regulating price	103

B.4	Amount of times downward regulating occurred with $P \leq €84,-/MWh$ with an activation time of 15 minutes or longer	104
B.5	Amount of times downward regulating occurred with $P \leq €84,-/MWh$ with an activation time of 30 minutes or longer	105
B.6	Amount of times downward regulating occurred with $P \leq €84,-/MWh$ with an activation time of 45 minutes or longer	105
B.7	Amount of times downward regulating occurred with $P \leq €84,-/MWh$ with an activation time of 60 minutes or longer	106
B.8	Amount of times downward regulating occurred with $P \leq €84,-/MWh$ with an activation time of 120 minutes or longer	106
B.9	Amount of times downward regulating occurred with $P \leq €63,-/MWh$ with an activation time of 15 minutes or longer	107
B.10	Amount of times downward regulating occurred with $P \leq €63,-/MWh$ with an activation time of 30 minutes or longer	107
B.11	Amount of times downward regulating occurred with $P \leq €63,-/MWh$ with an activation time of 45 minutes or longer	108
B.12	Amount of times downward regulating occurred with $P \leq €63,-/MWh$ with an activation time of 60 minutes or longer	108
B.13	Amount of times downward regulating occurred with $P \leq €63,-/MWh$ with an activation time of 120 minutes or longer	109
B.14	Amount of times downward regulating occurred with $P \leq €42,-/MWh$ with an activation time of 15 minutes or longer	110
B.15	Amount of times downward regulating occurred with $P \leq €42,-/MWh$ with an activation time of 30 minutes or longer	110
B.16	Amount of times downward regulating occurred with $P \leq €42,-/MWh$ with an activation time of 45 minutes or longer	111
B.17	Amount of times downward regulating occurred with $P \leq €42,-/MWh$ with an activation time of 60 minutes or longer	111
B.18	Amount of times downward regulating occurred with $P \leq €42,-/MWh$ with an activation time of 120 minutes or longer	112
B.19	Amount of times downward regulating occurred with $P \leq €31,50/MWh$ with an activation time of 15 minutes or longer	113
B.20	Amount of times downward regulating occurred with $P \leq €31,50/MWh$ with an activation time of 30 minutes or longer	113
B.21	Amount of times downward regulating occurred with $P \leq €31,50/MWh$ with an activation time of 45 minutes or longer	114
B.22	Amount of times downward regulating occurred with $P \leq €31,50/MWh$ with an activation time of 60 minutes or longer	114
B.23	Amount of times downward regulating occurred with $P \leq €31,50/MWh$ with an activation time of 120 minutes or longer	115
B.24	Amount of times downward regulating occurred with $P \leq €29,-/MWh$ with an activation time of 15 minutes or longer	116
B.25	Amount of times downward regulating occurred with $P \leq €29,-/MWh$ with an activation time of 30 minutes or longer	116
B.26	Amount of times downward regulating occurred with $P \leq €29,-/MWh$ with an activation time of 45 minutes or longer	117
B.27	Amount of times downward regulating occurred with $P \leq €29,-/MWh$ with an activation time of 60 minutes or longer	117
B.28	Amount of times downward regulating occurred with $P \leq €29,-/MWh$ with an activation time of 120 minutes or longer	118
B.29	Amount of times downward regulating occurred with $P \leq €21,-/MWh$ with an activation time of 15 minutes or longer	119
B.30	Amount of times downward regulating occurred with $P \leq €21,-/MWh$ with an activation time of 30 minutes or longer	119
B.31	Amount of times downward regulating occurred with $P \leq €21,-/MWh$ with an activation time of 45 minutes or longer	120

B.32	Amount of times downward regulating occurred with $P \leq \text{€}21,-/\text{MWh}$ with an activation time of 60 minutes or longer	120
B.33	Amount of times downward regulating occurred with $P \leq \text{€}21,-/\text{MWh}$ with an activation time of 120 minutes or longer	121
B.34	Amount of times downward regulating occurred with $P \leq \text{€}0,-/\text{MWh}$ with an activation time of 15 minutes or longer	122
B.35	Amount of times downward regulating occurred with $P \leq \text{€}0,-/\text{MWh}$ with an activation time of 30 minutes or longer	122
B.36	Amount of times downward regulating occurred with $P \leq \text{€}0,-/\text{MWh}$ with an activation time of 45 minutes or longer	123
B.37	Amount of times downward regulating occurred with $P \leq \text{€}0,-/\text{MWh}$ with an activation time of 60 minutes or longer	123
B.38	Amount of times downward regulating occurred with $P \leq \text{€}0,-/\text{MWh}$ with an activation time of 120 minutes or longer	124
C.1	Piecewise linearization Den Oever	126
C.2	Piecewise linearization Houtribsluis	127
C.3	Piecewise linearization Kornwederzand	127
C.4	Piecewise linearization Oranjesluizen	128
C.5	Piecewise linearization IJmuiden	129
C.6	Results optimization Gurobi	131
F.1	Time needed for discharge to become 0, for different wave heights	138

List of Tables

1.1	Potential capacity for ancillary services in households in the Netherlands in MW [4]	2
2.1	Pumping capacity discharging in the NZK-ARK[33]	7
2.2	Pump specifications of pumps installed at pumping station IJmuiden	8
3.1	Percentage of days activated per sequency length and bid-price [ENTSO-E] . . .	15
4.1	Model runs performed for sensitivity analysis	21
5.1	Q-dH curves	30
5.2	Pump power curves	30
6.1	Electricity production of the Netherlands by source [CBS]	33
6.2	Carbon intensity of energy sources [36]	34
6.3	Carbon intensity of German market data	35
7.1	aFRR bidding example	45
A.1	Yearly electricity production of the Netherlands by source [CBS]	91
B.1	Percentage of days activated per sequency length and bid-price [ENTSO-E] . . .	124

List of symbols

Q	Discharge
Q_{max}	Maximum discharge
n	Amount of gates
α	Gate coefficient
B	Width of gate
h_k	Height of throat of gate
h_g	Level of gate
h_{cr}	Crest level of gate
d_g	Depth of gate
h_i	Water level on the inside (upstream) of structure
h_o	Water level the outside (downstream) of structure
dH	Relevant water level difference between up- and downstream of structure
s	Slack variable to make dH 0 when smaller than minimum
g	Gravitational constant
W	Difference in water level due to wind influence
κ	Dimensionless wind constant
U_w	Wind speed 10m above water level
F	Undisturbed traveled length of wind
θ	Angle of wind relative to structure
d	Water depth
$h_{i,min}$	Lower water level bound
$h_{i,max}$	Upper water level bound
k	Slack for upper bound relaxation
N	Prediction horizon length
t	Timestep number
Δt	Timestep size
h_{nzk}	Water level of the Noordzeekanaal
h_{mar}	Water level of the Markermeer
h_{ijs}	Water level of the IJsselmeer
Q_{oranje}	Discharge through Oranjesluizen
Q_{waterb}	Discharge of waterboards
$Q_{ijm,sluice}$	Discharge through gates IJmuiden
$Q_{ijm,pump}$	Discharge pumping station IJmuiden
$Q_{houtrib}$	Discharge through Houtribsluis
Q_{korn}	Discharge through Kornwederzandsluis
Q_{den}	Discharge through Stevin- and Lorenz-sluis
Q_{olst}	Discharge measured in Olst
$Q_{maarssen}$	Discharge measured in Maarssen
A_{nzk}	Storage area of the Noordzeekanaal
A_{mar}	Storage area of the Markermeer
A_{ijs}	Storage area of the IJsselmeer
ρ	Density of substance
E	Energy use of pumping station
E_{plan}	Energy bid on day ahead market
P	Power consumption of pumping station
p_e	System efficiency

$c_{dayahead}$	Day ahead market price
$c_{intraday}$	Intraday market price
a	Curve-fit coefficient
b	Curve-fit coefficient
c	Curve-fit coefficient
p	Penalty height for objective function
γ	Scaling factor
δ	Constraint relaxation constant

Introduction

1.1. Demand response

With climate change as driving force, renewable energy is on the rise [35]. After the signing of the Paris agreement, the European Union has created a roadmap to a low-carbon economy. This roadmap aims to reduce carbon emissions by 20% before 2020, 40% before 2030, 60% before 2040 and 80% before 2050. This will be combined with 25% of the energy mix being renewable by 2020, and 27% by 2030. By 2050 the power sector is expected to be practically emission-free[13]. Some countries are even more ambitious, such as Germany (30% renewable energy generation by 2030), Denmark (35% by 2020, 100% by 2050), France (23% by 2020, 32% by 2030) and Portugal (40% renewable energy generation by 2030). The Netherlands has recently accepted a new climate-law, in which the country commits to a 49% reduction of CO₂ emission by 2030 and 95% reduction by 2050 (compared to the emissions in 1990). Solar and wind energy are promising choices of renewable energy, and also becoming more profitable due to technological advancements.

While these generating-techniques are valuable for the energy transition, they also bring some new problems. One of these problems is that the amount of energy generated at a certain time is as predictable as the weather. The current electricity-network is managed on the supply-side; a gas-turbine will run a bit harder, when more electricity is needed. The wind doesn't blow harder when we tell it to. Energy on demand will not come easily in the future. Energy storage, like home battery packs, can help with smaller appliances like lighting, computers and even dishwashers. But big consumers will have to be more active when energy is available, and less when it isn't. This principle is known as demand-side management, demand-side control or demand response (DR).

Instead of producing more energy when demand is high, it is necessary to consume more energy when more is produced (sustainably). Timing your consumption can be used to balance the grid in times of peak-production. Using less or no energy when no renewable energy is produced. Another possibility is to use more energy than is needed at the moment. This helps to balance the electricity grid. Figure 1.1 shows the load-shape adjustments that are possible due to the application of demand response. It comes down to either shifting your energy use, increasing it or decreasing it for the time being, in order to have a positive impact on the balance of the electricity grid and thus on the energy transition. This thesis will focus on the ability of a pumping station in IJmuiden to participate in DR.

Adjusted load shapes as a result of DSM (Chuang and Gellings, 2008; Gellings, 1985; Hakvoort and Koliou, 2014).

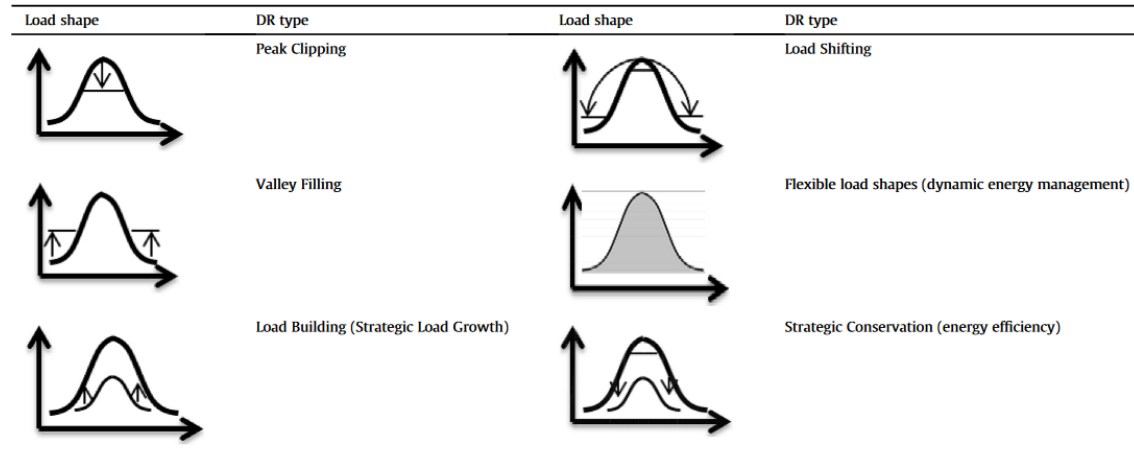


Figure 1.1: Load shape adjustments due to demand response [17]

Currently energy price is correlated with sustainable energy production, as showed in section 3.6. When an unpredicted gust of wind creates a peak in energy production, the market adjusts to help consume this extra amount; the price of energy goes down. Germany recently experienced such large sustainable energy generation that electricity prices became negative [44]. By consuming energy at the right time, money can be saved, or even earned. The principle of demand response is now being researched for the use of electrical vehicles, heating and even wet-appliances (laundry machine, dishwasher, etc)[51, 54, 56]. The total DR potential of household appliances in the Netherlands is not to be underestimated. Their potential to participate in demand response in can be seen in table 1.1

In most cases energy-costs are being minimized, giving demand response a business case.

Potential in MW	Summer		Winter	
	Up	Down	Up	Down
Regulating direction	Up	Down	Up	Down
<i>Freezer</i>	41	-12	41	-20
<i>Refrigerator</i>	70	-35	70	-35
<i>Air conditioner</i>	-	-20	-	-
<i>Electric water heater</i>	97	-29	97	-29
<i>Heat pump</i>	-	-	14	-37
Total	208	-105	222	-121

Table 1.1: Potential capacity for ancillary services in households in the Netherlands in MW [4]

The intraday market and imbalance market prices are influenced by the (expected) imbalance on the grid. By consuming energy when it is the cheapest, and producing when it is most expensive, imbalance is automatically positively influenced. This comes down to lower CO₂-emissions and lower energy costs for the flexible party, and a more balanced grid for the whole network. When the energy-mix will be 100% sustainable, CO₂-emissions savings are not expected to be possible anymore, but energy-costs and the stability of the grid will still be positively influenced.

1.2. The Dutch delta

The Netherlands is a low-lying country in the Rhine-Meuse delta. The rivers Rhine, Meuse and Scheldt flow through the Netherlands. Besides that, a large part of the country lies below mean sea level (MSL). After the 1953 flood that covered over 200.000 hectares of the country and killed 1863 people, the Delta plan was created. This plan consisted of creating flood-defense structures (dikes, dunes, etc) to create what is now the safest delta in the world.

The dikes next to the Rhine are designed to withstand high water levels with a return period of 1250 years. The dike-area of Zuid-Holland has a flood return period of 16.000 years, which includes the cities of Rotterdam, The Hague and Amsterdam[49].

The Netherlands is also known for its polders. All rainfall collected in these areas is pumped towards the sea in different stages. Historically, windmills were used to pump the water from one side of the dike to the other. This meant that storage capacity was needed, to store excess rainfall without flooding until the wind blows. Nowadays, these windmills hardly perform any work anymore. Windmills have been replaced by pumping stations, and storage capacity in urban areas was replaced by fast drainage.

Due to climate change an increase in rainfall is expected[38]. A recent research by HKV and the KNMI [29] showed that extreme rainfall has already increased in the last 20 years. The current drainage-system will be too expensive to maintain[18], bringing storage back to the cities. Old canals that were replaced with streets are being dug out[12, 57]. Newly built neighborhoods have more green and have separate rainwater sewers, making sewer overflows less damaging for the environment. These kind of measures increase the capacity and flexibility of the water system in the Netherlands.

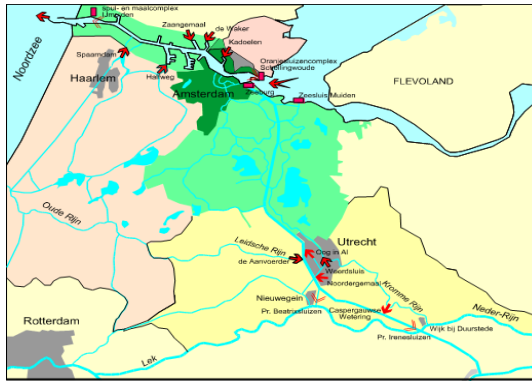
There are four different kinds of control strategies in water-level management applied in the Netherlands[53]:

- Regular management, where in summer the water level is kept at a higher level than in winter. This is typically applied in agricultural areas and the built-environment.
- Fixed management, where the water level is kept at a fixed level throughout the year. Typically applied in nature areas and the built environment.
- Flexible/natural management, where the water level can fluctuate freely between a pre-determined minimum and maximum water level. Typically applied in nature areas and large-scale water management. It can lead to fewer exchanges in water while keeping the water within safe boundaries.
- Dynamic management, where the water level is adjusted to the weather, crop growth and other agricultural needs. Only seen in agricultural areas.

The levels and type of management are decided locally by a Water board or nationally by Rijkswaterstaat (RWS), and are typically based on the agricultural needs, land-subsidence, shipping and flood probabilities. In the big canals and rivers there is room for more fluctuating water levels. This range makes it possible for the pumps to have a more flexible pump-schedule, to increase sustainable energy consumption. Demand response can be applied. This would reduce the carbon-emission caused by the pumping stations, and contribute to stabilizing the Dutch electricity-grid. It would be interesting to see if a more dynamic water-level can be applied in polders, but that would have to be researched and decided locally, involving local stakeholders like water boards, farmers and residents.

1.3. A new role for Rijkswaterstaat

In IJmuiden, the largest pump (in capacity) in Europe is located, with an estimated energy use equivalent to 3000 households[43]. It serves an important function in flood protection, since it is one open system with the Noordzeekanaal (NZK) including ports, the Amsterdam-Rijnkanaal (ARK), the IJ, the canals of Amsterdam, drainage canals of the water board Amstel, Gooi en Vecht and the Lekkanaal. See Figure 1.2 for an overview of the area.



(a) System with structures [source: HKV]



(b) Overview of study area [source: Nederlandse Hydrologische Vereniging]

Figure 1.2: The study area

Rijkswaterstaat (RWS) is the owner of the infrastructure, responsible for the water safety of the Netherlands. Their task is to manage water optimally, to prevent floods and act when droughts happen. With the UN Climate Agreement[41] and the Urgenda verdict[42] in mind, the Dutch government requires RWS to become CO₂ neutral by 2050. Optimizing the energy use of infrastructure is one part of the challenge. This can be done by installing efficient pumps, optimizing pump configurations or optimizing energy use.

Demand response is a tool RWS can use to take it one step further, as they are currently investigating in the "Pompen als het waait" project. They could use the water system of the NZK-ARK, and the assets they own, to help stabilize the grid. This doesn't only lower the energy bill for RWS, they could actively contribute to the energy transition, and to the energy-security of the Netherlands/Europe.

Extending the time to pump by a few hours or even minutes in case of a negative imbalance on the grid results in no energy being consumed at the time the price is the highest, unless completely necessary. This also has a positive effect on the stability of the frequency of the electricity grid. RWS could also pump extra water out in case of a positive imbalance. When there is a positive imbalance on the grid, you can get paid to consume energy, depending on which energy-market you are active. And you contribute to the stability of the frequency of the grid. Using the whole water system as a buffer, while using forecast models to anticipate to events, could give RWS a significant stabilizing capacity. With the energy transition coming up, and the expected increasing difficulty of stabilizing the grid, there is an interesting opportunity for RWS to be researched.

1.4. This research

In this research, we investigate to what extent Demand Response can be safely applied to the water system of the Noordzeekanaal-Amsterdam Rijnkanaal to optimize energy costs and CO₂ emissions. The following research questions will be answered:

To what extent can Demand Response (DR) be applied safely to pumping station IJmuiden, and the water system of the NZK-ARK, to optimize energy costs and CO₂-emission?

A model-predictive controller (MPC) will be built, using current and expected water levels and energy data as input. Energy availability, energy-price and market-imbalance can be used in the controller, and the differences in output will be investigated. The Pyomo package[30, 31] will be used to formulate the optimization problem in Python. A simulation-model of the water system, a bucket model, will be used to evaluate the consequences of the changes in pumping schedules on the water-system. In this study, the same model is used as the internal model of the MPC to simulate the effects of the MPC's output. It will be tested if the water-safety constraints are violated in any way, to make sure water-safety is not compromised for energy savings.

What electricity market(s) would be most suitable for pumping station IJmuiden to participate in?

Multiple markets will be researched, and various strategies will be considered. Besides that, also the risks of participating in each market will be elaborated on.

How large would the benefits of demand response be in terms of energy-costs, CO₂ emission and regulating volume?

The MPC-results will be compared with results for the current MPC strategy, where energy use is minimized. This information can be used to estimate the amount of CO₂ emitted for the pumping itself using historic energy-production data. The historic energy-production data can tell what the "energy-mix" looked like in the grid at a certain time. Multiple bidding strategies will be evaluated on different markets, to see which strategy would be most beneficial for both Rijkswaterstaat and the Dutch electricity grid.

What factors influence the performance of the controller, and what would be their optimal setting?

A sensitivity analysis will be performed on certain parameters of the optimization algorithm. The optimal prediction horizon, data uncertainty and simplifications will be taken into account in the sensitivity analysis. Besides that, market "rules" are evaluated for how accessible they make Demand Response.

Can the Markermeer and IJsselmeer contribute to the flexibility of the pumping station in IJmuiden?

The optimization problem for control with the Markermeer and IJsselmeer will be proposed, while the market analysis and system analysis will result in early conclusions on the possible added flexibility.

At IJmuiden, the sluices are opened at a difference in water level of 16cm, and closed at 12cm. This difference in pressure is needed to overcome the difference in density of fresh and salt water. The sluice is automatically controlled and has a maximum discharge of 500 m³/s. This maximum discharge is maintained to ensure stability of the bed of the sluice-complex.

Pumping station IJmuiden contains 6 pumps. Their specifications can be found in table 2.2. Their combined maximum power is around 4.9 MW. Two of the pumps have one setting, at 64.3 RPM (rounds per minute). While two can switch between 64.3 and 48.2 RPM. The last two, the newest, are variable speed pumps which are designed to discharge 55 m³/s at a water-level difference of 1.2m. The pumps can only pump up to a certain water level difference, when that is too high they will automatically shut down.

Currently, pumping station IJmuiden is controlled through Model Predictive Control (MPC). In this MPC, the prediction horizon is 24 hours, and the water level is kept between -0.3m NAP and -0.5m NAP.

Pump number	1&2	3&4	5&6
Manufacturer	Stork	Stork	Nijhuis
Type	OPH 400-V	OPH 400-V	HP1-4000.430
Design discharge - pump height	37.5 m ³ /s - 1.2m	37.5 m ³ /s - 1.2m 28.0 m ³ /s - 0.7m	55.5 m ³ /s - 1.2m
RPM	64.3	64.3/48.2	67-77
Engine	Electrical (direct drive)	Electrical (direct drive)	Electrical (direct drive)
Power	960 kW	960 kW	523 kW
Max. pump height	2.35	2.35	2.75

Table 2.2: Pump specifications of pumps installed at pumping station IJmuiden

2.2. Markermeer & IJsselmeer

The ARK turns into the IJ at Amsterdam, where it is connected with the IJmeer through the Oranjesluizen at Schellingwoude. The connection between the IJ and the IJmeer is made with the Oranjesluizen. The sluice-complex exists of three locks; Prins Willem Alexandersluis (used for shipping, and in rare cases for water management), Zuider- Midden- and Noorderschutsluis (can be used in winter as intake-sluice), and a sluice to the South of the other lock. The maximum discharge of the sluice-complex is 200 m³/s. The complex and Prins Willem Alexander-sluis can be seen in Figure 2.2.

The water from the Markermeer is used to limit salt water intrusion in the NZK and to guarantee the water level required for shipping.

At pumping station Zeeburg, the city water of Amsterdam are connected with the IJmeer. The station has three pumps with discharge capacity of 13.3 m³/s and one of 16.7 m³/s. The smaller pumps can either pump water from Amsterdam to the IJ, or the other way around. The bigger pump can only pump towards the IJ.

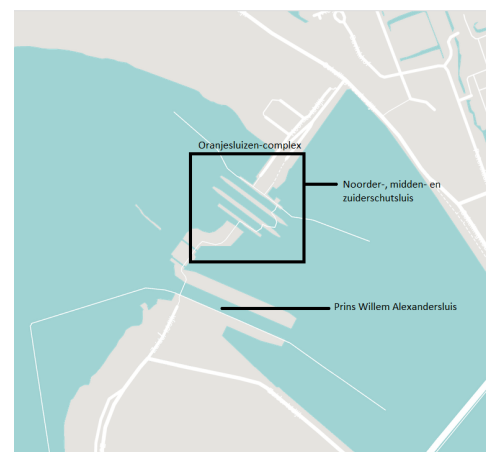


Figure 2.2: Oranjesluizen-complex [source: Google Maps]

In winter the same water level is maintained in the IJmeer and the NZK-ARK (-0.4m NAP). Through strong East-winds, the water level of the IJmeer at Schellingwoude can still significantly rise (to 0m NAP). With West-winds, the water level of the IJmeer can decrease a few centimeters. In summer, the desired water level of the IJmeer is -0.20m NAP, so water can flow to the NZK-ARK under gravity.

The IJ turns into the NZK at Amsterdam, which connects the ports of Amsterdam with the North Sea. The NZK discharges water into the North Sea through sluices and a pumping station. The NZK is controlled to maintain a water level of -0.4m NAP (daily average of water levels at the Oranjesluizen and Buitenhuisen). The drain possibilities are used maximally, giving water levels that deviate from -0.55m NAP to -0.3m NAP. This generally happens two times a day, but sometimes deviates from the tidal pattern due to wind. A strong west-wind (wind power 5) is enough to make discharge under gravity impossible. An east-wind is optimal for discharging under gravity, since it forces the water level of the NZK to be higher. The wind has more influence on the water system. Mainly with a North-West wind, the water level in the South of the ARK can be up to 30cm higher.

The IJmeer is connected to the Markermeer, which is separated from the IJsselmeer by a dam. The dam has two sluices; Krabbersgatsluis and Houtribsluis so water can be discharged in the IJsselmeer. The IJsselmeer is separated from the North Sea by the afsluitdijk. The Houtribsluis has a maximum discharge of 630 m³/s and is generally used to keep the chlorine-concentration in the Markermeer at respectable levels. The afsluitdijk also has two sluices; the Stevinsluis and the Lorentzsluis. The two lakes both have a desired water level of -0.2m NAP in winter, in summer the water level has an allowed deviation between -0.1m NAP and -0.3m NAP. The Lorentzsluizen consist of two structures with 5 discharge openings. There are plans to place turbines in the Lorentzsluizen for tidal energy. Every opening is 12m wide and 4m deep. The Stevinsluizen exist of three openings with a width of 12m.

The IJsselmeer is supplied with water by the discharge of the IJssel and the Vecht. The Markermeer is supplied with water through the sluices at the IJsselmeer, and through the Eem. The storage area of the NZK-ARK is, due to missing inundation-areas and floodplains, independent of the water level. The NZK has a storage area of 2.060 hectares, the ARK has a storage area of 821 hectares and the Boezem AGV has a storage area of 1.025 hectares. The Markermeer and IJsselmeer have a storage area of 70.000 hectares and 110.000 hectares respectively.

3

Electricity markets

The energy market is a complex system, which contains multiple market mechanisms. There are markets to buy and sell energy in the future, the near future and in real-time. The day-ahead market is where energy is bought and sold a day before consumption and generation. The intraday market, where energy is traded up to 5 minutes before consumption. The strips market is where standardized blocks of energy are traded up to two days before delivery. The imbalance market, where imbalances on the grid are solved in real-time in blocks of 15 minutes. And behind the imbalance market, there is the aFRR and mFRR market. Where imbalances are solved in near real-time and in 15 minute blocks. The electricity-market timeline can be seen in Figure 3.1

The buyers and sellers on the markets are certified BRP's (balance responsible parties). The TSO (transmission system operator), TenneT in the Netherlands, holds them accountable for imbalances on the grid. This results in them paying for the activation of balancing mechanisms. Smaller parties are contracted under a BRP, sometimes eliminating the risk for the small party (like in households), but sometimes the risk can be spread and evened out within the assets of one BRP (like an aggregator). In the next part, the markets will be further elaborated, and relevant markets will be further analyzed.

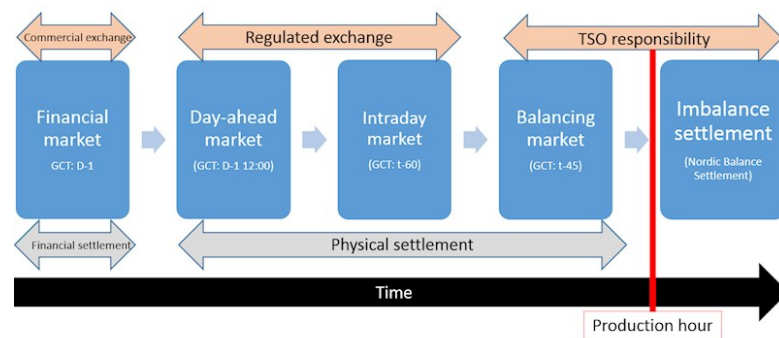


Figure 3.1: Timeline of energy markets [source: Norwegian Water Resources and Energy Directorate]

3.1. The day ahead market

The day-ahead market is where energy is traded on a day-to-day basis, and energy is bought and sold for the next day. Energy is sold per hour, and it has to be consumed within the period for which it is purchased; if you buy 1 MWh for 11:00-12:00, you have to use 1 MWh between 11:00 and 12:00.

In practice it is difficult, if not impossible, to exactly determine the planned energy consumption. This is registered as an imbalance, which in turn will be solved in the imbalance market(s). The required balancing will be charged to the BRP in hindsight, giving an incentive to predict energy use, and following the accepted bids on the market as accurately as possible.

Every day at 12:00 CET, producers bid their minimum selling price for the hours of the next day. Missing this deadline means no energy will be bought or sold by that party on that day. Buyers bid their maximum buying price for energy for the hours of the next day. Supply and demand are met, and the market price is calculated. In the Netherlands, this is done by EPEX, the market regulator. The economic “invisible hand” is EPEX’ hand that creates the equilibrium. In Figure 3.2, the day ahead price for the date 10-02-2016 can be seen. The first results are published at 12:42 CET, and are final at 12:55 CET: after publishing the price, it will not change anymore. The day ahead market for that day is closed.

The daily traded volume of energy is of the order of 100 GWh [27]. The day-ahead market shows a daily and weekly pattern. Prices of the hours of the day are correlated with the same hours of the previous day. This autocorrelation will be used in section 4.4.2 to create a predictive model for the APX price of the following days. This is needed in order to do a bidding on the market, before the actual market-price is known.

In order to participate on this market, no extra installations are needed. The regional TSO keeps track of the energy the actual energy use, and communicates this with TenneT. The difference between the planned energy use and the measured energy use is imbalance, which can be positive and negative.

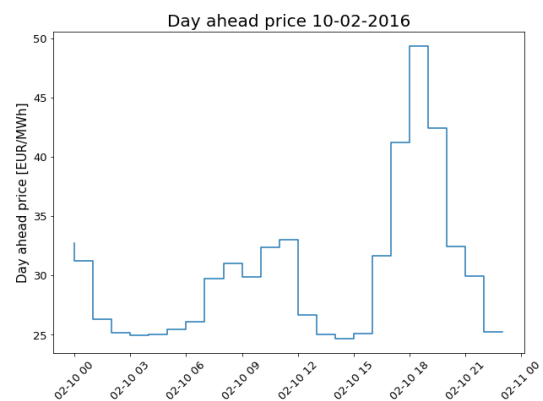


Figure 3.2: Day ahead price 10-02-2016 [source: ENTSO-E]

3.2. Intraday market

On the intraday market, quarterly blocks of energy are traded throughout the day, up to 5 minutes before consumption. This market makes it possible for BRP’s to reduce their caused imbalance. It is in theory an attractive market for sustainable energy, due to their unpredictable nature. The intraday market data is not available for download, so no price timeseries can be given. In the Netherlands, the intraday market is a relatively small market. This is due to an efficient imbalance system, experts at Sympower confirmed. A typical daily volume of the intraday market is of the order of 10 GWh [27]. However, the intraday market is seen as the market containing the most potential to trade sustainable energy in the future[15]. In Germany, this is the market where the energy price first became negative due to a surplus of wind energy. It can be expected that the national intraday markets will be harmonised to accommodate international/pan-European trade.

For participating in the intraday market, the same applies as with the day ahead market. No extra installations or measuring device are needed. The regional TSO is responsible for keeping track of actual energy use.

3.3. ENDEX

The ENDEX market is an international market where long-term or base-load products (coal, gas, electricity) can be traded. Currently Rijkswaterstaat (RWS) trades on this market, buying contracts (called futures) that guarantee a base-load. The price of the future is based on the day-ahead-prices of the APX market, and is €0.084/kWh on average for RWS, including transport costs [Rijkswaterstaat]. In the period of April 2017, the Dutch ENDEX price was around €31.50. The market does not stimulate flexible energy use, because the price is fixed. There is a minimum block order of 1 MW. In the Netherlands, the Dutch state buys the energy for all its assets on this market. Since base-load and long-term contracts are traded, this market is not suitable for demand response. However, it could be used for upward-regulation (increasing the energy on the grid) capacity. This would mean the pumping station would stop pumping, when it said it would pump. Due to time constraints, this research only focuses on downward regulating volume (decreasing the energy on the grid).

3.4. Imbalance market

The Dutch transmission system operator (TSO), TenneT, is responsible for balancing the grid. It does this through the imbalance market. Because large volumes of energy cannot yet be stored with economic efficiency, power supply and demand have to be matched continuously. Imbalance on the grid can negatively affect power quality or can even result in damage to the infrastructure itself. Devices like lights, clocks, rotating machines and transformers all rely on a certain frequency. Clocks might become incorrect, lights can flicker, and induction engines might stop working. Besides that, transmission and transforming of the energy is also a balance of frequency. Transmission is best done at low frequencies, while transforming is done more effectively at high frequency. And frequency deviations normally come paired with deviations in voltage, which can be detrimental for electrical appliances.

The imbalances are due to outages, unpredictable energy production and the inaccuracy of energy-use predictions. If the market projections would be perfect, no balancing of the grid would be needed. However, power flows between supply and demand (allocations) do not match the planned volumes (nominations). TenneT can balance the grid using back-up (emergency) production capacity or asking producers to stop/reduce. Another option is to ask large consumers to in- or decrease consumption, like what is currently done with greenhouses, hospitals and small industries. This is mostly done through automated control, powered by a near-real-time feed of imbalance and energy price[6]. Positive contributions to the imbalance (helping balance the grid) are rewarded, while negative contributions (increasing the imbalance) will be penalized. This is called "passive contribution", since the feed is freely available and BRP's can act on this market voluntarily.

The imbalance market is a highly unpredictable market, and is measured in timesteps of 15 minutes. In Figure 3.3, the imbalance on 10-05-2016 can be seen.

The imbalance market is known for its unpredictability and shows little correlation with the other markets. The mechanism behind the imbalance is very complex, since both production and consumption are complex mechanisms. Production is dependent on weather factors, which can be unpredictable. Weather conditions have a large impact on the demand and supply of energy: A heavy, unexpected, gust of wind can cause a positive imbalance. This is due to the fact that wind turbines will rotate faster, increasing the produced energy. Wind speed affects power-generation of turbines to the power

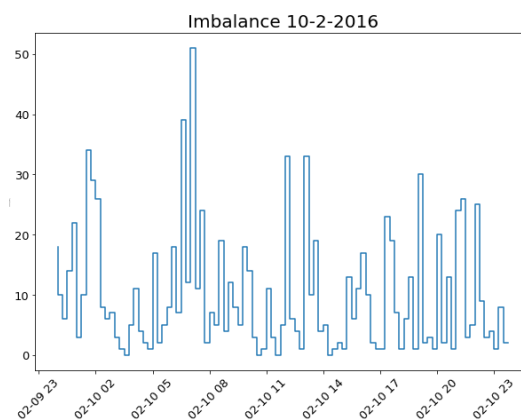


Figure 3.3: Imbalance 10-02-2016 [source: ENTSO-E]

three[37]. However, weather conditions also have a large effect on energy use. Wind speed affects the chilling of greenhouses, resulting in a higher energy use. An unexpected cloudy day results in greenhouse having to turn on their lights, while an unexpectedly sunny day does the opposite. Even though the effect of weather on energy consumption and production is well understood, predicting weather conditions accurately enough is still far away. The report of Gavin (2014)[24] elaborates further on the seasonal patterns of energy demand, which are caused by weather conditions.

The influence of forecasts can be seen in Figure 3.4, where the predicted wind and solar generation is plotted over the imbalance. It can be seen that if high renewable energy generation is expected, the imbalance is generally low. But when the predicted renewable generation is low, imbalance can be created due to unexpected weather conditions. This shows that the imbalance is also dependent on the accuracy of our weather forecasts, which affect planned allocations and nominations. For a customer/participant in the imbalance market, the imbalance price is also an important factor when being active on this market. The price is however dependent on supply/demand, the price of oil/coal, profitability of a wind-turbine, etc. Downward regulation volume (decreasing the energy on the grid) is preferably activated when there is an attractive price. Within 15 minutes, the balancing party would want to consume as much energy as possible to achieve as much profit as possible. This would also solve the most imbalance. For a pumping station like the one in IJmuiden, which takes about 15 minutes to boot-up and then keeps running for preferably one hour, participation on the the imbalance market would probably result in financial losses. The current players on this market are greenhouses (preferably with a combined heat- and power-unit; CHP), hydropower-plants and gas-turbines. These players can reacts fast, with high volume, and in both an upward and downward regulatory way. This gives the pumping station in IJmuiden a disadvantage on the imbalance market.

3.5. aFRR/mFRR

Behind the imbalance market, there is the aFRR and mFRR: the automatic and manual frequency restoration reserves. When the aFRR cannot supply the wanted regulating volume, the mFRR gets activated, where the activation is not done automatically (through control). On these markets, BRP's can bid for upward regulation (counteract negative imbalances) or downward regulation (counteract positive imbalances). This is done per 15 minutes, and the BRP gets a notice 15 minutes before activation. If TenneT expects an imbalance in 15 minutes, it will activate the aFRR first, since this is done automatically through control. The lowest bids will be chosen (on "merit" order) to be activated first, so the cheapest imbalance price is realized. In these first 15 minutes, a minimum power-deviation of 7% of the total bid is required per minute. After 15 minutes, the power should be as high as the bid. After this, the BRP can be notified to stay active for longer or shut down. However, if this is not possible, extra reserves will be called in place through the mFRR, which will be further calculated in the imbalance price on the imbalance market. These markets seems suitable for a pumping station like IJmuiden, with the downside that it operates in 15-minute slots. This means that a balancing party that can activate for smaller timeslots would probably get the preference over the pumping station. However, this does not mean that the pumping station would not be activated at all.

On the other side, due to the rapidly changing of the North Sea water level, the pumps will

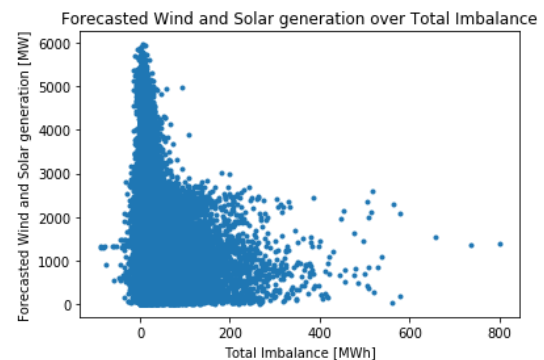


Figure 3.4: Forecasted REG over total imbalance [source: ENTSO-E]

have to be controlled frequently anyway.

Downward Activation Sequence length [min]	Percentage of days occurred					
	P [€/MWh] = 0	P = 21	P = 31.5	P = 42	P = 63	P = 84*
15 (+15) min	97.5%	99.3%	99.5%	99.5%	99.5%	99.5%
30 (+15) min	63.2%	89.8%	99.1%	99.1%	99.1%	99.1%
45 (+15) min	32.0%	71.5%	94.8%	97.9%	97.9%	97.9%
60 (+15) min	17.1%	55.4%	89.1%	95.4%	95.4%	95.4%
120 (+15) min	3.8%	22.5%	65.1%	79.0%	79.3%	79.3%

*RWS' current energy price

Table 3.1: Percentage of days activated per sequence length and bid-price [ENTSO-E]

In figures B.1, B.2 and B.3 the accepted downward regulating offers, activated downward regulating offers and downward regulating price can be seen. In Figure B.34, the amount of times the downward regulating price is lower or equal to €0,- during a day can be seen, while downward activation occurs. This means that either energy is for free, or you get payed to use energy. Which would be ideal for IJmuiden. The analysis shows that there are quite some opportunities for the pumping station to pump with an energy price lower than or equal to €0,-.

Another analysis has been performed about the length of activation time whilst the price was smaller than or equal to zero. The graphs show that a long sequential activation becomes more uncommon when the sequence gets longer. In table 3.1, the percentage of days a certain downward-activation sequence occurred together with certain bid-prices. The sequence time always comes along with a 15 min activation time. It can be seen that the higher RWS would bid, the more often they would be activated for downward regulation, and also in longer sequences. It shows that even with an energy price lower than half of the average day ahead price, longer sequences of activation are common.

The potential, possible gains and maintenance costs of applying DR to the pumping station is in this case dependent of the bid-price. A low bid price would decrease the length of sequences the pumping station would be turned on, which would increase the maintenance costs due to wear and tear. The low bid price could have as benefit that no energy costs will be made. Increasing the bid-price would mean RWS would still pay for energy, but less. This would have as a consequence that the activation sequencing of RWS would increase in length, and the costs of maintenance would decrease relatively to the before-mentioned option.

The aFRR does constrain its participants to a minimum bid of 1 MW. To investigate whether this is realistic for the pumping station, the feasible workspace was calculated and plotted. This can be seen in Figure 3.5. The Figure shows that a large part of the total workspace of the pumping station could be used for participating in the aFRR market. This is excluding a strategical decrease in efficiency to reach higher power with less pumping.

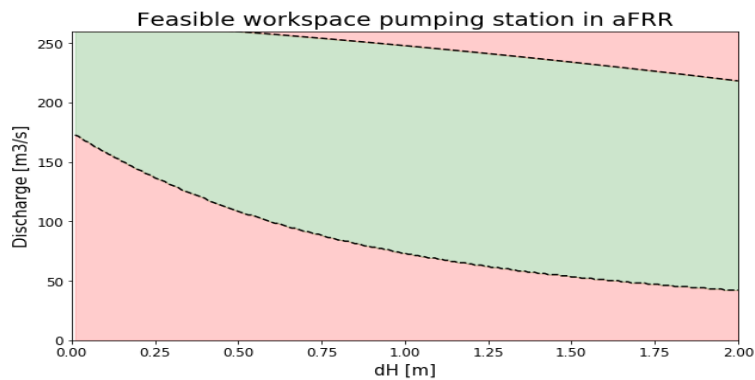


Figure 3.5: Feasible workspace pumping station IJmuiden for participating on the aFRR market

3.6. Correlation price and carbon intensity

The reason why optimization on energy costs, to give demand response a business case, leads to a decrease in CO₂ emission can be shown by the correlation between sustainable energy production and energy price. Two day ahead markets are evaluated; the Dutch and the German market. This is done since the Netherlands has a low share of sustainable energy production. In Germany, the energy mix contains a larger share of sustainable energy, which makes the correlation between low energy price and low carbon intensity more visible. First, a carbon intensity timeseries of the grid was calculated as described in section 6.1. The carbon intensity plotted together with the day ahead price (Figures 3.6, 3.7) already show that the time of the German price extremes coincide more with the carbon intensity extremes than in the Dutch case. However, Figure 3.8, where the carbon intensity of the two grids are plotted over the corresponding day ahead price, shows the correlation more clearly.

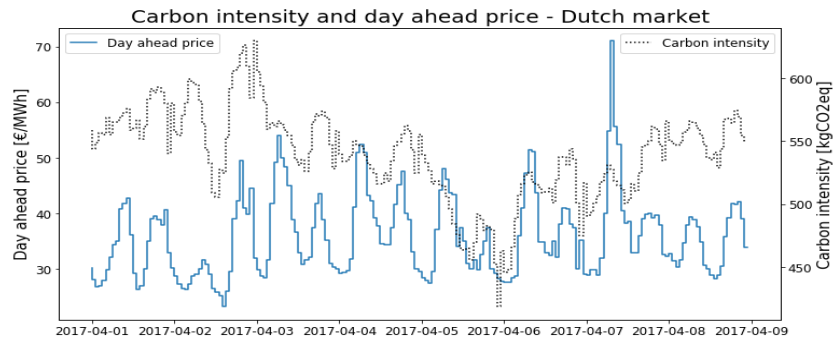


Figure 3.6: Carbon intensity and day ahead price - Dutch market

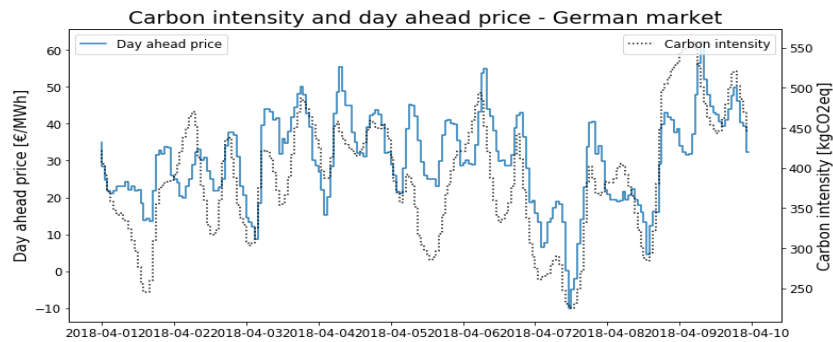
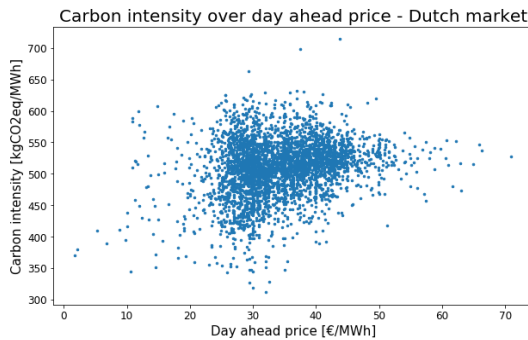
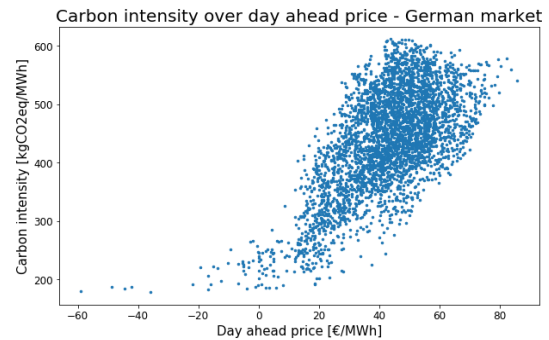


Figure 3.7: Carbon intensity and day ahead price - German market



(a) Dutch market 01-04-2017 - 31-08-2017



(b) German market 01-04-2018 - 31-08-2018

Figure 3.8: Carbon intensity over day ahead price

3.7. Future developments

Since the energy transition still brings a lot of uncertainties, the way the markets will act is still not sure either. However, the way the markets are moving on the short term is known. The European Commission is working towards a European grid. This means that the (flexibility) markets will adopt the same timeslots of 15 minutes. Besides that, more international high-voltage cables will be installed [19] to increase cross-border capacity. This will increase grid stability, since the market and grid will be bigger. This could mean that for example, peak solar energy supply in Spain due to a really sunny and clear day, could be balanced or bought by the Netherlands where a lack of wind is causing a shortage in supply.

Due to the increasing cross border capacity, and the aligning of European markets, national electricity prices will be driven towards each other. There will be less spread in energy prices around the European mean.

Another expected development is the increase in storage capacity. Some parties are exploring the use of salt-mines to store energy [2]. This will mean that a negative energy price will be less likely to happen, since cheap energy can be stored to be sold when the price is high. Having enough storage capacity is the key to a successful energy transition, but large technological advancements will have to be made to make it economically feasible. Until that time, demand response will have to play a large roll in stabilizing the grid. The more flexible the energy demand, the less energy storage is needed.

The German market already shows that fixed energy prices will become relatively expensive compared to the spot market prices. This is because inflexibility is punished through a higher price. When energy production becomes intermittent, it will cost more money to demand energy whenever it is needed. This is due to the higher marginal costs of non-renewable energy, or because of a relatively expensive energy storage unit.

4

Methodology

4.1. Model predictive control

To calculate the optimal configuration for the pumps and gates, a model predictive control (MPC) is created that makes use of a simplified internal model that represents reality accurately enough to estimate the effects of decisions. The controller scores certain combinations of settings based on an objective function, which represents the goal of the system. MPC's are now being applied in airplanes, robotics, chemical engineering, self-driving vehicles and many other applications.

The MPC can take setpoints, ranges and specific goals into account that a feedback or feed-forward control can't. It can take system dynamics into account, while also having a feedback loop to account for disturbances to the system. A big advantage of an MPC is that constraints can explicitly be taken into account [16]. A schematization of an MPC can be seen in Figure 4.1.

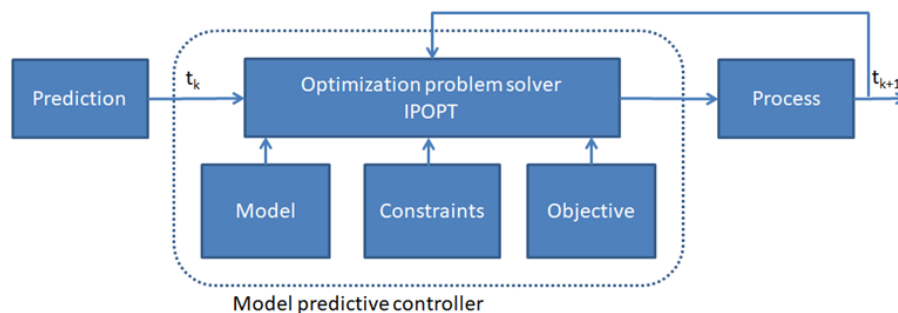


Figure 4.1: Model Predictive Control schematization

The key principle behind an MPC implementation is the receding horizon technique [10]. This is the principle that the controller predicts for a certain prediction horizon into the future, while only implementing the first step. After this, a step forward is taken, and the MPC is run again. The concept of the receding horizon is represented in Figure 4.2. The receding horizon principle implements only the first timestep of the prediction horizon, after which the horizon is shifted one step and the calculation is performed again. This allows for the use of up-to-date predictions and system states.

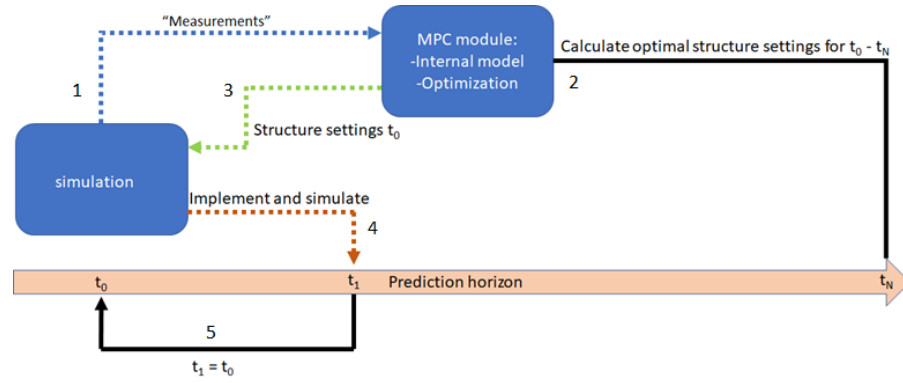


Figure 4.2: Depiction of receding horizon control

4.2. Solver

The optimization problem is solved using the open source software-library IPOPT[1]. IPOPT stands for Interior Point OPTimizer, which gives a hint to the method that is used to solve the problem. The solver uses the primal-dual interior point method to solve non-linear problems (NLP's). Python is used as an interface for IPOPT, through the Pyomo[30, 31] package. Since water systems have non-linear relationships, and the problem is a large scale problem (many decision variables), IPOPT is chosen as a suitable solver. The fact that IPOPT is open-source makes this research easier to reproduce, which is beneficial for its scientific value.

4.2.1. Theory

The goal of IPOPT is to iteratively approach the optimal solution from the interior of a feasible set.

It forces all iterates to stay within a feasible set by defining a barrier function. The objective function ($f(x)$) is then replaced with the barrier function in the optimization, for example with logarithmic barrier function (4.1)[25].

$$\mathfrak{B}(x, \mu) = f(x) - \mu \left(\sum_{i=1}^{m_1} \log(g_i(x)) + \sum_{l=1}^n \log(x_l) \right) \quad (4.1)$$

Where g_i is an inequality constraint, and μ is the barrier parameter which will be reduced to zero. This function is then transformed into Lagrange function (4.2).

$$\mathfrak{L}_\mu(x, \lambda) = f(x) - \mu \left(\sum_{i=1}^{m_1} \log(g_i(x)) + \sum_{l=1}^n \log(x_l) \right) - \sum_{j=1}^{m_2} \lambda_j * h_j \quad (4.2)$$

Then for a given μ , a vector x_μ is a minimum point of the problem if there is a Lagrange parameter λ_μ such that the pair (x_μ, λ_μ) satisfy the following conditions (4.3) and (4.4).

$$\nabla_\lambda * \mathfrak{L}_\mu(x, \lambda) = 0 \quad (4.3)$$

$$\nabla_x * \mathfrak{L}_\mu(x, \lambda) = 0 \quad (4.4)$$

This then gives the following system to be solved:

$$-h(x) = 0 \quad (4.5)$$

$$\nabla f(x) - \mu \left(\sum_{i=1}^{m_1} \frac{1}{g_i(x)} \nabla g_i(x) + \sum_{l=1}^n \frac{1}{x_l} e_l \right) + \sum_{j=1}^{m_2} \lambda_j \nabla h_j(x) = 0 \quad (4.6)$$

Where $\nabla f(x)$ is the gradient of $f(x)$, $\nabla g_i(x)$ the gradient of $g_i(x)$ and ∇h_j the gradient of h_j . Which is then commonly solved iteratively using the Newton method. The algorithm stops when a certain point of optimality is reached, which is measured by the size of μ , also called the duality gap. When the gap is sufficiently small, optimality is reached, and the problem is solved.

4.3. Simulation

4.3.1. Model

The internal model is described in chapter 5 is used to simulate the system. The solver output will be checked for feasibility. Infeasible output is changed to feasible output. For example: maximum discharge of a gate is calculated and if the output is higher, it will be changed to the maximum. These deviations act as a disturbance on the controller.

4.3.2. Energy use

To calculate the energy use of the pumping station, the fitted curve described in section 7.1.3 and Appendix C.2 was used.

4.3.3. Energy cost

In order to calculate the energy cost, the actual day ahead price was used to calculate the costs made at the times the bid was made. The difference between the energy that was bid and the actual consumed energy was calculated, and the intraday market price was used to calculate the intraday costs.

4.3.4. CO₂ emission

The CO₂ emission was calculated by multiplying the calculated energy use of a timestep with the corresponding carbon intensity of the grid, which is discussed in section 6.1.1.

4.3.5. Regulating volume

The amount of regulating volume that was generated by the MPC through intraday trading was calculated by taking the difference from the day ahead bids and the actual energy use. A decrease in energy use counts as upward regulating volume at the time of sell. An increase in energy use is downward regulating volume at the time of use. Upward regulation is assumed to be necessary when it is rewarding to sell energy. Downward regulating volume is assumed necessary when buying energy is rewarded through a low price. However, this is disturbed by unforeseen circumstances, like measurement errors. But since the overall measurement error is small, it is assumed that the energy that is bought or sold through the intraday market is fully because of price differences.

4.3.6. Model runs

The following scenario's were run in order to get the results.

Sensitivity analysis

All the simulations done for the sensitivity analysis were performed on the period of 01-04-2017 00:00 until 30-04-2017 23:45. The performed analysis can be seen in Table 4.1.

Sensitivity for	Price	Prediction horizon	Measurement error
Prediction horizon length	Actual	1.5, 2, 2.5 days	5%
Price uncertainty	SARIMA model	1.5, 2, 2.5 days	5%
Measurement errors	SARIMA model	1.5 day	5%, 10%, 15%

Table 4.1: Model runs performed for sensitivity analysis

Reference scenario

The reference scenario was created by using the same MPC and simulation model, but only minimizing energy use. This way the strategy that Rijkswaterstaat uses in practice can be evaluated in perspective to minimizing energy costs. These were done for a prediction horizon length of 1, 1.5, 2 and 2.5 days. Cost are calculated based on the ENDEX-price at that time, which was €31.50[40] for the Netherlands.

Future scenarios

Two future scenarios were created, one where the Dutch energy mix would be more sustainable. The German market data of 01-04-2018 - 30-04-2018 was used to optimize on and to calculate costs and CO₂, with a fixed energy price of and €35.35[22]. Besides that, a scenario where the North Sea would be 0.5m higher than it is now was simulated to estimate the effects of sea level rise. A reference was also simulated with higher sea levels. These simulations were done for the period of 01-04-2017 00:00 until 30-04-2017 23:45.

4-month run

A long simulation of 4 months was performed for the period of 01-04-2017 00:00 until 31-07-2017 23:45. This was done with a prediction horizon of 2 days, since a longer prediction horizon would take too long to simulate. This was done with a 5% measurement error, and with a predicted price. The reference with the same prediction horizon lengths was also run for this time period.

aFRR potential

To investigate the potential of participating on the aFRR market, an analysis will be performed on the results of participating on the day ahead market. There will be investigated how much extra pumping could have been done, and this will be linked with times downward activation occurred on the aFRR market. Besides that, the extra pumping that would result in a power consumption of 1 MW or more will be selected and the potential benefits will be calculated.

4.4. SARIMA model

In order to be able to make an educated guess on tomorrow's day ahead price a SARIMA model was used[32]. SARIMA stands for Seasonal Auto-Regressive Integrated Moving Average, and it uses historic data to predict the energy price for the future. In the case of the day ahead price, the price at a certain hour of the day is assumed independent of the other hours of the same day. This way, 24 SARIMA models are created; one for every hour of the day. The SARIMA model works on the assumption that the given timeseries is stationary; the mean, variance and autocorrelation of the data do not vary over time. The python Statsmodels[50] package was used to create and train the model.

4.4.1. Theory

Auto-regressive

The auto-regressive part of the SARIMA model assumes that the predicted value of a time-series is a linear function of its previous values. This can be written the following way:

$$X_t = c + \sum_{i=1}^p \phi_i * X_{t-i} + \varepsilon_t \quad (4.7)$$

Where X_t is the predicted value, c a constant, ϕ_i the model parameter for previous value with lag i and ε the error term. The value of p , which is the relevant lag, can be found using autocorrelation and partial autocorrelation functions. In those graphs can be seen after how much time (called lag) the values do not correlate anymore.

Integrated

This part of the model indicates the degree of non-stationarity of the timeseries. The model takes a first-difference of the data in order to take out the non-stationarity (like a gradual increase in mean price due to inflation). The first order difference is taken, in the case of a first order non-stationarity:

$$y'_t = y_t - y_{t-1} \quad (4.8)$$

A second order differencing is sometimes needed to create a stationary timeseries:

$$y_t^* = y'_t - y'_{t-1} \quad (4.9)$$

Where y is the observation, t the time, y' the first-order difference and y^* the second order difference. In the case of the day ahead market, a first order differencing was enough to create a stationary timeseries.

Moving average

The moving average model also assumes that the future value in a timeseries depends linearly on the current and past values in that timeseries:

$$X_t = \mu + \varepsilon_t + \sum_{i=1}^p \theta_i * \varepsilon_{t-i} \quad (4.10)$$

Where μ is the mean of the series, θ the model parameter and ε the error term. So the moving average term is a linear regression between the deviation from the mean of previous values. The relevant lag p can be determined through the (partial-) autocorrelation of the series.

Seasonality

Seasonality is when a certain pattern repeats over a given time, a season. In the case of the day ahead market, weekly and yearly seasonality are expected. Energy demand and production are influence by weather conditions, and they influence the price-mechanisms. But since there is not enough data to truly establish a record of yearly seasonality (3 years), this has been disregarded. .

The weekly pattern is included in the model; the energy price of a day of the week is correlated with the price of the same day last week.

This is taken into account by differencing the dataset:

$$y'_t = y_t - y_{t-m} \quad (4.11)$$

Where y is the observation, t the timestep and m is the seasonal length.

4.4.2. Market analysis**Stationarity**

Figure 4.3 shows the day ahead price of 3AM in the morning, before differencing (Figure 4.3a) and after differencing (Figure 4.3b). It can be seen that the rolling mean and standard deviation vary quite a bit over time, indicating the timeseries is not stationary. The differenced timeseries shows a more stable pattern, and is called stationary. This is proved by applying the augmented Dickey-Fuller test[14].

This test evaluates two hypothesis, which are contradicting, and gives the odd that the null-hypothesis is true based on the given data. The null-hypothesis is that there is a unit-root present in the timeseries, while the alternative hypothesis is that the timeseries is stationary or trend-stationary. The original p-value (probability that the null hypothesis is true) is 0.029 originally, after differencing it is $5.38 * 10^{-17}$. This gives us some certainty that there is no unit root present in the data, and the timeseries can be called stationary.

(Partial-) Auto-correlation

The autocorrelation (ACF) of the data gives the correlation of the data with itself at different lags. The partial autocorrelation (PACF) subtracts the autocorrelation of intermittent data-points to see the independent correlation of two points with each other. Since the data is splitted in hours of the day, every datapoint represents one day. A dashed line is added in the plots after the first and second week.

It can be seen that there is a relatively high correlation of the datapoints throughout the dataset. However, the PACF makes the seasonality more clear. Weekly patterns are visible.

Seasonality

The market seasonality can be seen as yearly. But since too little data is present to extract a yearly pattern, this has been disregarded. However, a weekly pattern is noticeable in the data, and is modelled in the form of seasonality. The weekly pattern can be seen in picture 4.4, where the dotted black line indicate the 7th and 14th lag day. The correlation factors peak at those days, indicating a strong correlation between prices of the same weekday and the same hour.

4.4.3. Extracting model parameters

The SARIMA model requires identification of certain parameters. The lag has to be identified to see until how far back the model has to look to predict new values. In the case of 6 am (figure 4.4), a lag of 3 days has been chosen, since that is the last day where the PACF is reaching out of the significance interval. The degree of differentiation is needed to create a stationary timeseries. In this case, a single differentiation was performed to create a stationary timeseries. Which gives us a degree of differentiation of 1. Seasonal parameters also have to be identified. In this case, it is clear there is a weekly patters, so the seasonal lag has been set to 7 days. Besides that, the stable seasonal pattern is modelled to be constant in time. In the above case, this is true, so this will be given to the model. Whether the ACF is positive or negative at the seasonal lag, is model input as well. In this case it is positive, and this was used when fitting the model.

4.4.4. Model training

The SARIMA models were trained using 9 months of data. The data was first corrected for daylight savings time, then split into the first 9 months and the remaining time, and then split by hour of the day.

Besides that, Not-a-Number-values (NaN) were linearly interpolated between the surrounding values.

The model is trained every day with an increasing window for the training data; the training set gets bigger as time proceeds. This gives the most realistic case of a price prediction, since new information is added to the model every day when the market prices are released.

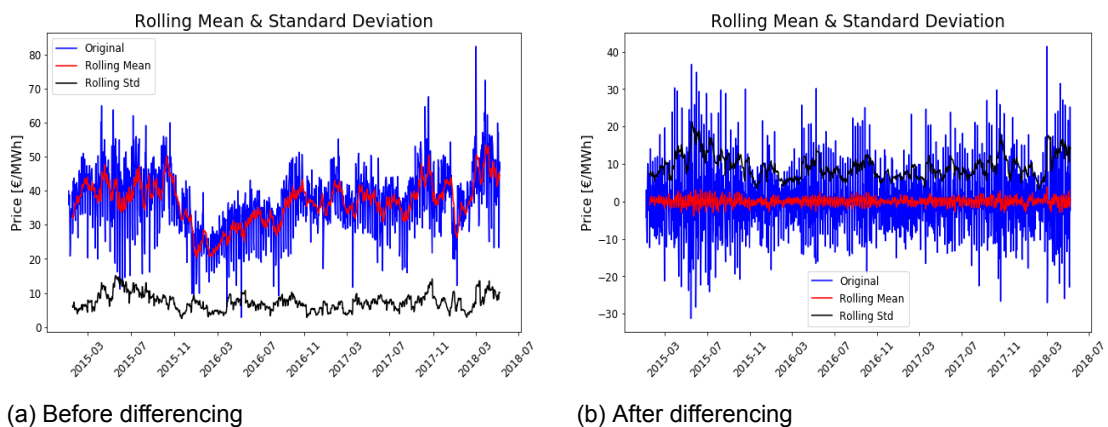


Figure 4.3: Stationarity testing

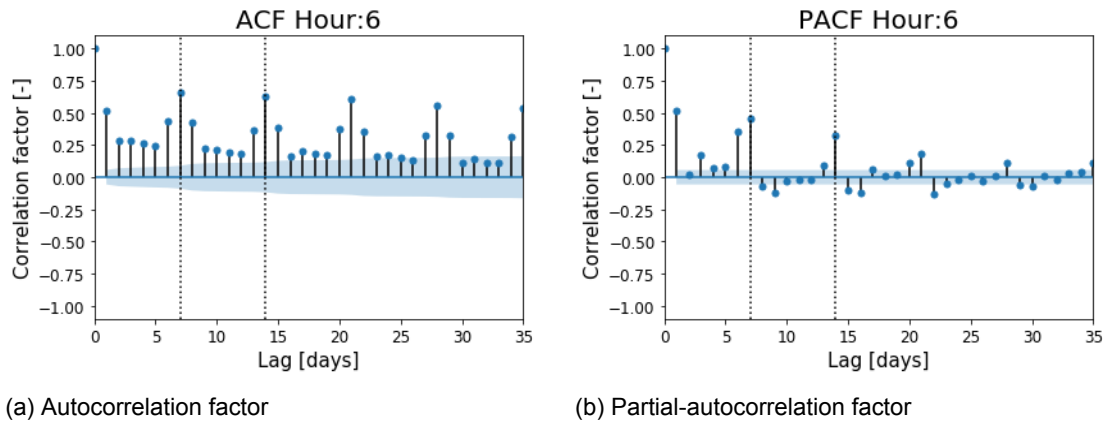


Figure 4.4: Market price timeseries autocorrelation

4.4.5. Model verification

The root mean squared error (RSME), the root of the sum of the squared difference between modelled and observed values, was used to verify model accuracy. Since the prediction horizon of a single optimization can span further than a day, the model is used to give prediction for a week. However, only the first day prediction is used to calculate the RMSE in this analysis, since that is what the bid price is based on.

The RMSE of the prediction over the remaining data-length is €5.21/MWh. Which is deemed acceptable for this study. The model-prediction plots with the actual data can be seen in Figure 4.5.

The actual accuracy of the model is of less importance, since the optimization bases its decisions on relative price differences. The times at which the maximum and minimum occurs are more important for planning energy use.

Another important factor is the uncertainty. Since the uncertainty increases with the prediction time, the optimal prediction horizon length is influenced. If the MPC predicts longer ahead, while the price is uncertain, there might not be an added benefit of predicting further ahead. The increase in uncertainty can be seen in Figure 4.6, where the daily extremes and average size of the confidence interval for April 1st 2017 are plotted over the prediction length. The figure shows an increase in uncertainty, but depending on the hour of the day this differs. This is because the price of the hour of the day are assumed statistically independent, resulting in 24 confidence intervals over a day. Figure 4.5 also shows this, through the varying size of the grey area surrounding the predicted price.

Figures 4.7 and 4.8 show the the performance of the SARIMA model for the German market. It can be seen that the confidence interval is larger in the German case, indicating a higher uncertainty. This can be explained by the higher amount of renewable energy sources on the German market, which are relatively unpredictable.

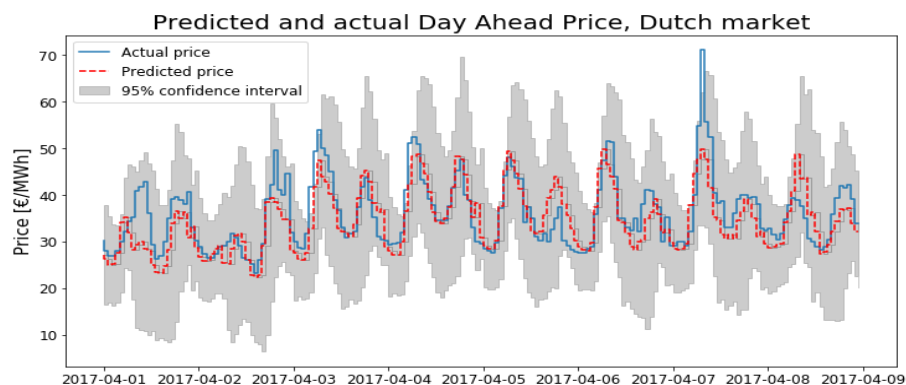


Figure 4.5: Receding horizon 1-Day ahead predicted and actual day ahead price, Dutch market

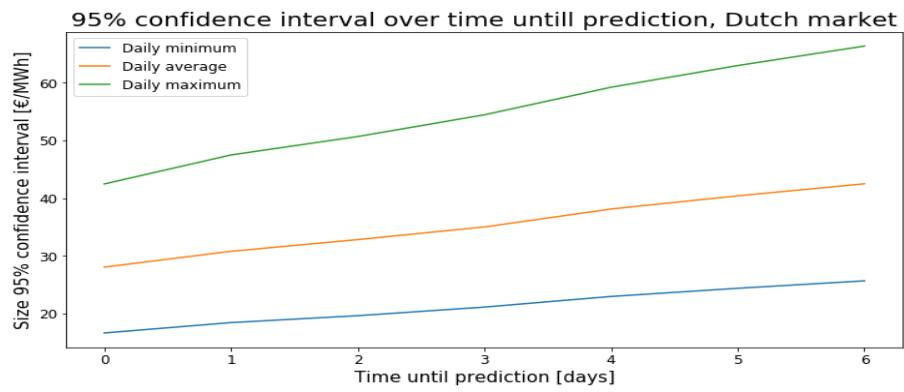


Figure 4.6: Size of daily minimum, maximum and average 95%-confidence interval of April 1st 2017, over prediction length, Dutch market

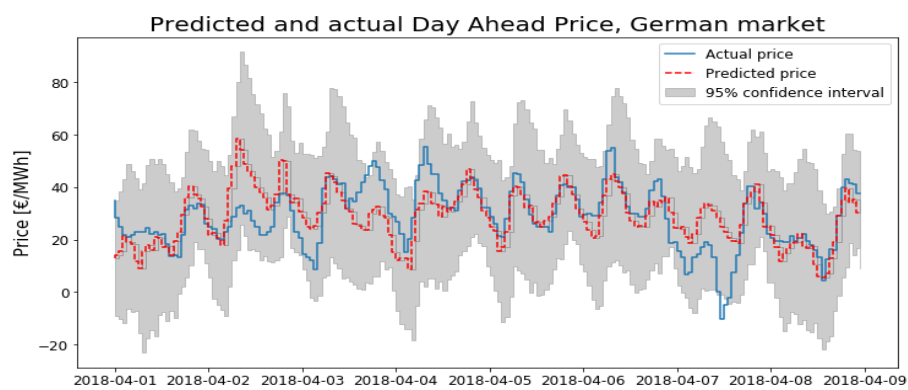


Figure 4.7: Receding horizon 1-Day ahead predicted and actual day ahead price, German market

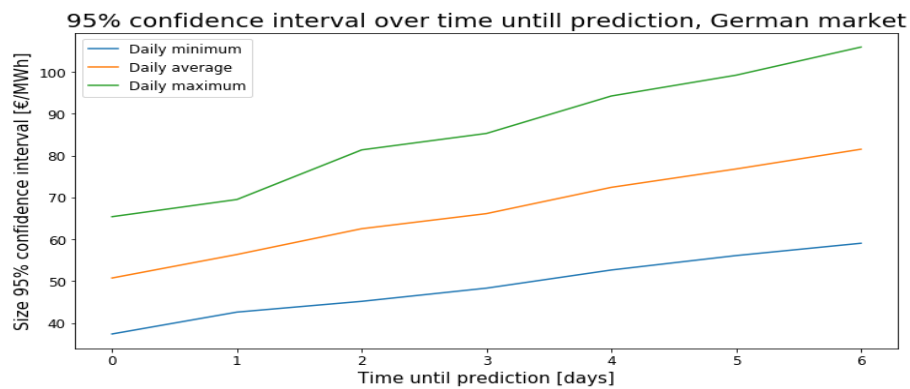


Figure 4.8: Size of daily minimum, maximum and average 95%-confidence interval of April 1st 2017, over prediction length, German market

5

Internal Model

In the internal model, the storage components of the system are represented as buckets. This comes down to three buckets with a fixed surface area that is used to describe the relationship between storage and water level. The concept of a bucket model can be seen in Figure 5.1. The Noordzeekanaal—Amsterdam-Rijnkanaal, Markermeer and IJsselmeer are represented in the model, as can be seen in Figure 5.3. Delay/routing is not taken into account, due to the low flow speeds in taking place in the system, and because of the directly discharging of one bucket in the other.

Two models were built in this thesis, one model using only the Noordzeekanaal with the Oranjesluizen's discharge as boundary condition. This model only controls the gates and pumping station in IJmuiden. The other model includes the Markermeer and IJsselmeer, to study the potential of the Markermeer and IJsselmeer to contribute to the flexibility of the system. This model includes the control of the Oranjesluizen, Houtrib-/Kornwederzandsluis and Stevin-/Lorenz-sluis. However, due to time constraints, only the model with the Noordzeekanaal has been simulated and tested.

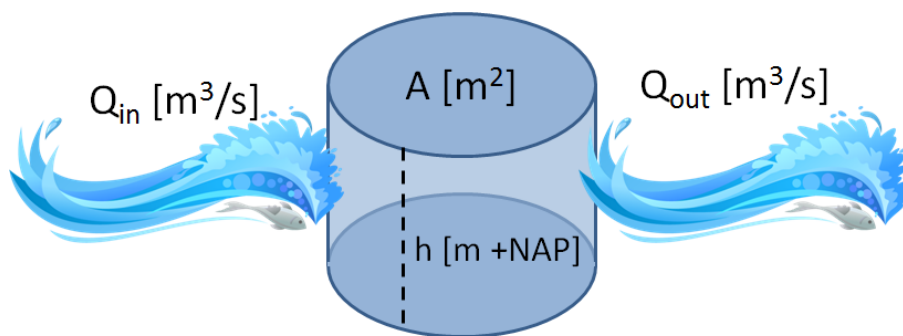


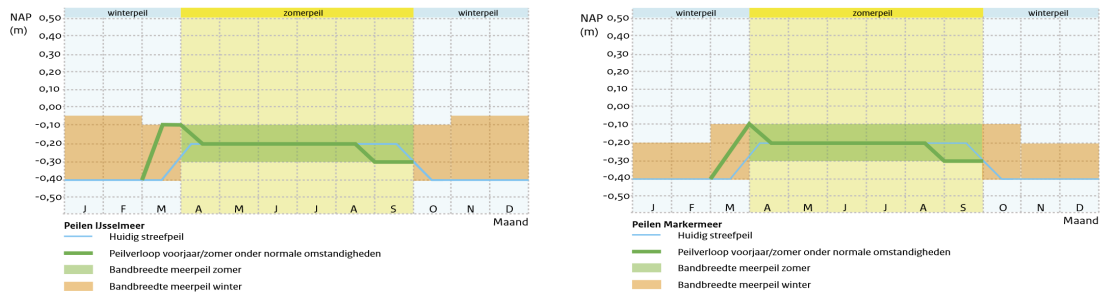
Figure 5.1: Concept bucket model

5.1. Flow model

The IJsselmeer is the largest storage possibility in the system, with a surface area of 1133 km²[46]. The river IJssel is discharging directly into the lake. This discharge is measured in Olst, and used as an inflow in the system. This data is collected from Rijkswaterstaat. Water from the IJsselmeer can either flow into the Markermeer, or into the Waddenzee. However, water from the Markermeer can also flow into the IJsselmeer if required. The allowed water level ranges are found in the peilbesluit [45] and can be seen in Figure 5.2a.

The Markermeer has a surface area of 700 km²[47] and receives water from the IJsselmeer and the Eem. Water from the Markermeer can flow back to the IJsselmeer, or continue to the NZK-ARK. The discharge of the Eem is on average about 10 m³/s [39], and a study by HKV [9] concluded that a peak-discharge of 50 m³/s has a return period of a year. Since this is an exploratory study applied to everyday scenarios, the discharge is not taken into account. A discharge of 10 m³/s would result in a water level difference of 0.12 mm per 15-minutes, which is smaller than the allowed constraint violations (accuracy) of the MPC.

The allowable water level ranges and setpoints of the Markermeer can be seen in figure 5.2b, as was found in public information published by Rijkswaterstaat[45].



(a) Peilbesluit IJsselmeer [source: Rijkswaterstaat]

(b) Peilbesluit Markermeer [source: Rijkswaterstaat]

Figure 5.2: Allowable water level ranges and setpoint level of IJsselmeer and Markermeer per month

The Noordzeekanaal—Amsterdam-Rijnkanaal is modelled as one waterbody with a storage area of 39 km²[7]. It receives water from waterboards, who discharge directly into the system, and from the Markermeer. In order to correctly estimate the discharge in the system, the discharge measurements in Maarsse are used as a base-discharge on which the discharge of local water boards and the Markermeer are added. The Noordzeekanaal is kept in a range of -0.3m NAP to -0.5m NAP, with a daily average water level of -0.4m NAP.

For the model with only the Noordzeekanaal, the Oranjesluizen's discharge is taken as a constant boundary condition, with a discharge of 20 m³/s. This amount is taken from a report published by Rijkswaterstaat, and is the average discharge of the Oranjesluizen in the year 2000 [8].

Direct rainfall is neglected in the model, since this is deemed negligible. The maximum hourly rainfall measured in the period of study is 21mm, which comes down to about 5mm in 15-minutes, the controller timestep. This maximum of 5mm is seen as negligible for the purposes of this study.

Pumping station Zeeburg is not taken into account in this model, due to the fact that this pumping station is only used in extreme situations, to pump water from the NZK to the Markermeer. The flexibility in energy use is expected to be most common during every-day situations, and not in extreme situations.

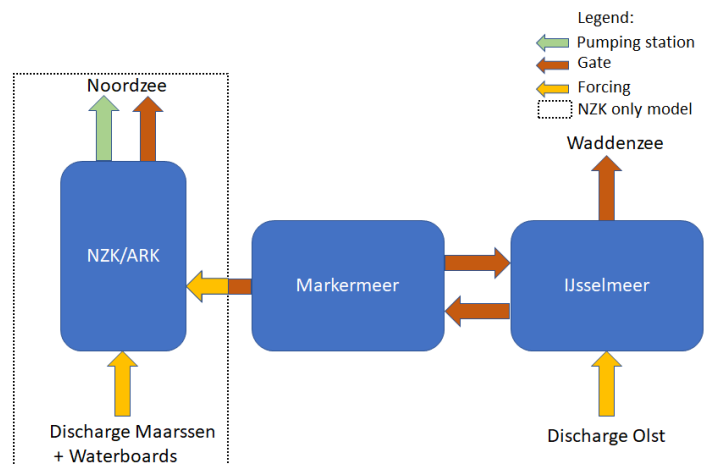


Figure 5.3: Internal model schematic

5.2. Structures

5.2.1. Undershot gates

The system contains 7 main structures: 6 gates and 1 pumping station. Two gates (Stevin- and Lorenz-sluizen) are situated between the IJsselmeer and the Waddenzee, two gates (Houtrib- and Krabbersgat-sluis) are in between the IJsselmeer and the Markermeer, one gate (Oranjesluizen) is in between the Markermeer and the Noordzeekanaal, and one gate (IJmuiden) is located in between the Noordzee and the Noordzeekanaal. The pumping station is also located in IJmuiden.

The Stevin- and Lorenzsluizen have 10 and 15 undershot gates in one complex. They have a width of 12m each, and a bottom level of -4.7m NAP[9]. They are modelled as one big complex with 25 gates.

The Houtrib- and Krabbersgatsluizen combined have 8 gates, with a bottom level of -4.5m NAP and a width of 18m [9]. Their combined maximum discharge is estimated to be around 1333 m³/s. They both allow bi-directional flow, but for modelling purposes they have been modelled as two separate, but identical, gates that allow one-directional flow in the opposite direction.

The Oranjesluizen has one gate which is designed for discharging water and for allowing boat-traffic to pass. It has a bottom level of -4.5m NAP and a width of 9.8m [9].

The sluice complex in IJmuiden has 7 square tubes, which contract in the middle to regulate discharge. They are 5.9m wide and the height of the “throat” of a tube is 4.8m above the bottom. It has a maximum discharge of 500 m³/s.

The gates are bound to have a maximum discharge the structure allows (due to stability of the bed and structure itself). However, the behaviour of the flow through a gate can also be described by equation. Whichever of the two is lower, is the acting constraint. The gate in IJmuiden has been simplified in a report by HKV [34]. There are seven square tubes that can be (partially) closed to regulate the flow. Equation (5.1) describes its behaviour [9].

$$Q_{max}[t] = n * \alpha * B * h_k * \sqrt{2 * g * (h_i[t] - h_o[t])} \quad (5.1)$$

With $Q_{max}[t]$ the maximum discharge at time t , n the amount of tubes, α the contraction coefficient, B the width of a tube, h_k the height of the center of the tube, g the gravitational constant, $h_i[t]$ the water level of the NZK at time t and $h_o[t]$ the water level of the North Sea at time t . This is depicted in Figure 5.4a. Equation (5.2) describes the behaviour of the other gates present in the system.

$$Q[t] = n * \alpha * B * (h_g[t] - h_{cr}) * \sqrt{2 * g * (h_i[t] - h_o[t])} \quad (5.2)$$

Where Q is the discharge in m³/s, n is the amount of gates in one complex, α is a sluice-constant, B is the width of the gates, h_g is the height of the gate in m, h_{cr} is the height of the crest of the gate, g is the gravitational constant (9.81 m/s²), h_i is the water level on the inside of the gate and h_o is the water level on the outside of the gate. As depicted in Figure 5.4b.

The equation used a difference in height as input, that makes sure that as long as the given heights are based on the same reference the equation will hold. When h_{cr} is subtracted from $h_g[t]$, the the height between the gate and the crest is calculated. When $h_o[t]$ is subtracted from $h_i[t]$ the difference of the water surfaces' height upstream and downstream of the structure. The effect of the wind has been implemented by by adding the water level difference caused by the wind to $h_i[t]$ and $h_o[t]$.

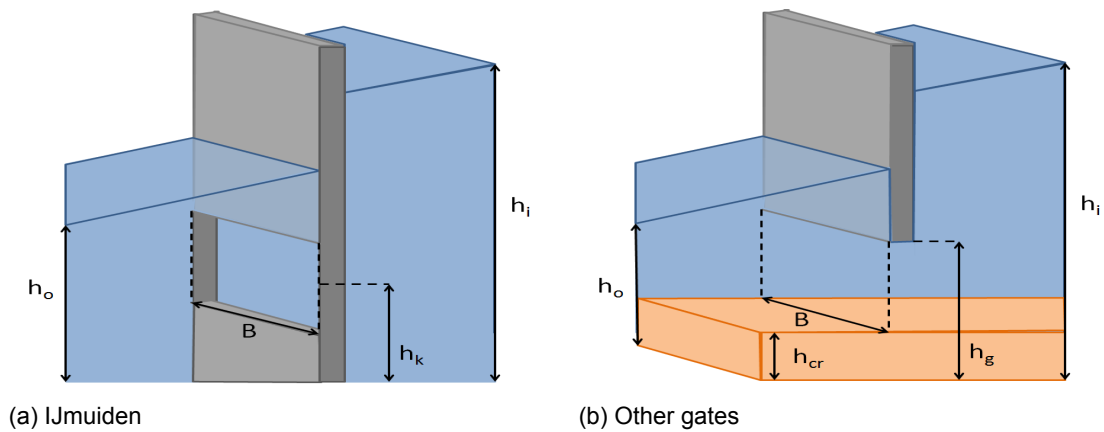


Figure 5.4: Explained equation for gates

5.2.2. Pumping station

The pumping station in IJmuiden consists of 6 pumps. Two fixed-speed pumps, two pumps with two settings, and two variable speed pumps. The combined maximum discharge is 260 m³/s. The pumping station is simplified to a single pump with a maximum discharge of 260 m³/s. Pump-characteristics are combined to estimate the equivalent characteristics.

In 2017, Tauw performed a research to find the Q-dH relationship of the different pumps. Since there are 6 pumps present in the pumping station, with different properties, multiple Q-dH curves are used to describe the station. Pump 1-4 have an Q-dH line that is estimated with a linear function. Pump 5 and 6 are varying speed pumps, which means that it is beneficial to be able to calculate a discharge with every pump-height and RPM. The Q-dH curves of these pumps are described by a second-degree polynomial. The coefficients of the pump Q-dH curves for different pump settings can be found in table 5.1.

Pump	RPM/Discharge	Q-dH relationship [m ³ /s],[m]
1&3	n = 64.3 rpm	$Q = -5.4174 \cdot dH + 44.93$
	n = 64.3 rpm	$Q = -5.4174 \cdot dH + 44.93$
2&4	n = 48.2 rpm	$Q = -6.4977 \cdot dH + 33.149$
	Q = 50 m ³ /s	$Q = -1.9822 \cdot dH^2 + 1.9726 \cdot dH + 44.93$
5&6	Q = 40 m ³ /s	$Q = 1.8544 \cdot dH^2 - 7.774 \cdot dH + 44.93$
	Q = 30 m ³ /s	$Q = -7.1021 \cdot dH + 48.164$

Table 5.1: Q-dH curves

Every pump has a different energy use at different pumping heights and discharges. The relationship between power and pumping height was researched by Weisenburch[59] and can be found in table 5.2. How the pump data is translated into a part of the optimization

Pump	RPM/Discharge	P-h relationship [kW], [m]
1&3	n = 64.3 rpm	$P = 208.02 \cdot dH + 536.85$
	n = 64.3 rpm	$P = 208.02 \cdot dH + 536.85$
2&4	n = 48.2 rpm	$P = 192.36 \cdot dH + 217.26$
	Q = 50 m ³ /s	$P = 443.91 \cdot dH + 476.3$
5&6	Q = 40 m ³ /s	$P = 379.09 \cdot dH + 373.18$
	Q = 30 m ³ /s	$P = 282.97 \cdot dH + 417.32$

Table 5.2: Pump power curves

problem is explained in section 7.1.3.

5.3. Wind effects

The effects of the wind on the water level is not negligible for the purposes of this study. It frequently occurs that the water level near the gates on the lakes is 20-30 cm higher than the average. To account for this effect, wind data of the stations in IJmuiden and the Houtribdijk have been used to estimate the effect of the water level. At the gates in the lakes, the same method as is used in SOBEK [23] has been applied to calculate the difference in water level. On the Noordzeekanaal, equation (5.3) has been used to estimate the effects of wind on the water level:

$$W = \frac{0.5 * \kappa * U_w^2 * F * \cos(\theta)}{g * d} \quad (5.3)$$

With W being the effect of the wind on the water level in [m], κ a dimensionless constant ($3.4 \cdot 10^{-6}$ [21]), U_w the wind speed at 10m above water level, g the gravitational constant in m/s^2 , d the water depth [m], F the undisturbed length of the wind [m] and θ the angle of the wind relative to the land. This is elaborated in figure The full calculations of the wind-effects can be found in Appendix D.

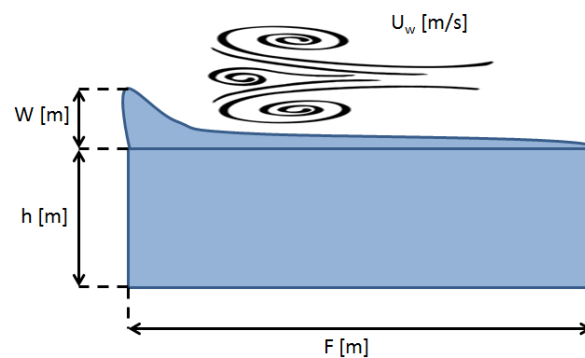


Figure 5.5: Wind effects explained

6

Data

6.1. Energy data

6.1.1. Dutch data

The energy generation data that was used was downloaded from European Network of Transmission System Operators - Europe (ENTSO-E). The data there is provided by national Transmission System Operators (TSO). In the case of the Netherlands, this is TenneT.

The Dutch "electricity production by source" data was incomplete when downloaded. According to the national statistics bureau, the total energy production of 2015, 2016 and 2017 was 110 million kWh, 115 million kWh and 116 million kWh [CBS]. The dataset downloaded from ENTSO-E, provided by the Dutch TSO, show a 65% lower total electricity production. Especially coal power-plant production was showing big gaps, as seen in picture [picture]. In this thesis, the energy sources and yearly production as seen in table 6.1 are taken into account. Further explanation on the data-corrections applied can be found in Appendix A.

Electricity production of the Netherlands [10^6 MWh]			
Energy source	2015	2016	2017
Gas	45.9	52.5	57.2
Coal	39.5	36.7	31.1
Solar	1.1	1.6	2.1
Wind	7.5	8.2	10.6
Biomass	4.9	4.9	4.6
Nuclear	4.1	4.0	3.4

Table 6.1: Electricity production of the Netherlands by source [CBS]

Filling the gaps

In the data sets of gas, solar, biomass and nuclear, the gaps were filled with a linear interpolation between the surrounding known days. However, the data was linearly interpolated between the same hours on those days, so daily patterns stay intact. The result can be seen in figure 6.1.

The dataset for coal was very incomplete. Only some months in the year 2015 were complete, so February and August 2015 were taken as reference months for cold and warm months. This was done so possible seasonal patterns would still be present. The transition of the months was filled through linear interpolation between the same hours on the surrounding known days.

The offshore wind production data was missing the first months of 2015. The production data of January and February 2016 were taken as representative patterns for these months. The absolute values will be corrected in the next section.

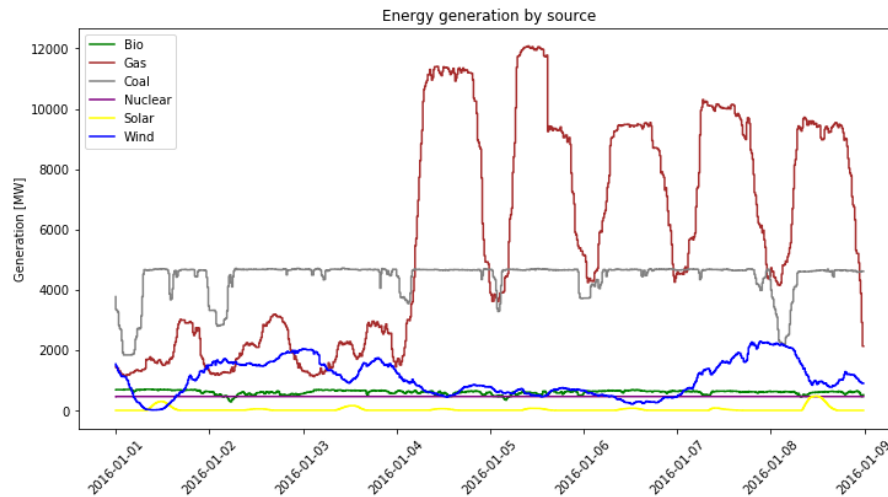


Figure 6.1: Energy production by source

Raising production

In every dataset, the yearly production was increased with a factor in such a way that the yearly production for this type would equal the amount CBS recorded. This method keeps the patterns recorded by TenneT intact, giving plausible energy production data. The assumption made here is that other, unrecorded, power-plants of the same production type have the exact same pattern as the recorded power-plants. Since the CBS makes no differentiation between offshore and onshore wind generation, the total wind energy was set equal to the onshore and offshore production. In other words: onshore and offshore wind energy production are raised with the same factor, so the total wind energy production would be equal to their sum.

Carbon intensity of the energy-mix

To get a dataset of the estimated carbon intensity of the energy-mix in the grid at a certain time, the carbon intensity of various sources was used [36]. By using an average carbon intensity of various generation sources (table 6.2), an estimate of the carbon intensity of the energy mix at a given time can be made. This is done by multiplying the amount of energy generated by a certain source with the corresponding carbon intensity. The resulting calculated carbon intensity of the Dutch grid can be seen in Figure 3.6.

This is an addition to the statistical analysis Rijkswaterstaat now uses found the assumption that a low energy price results in lower carbon emission. A deterministic approach is used in this thesis to estimate the CO₂ emission caused by the production of the energy that is used.

Generation source	Carbon intensity [g CO ₂ eq/kWh]
Biomass	230
Coal	820
Gas	490
Nuclear	12
Solar	45
Wind	11

Table 6.2: Carbon intensity of energy sources [36]

6.1.2. German market data

The German market data was far more complete than the Dutch production data. No extensive data verification was done. The German power mix does have more types of generation than the Dutch power mix.

In Table 6.3, the assumed carbon intensities of the energy sources present on the German grid can be found. The assumption is based on the IPCC report [36], however not all sources could be found. Electricity generated by coal-derived gas is assumed to have the same carbon intensity as coal. Brown coal is assumed to have a 38% higher carbon intensity as black coal[5]. Besides that, geothermal power is assumed to have the same carbon intensity as wind energy. And electricity generated through waste is assumed to have the same carbon intensity as biomass electricity generation.

For other renewables, carbon intensity is calculated through the weighted average of the renewable energy sources (biomass, geothermal, hydropower, solar and wind), with the volumetric presence on the grid as weight.

For other sources, the carbon intensity is calculated through the weighted average of the non-renewable energy sources (brown coal, coal-derived gas, gas, coal, oil, nuclear and waste) by volumetric presence on the grid.

The resulting calculated carbon intensity of the Dutch grid can be seen in Figure 3.7.

Generation source	Carbon intensity [CO ₂ eq/kWh]
Biomass	230
Coal	820
Gas	490
Nuclear	12
Solar	45
Wind	11
Brown coal	1130
Coal-derived gas	820
Oil	560
Pumped storage hydropower	348
Hydropower from runoff	24
Hydropower reservoir	348
Waste	230
Geothermal	11
Other renewables	134.5
Other	591.3

Table 6.3: Carbon intensity of German market data

6.2. Discharge data

The discharge data from waterboard Rijnland has been received with 10-minute interval. The NaN-values have been linearly interpolated, and the dataset has been resampled to 15-minute data, where the intermittent datapoints have been linearly interpolated.

Since no other data has been received from the waterboards, the maximum discharge present in the data was selected, and then the total maximum discharge as found in 2.1 was divided by this to get a magnification factor, which was then applied to the whole dataset of waterboard Rijnland. This comes down to the assumption that the other waterboards discharge at exactly the same pattern as Rijnland does, with similar discharge relative to their maximum discharge capacity.

6.3. Water level data

The models use the water level of the North Sea in IJmuiden and the Waddenzee at Den Oever as boundary condition. This data was obtained through Rijkswaterstaat's open data platform [48]. The data was supplied in 10-minute resolution, which was converted into 15-minute resolution. The intermittent data-points were filled with the maximum of the surrounding values, since an underestimation of discharge possibilities through the gates was preferred over an overestimation.

6.4. Wind data

Wind data was taken from KNMI stations IJmuiden and at the Houtribdijk. This was then processed to water-level difference data using the method described in section 5.3.

6.5. Day Ahead market data

For this study, the day ahead market data of the Netherlands and Germany was used to create a predictive model for the day ahead price. The model for the Netherlands is described in section 4.4, and a similar approach is used for the German market data. The day ahead price data on which the models are trained and verified was obtained through the ENTSO-E transparency platform[20].

6.6. Intraday market data

Intraday market data is not freely available for research, and is a limitation to this study. However, this study is about investigating the flexibility options. Which is why the intraday market data has been artificially created by assuming a strong correlation with the day ahead market price. The intraday market dataset was created with a random deviation between -25% and +25% from the day ahead market price on every 15-min block. An example week can be seen in figure 6.2.

It is expected that the intraday market data will become freely available in the future, in order to make research possible. For now, this is not the case and assumptions will have to do.

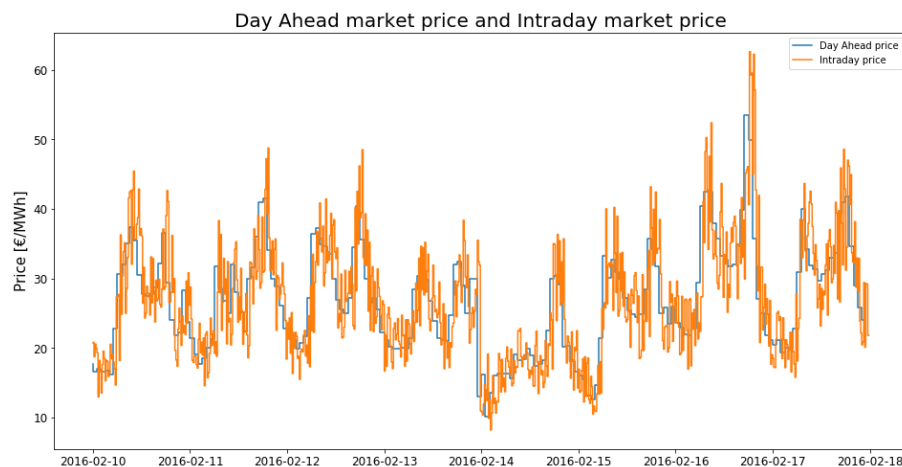


Figure 6.2: Day ahead and intraday market prices 10-02-2016 - 17-02-2016

7

Optimization problem

To be able to calculate optimal structure settings, the model needs to be expressed as an optimization problem. How this was done will be explained in this chapter.

7.1. Constraints

The MPC exists of multiple constraints to enforce realistic behaviour of the model.

7.1.1. Mass balance

In this subsection, the flow model as described in section 5.1 will be formulated as a constraint that can be used for an optimization problem.

Maximum and minimum water level

The water level ranges can be found in section 5.1. The upper bound of these ranges are relaxed with a slack variable, and a penalty for exceedance of the upper bound is introduced in the objective function. This was done to improve robustness of the model, so the problem would not become infeasible in extreme situations. The water level bound constraints can be seen in equations (7.1) and (7.2).

The slack variable was discretized in time in order to minimize the time a flood would occur as well. By discretizing the slack variable, the penalty is given for bound exceedance per timestep. If the slack variable wouldn't be discretized in time, no extra penalty would be introduced for bound exceedance in remaining timesteps once the upper bound would be exceeded in one timestep.

$$h_i[t] \geq h_{i,min} \quad (7.1)$$

$$h_i[t] \leq h_{i,max} + k_i[t] \quad (7.2)$$

Where h_i is the water level at location i (NZK-ARK, Markermeer or IJsselmeer), t the timestep number, $h_{i,min}$ the minimum water level at location i , $h_{i,max}$ the maximum water level at location i , and k the slack variable for upperbound relaxation.

Setpoint water level

Since a setpoint water level is applied in the current MPC, this option was investigated as well. A setpoint water level constraint was applied to the water level of the last timestep of the optimization. A positive deviation from the setpoint would be penalized, to keep a form of flexibility intact. The optimal value for the penalty was quickly decided to be zero, by investigating intermediate results. The constraint can be seen in equation (7.3).

$$h_i[N] - h_{i,setpoint} \leq k \quad (7.3)$$

Storage - Water level relationship

The water level associated the storage is calculated using a mass balance: the difference in water level is equal to the net flux that leaves or enters the body, divided by the surface area of the water body. This can be seen in equations (7.4), (7.5) and (7.6). Because water is assumed incompressible, a mass balance can be expressed in volume.

Equation (7.4) is used in both the model of the Noordzeekanaal/Amsterdam-Rijnkanaal (NZK/ARK) only, and the model including the Markermeer and IJsselmeer. Where in the model with only the NZK/ARK Q_{oranje} is taken as boundary condition, as described in section 5.1, while it is a controlled variable in the model including the Markermeer and IJsselmeer. Equations (7.5) and (7.6) are only used in the model with the Markermeer and IJsselmeer.

$$h_{\text{nz}}[t] = h_{\text{nz}}[t - 1] + \frac{\Delta t}{A_{\text{nz}}} * (Q_{\text{maarsse}}[t - 1] + Q_{\text{oranje}}[t - 1] + Q_{\text{waterb}}[t - 1] + Q_{\text{ijm;sluice}}[t - 1] - Q_{\text{ijm;pump}}[t - 1]) \quad (7.4)$$

Where $h_{\text{nz}}[t]$ is the water level [m +NAP] of the Noordzeekanaal at time t, Δt the timestep size [seconds], A_{nz} the surface area of the Noordzeekanaal [m^2], $Q_{\text{maarsse}}[t]$ the discharge [m^3/s] of the Amsterdam-Rijnkanaal measured in Maarsse at time t, $Q_{\text{oranje}}[t]$ the discharge [m^3/s] of the Oranjesluizen at time t, $Q_{\text{waterb}}[t]$ the discharge [m^3/s] of the waterboards at time t, $Q_{\text{ijm;sluice}}[t]$ the discharge [m^3/s] from the sluices in IJmuiden at time t and $Q_{\text{ijm;pump}}[t]$ the discharge [m^3/s] of the pumping station in IJmuiden at time t.

$$h_{\text{mar}}[t] = h_{\text{mar}}[t - 1] + \frac{\Delta t}{A_{\text{mar}}} * (Q_{\text{houtrib}}[t - 1] - Q_{\text{oranje}}[t - 1] - Q_{\text{korn}}[t - 1]) \quad (7.5)$$

Where $h_{\text{mar}}[t]$ is the water level [m +NAP] of the Markermeer at time t, Δt the timestep size [seconds], A_{mar} the surface area of the Markermeer [m^2], $Q_{\text{houtrib}}[t]$ the discharge [m^3/s] of the houtribsluis at time t, $Q_{\text{oranje}}[t]$ the discharge [m^3/s] of the Oranjesluizen at time t and $Q_{\text{korn}}[t]$ the discharge [m^3/s] of the kornwederzandsluis at time t.

$$h_{\text{ijs}}[t] = h_{\text{ijs}}[t - 1] + \frac{\Delta t}{A_{\text{ijs}}} * (Q_{\text{olst}}[t - 1] + Q_{\text{korn}}[t - 1] - Q_{\text{hout}}[t - 1] - Q_{\text{den}}[t - 1]) \quad (7.6)$$

Where $h_{\text{ijs}}[t]$ is the water level [m +NAP] of the IJsselmeer at time t, Δt the timestep size [seconds], A_{ijs} the surface area of the IJsselmeer [m^2], $Q_{\text{olst}}[t]$ the discharge [m^3/s] of the IJssel measured in Olst at time t, $Q_{\text{korn}}[t]$ the discharge [m^3/s] of the Kornwederzandsluis at time t, $Q_{\text{hout}}[t]$ the discharge [m^3/s] of the Houtribsluis at time t and $Q_{\text{den}}[t]$ the discharge [m^3/s] of the Stevin- and Lorenzsluizen at time t.

However, to ease the calculation by increasing the size of the feasible region, the mass balance of the Noordzeekanaal is implemented as the quadratic constraints seen in equations (7.7), (7.8) and (7.9).

$$(h_{\text{nz}}[t] - (h_{\text{nz}}[t - 1] - \frac{\Delta t}{A_{\text{nz}}} * (Q_{\text{maarsse}}[t - 1] + Q_{\text{oranje}}[t - 1] + Q_{\text{waterb}}[t - 1] + Q_{\text{ijm;sluice}}[t - 1] - Q_{\text{ijm;pump}}[t - 1])))^2 \leq 10^{-10} \quad (7.7)$$

$$(h_{\text{mar}}[t] - (h_{\text{mar}}[t - 1] + \frac{\Delta t}{A_{\text{mar}}} * (Q_{\text{houtrib}}[t - 1] - Q_{\text{oranje}}[t - 1] - Q_{\text{korn}}[t - 1])))^2 \leq 10^{-10} \quad (7.8)$$

$$(h_{\text{ijs}}[t] - (h_{\text{ijs}}[t - 1] + \frac{\Delta t}{A_{\text{ijs}}} * (Q_{\text{olst}}[t - 1] + Q_{\text{korn}}[t - 1] - Q_{\text{hout}}[t - 1] - Q_{\text{den}}[t - 1])))^2 \leq 10^{-10} \quad (7.9)$$

The allowed "constraint violation" of 10^{-10} is based on the fact that the constraint is in meters, and squared. A constraint violation of 10^{-10} in m^2 results in a $10^{-5}m$ constraint violation. Which is equal to an error of 0.1mm.

7.1.2. Gates

In this subsection, the undershot gates as described in section 5.2.1 will be formulated as a constraint that can be used for an optimization problem.

Maximum discharge

The maximum discharge is used as a constraint in the optimization algorithm, with $h_g = h_i - dH - d_g$. Where h_g = gate height, dH is the difference in water level ($h_i - h_o$) and d_g is the minimum depth required for the gate to ensure stable behaviour of the discharge. If the gate is too high, the water becomes free-flowing, which would change the way the discharge is calculated[58]. This comes down to the constraint seen in equation (7.10)

$$Q[t] \leq Q_{max}[t] = N * \alpha * B * (h_o[t] - d_g - h_{cr}) * \sqrt{2 * g * (h_i[t] - h_o[t])} \quad (7.10)$$

The internal model includes one gate at Den Oever that has the same properties as the Stevin- and Lorenz-gates combined. The Houtrib-gate is modelled as one-directional flow from the IJsselmeer to the Markermeer. The Krabbersgat-gate at Kornwederzand is modelled as one-directional flow from the Markermeer to the IJsselmeer. They have been modelled as separate one-directional flow, because of numerical issues in the equation. When bi-directional flow would be allowed, the root of a negative number would have to be calculated. This gives imaginary numbers, which are not compatible with the solver being used. Besides that, the term before the root is now dependent on the outside water-level. This would have to change in the case of bi-directional flow. These reasons combined explain why two opposite one-directional flow gates have been chosen, but with the same properties. A complementary constraint is added to ensure that the gates can never discharge at the same time, as seen in equation (7.11).

$$Q_{houtrib}[t] * Q_{kornwederzand}[t] = 0 \quad (7.11)$$

Linearization of gate-equations

Since IPOPT struggles with root-functions (due to similar numerical issues as seen with bi-directional flow), a simplification of the gate-equations was needed. The maximum discharge-extremes in feasible regions was plotted over the difference in water-level. The maximum-discharge occurs when the inside water-level is on the maximum feasible, and the minimum-discharge occurs when the inside water-level is on the minimum feasible. The gate-height then becomes a function of the difference in water level:

$$h_o[t] = h_{i,max} - dH[t] \rightarrow Q_{max}[t] = N * \alpha * B * (h_{i,max} - dH[t] - d_g - h_{cr}) * \sqrt{2 * g * dH[t]} \quad (7.12)$$

$$h_o[t] = h_{i,min} - dH[t] \rightarrow Q_{max}[t] = N * \alpha * B * (h_{i,min} - dH[t] - d_g - h_{cr}) * \sqrt{2 * g * dH[t]} \quad (7.13)$$

Where h_o is the water level [m +NAP] downstream of the gate, $h_{i,max}$ the maximum water level [m +NAP] upstream of the gate, $dH[t]$ the difference in water level [m] upstream and downstream of the gate, $Q_{max}[t]$ the maximum discharge [m^3] of the gate at time t , N the amount [-] of gates in the complex, α the gate-coefficient [-], B the width [m] of a gate, d_g the height of the gate [m +NAP], h_{cr} the height of the crest of the gate [m +NAP] and g the gravitational constant [m/s^2].

There is a minimum difference in water-level needed before the gates can open. For Ijmuiden, this is 12cm, Den Oever 10cm, Houtribsluis/Kornwederzand 2cm [Rijkswaterstaat] and Oranjesluizen is also assumed to be 2cm.

At Ijmuiden there is also a maximum discharge of $500 m^3/s$ imposed [Rijkswaterstaat], to ensure stability of the structures. For the remaining gates, the equation is constraining.

It is important that the optimal discharge the controller calculates is never higher than what is physically possible, so an underestimation of the maximum allowed discharge is preferred over an overestimation. This is why the minimum allowed water-level on the inside is used

to create the linearization, rather than the maximum.

An optimization problem that maximizes the surface-area of the feasible region with a 4-piece linearization was solved. The specifics of the problem can be found in the appendix C.1. The results of all piecewise linearizations can be found there as well. The linearization of the sluice in Den Oever can be seen in Figure 7.1. The green area represents the feasible region, the red area the infeasible region. In IJmuiden, the same method was applied. However, due to the already simplified equation, there is no extra dH -factor involved.

Slack variables and complementary constraints

To make sure the gates can only discharge when the water level on the outside of the gate is lower than the water-level on the inside, a slack variable is introduced. This method is based on Celeste et al (2010)[3]. This slack variable is a positive Real number, and is larger than or equal to zero. The slack variable is made to be the difference between the inside and outside water level, if this difference is negative. This is done with the following constraint:

$$h_i[t] - h_o[t] + s[t] \geq 0 \quad (7.14)$$

However, there is a minimum difference in water-level needed before the gates can discharge (to overcome internal friction or density differences in the water). So a minimum water-level difference is introduced: dH_{\min} . The constraint becomes the following:

$$h_i[t] - h_o[t] + s[t] \geq dH_{\min} \quad (7.15)$$

This makes sure that if the difference in water level is smaller than dH_{\min} , the total becomes dH_{\min} . The slack variable is added in the equation describing the gates' behaviour.

A complementary constraint is added to make sure that the gates can only discharge if the deficit is zero, which means the difference in water-level is equal to or larger than dH_{\min} :

$$Q[t] * s[t] = 0 \quad (7.16)$$

The final gate-discharge constraint can be seen in equation 7.17.

$$Q_i[t] \leq a_{i,j} * (h_i[t] - h_o[t] + s[t]) + b_{i,j} \quad (7.17)$$

Where Q_i is the discharge of structure i , and j stands for the lines that were fitted in the piecewise linearization. However, due to the inequality constraint, no integer variable is needed to keep track of which linear estimate is the active constraint. Any point in the feasible region is always lower any of the linear estimates.

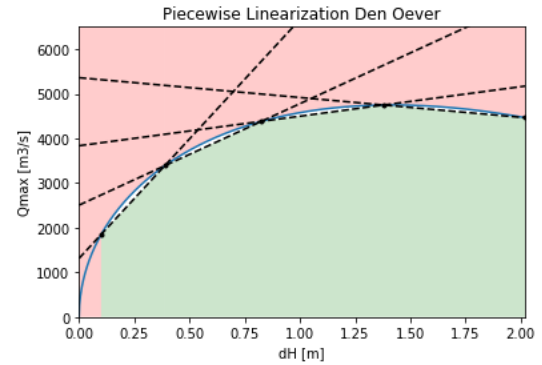


Figure 7.1: Linearization gate discharge equation Den Oever

7.1.3. Pumping station IJmuiden

In this subsection, the pumping station as described in section 5.2.2 will be formulated as a constraint that can be used for an optimization problem.

Q-h curve

Since the pumping station is represented as one big pump, the different Q-dH relationships are in need of simplification. The discharge of the total is equal to the sum of the discharge of all the pumps. In the optimization, it is assumed that all discharges below the Q-dH curve are possible due to smart configuration of the pumps, even though in the actual situation it might be possible that some ranges of discharge are not possible. The following constraint((7.18)) is applied:

$$Q_{pump}[t] \leq \sum_{i=1}^6 Q_i(dH[t]) \quad (7.18)$$

Where the highest RPM or discharge has been taken as the relevant Q-dH curve for pump 2 to 6. Combining the different curves gives (7.19).

$$Q_{pump}[t] \leq -3.976 * dH[t]^2 - 17.7244 * dH[t] + 269.58 \quad (7.19)$$

Power curve

In practice, the power of the pump can vary, depending on multiple operating conditions like pump configuration, pump height and discharge. In order to accurately model the pumping station's energy consumption, binary variables would be needed to act as an on/off switch. However, IPOPT only supports continuous variables.

To avoid using binary variables, a different optimization script was written using GUROBI[28]. GUROBI is a Mixed Integer Non Linear Problem (MINLP) solver, which does support integer variables.

The script, further elaborated in appendix C.2, optimizes energy use for different combinations of discharge and pump height. The results of this optimization can be found in Figure 7.2 and larger in Figure C.6. Pump power is physically described by equation (7.20). Since pump efficiency depends on its operating point, P-dH curves are used for separate pump modes. A fit was made through the optimized energy use at different operating points, using a function of Q and dH.

$$P = \rho * g * Q * dH / p_e \quad (7.20)$$

Where P is the power [W], ρ the density of water [kg/m^3], g the gravitational constant [m/s^2], Q the discharge [m^3/s], dH the pump-height [m] and p_e the efficiency of the pump [-].

The fit can be seen in (7.21)

The function seen in (7.21) was fitted through:

$$P = a * Q^2 + b * dH^2 * Q + c * dH * Q \quad (7.21)$$

Where P is the power [kW], Q the discharge [m^3/s], dH the pump-height [m], and a, b and c the fitted parameters. This function was chosen because: A linear trend can be observed between Q and dH, The curve becomes steeper at high dH and to find if there is a curve in the data at low pump-height.

The fit results are: a = 0.033, b = 0.061 and c = 11.306. The fit can be seen in figure 7.2b. However this is a physical constraint of the system, it is implemented in the objective function as the energy use per timestep as seen in equation (7.22):

$$E[t] = \frac{\Delta t}{3600 * 10^3} * (a * Q[t]^2 + b * Q[t] * dH[t]^2 + c * Q[t] * dH[t]) \quad (7.22)$$

7.1.4. Scaling of constraints and variables

Since the optimization performs best when all calculated values are of the order 1, scaling is applied. If scaling is not applied, a small constraint violation could be seen as large, only because the absolute value is large. This can complicate the optimization. Besides that, the derivatives of the equations should also be of order 1, for the interior point algorithm not to take too big steps when converging.

The next part is about how scaling is applied to enhance the optimization process.

Water level

The water level is expressed in m +NAP. For the model this mostly is between -0.4 and -0.6m NAP or -0.1 and -0.3m NAP. Some extremes are found in the water level at the North Sea and Waddenzee, but no scaling was applied.

Gates

The can gates have a widely varying discharge, which is why a scaling factor equal to the maximum discharge of the specific gate is applied. This way the maximum value of the constraint is 1; when the maximum discharge is reached.

Pump discharge

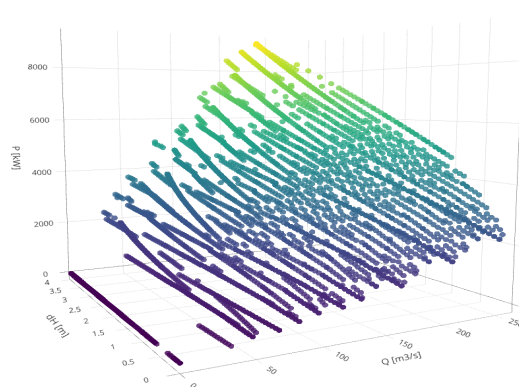
For the pumping station IJmuiden's discharge, a scaling of its maximum discharge (260 m³/s) is applied. This also results in a maximum value of 1 for the constraint.

Deficits

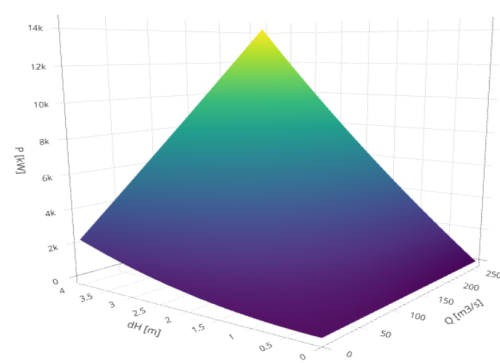
The deficit variables vary relatively little in value. That is why no scaling is applied.

7.1.5. Time

Besides constraints that describe the problem mathematically, the solver is also passed a constraint; a time constraint. It is important that every 15 minutes a solution is given. Since a non-convex optimization sometimes fails, a time constraint of 7.5 minutes is applied. If after 7.5 minutes a solution is not found, the solver restarts with a slightly disturbed starting point. This takes the optimization algorithm to a new point, possibly with higher convergence. Although on average, the solver can find an optimal solution within 10 seconds. An optimization can also be stopped after a time limit, to receive the most optimal solution after a certain time [52].



(a) Results of optimization



(b) Fitted power curve: $P = 0.033*Q^2 + 0.061*Q*dH^2 + 11.306*Q*dH$

Figure 7.2: Power curve fit with gurobi

7.2. Objectives

7.2.1. Day ahead market

The day ahead market optimization has two main phases: a planning and a follow phase. The day ahead planning phase is where the optimization decides on what hours to bid and for how much energy, where the follow phase minimizes the deviation from that bid, until the next bidding occurs.

Planning phase

For the strategy on the day ahead market, an indication of the price per hour of the next day is needed. That is why the SARIMA model was applied to predict tomorrow's market prices with the recently occurred prices.

Because the market works in hourly energy-prices, and the model works in timesteps of 15 minutes, the model is also told to keep the energy use within an hour on a stable level. This requires adjustment of the discharge, since deviating water levels cause deviating pump power.

The predicted hourly prices are loaded into the model, and the estimated energy costs are minimized. It is advised to bid higher than the predicted price, because if the bid isn't accepted, no energy is bought. What exact bidding strategy would prove "safest" or optimal for RWS is not within the scope of this research, and is recommended to study before implementing this strategy.

The formulation of the objective function can be seen in (7.23)

$$\min_P \sum_{t=0}^N P[t] * \frac{\Delta t}{3600} * c_{dayahead}[t] \quad (7.23)$$

Where P is the pumping power in MW, Δt the timestep size in seconds, 3600 is used to convert MWs to MWh, $c_{dayahead}$ is the predicted day ahead price in [€/MWh], t is the timestep indicator and N the prediction horizon length in amount of timesteps.

Follow phase

After the plan is made for the next day, the remaining period of the day will be following the plan. The plan is made at 11:45AM, since the bids have to be made at 12:00AM. This means that from 12:00AM until 11:30AM the MPC will try to follow the plan.

In order to keep the caused imbalances the lowest, the optimization should keep the differences with what is bought and what is consumed as low as possible. Since a deviation from the plan is imbalance. If an imbalance is caused by deviation from the plan, RWS would have to pay a fine.

When going further in time, the amount of timesteps included by the plan decrease. For the remaining time, the MPC minimizes costs.

The objective function can be seen in (7.24)

$$\min_P \left(\underbrace{\sum_{t_f=0}^{t_d} (E_{plan}[t_f] - P[t_f] * \frac{\Delta t}{3600})^2}_{\text{intraday trading}} + \underbrace{\sum_{t_r=t_d}^N P[t_r] * \frac{\Delta t}{3600} * c_{dayahead}[t_r]}_{\text{day ahead bid preparation}} \right) \quad (7.24)$$

Where E_{plan} is the energy-plan made in the planning phase. These are equal to the bids made on the day ahead market. P the power consumption, t_f the timesteps that need to follow the bids made for that day, and t_d the timestep where the day is over and the new planning would take over. From t_d to N are the timesteps where the new planning would have to be made, and t_r represents these timesteps.

Risks

The risk for participating on this market is that the predicted energy-price can be lower than the actual price, and the bid will not be accepted. This makes it necessary to increase the bid price to have a higher chance of acceptance. However, on holidays the price-prediction is normally off, according to experts at AgroEnergy. This is due to the relatively unpredictable consumption, since a holiday makes society use energy differently than at working days.

Another possibility is that more energy is needed than initially foreseen. This would lead to RWS causing imbalance, which they would be fined for. Whether this risk is worth it depends on the savings they make by participating on the day ahead market.

There is potential for filling this "energy gap" with the intraday market, which will be discussed in the next section.

After an early analysis of the results, it was concluded that due to the fast changing sea level, the day ahead market is only considered in combination with the intraday market. This will be discussed in the next section.

7.2.2. Day ahead + intraday market

The intraday market allows for extra flexibility. The market operates in hourly and 15-minute blocks of energy, that can be traded up to 5 minutes before consumption. This makes this market a valuable addition to the day ahead market, since the unpredicted influences could be made up for by trading the energy surpluses or deficits during the day. Since there is no market data available for the intraday market, this is simulated with assumptions as described in section 6.6.

The assumptions are that the intraday market has a random price deviation of 25% with the day ahead market, as explained in section 6.6. And that any bid on the market is accepted. These assumptions make the optimization the same as for the day-ahead market, since all the bidding's are done outside of the optimization. The deviation in energy use from the bidding's on the day-ahead market is sold or bought instead of penalized in the form of imbalance.

Another approach is possible, but more trading is required: keep optimizing costs by constantly updating the optimization with the current intraday price. This way, the profits of a trade could be calculated and the planned energy use could change more frequently. However, the profits this approach would give in this research would fully depend on the assumptions made on the intraday-market price. The profits of a trade on the intraday market, with respect to the energy bought on the day ahead market can be calculated with equation (7.25).

$$\sum_{t=0}^N (P[t] * \frac{\Delta t}{3600} - E_{plan}[t]) * (c_{intraday}[t] - c_{dayahead}[t]) \quad (7.25)$$

Where $P[t]$ is the power consumption at time t [MW], Δt the timestep size [seconds], $E_{plan}[t]$ the energy bought on the day ahead market at time t , $c_{intraday}[t]$ the intraday market price at time t and $c_{dayahead}[t]$ the day ahead price at time t .

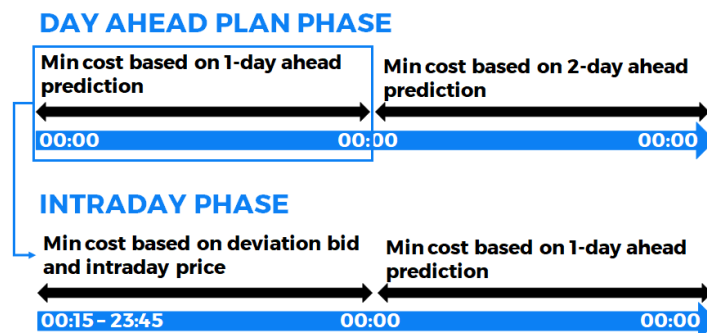


Figure 7.3: Day ahead plan and intraday phase

The MPC will minimize the costs by trading energy on the intraday market for the timeslots energy is bought on the day ahead market as well. For the remaining timesteps the MPC minimized the costs based on the day ahead price. The MPC first runs the day ahead planning phase, where a bid is made on the day ahead market. The day ahead planning phase minimizes the cost based on the predicted day ahead prices. After the bid is done, the MPC switches to the intraday phase until it is time to make another bid on the market. The intraday phase allows a deviation from the bid, at the cost of the intraday market price. Figure 7.3 show how the different phases of the MPC are set up.

The full objective function for the intraday phase can be seen in equation (7.26). The objective function for the day ahead plan phase is the same as discussed in the previous section, and can be seen in equation 7.23.

$$\min_P \left(\underbrace{\sum_{t=0}^{t_d} \left(P[t] * \frac{\Delta t}{3600} - E_{plan}[t] * c_{intraday}[t] \right)}_{\text{intraday trading}} + \underbrace{\sum_{t=t_d}^N P[t] * \frac{\Delta t}{3600} * c_{dayahead}}_{\text{day ahead bid preparation}} \right) \quad (7.26)$$

Where P is the power consumption, Δt the timestep, t_d the time at which the bid done on the day ahead market stops, E_{plan} the energy bought on the day ahead market, $c_{intraday}$ the intraday price and $c_{day ahead}$ the day ahead price.

Risk

The combination of these two markets is expected to bring the lowest risks for RWS. Energy can be bought the day before on the intraday market, and can be traded throughout the day to further optimize the energy use with updated predictions and with influence of the feedback loop that the measurements bring. The intraday market can also make it less detrimental of a bid on the day ahead market gets refused, since it is possible to trade it further on in time.

7.2.3. aFRR

The aFRR market offers the least flexibility, and demands the most from its participants. Besides that, the probability to be activated is also depending on the other players active on the market. It is important for the strategy to make sure the probability of being activated is high enough for the times that pumping is strictly necessary.

When bidding on the market, two optimizations can be performed. The one minimizes energy-use, and for these slots bids are done for a high bid-price, giving more certainty for activation. The price for which a bid is done will rely on a statistical analysis based on historic data. Besides minimizing energy use, a maximization is also performed. The times that the minimization would result in 0 energy use, and the maximization wouldn't, bids are done for a low/negative price. Varying this price can decrease the risk of not being activated. The scheme seen in table 7.1 shows a bid-selections procedure example.

Timestep	Minimized energy-use	Maximized energy-use	Energy bid	Bid price
1	0	10	10	Negative/0
2	0	0	0	No bid
3	5	7	5	Positive
4	2	4	2	Positive
5	0	3	3	Negative/0

Table 7.1: aFRR bidding example

The bids can be updated regularly. Energy use is minimized and maximized, while constraining the optimization to keep the bids for the next 30 minutes into account. Because the bids for the next 30 minutes are used to decide who will be activated. This would make sure these bids can be lived up to, while giving the flexibility to alter the system to satisfy the constraints in the remaining times. This also gives some flexibility in case of unforeseen circumstances (extreme rainfall, discharge, wind).

Another strategy, which would give a higher risk, would be to bid on the maximized energy use. When a time at which the minimization indicated pumping is necessary comes closer, the bid price is increased to increase activation probability. This strategy has a higher profit-potential since it is expected to be activated at generally lower prices, which indicate a higher imbalance.

The objective function can be seen in (7.27)

$$\min_P / \max_P \sum_{t=2}^N P[t] * \frac{\Delta t}{3600 * 10^3} \quad (7.27)$$

Where P is the power consumption in kW, Δt the timestep size in seconds, and then a conversion factor for kWh to MWh. Combined with constraints (7.28) and (7.29):

$$(E[0] - E_{plan}[0])^2 \leq 10^{-6} \quad (7.28)$$

$$(E[1] - E_{plan}[1])^2 \leq 10^{-6} \quad (7.29)$$

Where E is the energy use and E_{plan} the amount of energy that was bidden on the market. $E_{plan}[0]$ depends on the activation signal and the bid, while $E_{plan}[1]$ only depends on the bid. Since the activation signal comes from TenneT, if the signal is a yes, $E_{plan}[0]$ is what was bidden, if no it is 0. While $E_{plan}[1]$ is the possible activation. This is decided outside of the optimization, by using historical data to see if an activation would have been done. If downward activation occurred, and the activation price was lower than the bid-price done in the optimization, it is assumed the pumping station would be activated.

Due to time constraints, the aFRR market is not simulated, but its potential is investigated based on the results of the other markets.

Risk

The aFRR brings the highest risk, but possibly also the highest reward for RWS. It is theoretically possible to not be activated for a whole day, while pumping is necessary. However, in practice this does not occur, especially when the bid-price is high enough. The risk would be decreased if part of the energy used by the pumping station could be bought on the day-ahead/intraday market, and what could be pumped extra would be placed as bid on the aFRR. This will be further discussed in section 10.

7.2.4. Penalty functions

Upper water level bound

The penalty for exceeding the upper bound of the water level has been set on 100/mm violation per timestep. This comes down to a penalty of 100000 per m. Since the water level is measured in meters, so is the slack variable. A high penalty was chosen to ensure that it is never profitable for the MPC to trade a violation of the water level range for less energy use. Since the energy cost will be of order 1, it would be profitable to not consume any energy if the water level range would be exceeded by 10^{-5} m. The penalty function that was implemented in the objective function can be seen in (7.30).

$$\sum_{t=0}^N k_i[t] * 10^5 \quad (7.30)$$

Where N is the prediction horizon, k_i the slack variable of water body i and t the timestep.

Setpoint deviation

The penalty function for exceeding the setpoint-level at the last timestep was designed to give a lower penalty than exceeding the upper bound of the allowed water level range. Multiple degrees of penalties will be evaluated, and the function can be seen in (7.31).

$$k_i * p \quad (7.31)$$

Where k_i is the variable size at location i, and p the height of the penalty.

A penalty on setpoint deviation was not deemed necessary, since water level constraints were never exceeded. If Rijkswaterstaat would like to implement this on the lakes, it is advised to research the ideal penalty height first.

Slack variables

To increase stability of the optimization process, enabling the MPC to discharge more through the gates, the slack variables introduced in section 7.1.2 is minimized in the objective function. This makes sure the slacks are only larger than zero when the water level difference is negative.

$$\min_s \sum_{t=0}^N s_i[t] \quad (7.32)$$

Where $s_i[t]$ is the slack variable value of gate i at timestep t and N the prediction horizon length.

The slack variable part of the objective function is scaled by the prediction horizon length to get the average size of the slack variable. This was decided a posteriori, by looking at the resulting values of the objective function. The scaling results in a value of €0.5 in the objective function, in contrast to €0 - €200 for the energy cost part of the objective function.

7.2.5. Full optimization problem

NZK: Day ahead market + Intraday market

The full optimization problem for the model with only the Noordzeekanaal:

Day ahead plan phase:

$$\min_P \left(\underbrace{\sum_{t=0}^N (k_{nzk}[t] * \gamma_{nzk})}_{\text{robust control}} + \underbrace{\sum_{t=0}^N \left(P[t] * \frac{\Delta t}{3600 * 10^{-3}} * c_{dayahead}[t] \right)}_{\text{day ahead bid}} + \underbrace{\sum_{t=0}^N (s_{gate}[t] + s_{pump}[t]) * \gamma_{slack}}_{\text{slack variable minimization}} \right) \quad (7.33)$$

Intraday phase:

$$\begin{aligned} \min_P \left(\underbrace{\sum_{t=0}^N (k_{nzk}[t] * \gamma_{nzk})}_{\text{robust control}} + \underbrace{\left(\sum_{t_f=0}^{t_d} \left(P[t] * \frac{\Delta t}{3600 * 10^{-3}} - E_{plan}[t] \right) * c_{intraday}[t] \right)}_{\text{intraday trading}} \right. \\ \left. + \underbrace{\sum_{t_r=t_d}^N \left(P[t] * \frac{\Delta t}{3600 * 10^{-3}} * c_{dayahead} \right)}_{\text{day ahead bid preparation}} + \underbrace{\sum_{t=0}^N (s_{gate}[t] + s_{pump}[t]) * \gamma_{slack}}_{\text{slack variable minimization}} \right) \quad (7.34) \end{aligned}$$

$$\gamma_{nzk} = 10^5 \quad (7.35)$$

$$\gamma_{slack} = \frac{1}{N} \quad (7.36)$$

$$P[t] = a_{ijm,p} * Q_{ijm,p}[t]^2 + b_{ijm,p} * dH_p[t]^2 * Q_{ijm,p}[t] + c_{ijm,p} * Q_{ijm,p}[t] * dH_p[t] \quad (7.37)$$

Subject to:

$$h_{nzk}[t] \geq h_{nzk,min} \quad (7.38)$$

$$h_{nzk}[t] \leq h_{nzk,max} + k_{nzk}[t] \quad (7.39)$$

$$\begin{aligned} & (h_{nzk}[t] - (h_{nzk}[t-1] \\ & - \frac{\Delta t}{A_{nzk}} * (Q_{maarssen}[t-1] + Q_{oranje}[t-1] + Q_{waterb}[t-1] + Q_{ijm,stuice}[t-1] - Q_{ijm,pump}[t-1]))^2 \leq \delta_{WB} \end{aligned} \quad (7.40)$$

$$\delta_{WB} = 10^{-10} \quad (7.41)$$

$$Q_{ijm,s} \leq a_{ijm,s} * dH_s[t] + b_{ijm,s} \quad (7.42)$$

$$dH_s[t] \geq dH_{s,min} \quad (7.43)$$

$$dH_s[t] = h_{nzk}[t-1] + W_{ijm}[t-1] - h_{NS}[t-1] + s_{ijm,s}[t] \quad (7.44)$$

$$Q_{ijm,s}[t] * s_{ijm,s}[t] = 0 \quad (7.45)$$

$$Q_{ijm,p}[t] \leq a_{ijm,p} * dH_p[t]^2 - b_{ijm,p} * dH_p[t] + c_{ijm,p} \quad (7.46)$$

$$dH_p[t] \geq dH_{p,min} \quad (7.47)$$

$$dH_p[t] = h_{NS}[t-1] - h_{nzk}[t-1] - W_{ijm}[t-1] + s_{ijm,p}[t] \quad (7.48)$$

$$Q_{ijm,p}[t] * s_{ijm,p}[t] = 0 \quad (7.49)$$

NZK + MAR + IJS: Day ahead market + Intraday market

The full optimization problem for the model with the Noordzeekanaal, Markermeer and IJsselmeer:

Day ahead plan phase:

$$\begin{aligned} & \min_P \left(\underbrace{\sum_{t=0}^N (k_{nzk}[t] * \gamma_{nzk} + k_{mar}[t] * \gamma_{mar} + k_{ijs}[t] * \gamma_{ijs})}_{\text{robust control}} \right) \\ & + \underbrace{\sum_{t=0}^N (P[t] * \frac{\Delta t}{3600 * 10^{-3}} * c_{dayahead}[t])}_{\text{day ahead bid}} + \underbrace{\sum_{t=0}^N (s_{gate}[t] + s_{pump}[t] + s_{oranje}[t] + s_{hout}[t] + s_{korn}[t] + s_{den}[t]) * \gamma_{slack}}_{\text{slack variable minimization}} \end{aligned} \quad (7.50)$$

Intraday phase:

$$\begin{aligned} & \min_P \left(\underbrace{\sum_{t=0}^N (k_{nzk}[t] * \gamma_{nzk} + k_{mar}[t] * \gamma_{mar} + k_{ijs}[t] * \gamma_{ijs})}_{\text{robust control}} \right) \\ & + \underbrace{\left(\sum_{t_f=0}^{t_d} \left((P[t] * \frac{\Delta t}{3600 * 10^{-3}} - E_{plan}[t]) * c_{intraday}[t] \right) \right)}_{\text{intraday trading}} + \underbrace{\sum_{t_r=t_d}^N (P[t] * \frac{\Delta t}{3600 * 10^{-3}} * c_{dayahead})}_{\text{day ahead bid preparation}} \\ & + \underbrace{\sum_{t=0}^N (s_{gate}[t] + s_{pump}[t] + s_{oranje}[t] + s_{hout}[t] + s_{korn}[t] + s_{den}[t]) * \gamma_{slack}}_{\text{slack variable minimization}} \end{aligned} \quad (7.51)$$

$$\gamma_{nzk} = 10^5 \quad (7.52)$$

$$\gamma_{mar} = 10^5 * \frac{A_{ijs}}{A_{ijs} + A_{mar}} \quad (7.53)$$

$$\gamma_{ijs} = 10^5 * \frac{A_{mar}}{A_{ijs} + A_{mar}} \quad (7.54)$$

$$\gamma_{cost} = \frac{1}{\max_t(\text{price}[t]) * N} \quad (7.55)$$

$$\gamma_{slack} = \frac{1}{N} \quad (7.56)$$

$$P[t] = a_{ijm,p} * Q_{ijm,p}[t]^2 + b_{ijm,p} * dH_{ijm,p}[t]^2 * Q_{ijm,p}[t] + c_{ijm,p} * Q_{ijm,p}[t] * dH_{ijm,p}[t] \quad (7.57)$$

Subject to:

$$h_{nzk}[t] \geq h_{nzk,min} \quad (7.58)$$

$$h_{nzk}[t] \leq h_{nzk,max} + k_{nzk}[t] \quad (7.59)$$

$$h_{mar}[t] \geq h_{mar,min} \quad (7.60)$$

$$h_{mar}[t] \leq h_{mar,max} + k_{mar}[t] \quad (7.61)$$

$$h_{ijs}[t] \geq h_{ijs,min} \quad (7.62)$$

$$h_{ijs}[t] \leq h_{ijs,max} + k_{ijs}[t] \quad (7.63)$$

$$(h_{nzk}[t] - (h_{nzk}[t-1] + \frac{\Delta t}{A_{nzk}} * (Q_{maarssen}[t-1] + Q_{oranje}[t-1] + Q_{waterb}[t-1] + Q_{ijm;sluice}[t-1] - Q_{ijm;pump}[t-1])))^2 \leq \delta_{WB} \quad (7.64)$$

$$(h_{mar}[t] - (h_{mar}[t-1] + \frac{\Delta t}{A_{mar}} * (Q_{houtrib}[t-1] - Q_{oranje}[t-1] - Q_{korn}[t-1])))^2 \leq \delta_{WB} \quad (7.65)$$

$$(h_{ijs}[t] - (h_{ijs}[t-1] + \frac{\Delta t}{A_{ijs}} * (Q_{olst}[t-1] + Q_{korn}[t-1] - Q_{hout}[t-1] - Q_{den}[t-1])))^2 \leq \delta_{WB} \quad (7.66)$$

$$\delta_{WB} = 10^{-10} \quad (7.67)$$

$$Q_{ijm,s}[t] \leq a_{ijm,s} * dH_{ijm,s}[t] + b_{ijm,s} \quad (7.68)$$

$$dH_{ijm,s}[t] \geq dH_{ijm,s,min} \quad (7.69)$$

$$dH_{ijm,s}[t] = h_{nzk}[t-1] + W_{ijm}[t-1] - h_{NS}[t-1] + s_{ijm,s}[t] \quad (7.70)$$

$$Q_{ijm,s}[t] * s_{ijm,s}[t] = 0 \quad (7.71)$$

$$Q_{ijm,p}[t] \leq a_{ijm,p} * dH_p[t]^2 - b_{ijm,p} * dH_{ijm,p}[t] + c_{ijm,p} \quad (7.72)$$

$$dH_{ijm,p}[t] \geq dH_{ijm,p,min} \quad (7.73)$$

$$dH_{ijm,p}[t] = h_{NS}[t-1] - h_{nzk}[t-1] - W_{ijm}[t-1] + s_{ijm,p}[t] \quad (7.74)$$

$$Q_{ijm,p}[t] * s_{ijm,p}[t] = 0 \quad (7.75)$$

$$Q_{oranje}[t] \leq a_{oranje} * dH_{oranje}[t] + b_{oranje} \quad (7.76)$$

$$dH_{oranje}[t] \geq dH_{or,s,min} \quad (7.77)$$

$$dH_{oranje}[t] = h_{mar}[t-1] + W_{mar,or}[t-1] - h_{nzk}[t-1] - W_{nzk,or}[t-1] + s_{oranje}[t] \quad (7.78)$$

$$Q_{oranje}[t] * s_{oranje}[t] = 0 \quad (7.79)$$

$$Q_{houtrib}[t] \leq a_{houtrib} * dH_{houtrib}[t] + b_{houtrib} \quad (7.80)$$

$$dH_{houtrib}[t] \geq dH_{hout,s,min} \quad (7.81)$$

$$dH_{houtrib}[t] = h_{ijs}[t-1] + W_{ijs,hout}[t-1] - h_{mar}[t-1] - W_{mar,hout}[t-1] + s_{houtrib}[t] \quad (7.82)$$

$$Q_{houtrib}[t] * s_{houtrib}[t] = 0 \quad (7.83)$$

$$Q_{kornwederzand}[t] \leq a_{kornwederzand} * dH_{kornwederzand}[t] + b_{kornwederzand} \quad (7.84)$$

$$dH_{kornwederzand}[t] \geq dH_{korn,s,min} \quad (7.85)$$

$$dH_{kornwederzand}[t] = h_{mar}[t-1] + W_{mar,korn}[t-1] - h_{ijs}[t-1] - W_{ijs,korn}[t-1] + s_{kornwederzand}[t] \quad (7.86)$$

$$Q_{kornwederzand}[t] * s_{kornwederzand}[t] = 0 \quad (7.87)$$

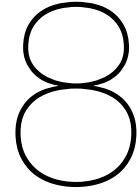
$$Q_{houtrib}[t] * Q_{kornwederzand}[t] = 0 \quad (7.88)$$

$$Q_{denoever}[t] \leq a_{denoever} * dH_{denoever}[t] + b_{denoever} \quad (7.89)$$

$$dH_{denoever}[t] \geq dH_{den,s,min} \quad (7.90)$$

$$dH_{denoever}[t] = h_{ijs}[t-1] + W_{ijs,den}[t-1] - h_{WZ}[t-1] + s_{denoever}[t] \quad (7.91)$$

$$Q_{denoever}[t] * s_{denoever}[t] = 0 \quad (7.92)$$



Results and Discussion

8.1. Verification of MPC

The optimization performed every timestep contains a plan for the coming prediction horizon. The planning phase decides the optimal pump schedule in order to minimize the costs. In the planning phase, only the predicted day ahead energy price is taken into account. The plan is made at midnight, after which the MPC switches to the following phase, where it is allowed to trade energy on the intraday market for the remaining time of the plan. The time after the plan, the predicted day ahead time is used to make a plan.

Figure 8.1 shows the actual and planned fluxes of the NZK. It can be seen that the water level constraint is not violated. It can also be seen that the MPC tends to focus the time of pumping around times where the water level difference between the NZK and the sea is low, which decreases the energy demand for pumping. The gates are only discharging when the sea level is lower than the NZK, and the pumps only discharge when the sea water level is higher than the NZK's water level.

Figure 8.2 shows the actual and planned energy use of the pumping station and the market energy prices. It can be seen that at first, the MPC decides to pump where the day ahead price is relatively high, but the energy use would be small. After the plan was made, the intraday prices were advantageous, causing the MPC to trade its bought energy between 02:00 and 11:00, to increase its energy use between 20:00 and midnight where the intraday prices are generally cheaper than the previous day ahead prices. It can be seen that the peaks in energy use are generally a time the intraday price is low.

It can also be seen in Figure 8.1 that the MPC decides to decrease to discharge through the gates around 12:00. This might be because it would increase the water level difference later on, when pumping is scheduled. This would increase the energy needed to pump the water to the sea, while Figure 8.2 shows that the energy price is positive at that time, and water level constraints won't be violated. This makes it likely that the MPC is saving money by keeping the water level difference low to decrease energy use.

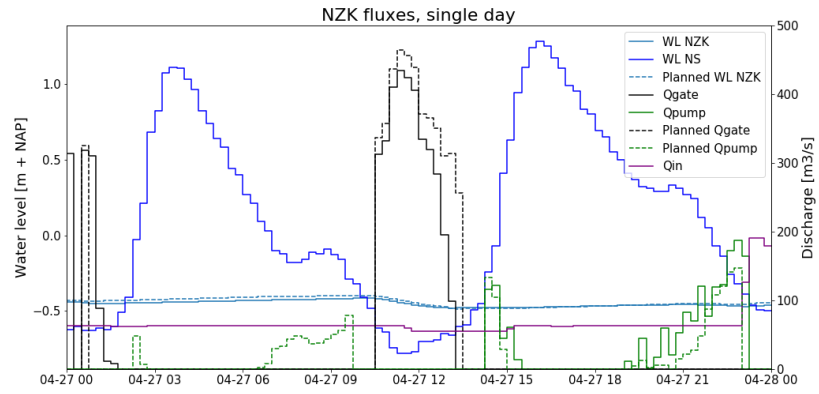


Figure 8.1: Optimized fluxes of the North Sea canal

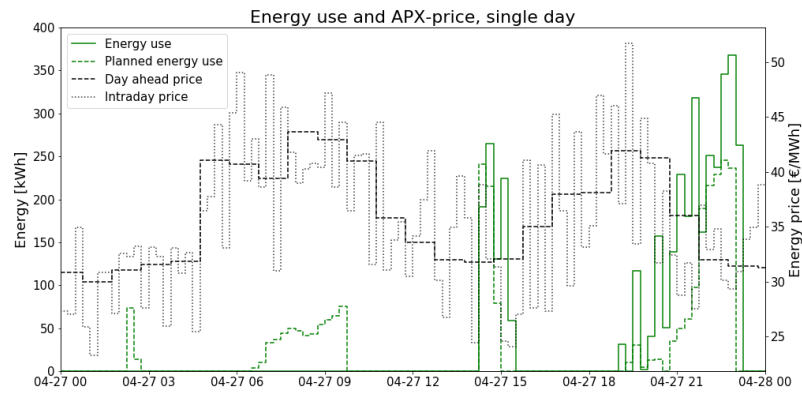


Figure 8.2: Optimized pump energy and energy prices

8.2. Sensitivity analysis

The sensitivity analysis simulation were done as described in Table 4.1. Multiple prediction horizons were tested in combination with a predicted and unpredicted day ahead price. Incoming discharge is certain, but a discharge measurement error of 5% is taken as minimum. For the penalty on setpoint deviation, the intermediate results already showed that no penalty was needed to keep the water level within constraints. For that reason, this sensitivity analysis was skipped and no penalty was implemented.

Then the prediction horizon is varied to check for an optimal setting. This is done for a predicted price (generated by the SARIMA model) and unpredicted price. This is to estimate the effect the prediction has on the performance. When looking further in the future, uncertainty of the predicted price increases, which could lead to a worse plan. However, the MPC would be updated with the a less uncertain price prediction as soon as the day passes. While the MPC is also allowed to correct for sub-optimality by trading on the intraday market. The sensitivity analysis has been performed on the model of the Noordzeekanaal, without the Markermeer and IJsselmeer, with the discharge of the Oranjesluizen as boundary condition.

8.2.1. Prediction horizon

To see what prediction horizon would be optimal for the MPC, a prediction horizon of 1.5 (the minimum to participate in the day ahead market), 2 and 2.5 have been simulated. The resulting water level can be seen in figure 8.3. The figure shows that the water level constraints are not violated. The simulated water levels follow the same pattern.

In figure 8.4, the overall result of the simulations can be seen. It can be seen that a longer prediction horizon gives a trend to lower energy use, costs and CO₂ emission. The MPC can make a longer plan to minimize the energy costs, and has more time to anticipate to events. The reduction in CO₂ emission and energy use due to the increased prediction horizon length are of the same order. However, the reduction in cost is a little bit more, although very small. This can be explained by the low correlation between price and carbon intensity of the Dutch market, causing the CO₂ emission and cost savings to be of different orders. That reduction in CO₂ emission is in the same order as the energy reduction can be explained by the low correlation between energy price and carbon intensity of energy on the Dutch market, as discussed in section 3.6. When sustainable energy becomes a larger part of Dutch the energy mix, more CO₂ emission savings are expected.

Figure 8.5 shows that the day ahead costs are higher than the total costs. This indicates that the MPC makes a profit by selling energy on the intraday market. Interesting is that the day ahead costs are higher with a longer prediction horizon, but the total costs are lower. The main gap between the day ahead costs and the total costs is created around 16-04-2017, when relatively much pumping is needed. This could be due to the MPC making a plan that is on the safe side, after which it sees opportunities to pump less, causing it to sell energy on the intraday market. However, this could also be due to the relative size of the energy cost part of the objective function, compared to the slack variable part. This could make the MPC see less discharge opportunity than there is, or see less benefit in terms of convergence when minimizing the energy cost. This can also be seen in Figure 8.7, where the cumulative gate discharge is plotted. The Longer prediction horizon can make better use of the gate discharge opportunities, causing it to have a larger overall discharged volume. This will be further discussed in section 10.

Besides costs, Figures 8.4b and 8.4c show that the energy use and carbon emission are in a similar pattern, and large deviations also start occurring after 17-04-2017. Figure 8.9 shows the amount of regulating volume that was produced due to shifting the energy demand. A negative value means there was a negative deviation from the day ahead plan, which means energy was sold where it was relatively more expensive than the intraday price. It can be seen that with a longer prediction horizon, the amount of energy traded on the intraday market increases significantly.

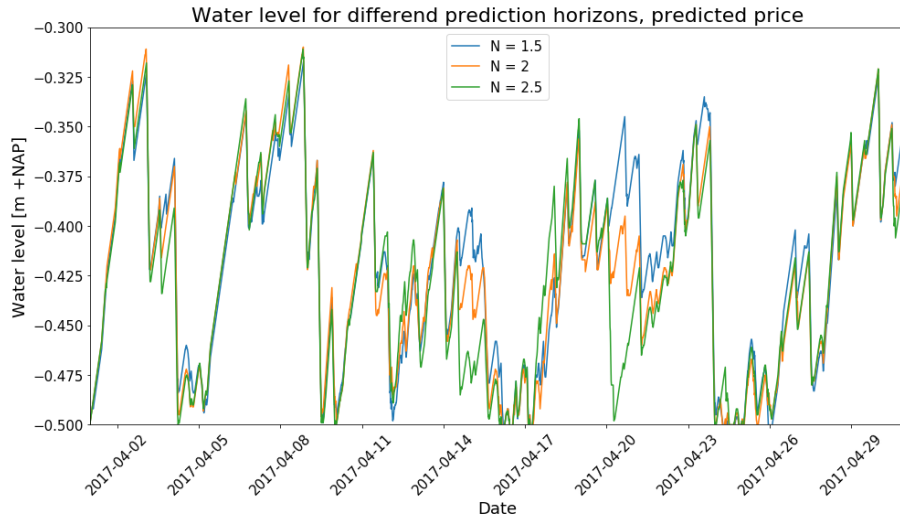


Figure 8.3: Simulated water level of the North Sea canal for different prediction horizons

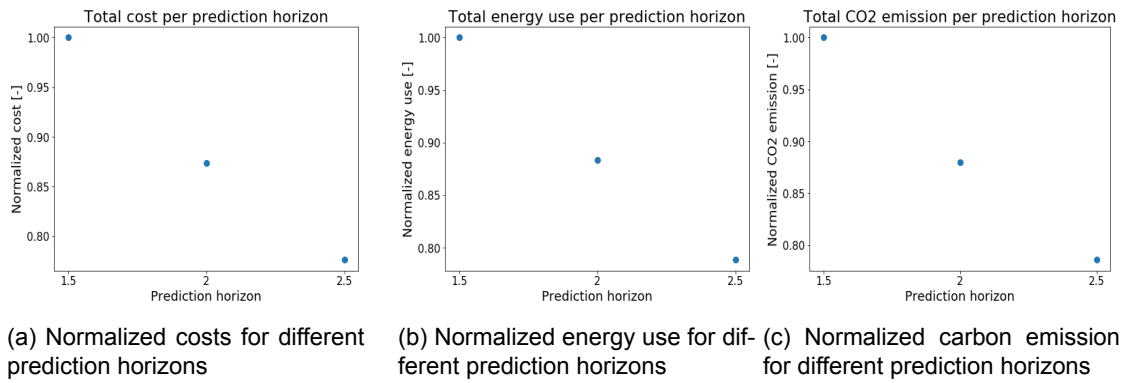


Figure 8.4: Relative performance for different prediction horizons

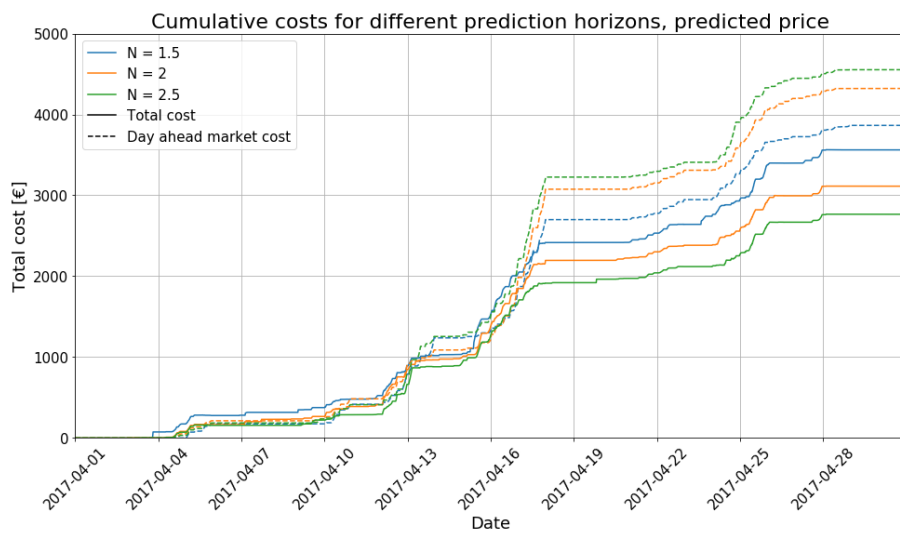


Figure 8.5: Cumulative cost for different prediction horizons

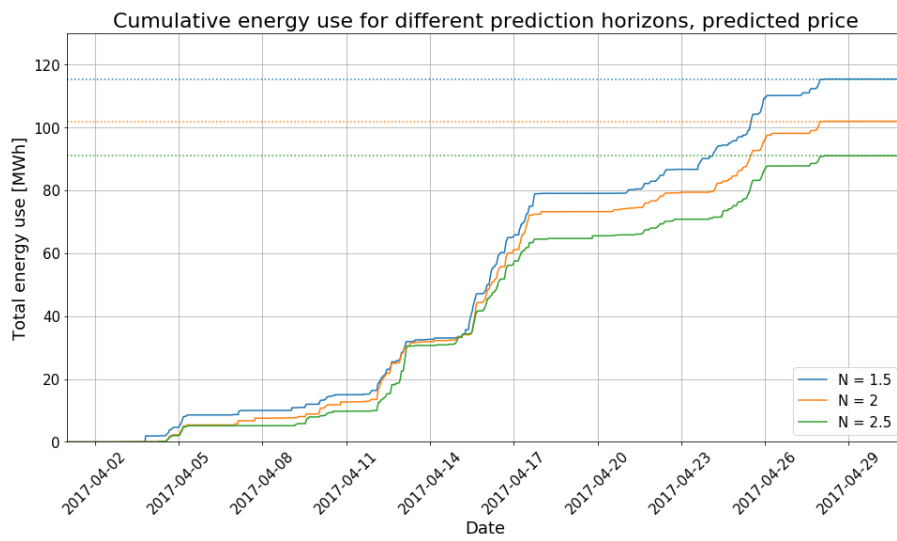


Figure 8.6: Cumulative energy use for different prediction horizons

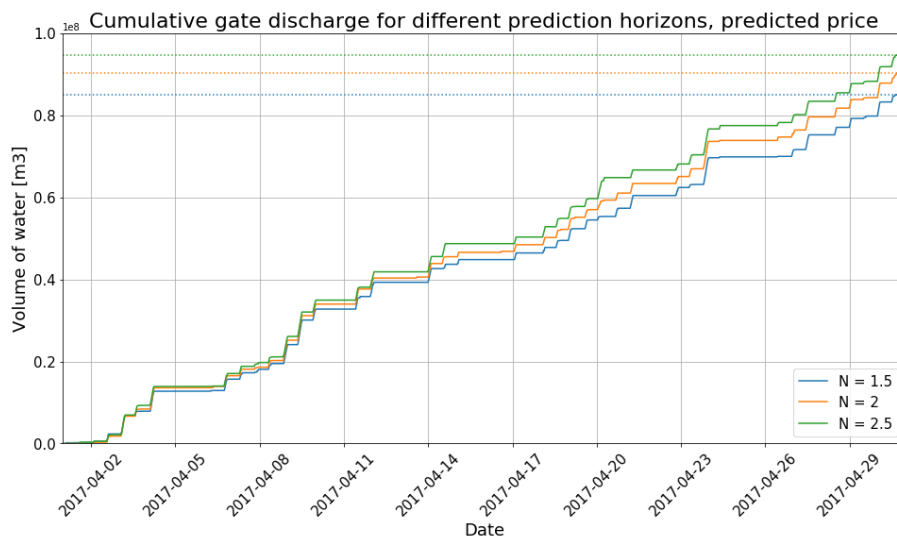


Figure 8.7: Cumulative gate discharge in IJmuiden for different prediction horizons

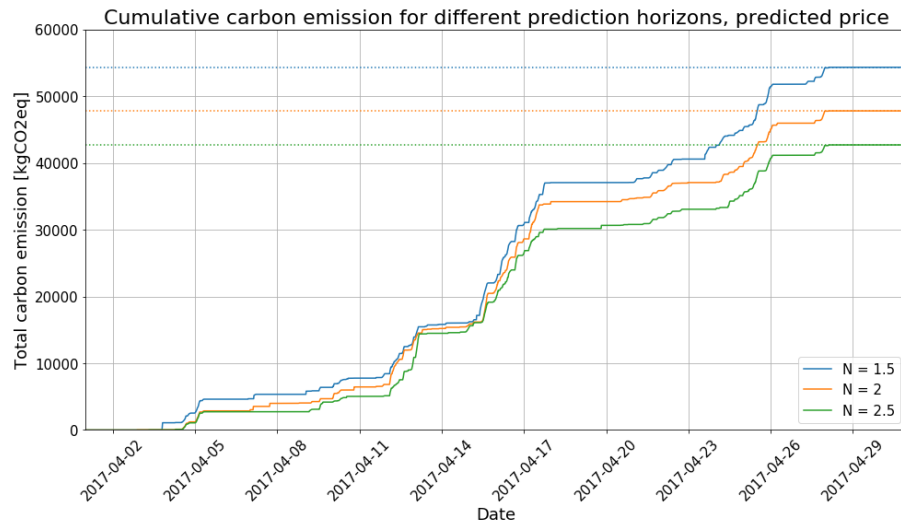


Figure 8.8: Cumulative carbon emission for different prediction horizons

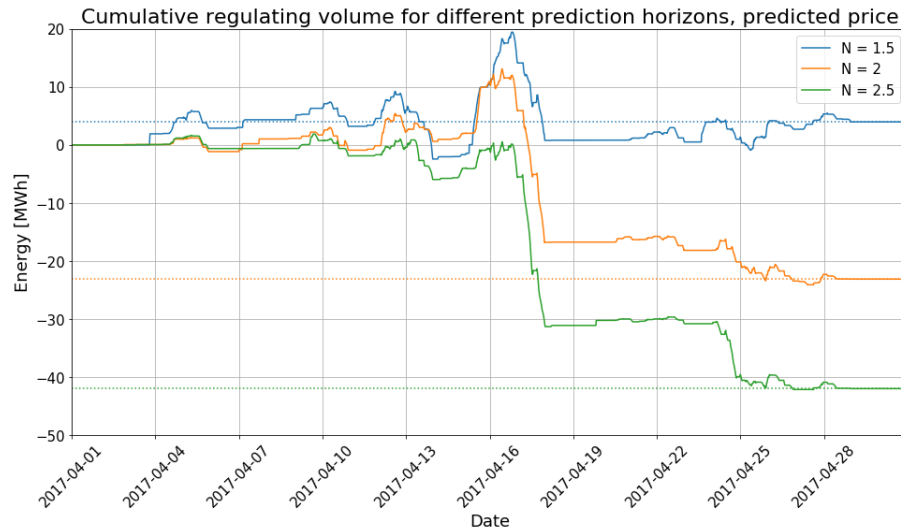


Figure 8.9: Cumulative regulating volume for different prediction horizons

8.2.2. Price prediction

The actual predicted day ahead price will be used in this section to test the influence of price uncertainty for multiple prediction horizons. This is done since price uncertainty might influence the useful prediction horizon length. Looking far into the future might have less benefits if the uncertainty is too high. This can be seen in section 4.4.5 Figure 4.6, where the increase of the 95% confidence interval is shown to increase when predicting further into the future. This should be taken into account when deciding on a prediction horizon length.

Figure 8.10 shows the cumulative total costs for simulations with predicted and actual prices. The figure shows that for a prediction horizon of 1.5 day, the MPC actually performs better with a predicted price than with the actual price. This can be explained by advantageous intraday prices. It can also be seen in the figure that whether a predicted or actual price is used to make the day ahead plan has relatively little influence on the performance. This shows that the SARIMA model, discussed in section 4.4.5 is working sufficiently to make a plan. However, this is also influenced by the lack of uncertainty of the intraday price, which is known after the bid is done. This is the same for both simulations, and is expected to have a converging influence on the results.

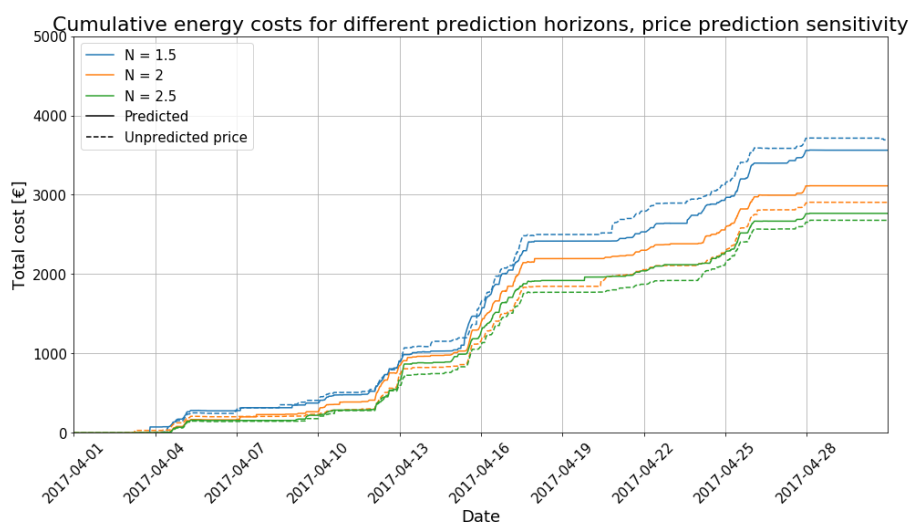


Figure 8.10: Cumulative cost comparison predicted and actual day ahead price

8.2.3. Measurement error

Since the measured discharge in Maarsssen is done by Q-h curve, there is some error in the discharge measurements. However, since the system of the NZK is well regulated, the error in estimated discharge is assumed to be small. Which is why a random variation of 5%, 10% and 15% has been applied to the incoming discharge in the NZK, in the simulation model. The sensitivity to measurement errors was tested with a prediction horizon of 1.5 day.

Figure 8.12, the cumulative costs for the different measurement errors. It can be seen that a 10% error gives the best performance. However, when looking at Figure 8.11 it can be seen that this can be explained by the relatively low discharge going out of the system. This can be since the random deviations are regenerated for every measurement error, causing slight differences in total volume coming into the system. This will be further discussed in sections 8.7 and 10.

Overall it can be said that the MPC is relatively insensitive to measurement errors, given these results. This can be explained by the ability to trade energy on the intraday market, which allows the MPC to correct for unforeseen influences like a measurement error.

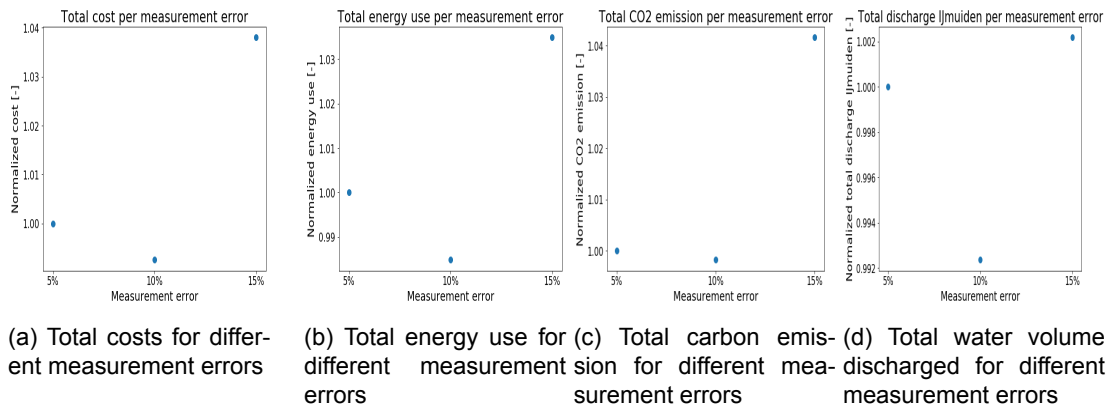


Figure 8.11: Relative performance of MPC with different measurement errors

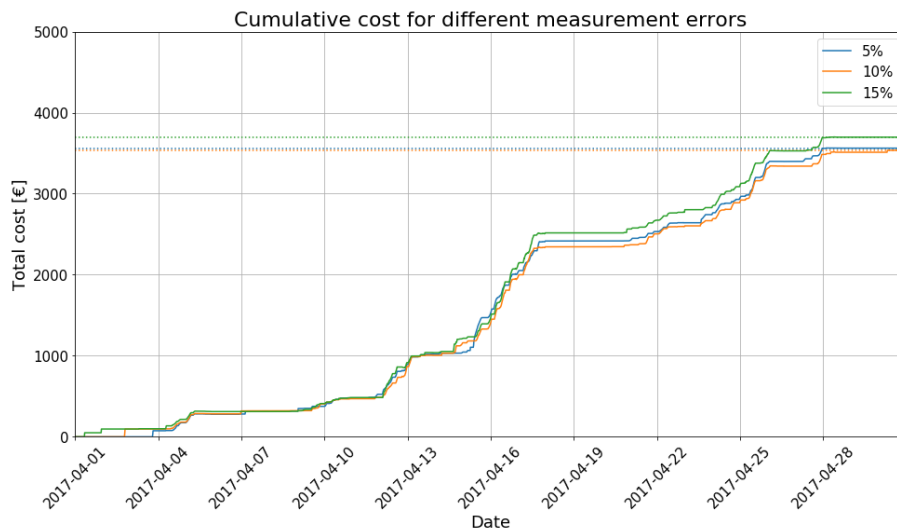


Figure 8.12: Cumulative costs with $N=1.5$ and measurement errors

8.3. Reference

As a reference scenario, the MPC created in this thesis has been modified to only minimize energy use over all timesteps, not taking price into account. Besides that, the monthly ENDEX-market energy price was taken for the period of simulation.

The cumulative cost of the reference and Dutch market simulations can be seen in Figure 8.13.

It can be seen that the MPC performs better when minimizing energy use, than when it is minimizing energy cost. This could be caused because the market is not rewarding demand response, through a varying energy price. However, the ENDEX market price is also relatively low compared to the German ENDEX price. This can be explained by the lack of renewable sources in the Dutch electricity mix. A large share of sustainable energy causes flexibility to be rewarded with low prices, and inflexibility to be punished with high prices.

It can be seen that with longer prediction horizons, the costs of minimizing energy and cost converge. The consequence of a longer prediction horizon is that the energy cost part of the objective function makes up a larger share of the total value of the objective function. This makes the MPC search harder for a minimum energy cost solution. A shorter prediction horizon causes slack variable part to grow in relative size.

The pattern same pattern can be seen in Figures 8.14 and 8.15, where the cumulative energy use and CO₂ emission can be seen. Interesting to see is that the prediction horizon of 2 and 2.5 day show similar results when minimizing energy, indicating that a prediction horizon of 2 days would be sufficient to achieve optimal results.

Figure 8.16 shows that with longer prediction horizons, the MPC is able to discharge more water through the gate. This could be due to efficient water level scheduling, allowing for a higher discharge. However, this could also be due to the relative size of the energy cost in the objective function, causing the MPC to get a higher convergence when discharging water through the gates, saving energy costs.

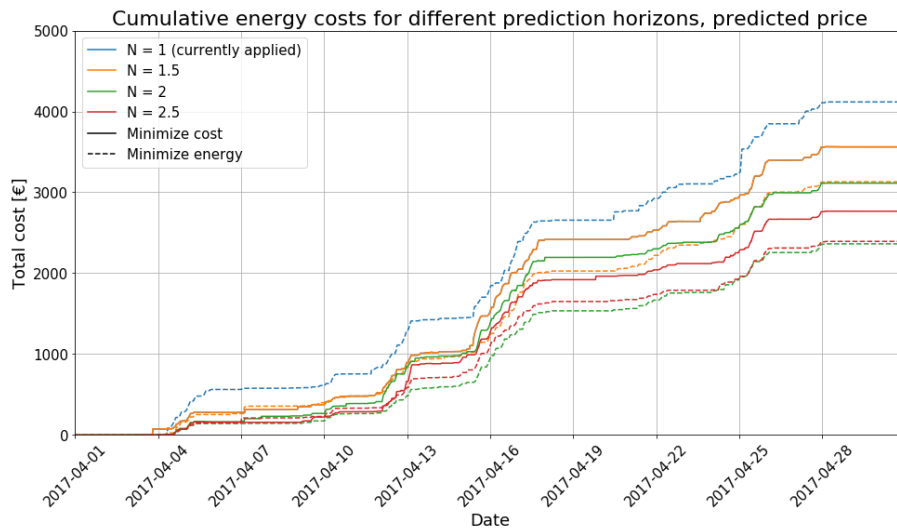


Figure 8.13: Cumulative costs for different prediction horizons, including reference

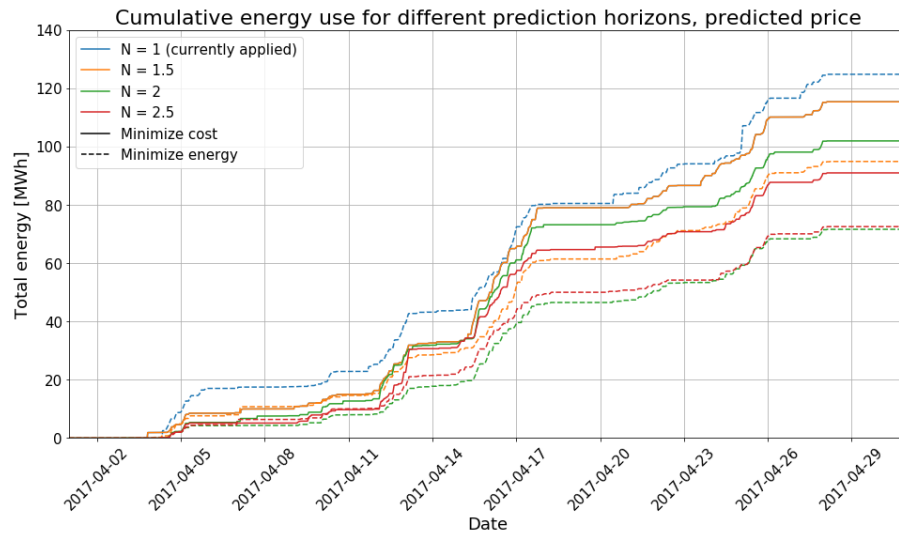


Figure 8.14: Cumulative energy use for different prediction horizons, including reference

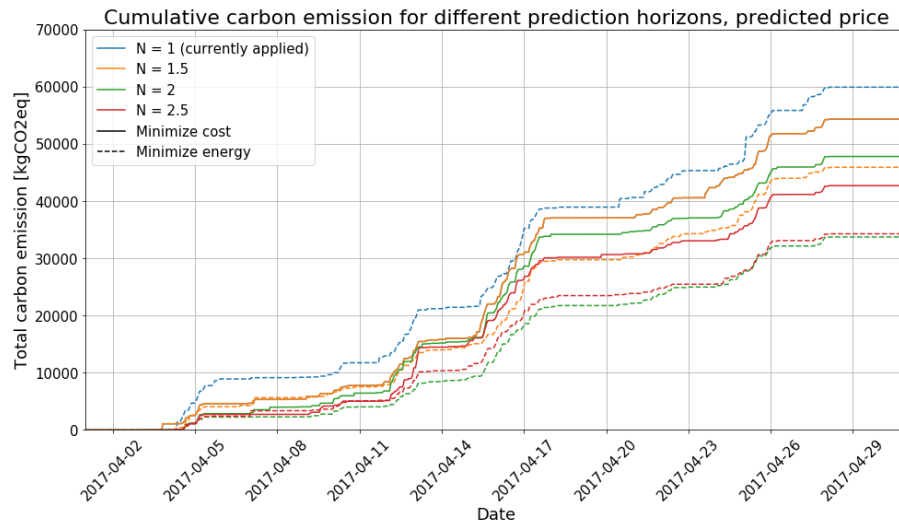


Figure 8.15: Cumulative CO₂ emission for different prediction horizons, including reference

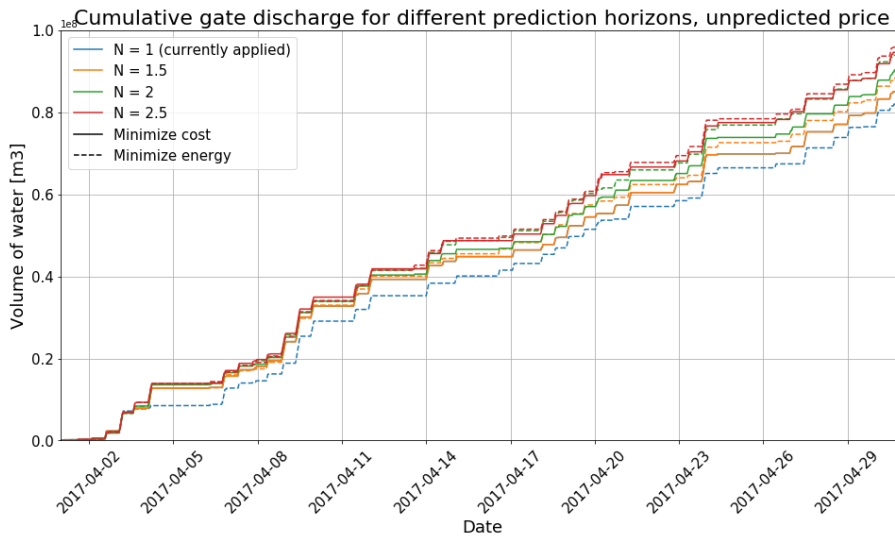
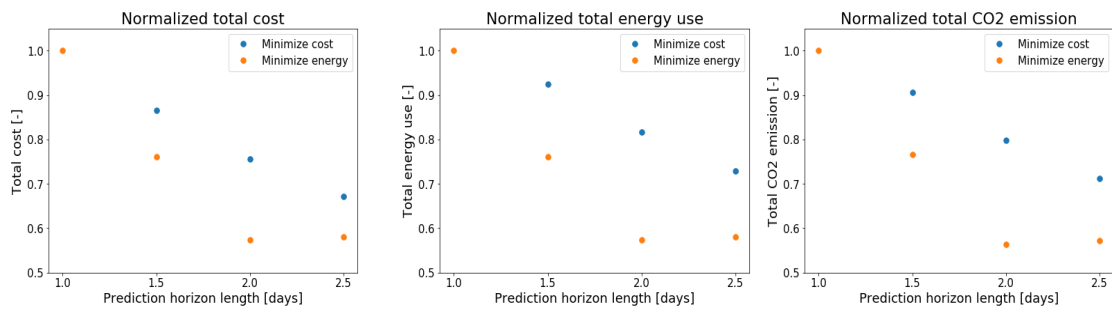


Figure 8.16: Cumulative gate discharge for different prediction horizons, including reference



(a) Normalized costs for different reference scenario's

(b) Normalized energy use for different reference scenario's

(c) Normalized carbon emission for different reference scenario's

Figure 8.17: Relative performance of different prediction horizons with reference scenario's

8.4. Long simulation with optimal settings

In this section, the optimal settings found through in the earlier results are used in the MPC to simulate 4-month (01-04-2017 00:00 - 31-07-2017 23:45) periods. The optimal settings are: no penalty on setpoint deviation at the end of the prediction horizon and a prediction horizon of 2 days.

Figure 8.18 shows the cumulative cost for the simulated period. The black dotted line indicates where previous simulations stopped. It can be seen that the relative cost difference is decreasing. The same can be said for the cumulative energy use shown in Figure 8.19. The difference in energy use decreases less than the difference in CO₂ emission seen in Figure 8.20, which indicates that the correlation between carbon intensity and energy price is a bit more present in the months of May - July. These results indicate that further research on the MPC can be rewarded, and longer simulation periods are needed to be able to give a trustworthy indication of relative savings.

Figure 8.21 shows that the amount of regulating volume sold on the intraday market is increased by 5-fold, which indicates the MPC found more flexibility to be used. The root mean squared deviation in the day ahead price from the mean is €6.88 in April, while it is €7.17 in April - July. This indicates that the price is fluctuating more in the long scenario, rewarding picking your time to consume energy more.

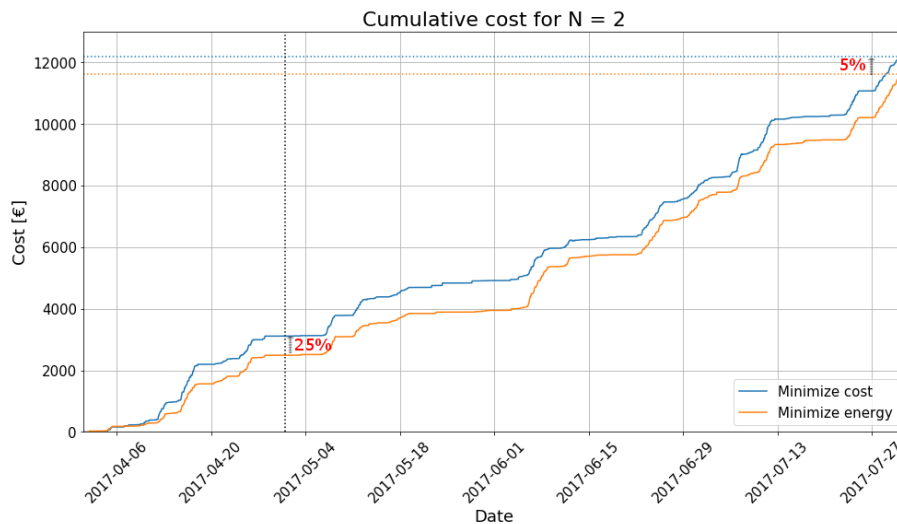


Figure 8.18: Cumulative cost for long run, N=2, including reference

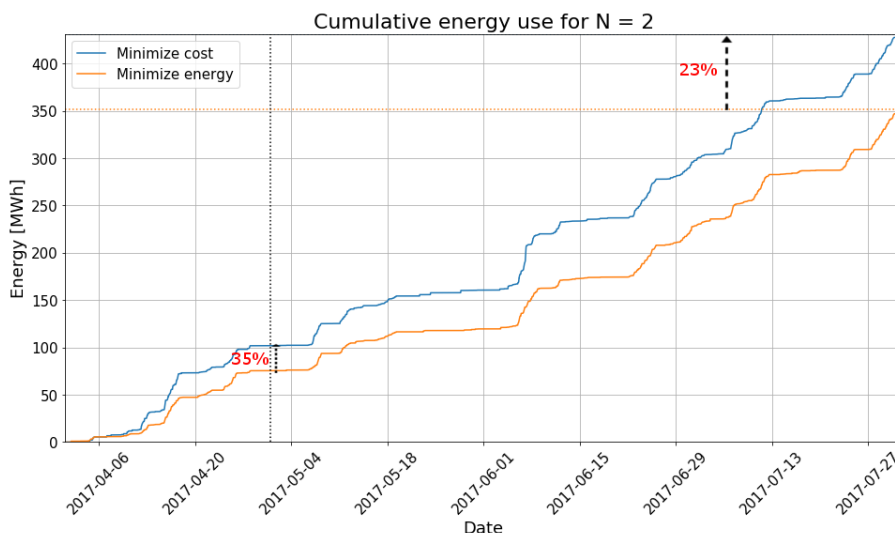


Figure 8.19: Cumulative energy use for long run, N=2, including reference

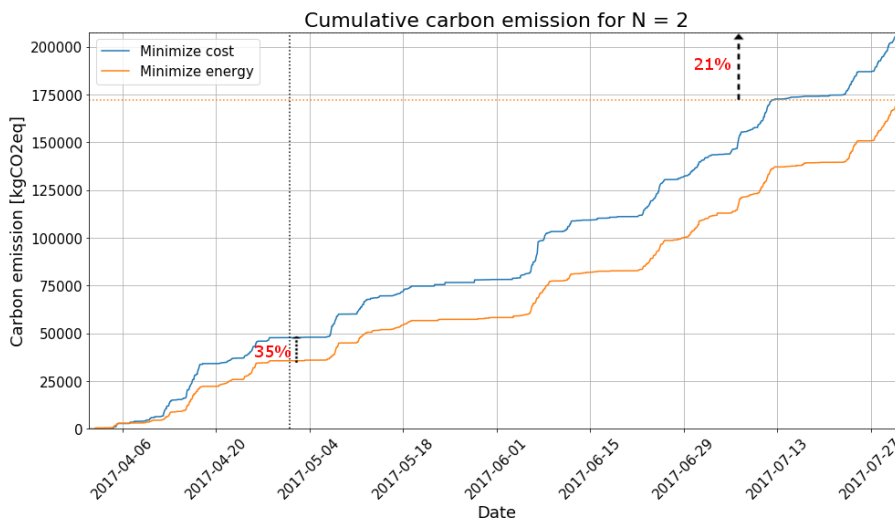


Figure 8.20: Cumulative carbon emission for long run, N=2, including reference

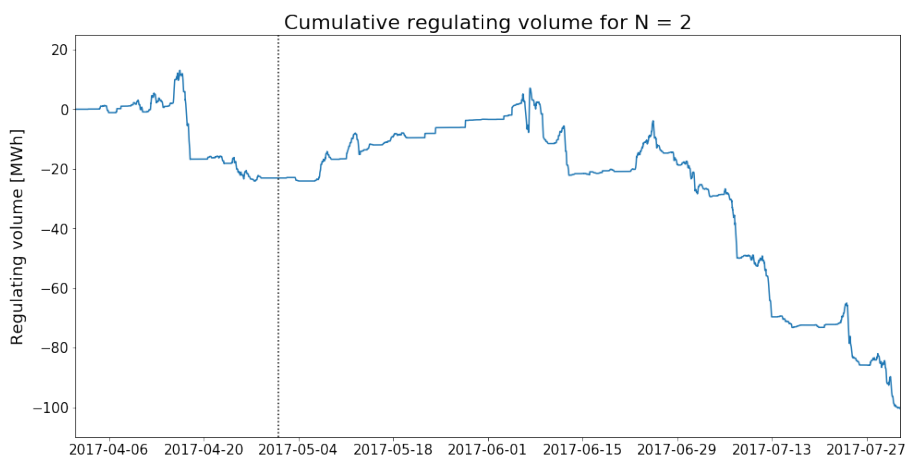


Figure 8.21: Cumulative regulating volume for long run, N=2, including reference

8.5. Future scenario

8.5.1. German market

To estimate the market prices and carbon intensity of the future Dutch grid, the German market was picked as representative. This is done in order to estimate the benefits of demand response when renewable energy will be more present in the Dutch electricity mix.

Figure 8.22 shows that minimizing cost now brings lower cost than the reference scenario where energy is minimized. This can be explained by a more fluctuating energy price, which rewards picking the right time to use energy more.

Figure 8.23 shows a significant difference in energy use, which reflects in the carbon emission seen in 8.24. The largest increase can be seen at 07-04-2018. When looking back at the same date in Figure 8.22, it can be seen that the MPC made profit on that time, while consuming energy. Figure 8.27 confirms that the MPC indeed decided to pump at its maximum capacity, while the reference did not. The reference MPC decided that a lot more water could be discharged through the gates. While the MPC that minimizes costs decided to discharge a lot of water before pumping, increasing the pump height, which increases the energy use. This is explained by Figure 8.28, where it can be seen that a negative energy price occurred in the time the MPC decided to maximize its energy use. When looking at the carbon intensity of the German grid at that period, seen in Figure 8.29 it shows that the carbon intensity indeed was very low. But the decrease in carbon intensity did not compensate for the increase in energy use, resulting in a higher CO₂ emission.

However, the intraday price was assumed to be a 25% random deviation around the day ahead market price. This does not reflect the correlation between carbon intensity and energy price that is present. The intraday market is expected to show a higher correlation between carbon intensity and energy price than the day ahead market is. This will be further discussed in section 10.

In Figure 8.25 the day ahead and total cost of the Dutch and German scenarios can be seen. The German market is cheaper, resulting in lower cost. However, the day ahead costs of the German market scenario exceed the day ahead cost of the Dutch scenario. This results in a higher amount regulating volume, as seen in 8.26. This can be explained by a higher incentive to sell energy on through the intraday market through a more fluctuating price. This energy is then later on bought on the day ahead market, resulting in higher bids.



Figure 8.22: Cumulative costs with N=2, German market scenario

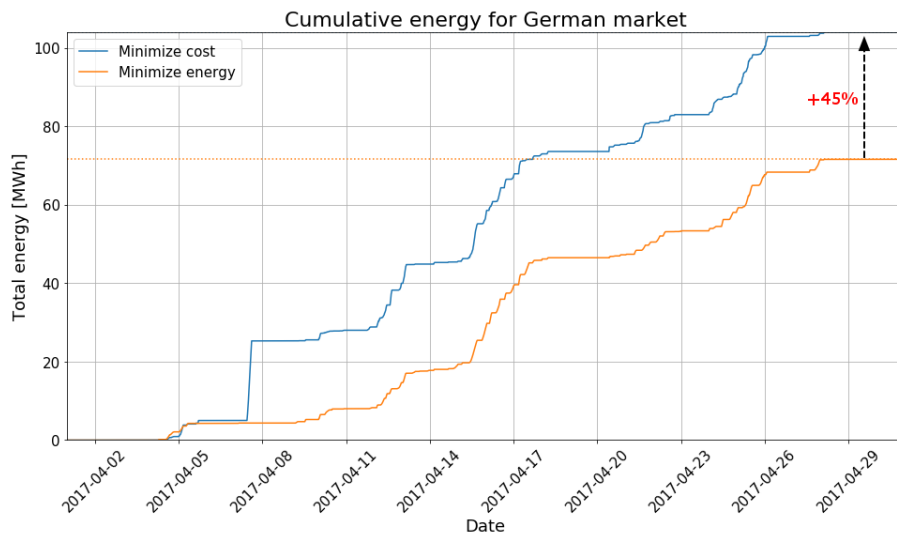


Figure 8.23: Cumulative energy use with N=2, German market scenario

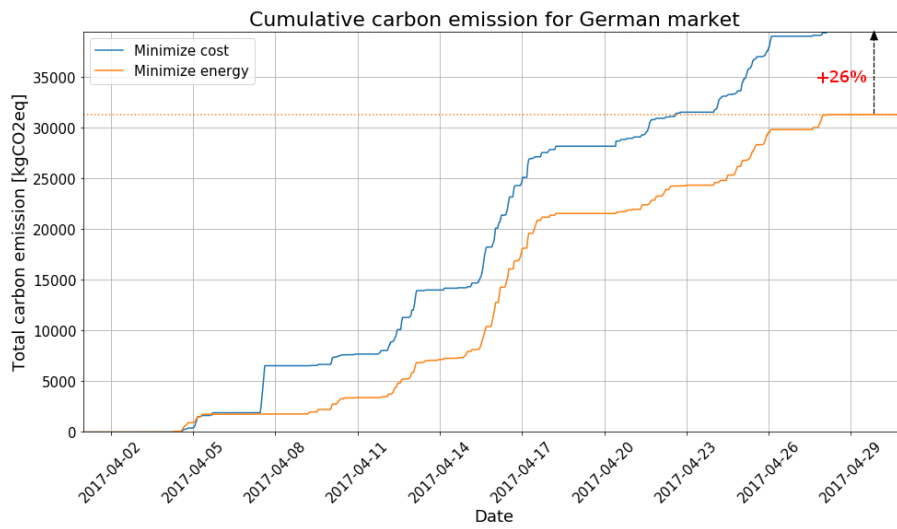


Figure 8.24: Cumulative carbon emission with N=2, German market scenario

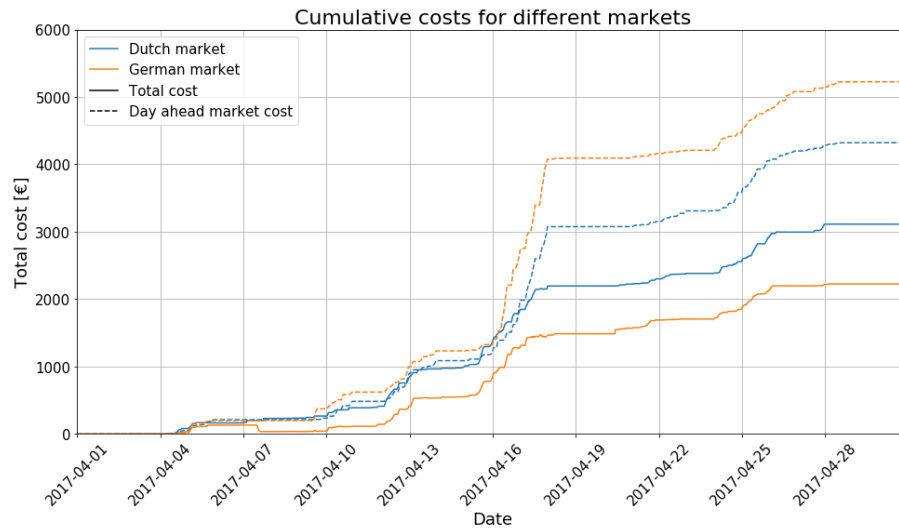


Figure 8.25: Cumulative cost with N=2, Dutch and German market scenario



Figure 8.26: Cumulative regulating volume with N=2, Dutch and German market scenario

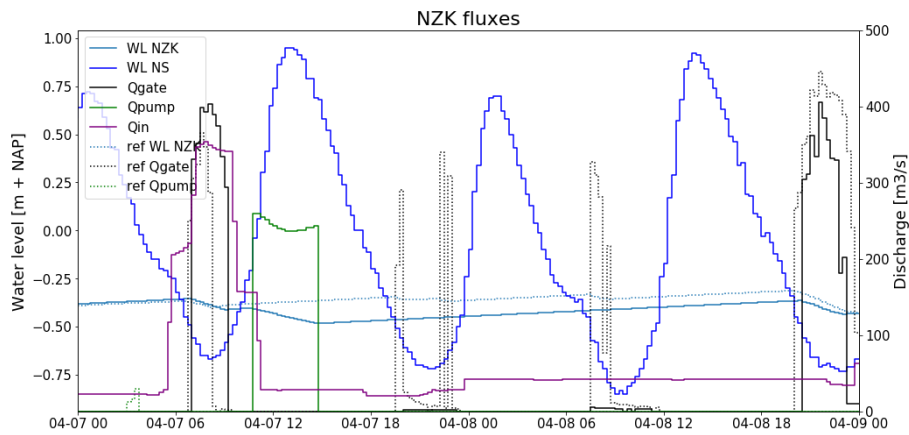


Figure 8.27: Fluxes NZK 07-04-2017 - 09-04-2017, German market scenario

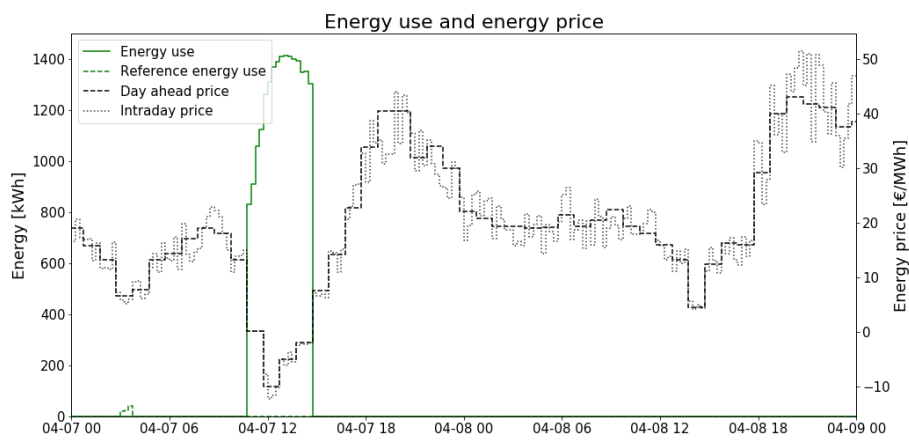


Figure 8.28: Energy use and energy price 07-04-2017 - 09-04-2017, German market scenario

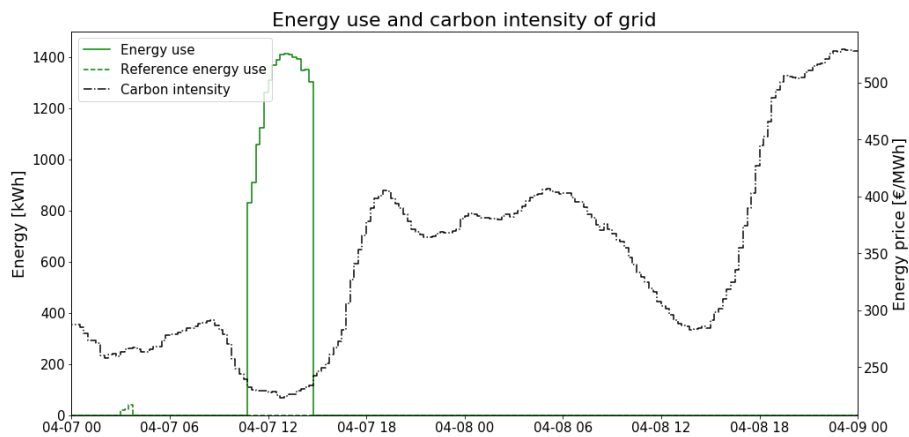


Figure 8.29: Energy use and carbon intensity 07-04-2017 - 09-04-2017, German market scenario

8.5.2. Sea level rise

To estimate the effect climate change will have on the MPC's performance, and to see whether the pumping capacity present would still be sufficient, a scenario was simulated with a sea level increase of 0.5m.

Figure 8.30 shows that cost are lower when minimizing energy with a constant price, than for acting on the day ahead market. This could be explained by the relatively large part of the slack variables on the objective function, rewarding a decrease in energy costs less. It is expected that a fixed energy price will be more expensive in the future, when energy supply will be more intermittent. Besides that, the total cost are now closer to each other than in the reference scenario described in section 8.3. Figures 8.31 and 8.32, where cumulative energy use and carbon emission can be seen, show a similar difference as seen in the costs. But Figure 8.33 does not show a significant difference in pumped volume.

The results show that the MPC is indeed able to keep the water level within constraints, however it would be interesting how much extra pumping capacity would be needed to optimize flexibility in pump schedule, this will be discussed in section 10.

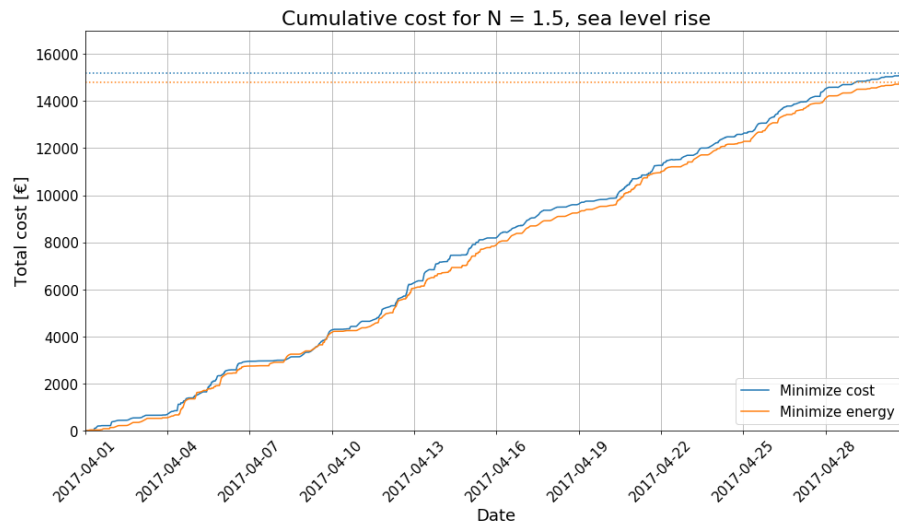


Figure 8.30: Cumulative cost N1.5, +0.5m sea level

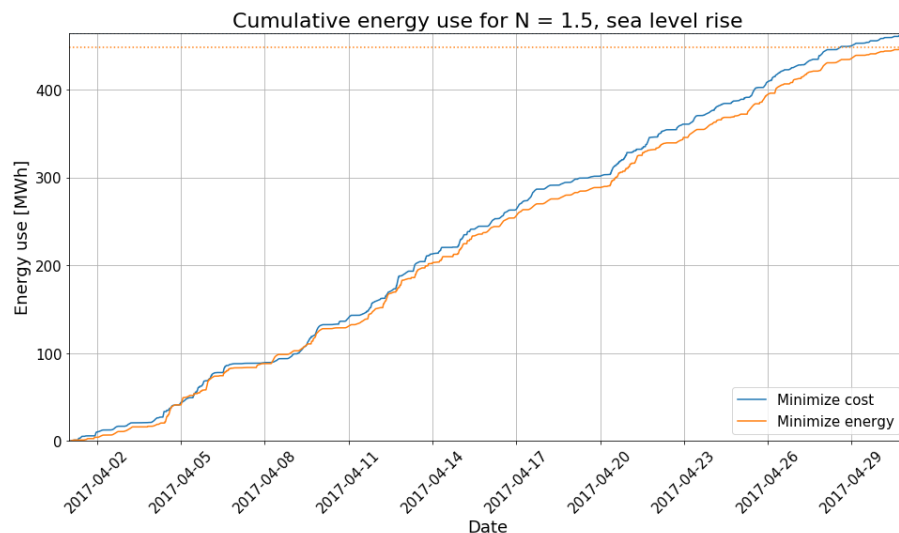


Figure 8.31: Cumulative energy use N=1.5, +0.5m sea level

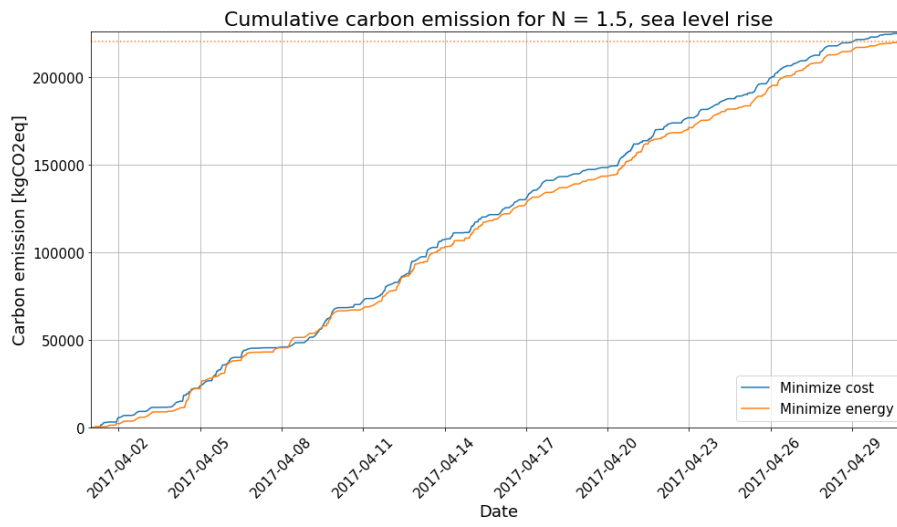


Figure 8.32: Cumulative carbon emission N=1.5, +0.5m sea level

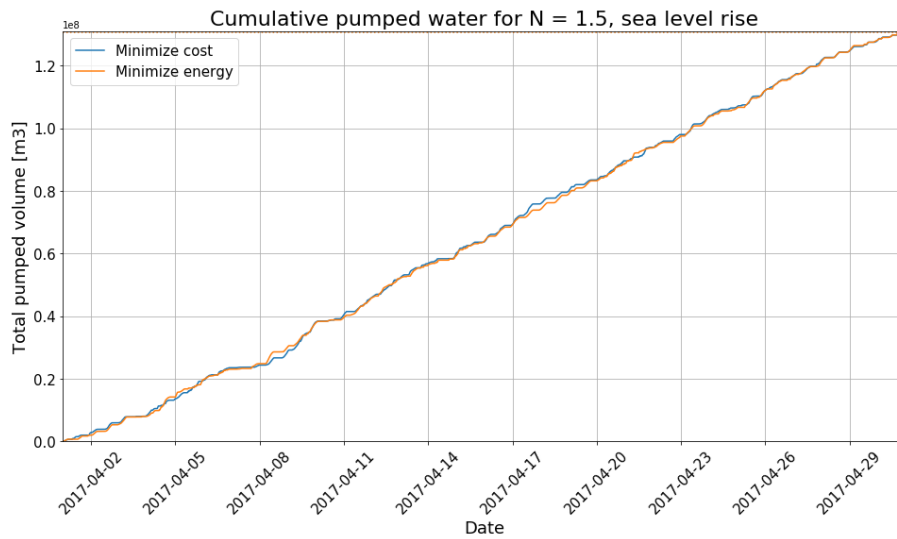


Figure 8.33: Cumulative pumped volume N=1.5, +0.5m sea level

8.6. Possibilities for the aFRR

To investigate the potential for pumping station IJmuiden to be active on the aFRR market, an analysis was performed on the previous results where IJmuiden would be active on the day ahead and intraday market.

The simulation of the 2-day prediction horizon on the Dutch market, with predicted price, was used to see where the MPC decided not to pump, while pumping was possible. After which the maximum amount of energy that could have been used was calculated, and the values above 0.25 MWh (1 MW power) were selected. After that, the periods where downward activation in the aFRR market occurred were selected. This gives the maximum extra amount of energy that could have been used for purposes of grid balance per timestep, as can be seen in Figure 8.34.

These energy amounts were then multiplied with the acting downward activation price. The result can be seen in Figure 8.35. The figure shows that indeed it would have been possible to make extra bids on the aFRR market, in order to achieve a profit and supply regulating volume.

For further analysis, the timeslots where the downward activation price is 0 or negative were selected to estimate the maximum amount of regulating volume that was possible, without making costs. Figure 8.36 shows that a maximum amount of regulating volume, without making costs, of 120 MWh was possible. Figure 8.37 shows that a profit of €3000 would have been realized, which is of the same order as the cost calculated in section 8.2.1. This can be seen in Figure 8.38, where the aFRR profit is subtracted from the total cost for being active on the day ahead and intraday market. The figure shows that the aFRR market has the potential to almost fully compensate the energy cost for pumping station IJmuiden. This is excluding the decrease in energy bought on the day ahead and intraday market that is possible due to the extra pumping done for grid balancing purposes, and excluding the effect of pumping for grid balancing purposes on the possibilities for pumping for grid balancing purposes.

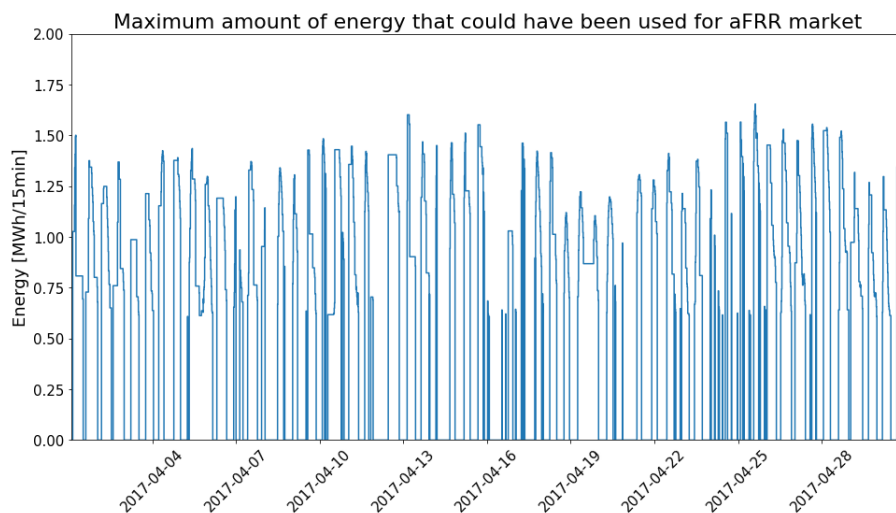


Figure 8.34: Maximum possible extra energy use per timestep, while downward activation occurred

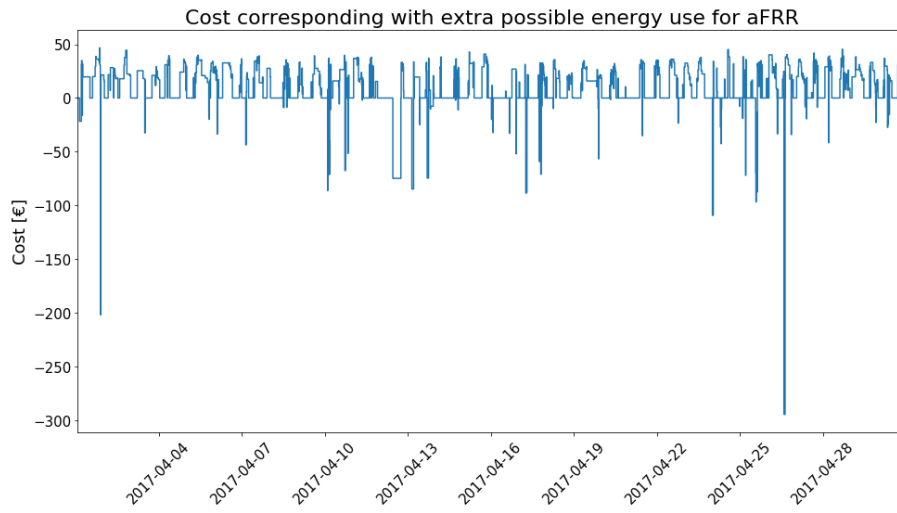


Figure 8.35: Maximum cost per timestep due to downward activation

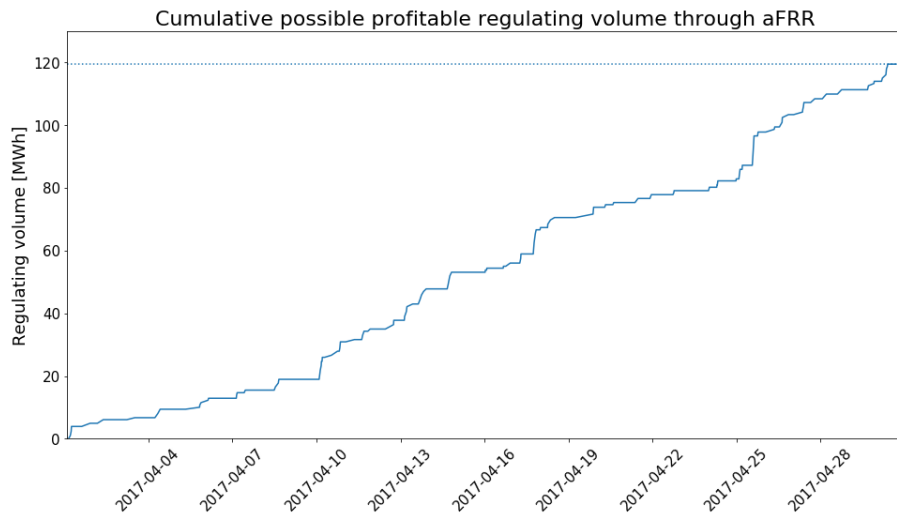


Figure 8.36: Cumulative maximum regulating volume without costs

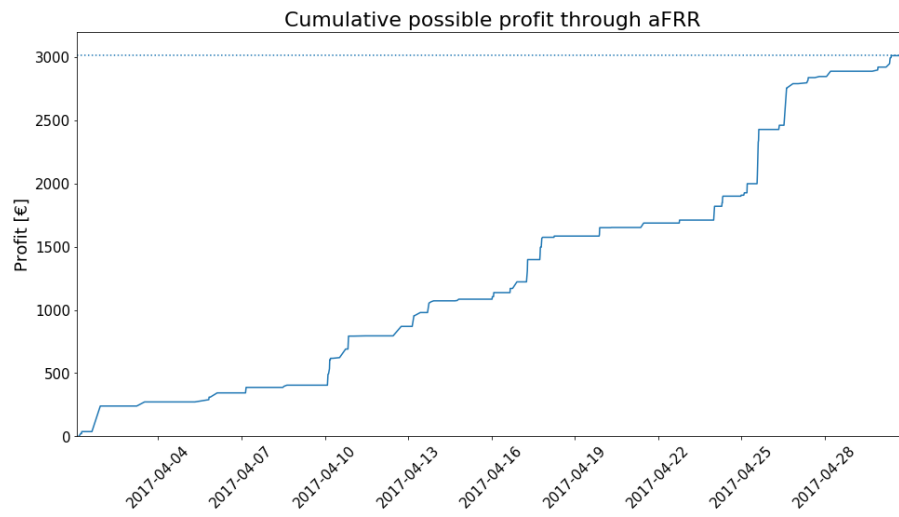


Figure 8.37: Cumulative maximum profit through downward activation

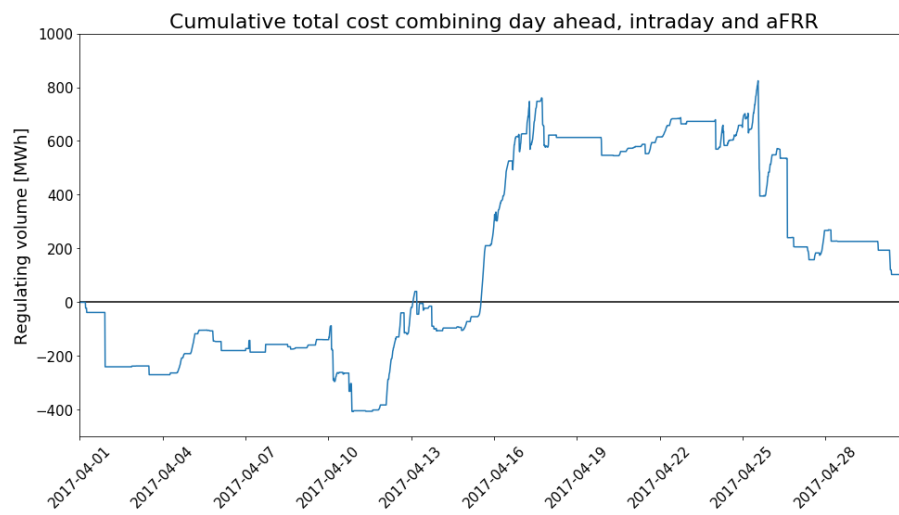


Figure 8.38: Cumulative total cost for being active on day ahead, intraday and aFRR market

8.7. Study limitations

8.7.1. Optimal parameter choices

These results show that it is possible for the pumping station and water system to participate in Demand Response. The current results show that for these scenarios and simulated times, a prediction horizon of 2 days and no penalty on setpoint deviation would be optimal. This way the controller can deal with price and data uncertainty, while still being flexible enough to trade energy on the intraday market. This could change when simulating a longer or different period, since these simulations were done for one week.

8.7.2. Data limitations

Discharge data availability

Since insufficient historic discharge data was available for this study, the assumption that all waterboards discharge at the exact same pattern as Rijnland, was made. When Rijnland discharges at its maximum capacity, the other waterboards do as well. This is unlikely, since this is dependent of the local storage and delays in the system. Besides that, rainfall is non-uniformly distributed, resulting in different needs for pumping. However, this assumption is probably a disadvantageous effect on the results. Since it is unlikely that the waterboards discharge at the maximum capacity at the same time, the actual discharges in the system are probably more averaged out. This is disadvantageous to the results, since the need for pumping is higher when the discharge is extreme, making the pump schedule less flexible.

Uncertainty in discharge

The discharges of the waterboards were assumed to be known. In reality, this is not true. Rainfall-runoff predictions have a relatively high uncertainty, and in this case is also dependent on local policies (setpoint levels, pre-pumping, energy market price). This is beneficial to the results, since the MPC is able to create a better plan based on certainties. However, the MPC would be able to correct for this as soon as the prediction is better. The MPC could then buy more energy on the intraday market to correct its pump schedule.

Including a form of uncertainty in the discharge is relatively difficult, which is why this was not done for this study. Since rainfall has a temporal and spatial variability, the discharge of separate waterboard would be dependent of the timing of the rainfall and whether the rain falls there or not. Besides that, the local (urban) water system would have to be modelled to estimate when the waterboards would pump water into the NZK/ARK. This could be a study by itself, which is why this has not been taken into account in this thesis. However, this is recommended for further research. As will be discussed in section 10.

Sea water level uncertainty

The water level of the sea is assumed to be known. No uncertainty was applied, which has a beneficial effect on the results. The MPC knows exactly when it could use the gates, and when it could pump. In reality there is some uncertainty in the sea water level prediction. However, the tides do have a relatively predictable nature. This limits the beneficial effect of the lack in data uncertainty on the results.

Rijkswaterstaat's energy price

Rijkswaterstaat provided an energy price that is used internally for calculations. This was found to be €87,-/MWh. However, this is including the delivery costs of energy. Which is why the ENDEX price has been taken as a reference price. What the actual raw energy price is and was is not known, and is dependent of the type of contract and the negotiations around it.

However, it is still to be expected that a fixed energy price will become relatively expensive in the future compared to flexible tariffs.

Intraday market price data availability

The data for the intraday market price is not freely available, and was not used for this study. The intraday market price timeseries was created by assuming a correlation with the day ahead market price, and adding a random 25% deviation as explained in section 6.6. This makes the absolute value of the costs not comparable with a real situation. However, it does show that the presence of the intraday market gives the pumping station more flexibility since it allows for changes in energy use up to 5 minutes before consumption, increasing the ability to participate in demand response.

Intraday market uncertainty

In this study the MPC knew the intraday market prices for the whole day as soon as the bids on the day ahead market were done, and after that fixed. In reality, the intraday market is varying throughout the day, depending on (unpredicted) supply and demand of energy. This allows for the MPC to make a plan based on certain prices.

Besides that, the time at which the energy is bought doesn't matter either, since the price is fixed. While in reality the energy price could be higher or lower when it is bought at a later time.

This could either positively or negatively affect the results, depending on the intraday strategy, like how far into the future the MPC is allowed to trade, and actual intraday energy prices.

Energy production data quality

The energy production data of the Netherlands had to be adjusted to match with the statistics provided by CBS. These many assumptions to fill gaps and make total volume of energy production match influence the estimation of the carbon intensity of the grid. This is further explained in section 6.1.

8.7.3. Market assumptions**Bids are always accepted**

The MPC makes a bid based on the predicted energy price. After the bid is done, it is automatically accepted, but the actual day ahead price was charged. In reality, a bid can be rejected if it was lower than the equilibrium day ahead price. The same counts for the intraday market, where energy can always be bought in these simulations.

For the day ahead market, this could be realized in reality as well by bidding higher than the expected price. As long as the bid is higher than the final equilibrium day ahead price, it will be accepted. This does influence the height of the price itself, since a bid is done with a high price.

If a bid would be rejected, this could be implemented as a hard constraint for the MPC not to use that timeslot for pumping. Or if a day ahead bid is rejected, it could still be traded on the intraday market.

In the end, the time until the bid that was rejected is the decisive factor in how it would influence the system.

Time of day ahead plan

In this study, the day ahead plan was made at midnight. However, in reality this is done at 12:00. This gives the MPC used in this thesis half a day extra knowledge about the system state. This is expected to have a beneficial effect on the results, since a better plan can be made. If the plan was made at 12:00, the MPC would probably trade more energy on the intraday market to optimize for the unforeseen system state.

Carbon intensity assumptions

When calculating the carbon intensity of the grid at a certain time, assumptions were made on the carbon intensity of various energy sources. It is known that there is a difference in lifetime CO₂ emission between off- and onshore wind turbines. This difference could not be verified from a reliable source, which is why the IPCC's general carbon intensity for wind energy was taken.

More assumptions were made on carbon intensities not specified by the IPCC, like brown-coal, or specific types of hydropower.

These assumptions influence the estimated CO₂ emitted by the energy use of the pumping station. It is not known what the effect is, since the actual numbers are not known.

Due to the inavailability of the intraday market data, and the assumed 25% deviation around the day ahead price, the correlation between carbon intensity and energy price is disturbed for this market. This could have influence on the amount of CO₂ that is expected to be saved, since usually cheap energy would be more sustainable. However, when simulating the intraday market with a random 25% deviation, it could be that a cheap energy price occurs during a very polluting moment, and vice versa. This effect is expected to have a larger influence on the German market results, since renewable energy is more present in the German (intraday) market, making the 25% random deviation less accurate.

aFRR results

The aFRR results are based on the results coming from the simulation where the MPC is active on the day ahead and intraday market. This neglects the influence of the extra pumping for grid balancing purposes. These effects however are likely to result in a lower amount of energy that would be needed to be bought on the spot markets, which would also increase the amount of timeslots extra pumping is possible. However, the extra pumping for grid balancing purposes could also decrease the possibilities for extra pumping if the water level is brought near the lower bound.

8.7.4. Model limitations

Bucket model

The water bodies are modelled as a bucket in this MPC. This neglects the effect of delay in the system, affecting the response time of the system. When the pump is activated, the effect is immediately noticed throughout the whole water body, while in reality this is not the case. The effect would travel through the system like a wave.

Besides that, the location of discharge into the system also doesn't matter in this MPC. Since it is one bucket. In reality the discharge is distributed along the water body, having different effects on the system.

Timestep size

In this MPC, a timestep size of 15 minutes was used. Within these 15 minutes, the system state can already vary. Besides that, the sea water level is probably changing more notable. This would effect the system performance. The actual pump-height or difference in water level is varying, resulting in varying discharges or energy use. This could disturb the system, but the feedback loop should prevent constraint violations.

Linearizations

The maximum discharge that can possibly go through a gate is linearized in this MPC. The linearizations are chosen in such a way that they only have a negative effect on system performance, not on water safety. The linearizations are created in such a way that they underestimate the maximum discharge, making the MPC believe there would be a need for pumping rather than making the MPC believe it can discharge more than it can through the gates. The result is that this simplification could only cause higher energy costs, rather than a higher water level. The linearizations are further elaborated in section 7.1.2.

Rainfall/evaporation

Rainfall and evaporation are neglected in this study, due to the estimated small effect on the water levels. However, to be truly precise these should be accounted for in at least the simulation model. This would have a slightly disturbing effect on the system state, which should be corrected by the feedback loop.

Effect of waves on discharge gates

There are waves on the sea that could disrupt the discharge coming through the gates. This has a decreasing effect on the discharge of the gates. This has not been taken into account in the model, but is partially taken into account in the water-level data, since it is a 10-minute average. To estimate whether the effect of a short wave is negligible or not, the amount of time needed for a step-shaped wave fully stop a discharge was calculated based on an impulse-

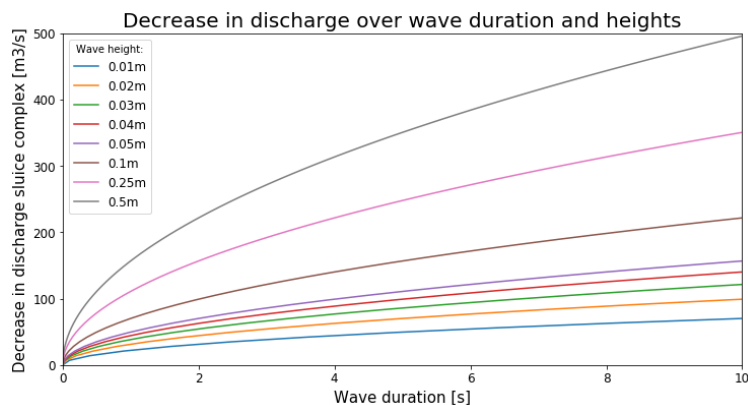


Figure 8.39: Decrease in discharge per step-wave time and height

balance, as described in Appendix F. The result can be seen in Figure 8.39. The figure shows that for a long time span, the decrease in discharge can be high. But this is done with a step wave, the actual wave don't have a step-shape, which means this figure is overestimating the effect of the waves on discharge. But even with a 10-second stop of the maximum discharge ($500 \text{ m}^3/\text{s}$), the effect on the water-level of the Noordzeekanaal would be 0.12mm , which is negligible.

8.7.5. Simulation limitations

Accurate simulation software

The results don't prove if the MPC works in a real situation, which is why the use of SOBEK was planned as reliable non-linear estimator of state. But due to software limitations this was not possible. It is advised to at least simulate the water system with this MPC using a model based on the St. Venant equations to describe the flow and water level of the water. However, the current MPC used in IJmuiden is also based on a bucket model, and the surface area used in the current MPC's model was used in the MPC created for this research as well. This does not give a guarantee that this controller will work, but it does give some indication on whether the model assumptions represent the physical system well enough for control-purposes.

Energy use

The energy use is calculated through the fitted function used in the MPC. However, the combination of discharge and pump-height is not checked for feasibility and for actual energy use. Besides that, energy use of the pump is calculated through the fitted function, while there is some error in this fit. This is better described in Appendix C.2. This assumptions makes the MPC know exactly what the energy use of the pumping station is or would be, while it could use more or less energy for specific working points.

9

Conclusion

The goal of this thesis was to find out whether demand response could be safely applied to the water system of the Noordzeekanaal–Amsterdam-Rijnkanaal. This was done by writing an MPC that uses expected discharge, wind speed and direction and energy prices to optimize its pump schedule to minimize energy costs.

9.1. Electricity markets

Based on the analysis (section 3) and simulations performed for this thesis can be concluded that a combination of the day ahead market and intraday market is feasible. The SARIMA model (section 4.4) seems to perform well enough in predicting the day ahead price to base a plan on. Besides that, including the day ahead market gives more certainty of supply and costs. However, the intraday market allows for short-notice trading, to make up for unforeseen events. The intraday market also has a large potential for the trading of renewable energy, making the market more interesting. The MPC seems to create a larger profit when prices fluctuate more, which is expected on the intraday market. Besides that, the MPC steadily makes a profit through intraday trading. This is also due to the shifting of its energy use in time, placing it on the day ahead bid. And the intraday price is known and fixed after the day ahead market is closed. Still it can be said that the intraday market seems a valuable addition to the market strategy.

The imbalance market seems unfeasible, because of its unpredictable nature and fast acting players. Pumping station IJmuiden can't start and stop quickly enough for it to be profitable. However, the aFRR market does show a large potential. Receiving a warning signal 15-minutes before activation makes the market feasible for the pumping station to be active on. The results also show that a minimum power of 1 MW is achievable for the pumping station, and the addition of the aFRR-strategy to the day ahead- and intraday-strategy seems like a way to be certain that pumping can be done when it is crucial, while counteracting imbalance on the grid.

9.2. Controller sensitivity

Based on the results can be said that the performance of the MPC seems to be sensitive to prediction horizon length. The different prediction horizons that were tested in this thesis did not yet converge to a stable performance. However, the calculation time increases significantly when increasing the prediction horizon. A prediction horizon of 2 days seemed to be optimal in sense of calculation speed and performance. Since this thesis did not include uncertainty in discharge, the optimal prediction horizon length cannot be determined fully. A higher uncertainty could decrease the effectiveness of a longer prediction horizon. The MPC seems insensitive to (random) measurement errors. The results do not vary significantly for different measurement errors. The ability to correct for disturbances through intraday trading is expected to have a play a large role in the property of the MPC.

Price uncertainty does not seem to have a large influence on the performance of the controller. The SARIMA model seems to predict the day ahead price well enough for the controller to base its plan on. However, no intraday price uncertainty/variety is taken into account. The intraday market price varies throughout the day, and therefore the trading mechanism would resemble stock market trading. The time at which a trade is done influences the costs, which is a factor that is not taken into account in this thesis.

The controller also seems to be sensitive for the scaling of the objective function, and its influence on complementary constraints. It is likely that the MPC is not performing optimally, since the differences in performance between minimizing cost and minimizing energy vary significantly. This could be due to the influence of the slack variables used in the gates on the allowable maximum discharge of the gates. Besides that, the objective problem has to converge towards a solution with lower energy costs. The relative scaling of the energy cost part and the slack variable part of the objective function seems to have a large influence.

9.3. Benefits

The benefits are momentarily hard to be sure of. However, it can be said that an increase in prediction horizon can give up to 40% less costs, energy use and CO₂ emission. The 40% is a maximum, since this number is likely to be influenced by the unequal scaling of the objective function.

It can be said that in a future scenario, optimizing cost can bring low energy costs. But a negative energy price can increase the energy consumed and CO₂ emitted significantly. On the one hand energy is being wasted, since more is used than necessary. On the other side, a negative energy price is not something the market prefers. It is negative since there is simply too much, and storing it or turn off generative sources would cost more. A negative price on the day ahead or intraday market can be seen as an early balancing mechanism.

The future scenario with the German market shows that a 13% cost decrease compared with the reference is possible with the current MPC. The negative energy price that occurs on the German market results in a large increase in energy use and CO₂ emission, but this is not the full source of the difference. This could again be influenced by the complementary constraint for the gates, combined with the relative scaling of the objective function.

In terms of regulating volume can be seen that in the future scenario, where prices fluctuate more, can result in up to 78% more upward regulating volume is created through selling on the intraday market.

The inclusion of the aFRR market could possibly make pumping station IJmuiden save significantly in cost by acting on imbalances on the grid. The analysis shows that over 90% of the cost made on the day ahead and intraday market could be regained through the aFRR market. However, this is only an analysis based on the results of being active on the day ahead and intraday market, and no simulation was performed. Still it can be said that the aFRR holds a lot of potential for the pumping station.

9.4. Markermeer and IJsselmeer

It seems that in the current strategy, the Markermeer and IJsselmeer cannot contribute much. The lakes are only allowed to discharge water into the Noordzeekanaal, and not the other way around. This results in the lakes only being a useful addition in case of negative energy prices or large positive imbalances. Since the Dutch market does not know many negative energy prices, and these are expected to be stored efficiently in the future, the lakes can't contribute much.

When combining the aFRR strategy with the day ahead and intraday strategy, the lakes can give a valuable addition. Positive imbalances are likely to remain, although on smaller scale. Besides that, Rijkswaterstaat could sell their (already bought) energy as upward regulating volume by turning off the pumping station.

The afsluitdijk will contain a large pumping station in the future, and possibly turbines in the gates. This would increase the balancing capacity and possibilities for the whole water system. Therefore it is advised to further research the inclusion of the Markermeer and IJsselmeer, centralizing the control of the structures.

9.5. Final

Overall can be said that demand response can be applied safely to the water system. The water levels stay within constraints, however this should be further tested with a more reliable simulation software.

The results do not show cost, energy or CO₂-emission savings on the Dutch market in comparison with the reference scenario. However, this could be influenced by the scaling of the objective function and the complementary constraint for the gate. This should certainly be further researched. The costs do seem to converge when simulating for a longer period, also giving reason for further research and simulations for longer periods. On the German market there were already cost savings, but no energy or CO₂ emission savings. This can be explained due to the fact that in Germany, the ENDEX price was relatively high compared to the day ahead market prices since sustainable energy makes up a larger share of the energy mix.

Still, a significant amount of regulating volume of over 20 MWh was simulated through intraday trading on the Dutch market. Which was over 40 MWh on the German market. This shows that the MPC can take different market prices into account.

The analysis on the aFRR market shows that the addition of the balancing mechanism could have a significant impact on the balance of the grid, and this strategy should be simulated in further research.

The Dutch water system as a whole contains many pumping stations. Aggregating them and collectively help balance the grid could prove a valuable service to the Dutch and possibly European grid stability.

Perhaps the most important thing this research showed is that by creating an MPC for the water system, it can be fine-tuned by adding constraints and adjusting the objective function to participate on different markets. This is valuable information, since the markets are changing and new rules are likely to come with those changes.

10

Recommendations

This study had some limitations, resulting in a few recommendations for further research as regards the optimization. Furthermore there are some recommendations on a more personal note. Problems that were run in to, personal views, and about signals received when talking with the people involved in similar problems.

10.1. Optimization

10.1.1. Bucket model

The internal model of the MPC now uses a bucket model to estimate effects of control on the water level. However, this disregards delay in the system. It would be especially interesting to research the effect of delay in the Noordzeekanaal on the system performance. I recommend the following two approaches:

- Split the Noordzeekanaal in a 10-bucket model, as depicted in Figure 10.1. This was also researched by Goedbloed [26]. The advantage would be that delays in the system can be taken into account, but simplified. Besides that, a spatial distribution of the water level would be calculated and constrained. This would partially prevent the water level bounds to be exceeded, even though according to the MPC it is not exceeded. But only partially, because within one of the 10 buckets this could still happen.

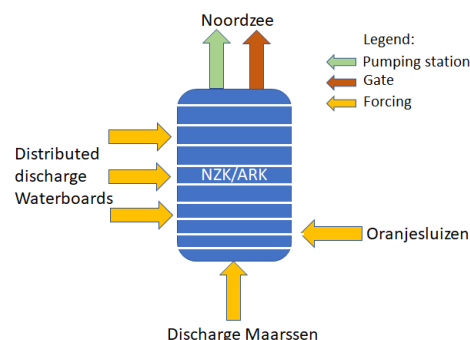


Figure 10.1: 10-bucket model Noordzeekanaal

- Another option is to use (linearized) St. Venant equations to describe the relationship between water-level, discharge and storage as done by Tian [55]. This would give a more accurate representation of the water level present in the system, by taking friction and flow speed into account. However, it is still advised to split the NZK and possibly the IJsselmeer and Markermeer in smaller parts to have a spatial distribution of the water level.

10.1.2. Pump configuration

In this thesis, the MPC uses a simplified power-curve to estimate energy use by the pumping station. All possible combinations of pump height and discharge are possible. However, in the real case this is not. By using a Mixed Integer Non-Linear Problem solver, like GUROBI [28], the pumping station could be modelled similarly as done in section C.2. This way the exact optimal pump configuration can be calculated, and the energy use is better estimated.

10.1.3. Optimization process

A non-convex optimization can sometimes fail. In the case of the MPC created for this thesis, a slight disturbance in the start points or not specifying a warm start was enough to find an optimal result. Besides that, a time constraint was implemented so the optimization would stop after 7.5min. Since a decision needs to be made in 15 minutes, the MPC would have two tries. However, normally the solver could solve a single timestep in 10 seconds. When a decision is vital, it is advised to not let the decision depend on a single optimization process. Rijkswaterstaat could consider running multiple processes at once, and pick the optimal result after 15 minutes. Or they could implement a time constraint to give the same calculating unit multiple shots. In this study, the time constraint was applied after which the starting point was (slightly) altered and the option warm-start option for IPOPT was altered. These modifications to the problem were enough to make the solver return an optimal solution.

10.1.4. Fish migration/maximum discharge

This MPC does not regard fish migration, salt water intrusion and maximum discharge in the NZK, things that are taken into account in practice. It is possible to include these constraints in the MPC. Fish migration could be taken into account by penalizing pumping on the maximum discharge, which is the way it is taken into account currently. Salt water intrusion could be taken into account by measuring salinity at certain locations, to constrain the minimum discharge of the NZK when it is above a certain threshold. The maximum discharge of the NZK is applied to enable ship traffic. This is trivial for a single-bucket model. However, when using St. Venant equations and/or multiple buckets in the NZK, this can be taken into account more accurately.

10.2. Simulation

10.2.1. Non-linear estimator of state

Simulate the MPC with a reliable non-linear estimator of state. This gives a higher certainty that the control works on the real system. Software like SOBEK or MIKE11 could be used to simulate the real system in a more reliable way. It was planned to use SOBEK for this study, but the software was not fully developed yet for the implementation of an MPC written in python. Using a reliable simulation software would help with testing whether water-safety constraints are actually never violated. It is recommended to simulate with SOBEK or MIKE11 before implementation in the real system.

10.2.2. Energy use

The energy use of the pumping station is now calculated through the simplified power curve. It is advised to calculate the actual pump-configuration and energy use through the algorithm described in section C.2, or the data-points resulting from that algorithm. This could also be implemented directly in the MPC by changing the solver, as stated before.

10.3. Strategy

10.3.1. Markets

Since the conclusion of this thesis is that the inclusion of the aFRR market could be a valuable addition to the strategy, and Dutch grid. It would be interesting to research the possibility of combining the aFRR with the day ahead market and/or intraday market. The day ahead market could be used to buy the minimum energy needed, and the aFRR could make up the difference between minimum and maximum energy use. This way the risk of not being activated on the aFRR is not important anymore.

Another possible strategy is to bid on the aFRR, but when it is likely to not be activated, buy the energy on the intraday market. However, it is possible that the moment where no downward activation takes place, energy will be scarce and expensive.

10.3.2. Clustering energy use

Rijkswaterstaat possesses many asset. Clustering the energy use of all assets, possibly through an aggregator, could help Rijkswaterstaat participate more in Demand Response. They could use highway lighting for downward activation, by turning on the lights during the day. Highway-tunnel ventilation are also large energy consumers, which could turn off for short times and more often. The ventilation could even be used for the imbalance market. And this way, even pumping station IJmuiden could participate in the balancing markets, since the risks are spread over multiple assets. This increases the total flexibility of the clustered assets.

Besides Rijkswaterstaat's assets, there are many other pumping stations in the Netherlands owned by Waterboards. Clustering the energy use of all pumping stations is also a possibility to increase the flexibility in energy use of pumping stations. The risks can be spread again, and only a minimum amount of energy would be bought on the day ahead market or intraday market. The rest of the energy could be consumed for balancing purposes, and against lower prices.

10.3.3. Optimizing on sustainable energy generation

Rijkswaterstaat indicated that they want to focus on lowering their carbon footprint. This could be achieved through optimization on the day ahead predicted sustainable energy generation and the day ahead predicted total energy generation. This strategy is explained in Appendix E. The uncertainties of these predictions are not publicly available at the data source, so this should be investigated as well.

Even though this could help with achieving extra CO₂-emission savings for Rijkswaterstaat, optimizing on the scarcity in the market would be more beneficial for the energy transition as a whole. Besides that, public money can be saved, which could be invested in other sustainable projects. It is the difference between being a symptom of the energy transition (consuming renewable energy) and enabling the energy transition (actively try to match demand with supply).

10.4. Data availability

Data availability and validity was a large limitation to this study. Optimizations requires large amounts of data, to make its prediction as accurate as possible.

10.4.1. Electricity generation data

The Dutch electricity generation data is very flawed. In Appendix A can be seen how much it was flawed, and how it was edited in such a way that it could be used. Having correct and verified electricity production data publicly available would help to estimate the carbon intensity of the grid. Besides that, many other types of research can be thought of in which this data could be used. It would be advised to legally enforce data availability of energy production, starting at the source. TenneT already shares the data it has with ENTSO-E, but TenneT seemingly does not receive all data from energy producers. It would be advised to implement a law, like the CBS now has to gather data, which forces energy producers to share the generation data with TenneT.

10.4.2. Water system data

Even though there is a dashboard available for water system related data in the Netherlands, it is lacking. Discharge data of rivers is scarce and only daily averages were available. Discharge through structures was not available at all. Besides that, the discharges from the waterboards are not publicly available. Some waterboards could only supply a monthly volume of water. This made it difficult to construct the real scenario in the model.

Rijkswaterstaat and the waterboards are constructing a dashboard in which they all upload their data. I would advise for this dashboard to include predictions of discharge. Either based on a rainfall-runoff model of the area combined with weather predictions, or what the local MPC predicts will be discharged. The latter can make it easier to include all data that might be useful to optimally control the water system.

10.4.3. Intraday market data

The market data is not publicly available. The data was queried at EPEX Group to be used for scientific purposes, but would only be given for a fee of a few thousand euro's. This makes it very difficult to perform research on the market data. The day ahead Market data is publicly available by law. I would recommend to enforce market data availability by law as well. Especially since the market has a high potential for renewable energy trading, research on this market is crucial. Making the data freely available, at least for scientific purposes, would be beneficial for the whole society.

10.5. Further research

10.5.1. Discharge uncertainty

To simulate the effect of discharge uncertainty, the timeseries provided by Rijnland could be decomposed by frequency. This would make it possible to shift the long-frequency data in time and amount. This is a more realistic method than a random deviation, since the uncertainty is not random. The expected discharge could change in shape, damping the peak. Or the peak could be increased, but the length of the peak decreased. This could be simulated with a frequency decomposed signal of the discharge, and then different kinds of changes in expected discharge could be simulated by playing with the decomposed signals.

10.5.2. System's sensitivity to waterboard discharge

It would be interesting to investigate how quickly the system responds to discharge from waterboards. This could make the difference in whether the assumed bucket model is valid or not in the Noordzeekanaal.

10.5.3. Day ahead market deadline

Currently, the bids for the day ahead market are closed at 12:00. Extending the deadline would decrease the uncertainty in predictions that are used for optimization. The easiest solution would be to extend the deadline to the end of the working day (around 18:00) or even to the end of the day (23:00). This would decrease the prediction horizon that is needed by 6 to 11 hours, which would increase the accuracy of the predictions. This would allow for MPC's to make a better plan before bidding on the market.

Another possibility is to implement a receding horizon deadline for the day ahead Market. This way energy could be bought up to 24h before consumption. This would also give better price predictions, since the price of the previous hours is known instead of the whole day at once.

Whether this is possible would depend on the reason why these regulations are in place at the moment. Which is why these new market deadlines should be investigated.

10.5.4. Prediction horizon MPC currently applied

It was brought to my knowledge that the current MPC being applied in IJmuiden is not suitable for a prediction horizon of longer than a day. It should be investigated why this is the case. If this is because of data availability, the planned new dashboard could be the solution. If indeed the prediction horizon could not be longer than a day for this water system, the day ahead market would not be a feasible option anymore. Since a minimum of 1.5 day prediction horizon is currently needed to be able to make a full plan for the next day at the time the bids close.

10.5.5. Price prediction

More work could be put in prediction the day ahead price more accurately. Including exogenous variable (wind, sun-hours, oil prices, ...), which have an influence on the day ahead Price, could make the prediction more accurate. This way, the plan could be improved and the uncertainty over time decreased.

10.5.6. Upscaling

Even though the pumping station in IJmuiden is the largest pumping station in Europe (for now), there are bigger pumping stations in the world.

Rijkswaterstaat is planning on building a pumping station in the Afsluitdijk, and placing generators in the gates. This way the Afsluitdijk could produce as upward and downward regulating volume. It would be interesting to investigate the potential for the Afsluitdijk to participate in Demand Response.

New Orleans also has a large pumping station present since hurricane Katrina, as part of the floodwall. The same methodology as presented in this thesis could be applied to investigate the potential of that pumping station to participate in Demand Response, if it is an electricity-powered pump.

In Abu Dhabi, a large wastewater pump is installed. If retention facilities are present in the system, it could be possible to apply Demand Response on this pump as well. This would be interesting to investigate in the UAE, since solar energy is expected to be or become a large part of the local energy-mix.

Besides international upscaling, smaller Dutch pumping stations are certainly suitable for Demand Response if IJmuiden's pumping station is as well. The case in IJmuiden is a relatively complex one, because of the changes sea-level, many parties discharging into the system and the strict water-safety constraints applied. If Demand Response has potential here, where flexibility is expected to be one of the least, it can be applied on other systems in the Netherlands as well.

10.5.7. Penalty on setpoint deviation

The IJsselmeer and Markermeer have other goals than stabilizing the grid. If a setpoint would be preferred, it is advised to research the ideal setpoint penalty level and function, with respect to with the grid imbalance or energy cost.

10.5.8. Scaling of the objective function

The MPC seems to have difficulties solving the complementary constraint optimally. The optimal relative scaling should be researched, and would probably have to vary every optimization. This could be done by iteratively changing the relative scales until to keep them on optimal relative magnitudes.

10.5.9. Uncertainty of data

The data that was used in this thesis, like the discharge data from Rijkswaterstaat, does not include a description of the measurement error. The same counts for the uncertainty in the predicted energy generation discussed in Appendix E. It would be interesting to research these uncertainty and measurement errors that are present in the data and predictions, to test how well the MPC would perform in reality.

10.6. Personal recommendations

10.6.1. Extending pumping capacity

Rijkswaterstaat is about to start a process of extending the pumping capacity of IJmuiden. When buying extra pumps, it is advised to explore the possibilities for pumps that can quickly turn on and off, and that can change mode more often. This way the concern for increasing maintenance cost due to the wear and tear of starting the pumps more often would be taken away. Besides that, Rijkswaterstaat is planning to place pumps in the Afsluitdijk. The IJsselmeer has a large storage capacity, and adding pumps could increase the balancing capacity of the whole water system.

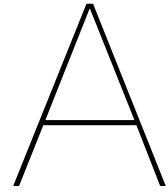
Bibliography

- [1] L.T. Biegler A. Wächter. On the implementation of a primal-dual interior point filter line search algorithm for large-scale nonlinear programming. *Mathematical Programming*, 106(1):25–57, 2006.
- [2] AkzoNobel. Energieopslag in zoutcavernes, 2018. URL <https://www.akzonobel.com/nl/generic-content/energieopslag-zoutcavernes>.
- [3] Max Billib Alcigeimes B. Celeste. The role of spill and evaporation in reservoir optimization models. *Water Resources Managemen*, 2010. doi: 10.1007/s11269-009-9468.
- [4] Remco Bal. Development of the imbalance on the Dutch electricity grid. Master’s thesis, Universiteit Utrecht, 2013.
- [5] Charles Berger. Greenhouse pollution intensity in the victorian brown coal power industry. Technical report, Environment Victoria, Greenpeace, Australian Conservation Foundation, 2005. URL http://environmentvictoria.org.au/wp-content/uploads/2017/03/Greenhouse_Brown_Coal_05.pdf.
- [6] Paolo Bertoldi, Paolo Zancanella, and Benigna Boza-Kiss. Demand Response status in EU Member States. Technical report, European Commission, 2016. URL <https://iet.jrc.ec.europa.eu/energyefficiency/sites/energyefficiency/files/publications/demand{ }response{ }status{ }in{ }eu28{ }member{ }states-online.pdf>.
- [7] P.H. Beuse. Oppervlakte noordzeekanaal/amsterdam-rijnkanaal. Technical report, Rijkswaterstaat Noord-Holland, 2004.
- [8] M.T. Brouwer. Waterbalans noordzeekanaal/amsterdam-rijnkanaal 1998-2000. Technical report, Rijkswaterstaat, 2003. URL <http://edepot.wur.nl/116414>.
- [9] B. Kuijper C. Geerse. Probabilistisch model frequentielijnen ijsselmeergebied: Hoofdrapport van model dezy. Technical report, HKV, 2015.
- [10] David M. Prett Carlos E. Garcia and Manfred Morari. Model predictive control: Theory and practice survey. *Automatica*, 25(3):335–348, 1989. ISSN 09624929. doi: 10.1016/0005-1098(89)90002-2.
- [11] Jesuina Chipindula, Venkata Sai Vamsi Botlaguduru, Hongbo Du, Raghava Rao Kommalapati, and Ziaul Huque. Life cycle environmental impact of onshore and offshore wind farms in Texas. *Sustainability (Switzerland)*, 10(6):1–18, 2018. ISSN 20711050. doi: 10.3390/su10062022.
- [12] Cobouw. Stadsgracht veenendaal, 2009. URL <https://www.cobouw.nl/infra/nieuws/2009/12/stadsgracht-veenendaal-101181756?vakmedianet-approve-cookies=1>.
- [13] European Commission. 2050 low-carbon economy roadmap. Technical report, European Commission, 2016. URL https://ec.europa.eu/clima/policies/strategies/2050_en.
- [14] W.A. Fuller D.A. Dickey. Likelihood ratio statistics for autoregressive time series with a unit root. *Econometrica*, 1981.

- [15] Jacques De Jong, Arndt Hassel, Jaap Jansen, Christian Egenhofer, and Zheng Xu. Improving the Market for Flexibility in the Electricity Sector. Technical report, Centre for European Policy Studies, 2017. URL http://aei.pitt.edu/92294/1/CEPS_{_}TFR_{_}Flexibility_{_}Electricity_{_}Markets.pdf.
- [16] Carlos Bordons Alba Eduardo F. Camacho and C Bordons. *Model Predictive Control*. Springer, 2007. ISBN 9781852336943. doi: 10.1007/978-0-85729-398-5.
- [17] C Eid. Time-based pricing and electricity demand response: Existing barriers and next steps. *Utilities Policy*, 2016. URL <https://www.sciencedirect.com/science/article/pii/S0957178716300947?via%3Dihub>.
- [18] Nationaal Kennis en Innovatieprogramma Water en Klimaat. Hevige buien: het rioolstelsel voorbij, 2012. URL <https://waterenklimaat.nl/onderzoekslijnen/klimaatbestendige-stad/kenniskrant-voor-een-klimaatbestendige-stad/natte-krant/hevige-buien-het-rioolstelsel-voorbij/>.
- [19] ENTSO-E. Entso-e grid map, 2018. URL <https://www.entsoe.eu/data/map/>.
- [20] ENTSO-E. Entso-e transparency platform, 2018. URL <https://transparency.entsoe.eu/>.
- [21] A.G. Maris et al. Rapport deltacommissie. deel 4. bijdragen 3: Beschouwingen over stormvloeden en getijbeweging. Technical report, Rijkswaterstaat, 1961. URL <https://repository.tudelft.nl/islandora/object/uuid:e32906b8-a248-412a-9611-ea28d8a08231?collection=research>.
- [22] European Energy Exchange. Phelix-de futures, 2019. URL <https://www.eex.com/en/market-data/power/futures/phelix-de-futures#!/2018/03/29>.
- [23] R. J. Fokkink. Wind opzet SOBEK-Bekken. Technical report, Rijkswaterstaat, 1998.
- [24] Claire Gavin. Seasonal variations in electricity demand. Technical report, Department of Energy and Climate Change, 2014. URL https://assets.publishing.service.gov.uk/government/uploads/system/uploads/attachment_data/file/295225/Seasonal_variations_in_electricity_demand.pdf.
- [25] Abebe Geletu. Introduction to interior point methods, 2013. URL https://www.tu-ilmeneau.de/fileadmin/media/simulation/Lehre/Vorlesungsskripte/Lecture_{_}materials_{_}Abebe/IPM_{_}Slides.pdf.
- [26] A Goedbloed. Kwaliteitsanalyse Beslissingen Ondersteunend Systeem Noordzeekanaal / Amsterdam-Rijnkanaal. Master's thesis, TU Delft, 2006.
- [27] APX Group. Market results, 2018. URL <https://www.apxgroup.com/market-results/apx-power-nl/dashboard>.
- [28] LLC Gurobi Optimization. Gurobi optimizer reference manual, 2018. URL <http://www.gurobi.com>.
- [29] Theo Brandsma Rudolf Versteeg Kees Peerdeman Hans Hakvoort, Jules Beersma. Nieuwe statistieken: extreme neerslag neemt toe en komt vaker voor. Technical report, HKV, KNMI, 2015. URL <http://edepot.wur.nl/382198>.
- [30] William E Hart, Jean-Paul Watson, and David L Woodruff. Pyomo: modeling and solving mathematical programs in python. *Mathematical Programming Computation*, 3(3):219–260, 2011.
- [31] William E. Hart, Carl D. Laird, Jean-Paul Watson, David L. Woodruff, Gabriel A. Hackebeil, Bethany L. Nicholson, and John D. Sirola. *Pyomo—optimization modeling in python*, volume 67. Springer Science & Business Media, second edition, 2017.

- [32] Chuan et al. He. On the solution of revenue- and network-constrained day-ahead market clearing under marginal pricing-part ii: Case studies. *IEEE Transactions on Power Systems*, 32, 2017.
- [33] HKV. Definitief eindrapport De Ronde Hoep met aanvullingen, 2005.
- [34] HKV. Doorontwikkeling DEZY 2.0. Technical report, HKV, 2016.
- [35] International Energy Agency (IEA). Renewables 2017: Analysis and forecast to 2022. Technical report, International Energy Agency (IEA), 2017.
- [36] IPCC. Climate change 2014: Mitigation of climate change. Technical report, Intergovernmental Panel on Climate Change, 2014. URL https://www.ipcc.ch/pdf/assessment-report/ar5/wg3/WGIIIAR5_SPM_TS_Volume.pdf.
- [37] A. Kalmikov. Wind power fundamentals, 2011. URL <http://web.mit.edu/windenergy/windweek/Presentations/Wind%20Energy%20101.pdf>.
- [38] KNMI. Knmi'14 klimaatscenario's, 2014. URL http://www.klimaatscenarios.nl/scenarios_samengevat/index.html.
- [39] W.F. Koopmans. Een studie naar het afvoerverloop van het stroomgebied van de Eem. Technical report, Provinciale Waterstaat Utrecht, 1982.
- [40] Energie markt informatie. Endex dutch power, 2019. URL https://www.energiemarktinformatie.nl/beurzen/elektra/#stockchart_dpb.
- [41] United Nations. The paris agreement, 2018. URL <https://unfccc.int/process-and-meetings/the-paris-agreement/the-paris-agreement>.
- [42] Arthur Nelsen. Dutch appeals court upholds landmark climate change ruling. *The Guardian*, 2018. URL <https://www.theguardian.com/environment/2018/oct/09/dutch-appeals-court-upholds-landmark-climate-change-ruling>.
- [43] Projectbureau Energiebesparing GWW. Het grootste en zuinigste gemaal van europa, 2004. URL <https://datachallenge.nl/files/Energie%20RWS%20-%20Artikel%20het-grootste-en-zuinigste-gemaal-van-europa.pdf>.
- [44] S Reed. Power prices go negative in germany, a positive for energy users. *New York Times*, 2017. URL <https://www.nytimes.com/2017/12/25/business/energy-environment/germany-electricity-negative-prices.html>.
- [45] Rijkswaterstaat. Publieksfolder peilbesluit ijsselmeergebied. Technical report, Rijkswaterstaat, 2017. URL https://staticresources.rijkswaterstaat.nl/binaries/peilbesluit-ijsselmeergebied-publieksfolder_tcm21-121658.pdf.
- [46] Rijkswaterstaat. Kenmerken ijsselmeer, 2018. URL <https://www.rijkswaterstaat.nl/water/vaarwegenoverzicht/ijsselmeer/index.aspx#21018>.
- [47] Rijkswaterstaat. Kenmerken markermeer, 2018. URL <https://www.rijkswaterstaat.nl/water/vaarwegenoverzicht/markermeer/index.aspx#21018>.
- [48] Rijkswaterstaat. Waterinfo rws, 2018. URL <https://waterinfo.rws.nl/#!/nav/index/>.
- [49] Rijkswaterstaat. Eindrapport "de veiligheid nederland in kaart". Technical report, Rijkswaterstaat, 2014. URL https://staticresources.rijkswaterstaat.nl/binaries/Eindrapport%20Veiligheid%20Nederland%20in%20Kaart_tcm21-63921.pdf.

- [50] J. Perktold S. Seabold. Statsmodels: Econometric and statistical modeling with python. *PROC. OF THE 9th PYTHON IN SCIENCE CONF*, 2010. doi: 10.1007/s00367-011-0258-7. URL <http://statsmodels.sourceforge.net/>.
- [51] M.R. Staats. Using wet appliances for demand side management: current state assessment and potential exploration. Master's thesis, Universiteit Utrecht, 2015. URL <https://dspace.library.uu.nl/handle/1874/316928>.
- [52] Filippo Pecci; Edo Abraham; Ivan Stoianov. Global optimality bounds for the placement of control valves in water supply networks. *Optimization and Engineering*, 2018. doi: 10.1007/s11081-018-9412-7.
- [53] STOWA. Dynamisch peilbeheer. Technical report, STOWA, 2017. URL http://deltaproof.stowa.nl/pdf/Dynamisch_peilbeheer?rId=6.
- [54] T. Gnann et al. The load shift potential of plug-in electric vehicles with different amounts of charging infrastructure. *Journal of Power sources*, 2018. URL <https://www.sciencedirect.com/science/article/pii/S0378775318303720>.
- [55] Xin Tian, Peter Jules van Overloop, Rudy R. Negenborn, and Nick van de Giesen. Operational flood control of a low-lying delta system using large time step Model Predictive Control. *Advances in Water Resources*, 75:1–13, 2015. ISSN 03091708. doi: 10.1016/j.advwatres.2014.10.010. URL <http://dx.doi.org/10.1016/j.advwatres.2014.10.010>.
- [56] T.Q. Péan et al. Review of control strategies for improving the energy flexibility provided by heat pump systems in buildings. *Journal of Process control*, 2017. URL <https://www.sciencedirect.com/science/article/pii/S0959152418300489>.
- [57] Bouwput Utrecht. Herstel singel, 2010. URL <http://www.bouwpututrecht.nl/herstelde-singel/>.
- [58] P.J. van Overloop. *Model Predictive Control on Open Water Systems*. PhD thesis, TU Delft, 2006.
- [59] R.D. van Weissenbruch. Onderzoek energieverbruik gemaal ijmuiden. Master's thesis, TU Delft, 2003.



Appendix A

A.1. Energy production data correction

When the energy production data was downloaded from the ENTSO-E transparency platform, there were holes in the data and the total amount of energy generated was not in line with what the Centraal bureau van de Statistiek (CBS) reports. In this appendix will be discussed how the data was edited to get a more complete view of the actual power generation in the Netherlands.

Yearly electricity generation [MWh] of the Netherlands by source (CBS)

Year	Biomass	Coal	Gas	Nuclear	Solar	Wind	Total
2015	4930000	39534307	45881465	4078041	1121509	7549873	110086512
2016	4904580	36720172	52567425	3960278	1559424	8170458	115170275
2017	4645000	31134229	57216971	3402478	2149000	10569000	116412928

Table A.1: Yearly electricity production of the Netherlands by source [CBS]

A.1.1. Biomass

The amount of electricity generated with biomass was grossly underestimated by the data. But as can be seen in picture A.1, there is only a relatively small gap in the data in 2017. The gap was filled by linearly interpolating between the hours of the days around the data-gap, keeping a daily pattern in place.

Besides that, CBS' report of the total amount of electricity generated with biomass can be seen in table A.1. The data provided by ENTSO-E was linearly increased to achieve the same total energy generation. The factor with which the data was increased for 2015 was 15.5, for 2016 it was 14.2 and for 2017 it was 13.5. The resulting generation timeseries can be seen in picture A.2.

A.1.2. Coal

The amount of energy generated by coal power-plants (CPP) in the Netherlands is relatively high in the Netherlands, as can be seen in table A.1. Only electricity generated with gas exceeds this amount. However, the generation data for coal is almost empty from 2016 onward. In 2015, some full months without gaps are present. The raw data can be seen in picture A.3. Two months were taken as representative months for a year; February and August. A warm and a cold month in order to maintain a seasonal difference. The cold month (February) was used to represent the pattern of generation in January, February, March, November and December. The warm month (August) was used to represent the pattern in May, June, July, August and September. For the months of April and October a mix of the warm and cold months was taken. The pattern of the warm and cold months have been

applied with a weight of how close the cold and warm months are. So at the 1st of April, the pattern is the one of the cold months, while on the 30th of April the pattern is the one of the warm months. On the 15th of April, it is 50% influenced by the warm-pattern and 50% influenced by the cold-pattern.

After this was done, the timeseries was linearly increased by year to have the same total production as CBS reported. The resulting timeseries can be seen in figure A.4. The factors by which the data was increased are 11.2 in 2015, 10.4 in 2016 and 8.8 in 2017.

A.1.3. Gas

Gas is the largest energy-source in the Netherlands, and the timeseries provided by ENTSO-E is hardly showing any gaps (see figure A.5). The small gaps that were there were linearly interpolated between the same times of the days surrounding the data-gap. However, the total amount of energy produces is still too little. The factors that were used to make the total yearly production equal to CBS' report are 2.2 in 2015, 2.1n in 2016 and 1.7 in 2017. The resulting timeseries can be seen in figure A.6.

A.1.4. Nuclear

The data of nuclear energy produced in the Netherlands was showing some gaps and what are assumed to be faulty-zeros (see figure A.7). This assumption is based on the fact that it is hard, if not impossible, but at least very impractical, to shut down a nuclear power plant to boot it up again later. This is why all the datapoints that show less than 500 MW generation are put to NaN values, which are later linearly interpolated between the same times of the surrounding days. By doing this, the total amount of nuclear energy produced in a year according to CBS is more than the timeseries show. The dataset was decreased with a factor 0.86 in 2015, 0.84 in 2016 and 0.73 in 2017. The resulting timeseries can be seen in figure A.8.

A.1.5. Solar

Solar energy is on the rise in the Netherlands. CBS' report show an increase of almost 50% per year. The data is also showing relatively little gaps compared to other sources (figure A.9). The gaps that were present were filled by linearly interpolating between the hours of the surrounding days. After that, the annual solar energy production was still off, so the complete series was multiplied by a factor 1.1 in 2015, 1.01 in 2016 and 1.14 in 2017. The resulting timeseries can be seen in figure A.10.

A.1.6. Wind

Wind energy is recorded from two separate sources; onshore and offshore wind energy. However, CBS only records the amount of wind energy that is produced in total. The timeseries were kept separate, since lifetime CO₂ emissions are higher for offshore wind than onshore wind [11]. The data of offshore wind generation shows a big gap in the beginning of the time-series (see figure A.12), the same months the next year were taken as representative patterns for these months. The onshore wind energy production shows little to no gaps (figure A.11). The gaps in either the on- or offshore wind production data were linearly interpolated between the same hours of the surrounding days. After which the sum of the two was taken and compared with CBS' report. Both datasets were decreased with a factor 0.93 in 2015, 0.97 in 2016 and 0.96 in 2017 to have the same total amount of wind energy as CBS reported. The resulting timeseries can be seen in figures A.13 and A.14.

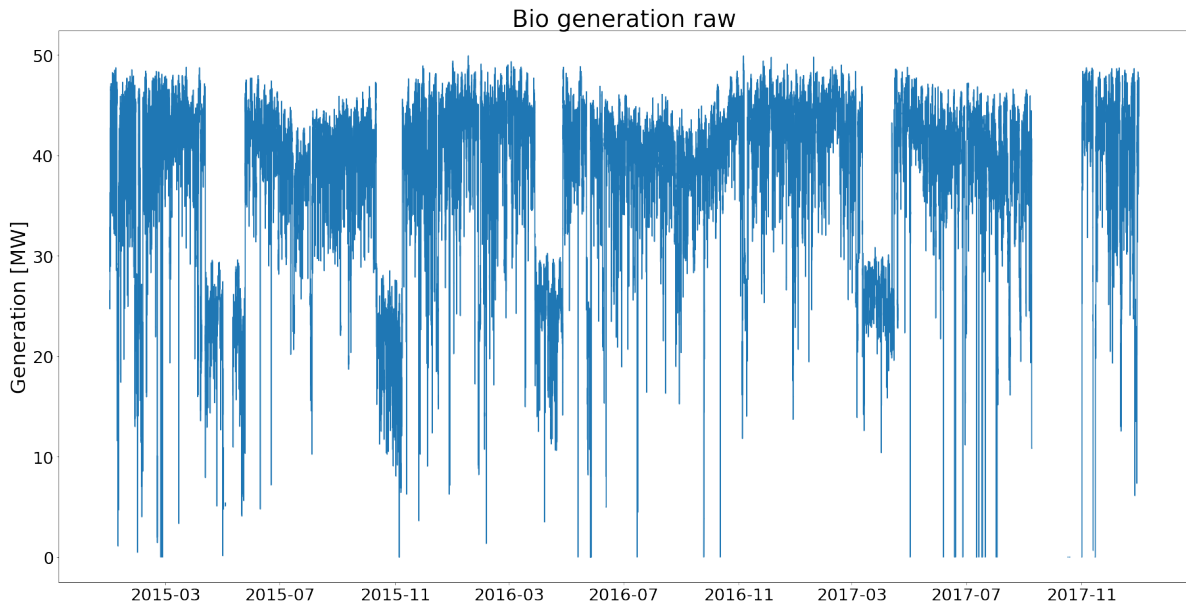


Figure A.1: Electricity generation with biomass, raw data. [ENTSO-E]

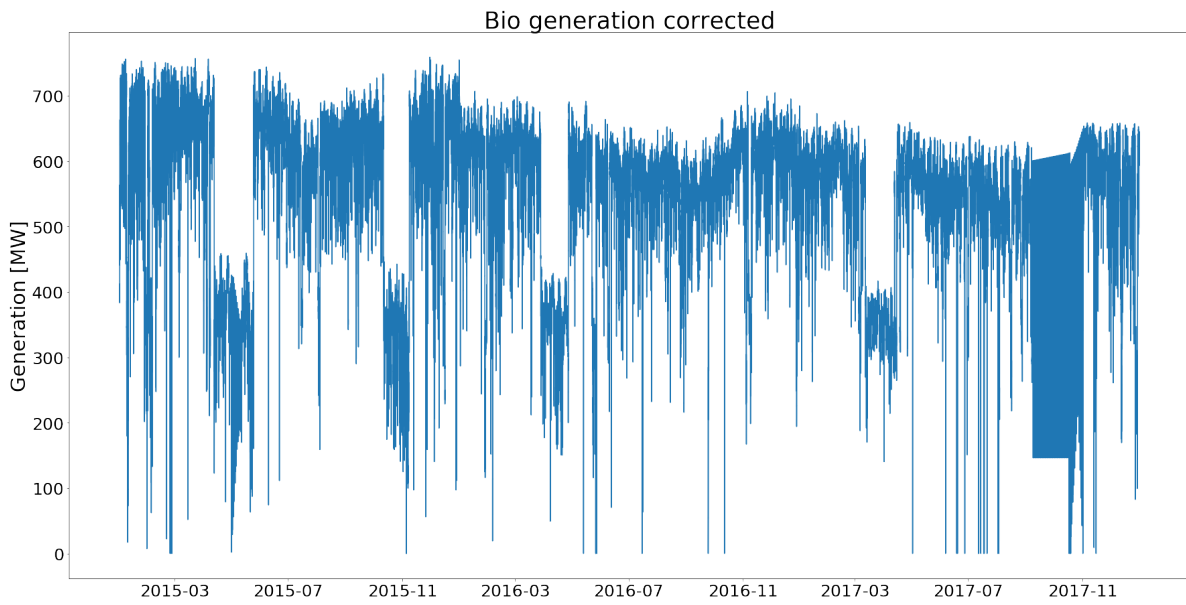


Figure A.2: Electricity generation with biomass, corrected data.

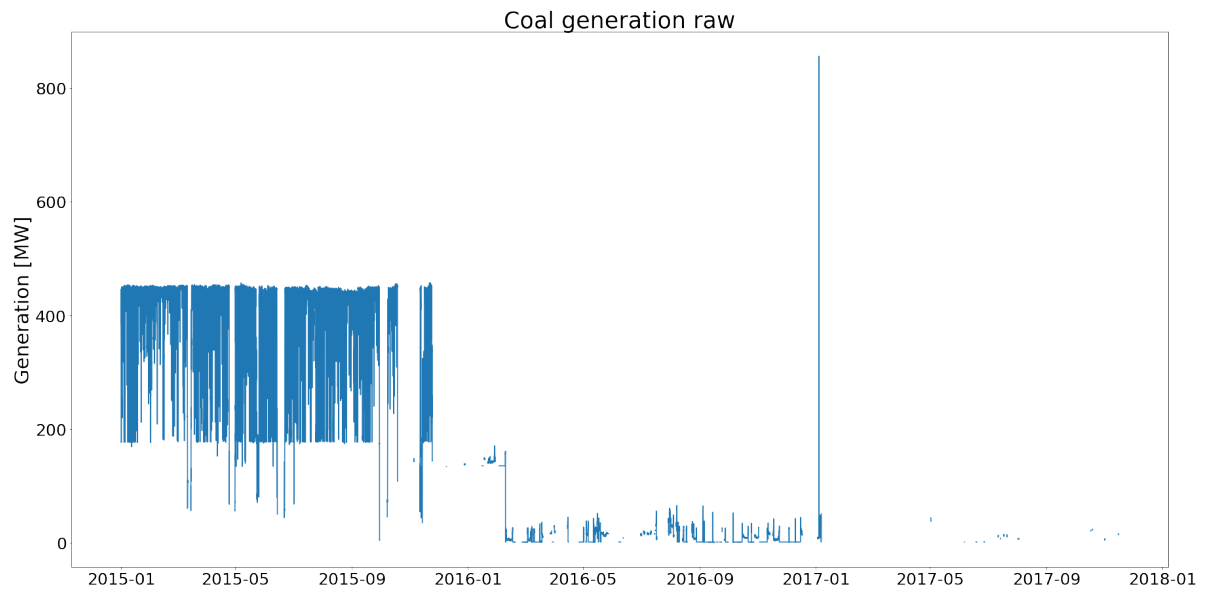


Figure A.3: Electricity generation with coal, raw data. [ENTSO-E]

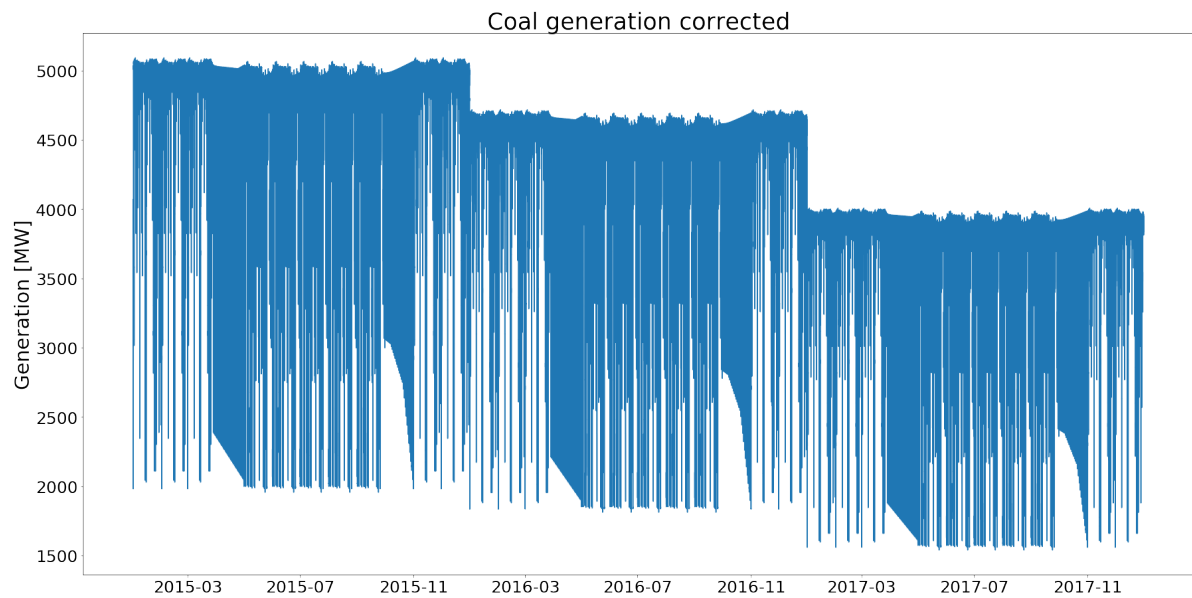


Figure A.4: Electricity generation with coal, corrected data.

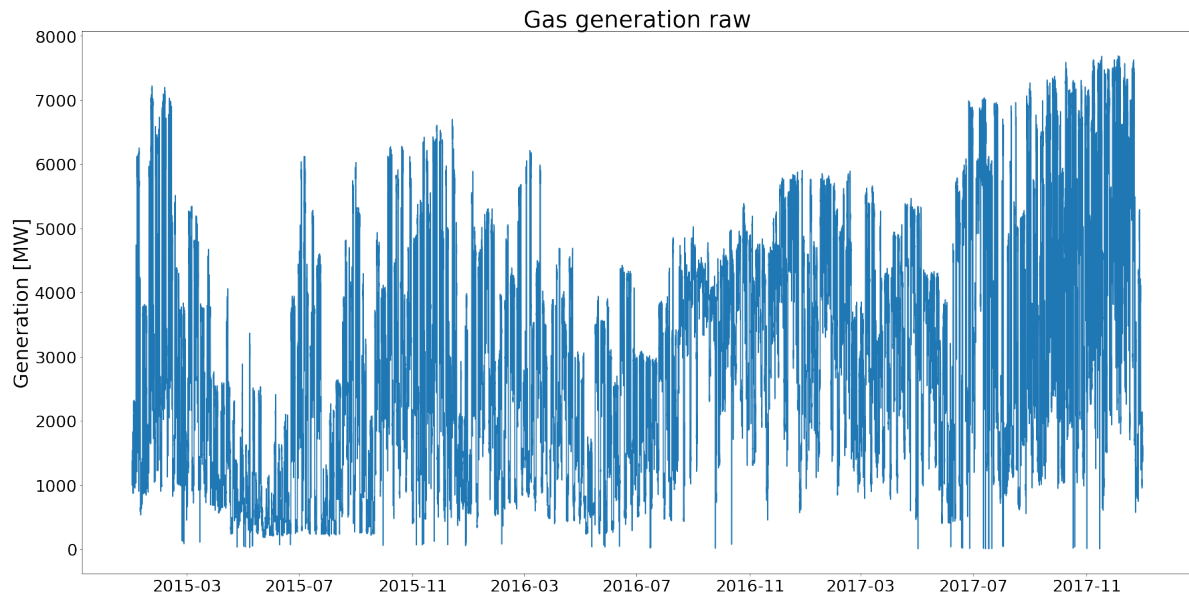


Figure A.5: Electricity generation with gas, raw data. [ENTSO-E]

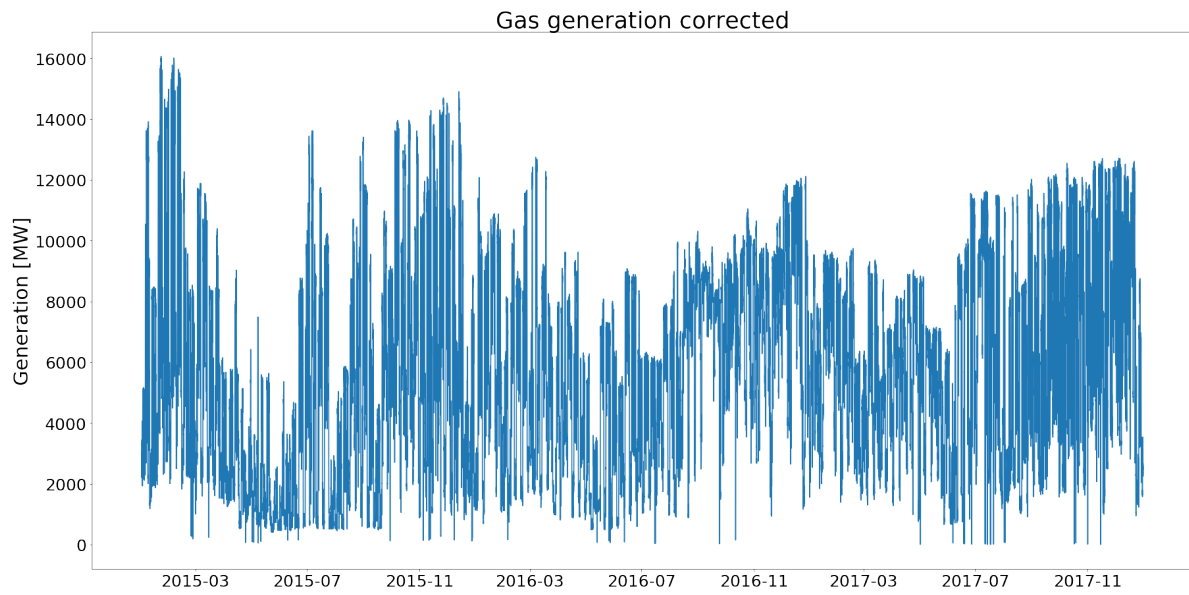


Figure A.6: Electricity generation with gas, corrected data.

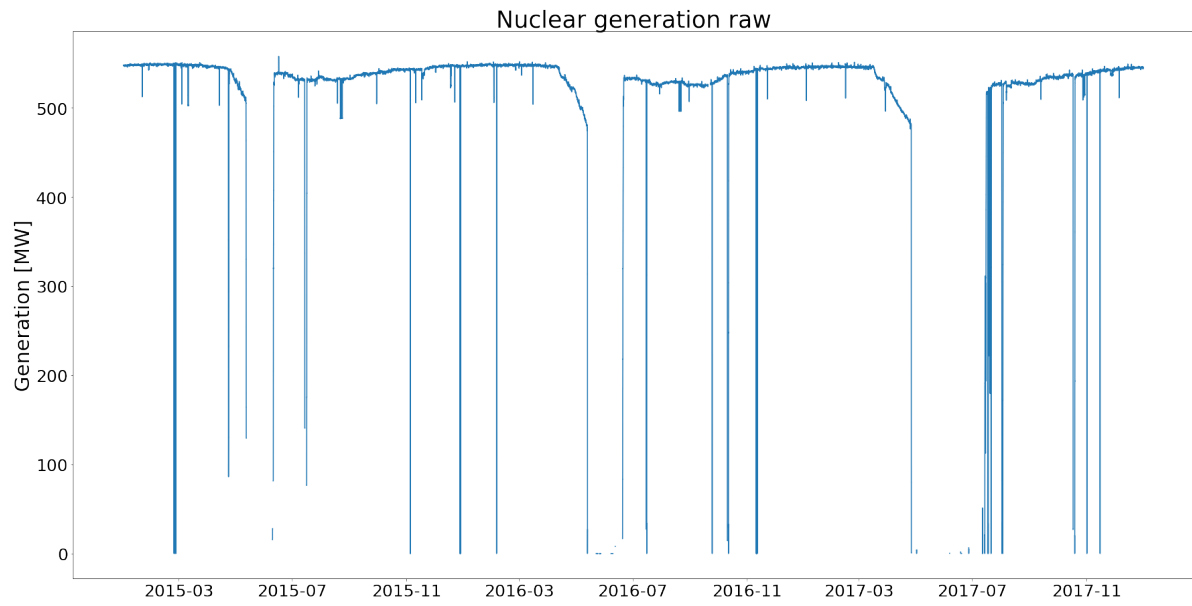


Figure A.7: Electricity generation by nuclear energy, raw data. [ENTSO-E]

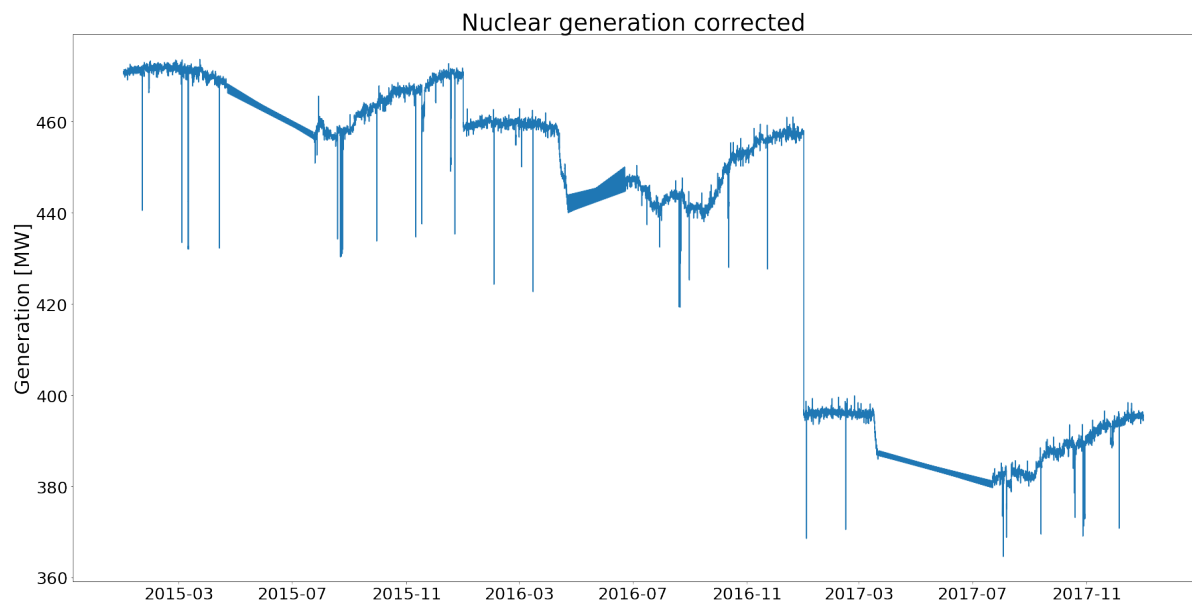


Figure A.8: Electricity generation by nuclear energy, corrected data.

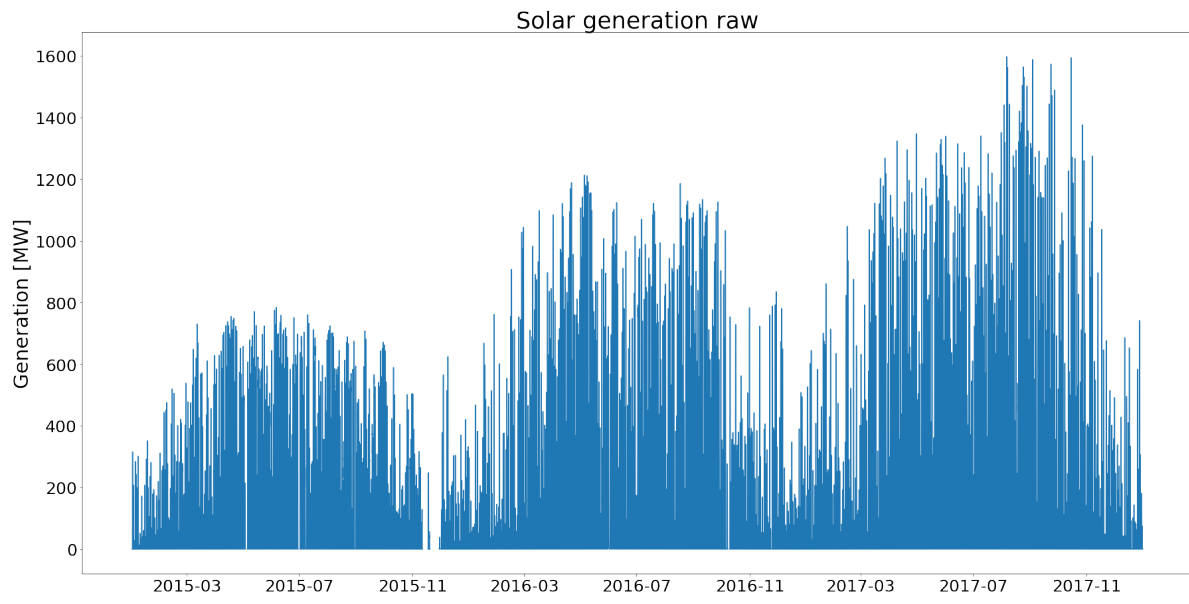


Figure A.9: Electricity generation with solar energy, raw data. [ENTSO-E]

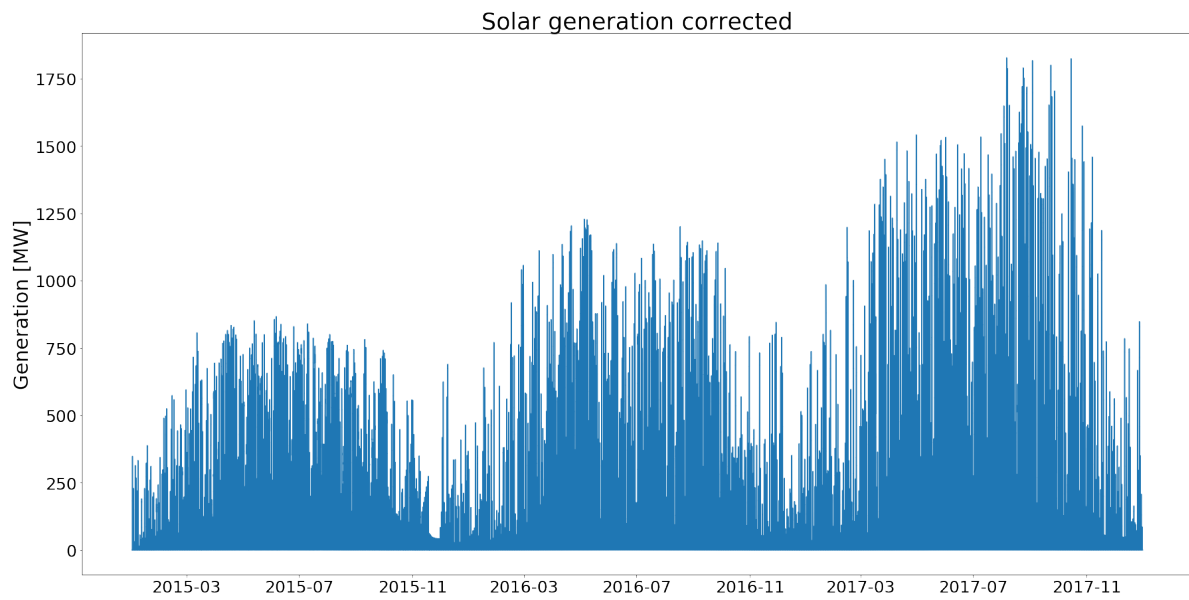


Figure A.10: Electricity generation with solar energy, corrected data.

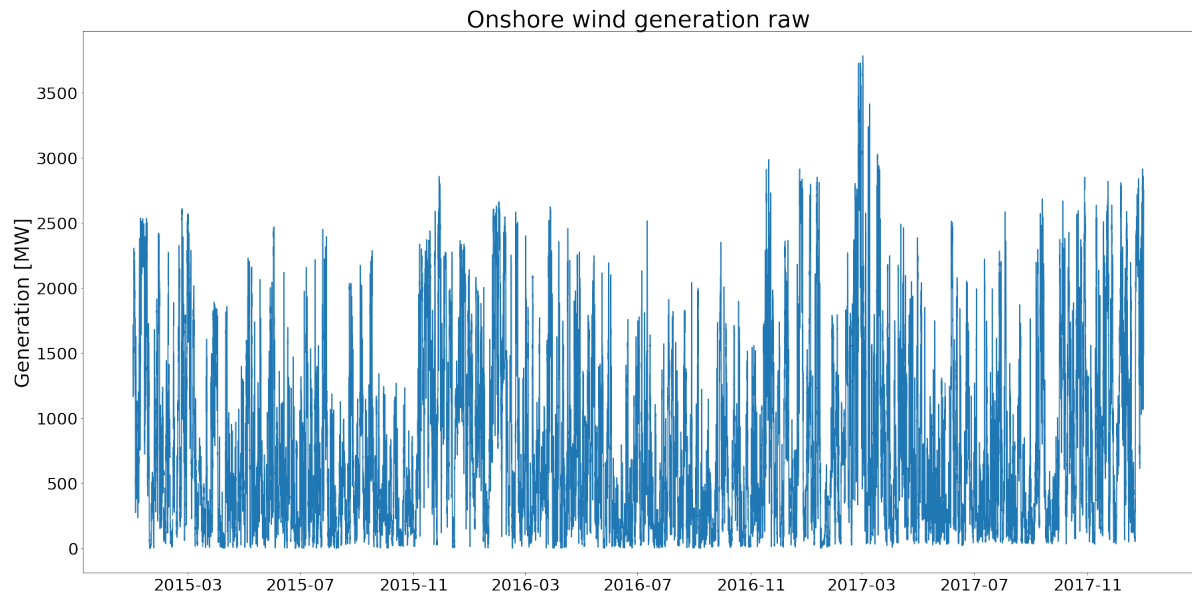


Figure A.11: Electricity generation with onshore wind energy, raw data. [ENTSO-E]

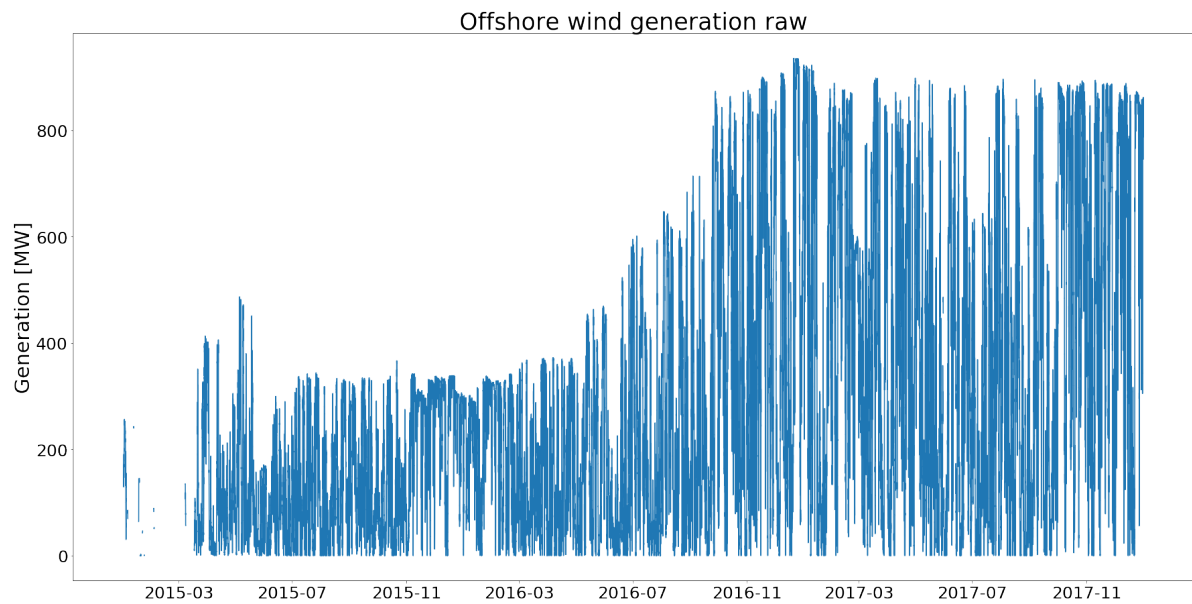


Figure A.12: Electricity generation with offshore wind energy, raw data. [ENTSO-E]

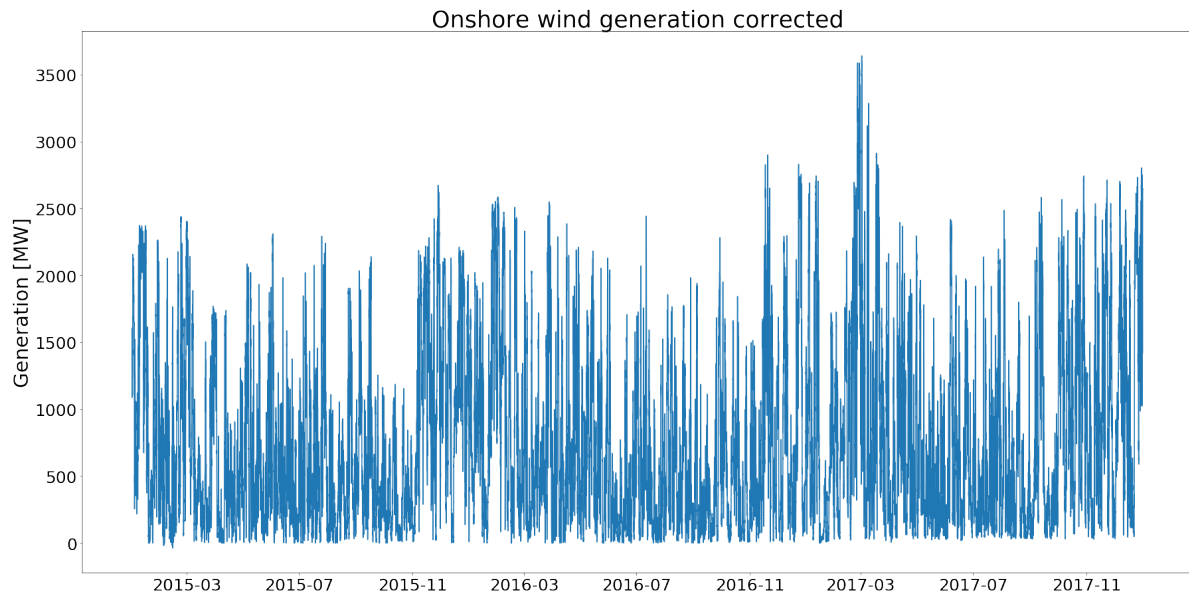


Figure A.13: Electricity generation with onshore wind energy, corrected data.

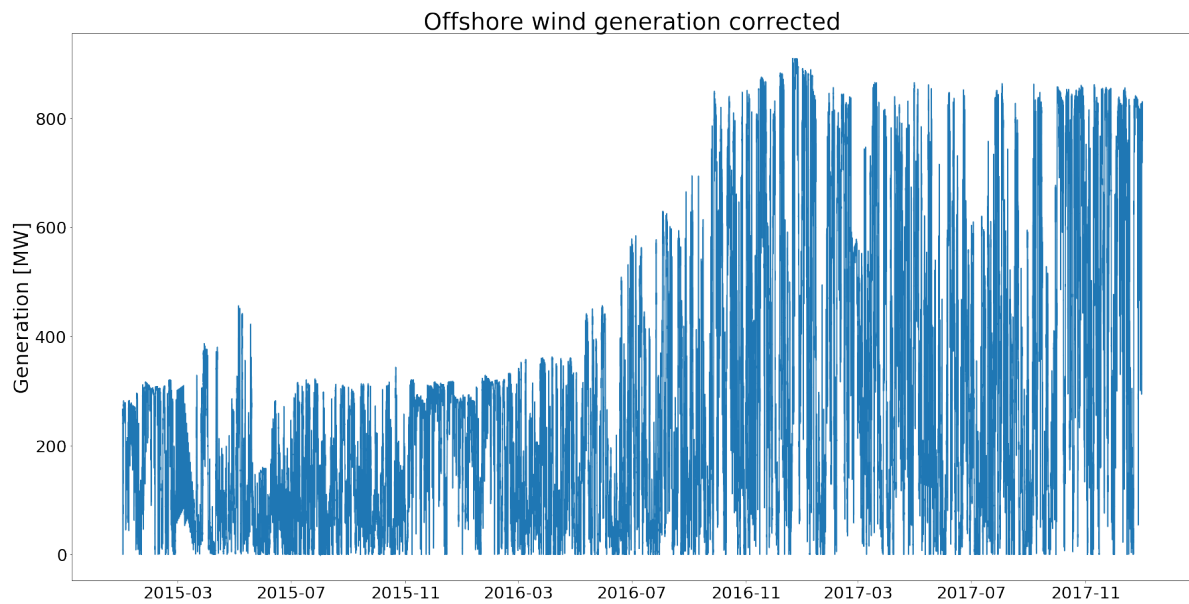


Figure A.14: Electricity generation with offshore wind energy, corrected data.

B

Appendix B

B.1. aFRR market analysis

To analyze the amount of times the pumping station would be activated on the aFRR market, an analysis has been performed based on historic market data. Multiple fixed bid-prices have been determined, with the current energy-price RWS (€84,-/MWh) pays as maximum. In this analysis, only downward regulating volume was analyzed, since this study focusses on energy consumption. For further research it might be interesting to investigate the upward regulating possibilities for IJmuiden.

B.1.1. Downward regulating bids, activations and price

The bids for the markets were analyzed and can be seen in figure B.1. The bids are done in power [MW] and for a duration of 15 minutes (excluding the 15min activation time). It can be seen that from March 2016 it never occurred anymore that no downward regulating bids were made. This helps with the balance of the grid.

In figure B.2, the amount of downward regulating volume that was activated in that period can be seen. The volume is shown in energy [MWh], instead of power [MW]. The graph shows that it almost never occurs that no downward regulating volume is active, which is a good sign for IJmuiden and RWS.

In figure B.3, the downward regulating price can be seen. This is the price that the balancing party pays to activate; a negative price means the balancing party receives money to use energy. Generally, one needs to pay to use energy. But when the imbalance is high enough, highly negative bid prices will be activated, which means the balancing party can receive up to €500,-/MWh to consume energy.

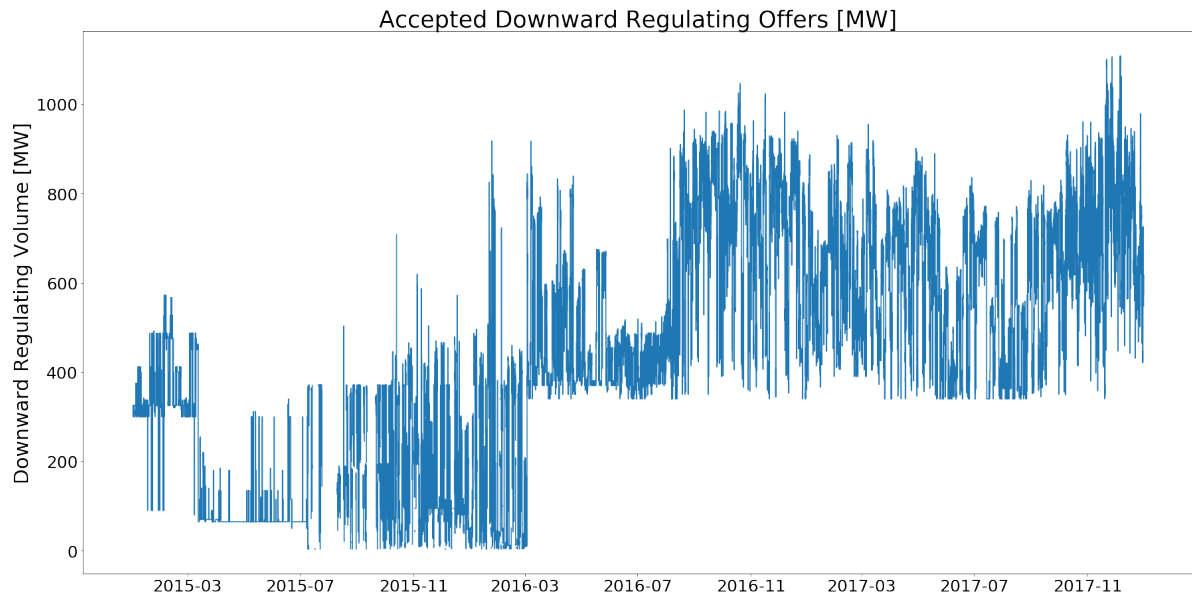


Figure B.1: Downward regulating bids

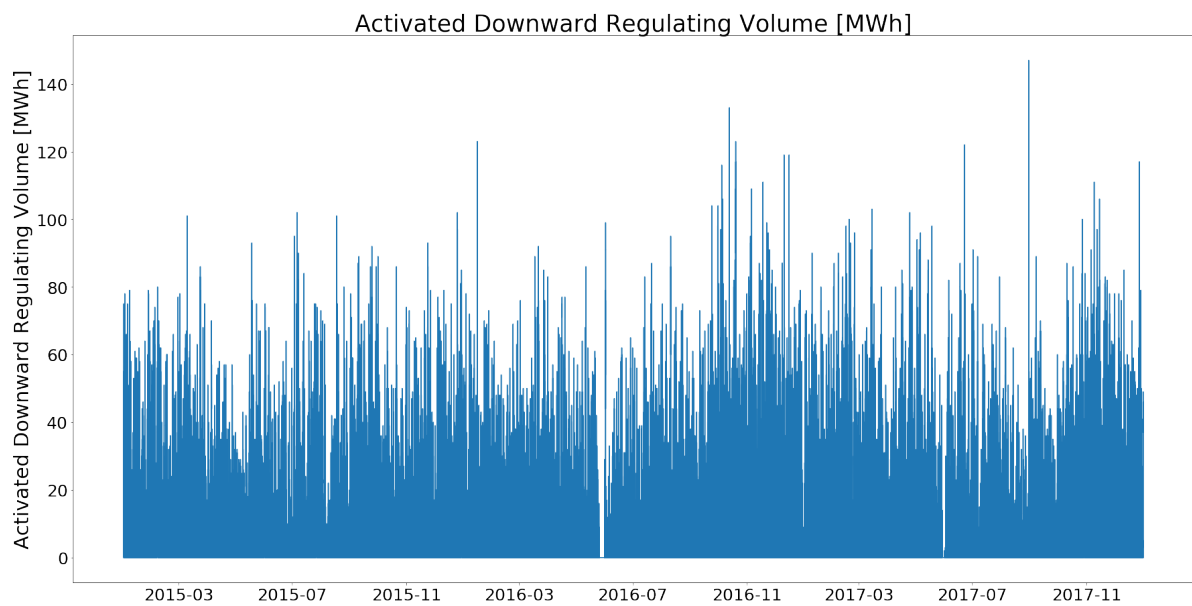


Figure B.2: Activated downward regulating volume

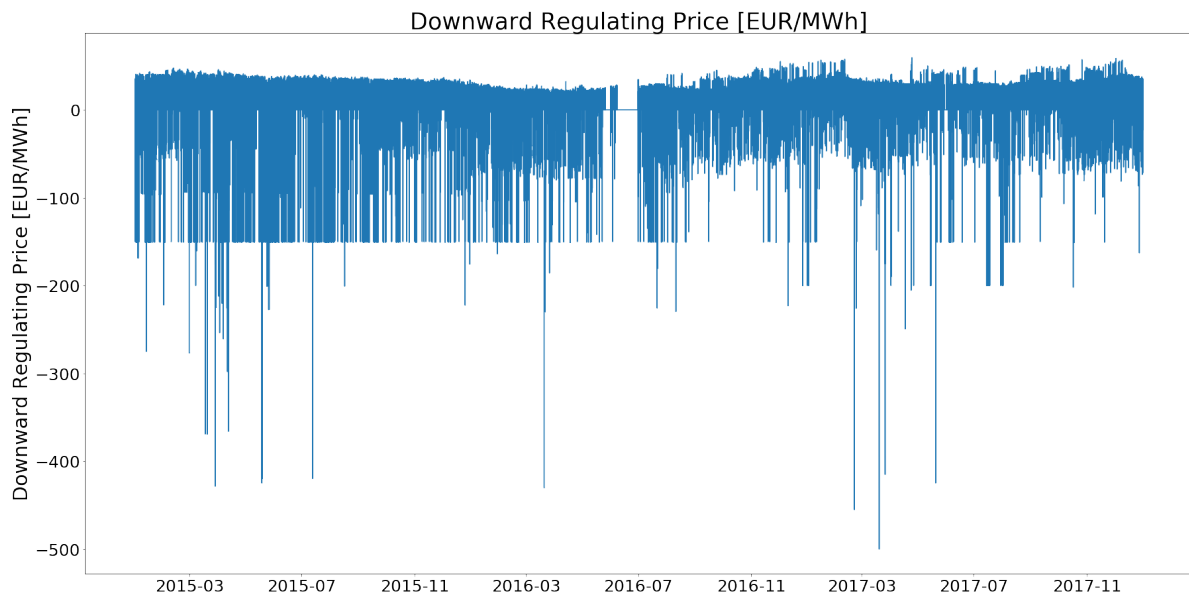


Figure B.3: Downward regulating price

B.1.2. Activation time and probability

To investigate the ideal bid-price for RWS when participating on the aFRR market, multiple prices are analyzed, together with an activation sequence. It is assumed that when RWS' bid would be higher (RWS would pay more to be activated) than the downward regulating price at that moment, while a downward regulating volume is activated, pumping station IJmuiden would be activated.

Then the analysis looks at the amount of times this occurs in a sequence (of 15 minutes per slot). Since RWS indicated that a longer activation sequence is preferred to prevent maintenance costs from rising too much, sequence lengths of 15, 30, 45, 60 and 120 minutes are investigated.

B.1.2.1. P = €84,-/MWh

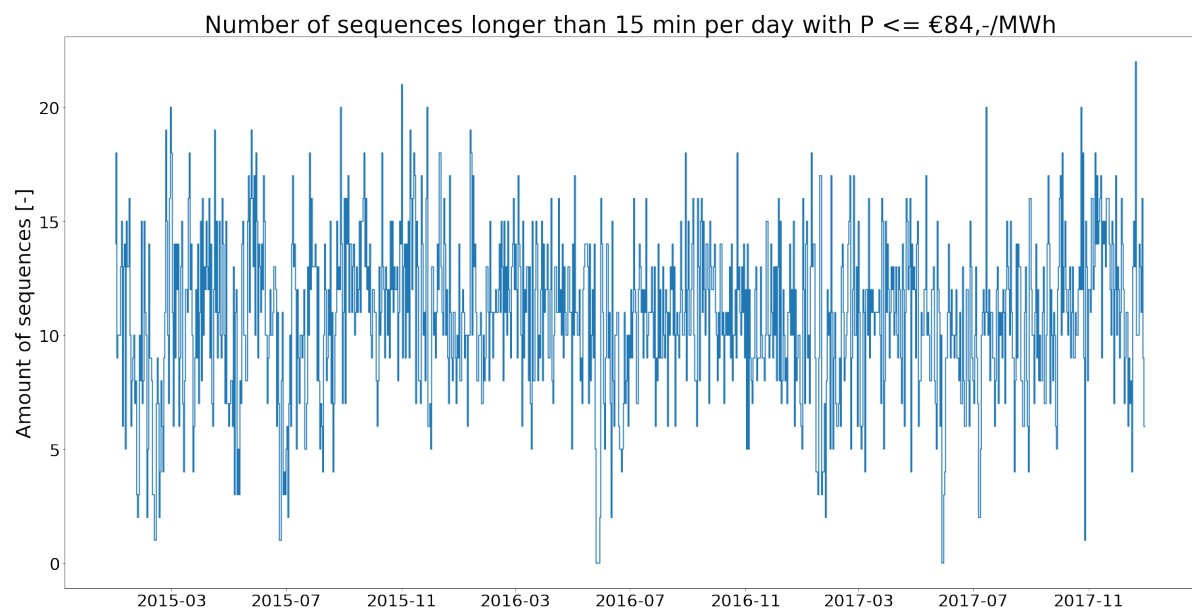


Figure B.4: Amount of times downward regulating occurred with P ≤ €84,-/MWh with an activation time of 15 minutes or longer

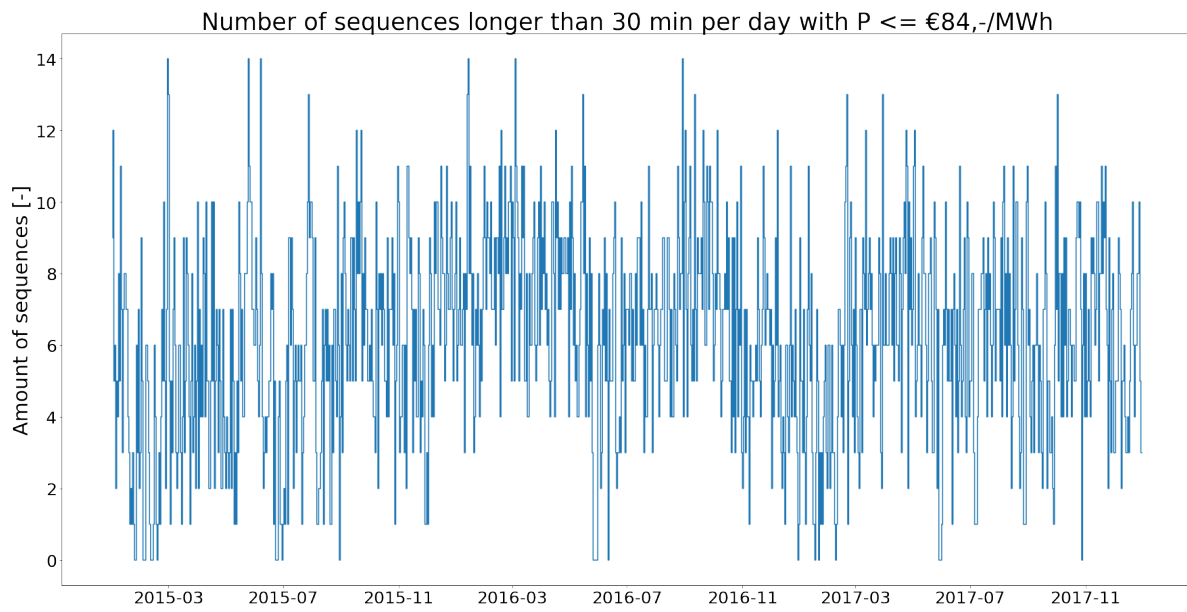


Figure B.5: Amount of times downward regulating occurred with $P \leq €84,-/MWh$ with an activation time of 30 minutes or longer

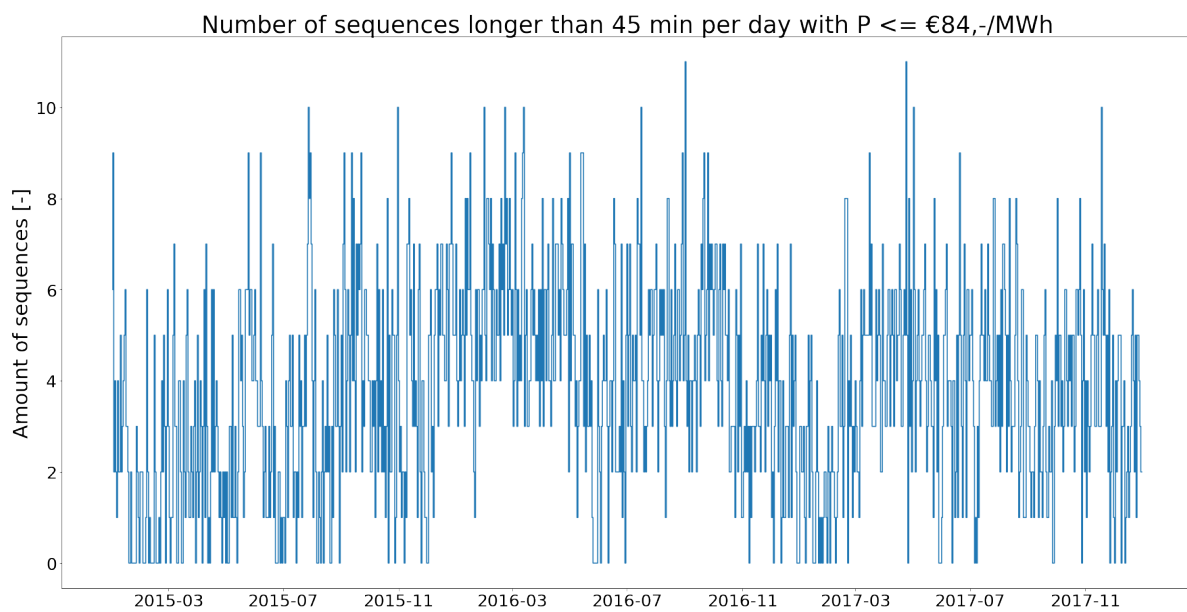


Figure B.6: Amount of times downward regulating occurred with $P \leq €84,-/MWh$ with an activation time of 45 minutes or longer

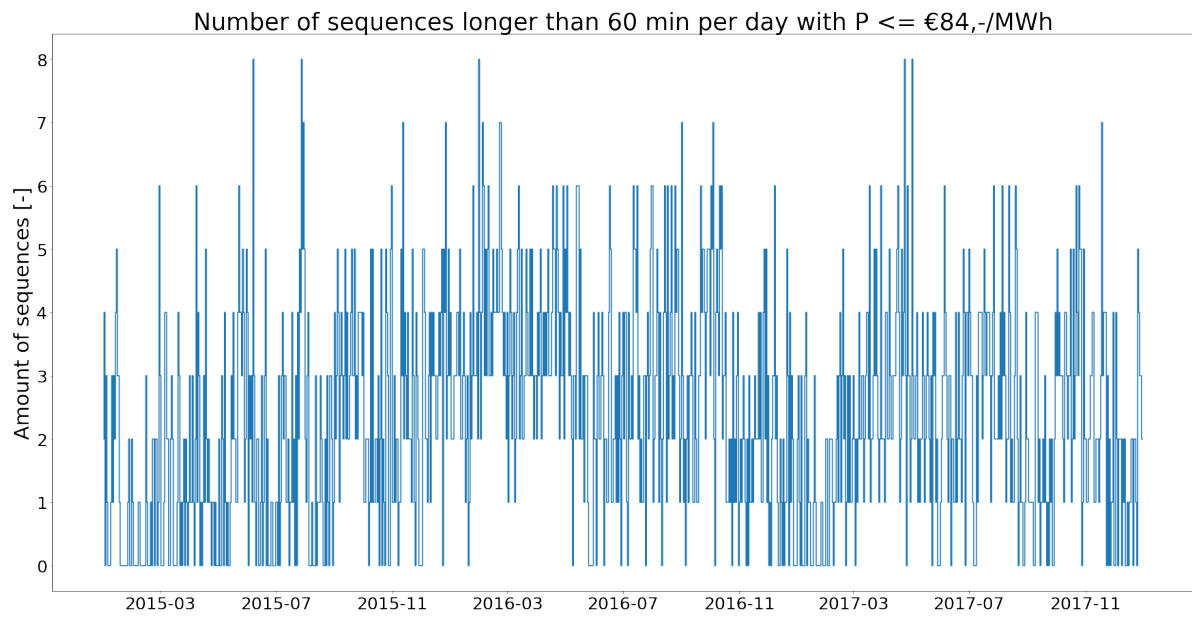


Figure B.7: Amount of times downward regulating occurred with $P \leq \text{€}84,-/\text{MWh}$ with an activation time of 60 minutes or longer

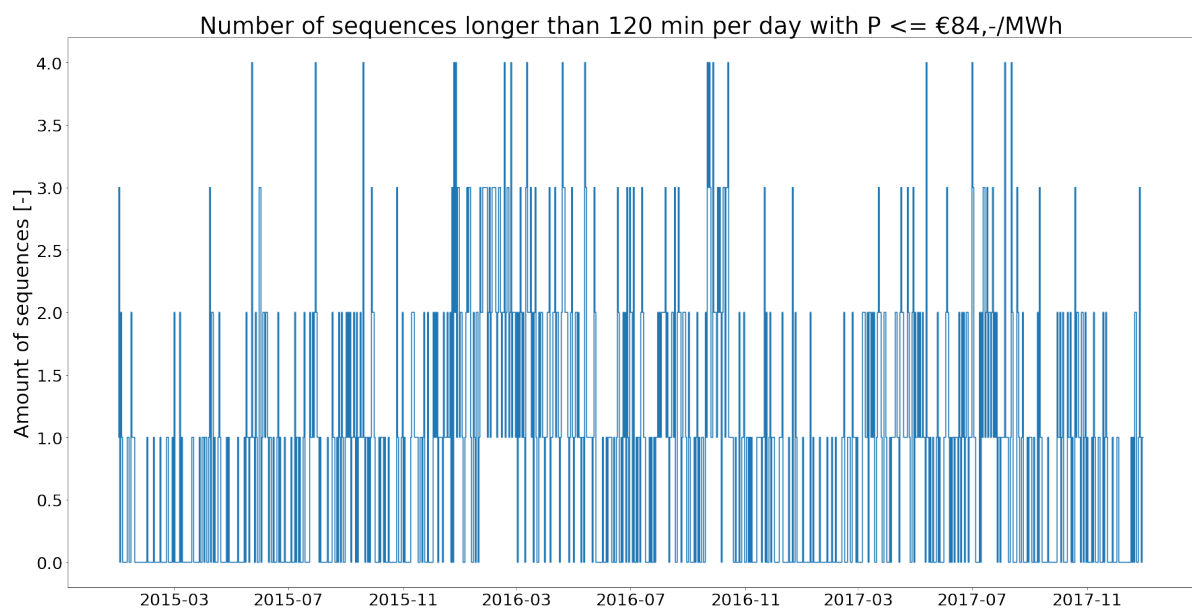
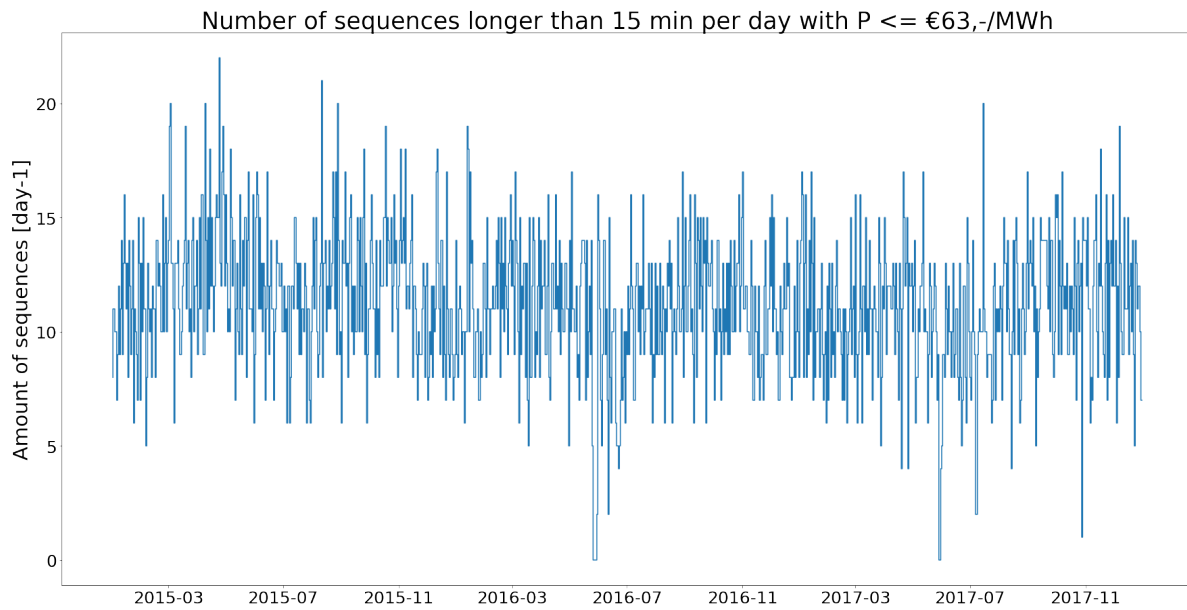
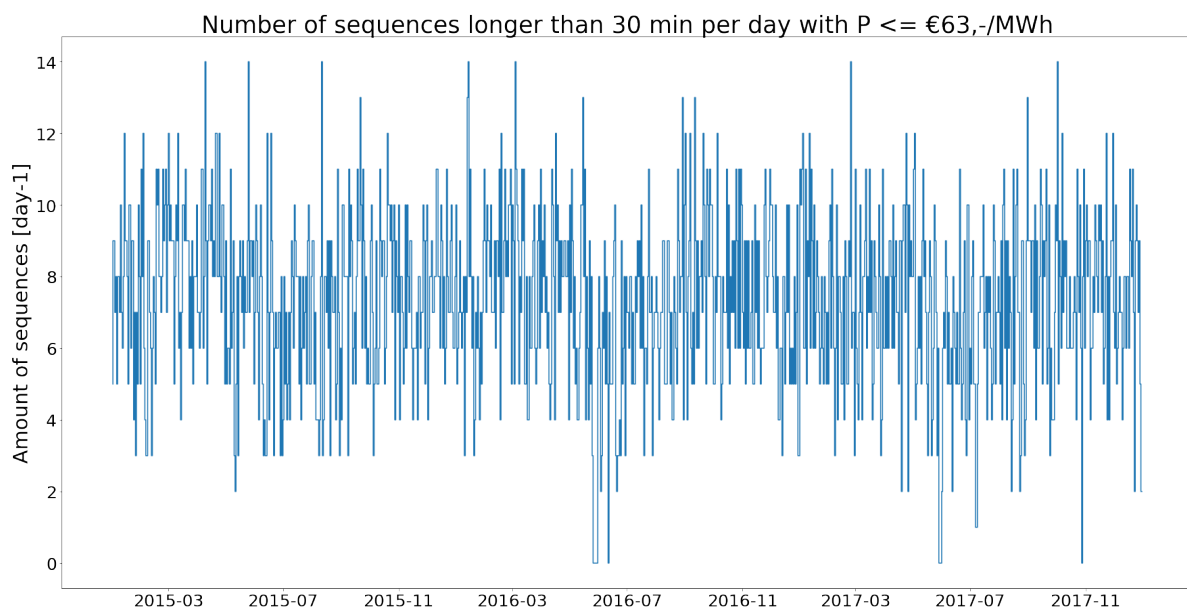


Figure B.8: Amount of times downward regulating occurred with $P \leq \text{€}84,-/\text{MWh}$ with an activation time of 120 minutes or longer

B.1.2.2. P = €63,-/MWhFigure B.9: Amount of times downward regulating occurred with $P \leq €63,-/MWh$ with an activation time of 15 minutes or longerFigure B.10: Amount of times downward regulating occurred with $P \leq €63,-/MWh$ with an activation time of 30 minutes or longer

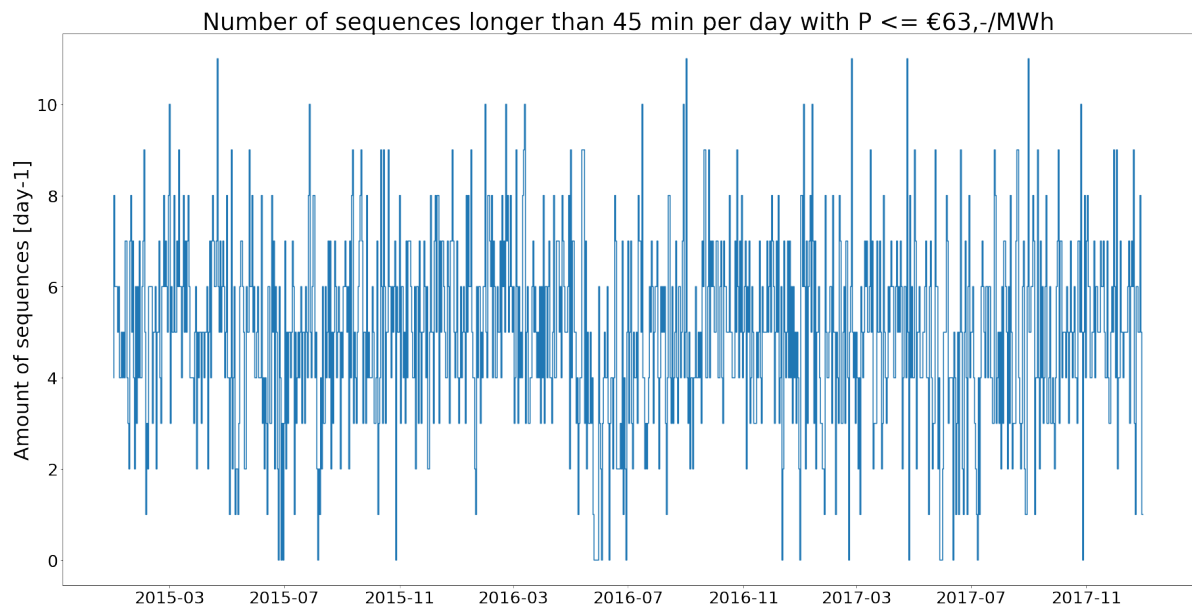


Figure B.11: Amount of times downward regulating occurred with $P \leq \text{€}63,-/\text{MWh}$ with an activation time of 45 minutes or longer

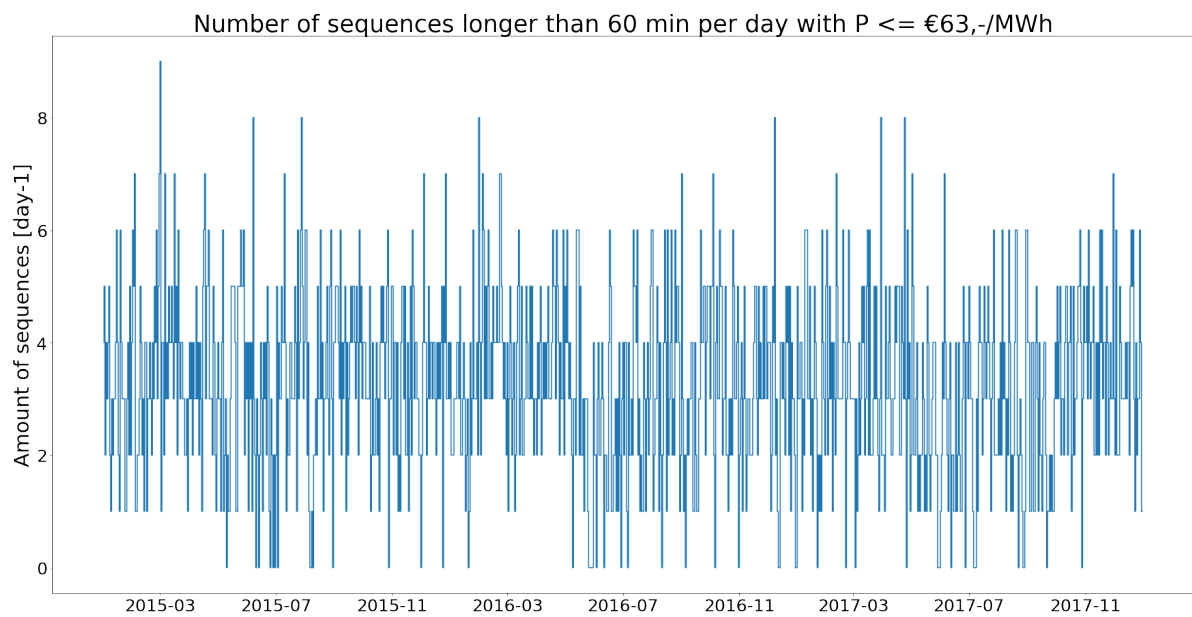


Figure B.12: Amount of times downward regulating occurred with $P \leq \text{€}63,-/\text{MWh}$ with an activation time of 60 minutes or longer

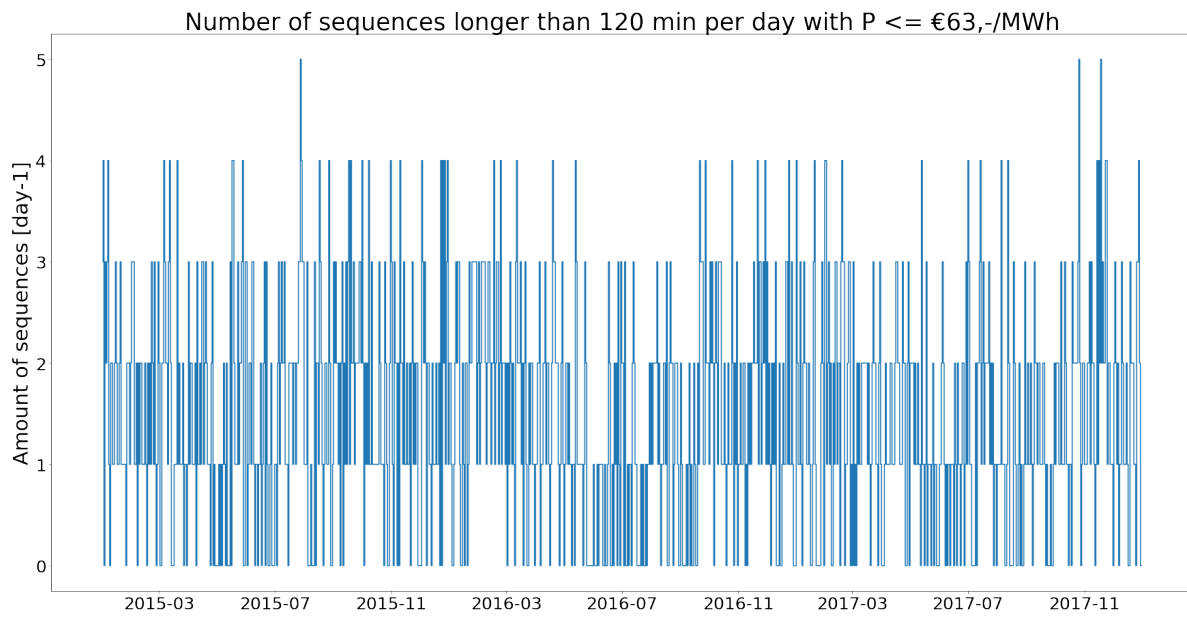


Figure B.13: Amount of times downward regulating occurred with $P \leq €63,-/MWh$ with an activation time of 120 minutes or longer

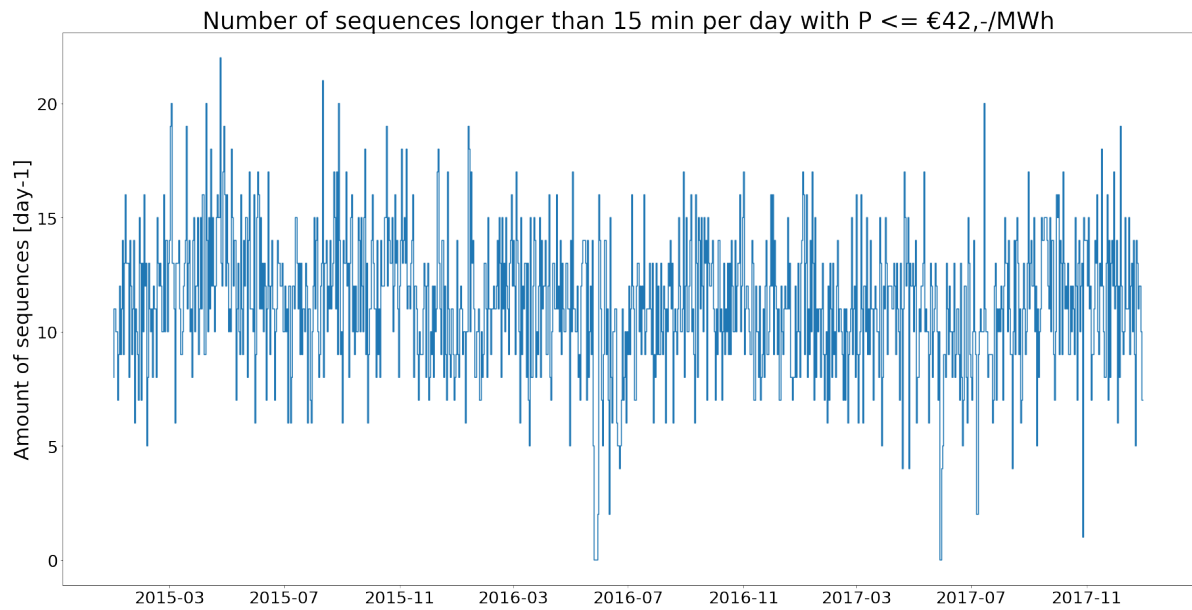
B.1.2.3. P = €42,-/MWh

Figure B.14: Amount of times downward regulating occurred with P ≤ €42,-/MWh with an activation time of 15 minutes or longer

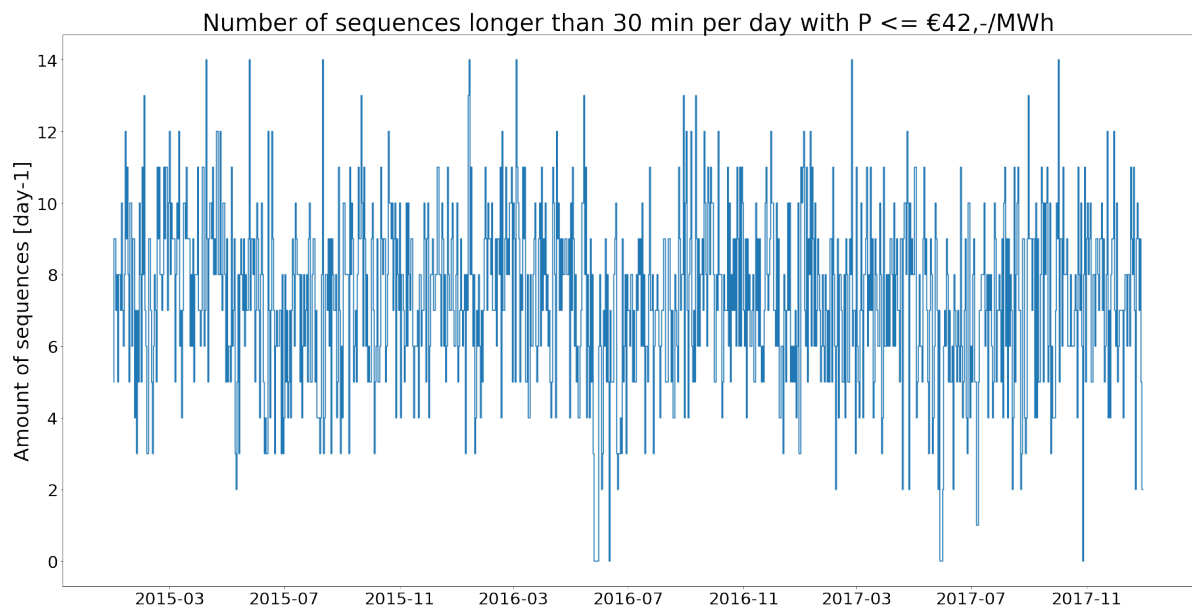


Figure B.15: Amount of times downward regulating occurred with P ≤ €42,-/MWh with an activation time of 30 minutes or longer

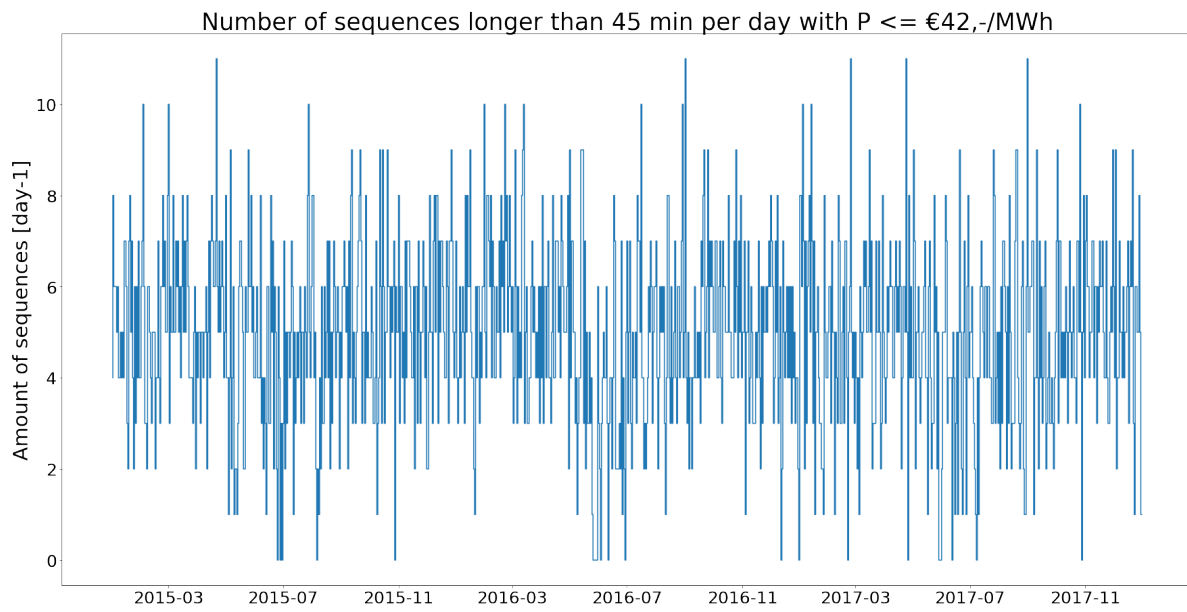


Figure B.16: Amount of times downward regulating occurred with $P \leq \text{€}42,-/\text{MWh}$ with an activation time of 45 minutes or longer

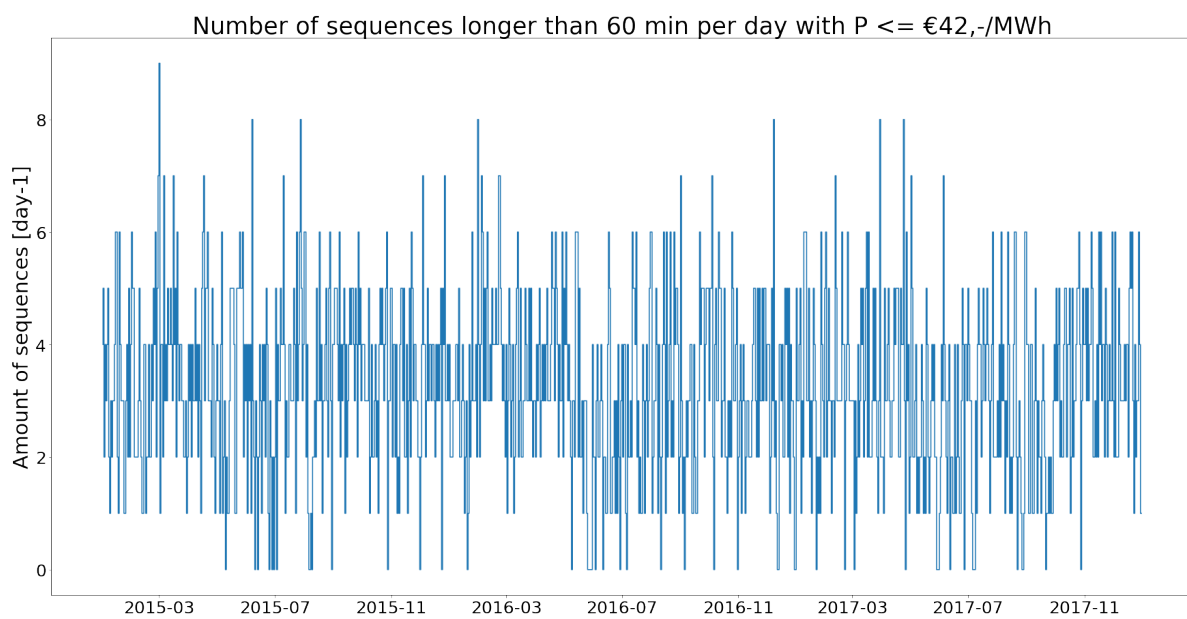


Figure B.17: Amount of times downward regulating occurred with $P \leq \text{€}42,-/\text{MWh}$ with an activation time of 60 minutes or longer

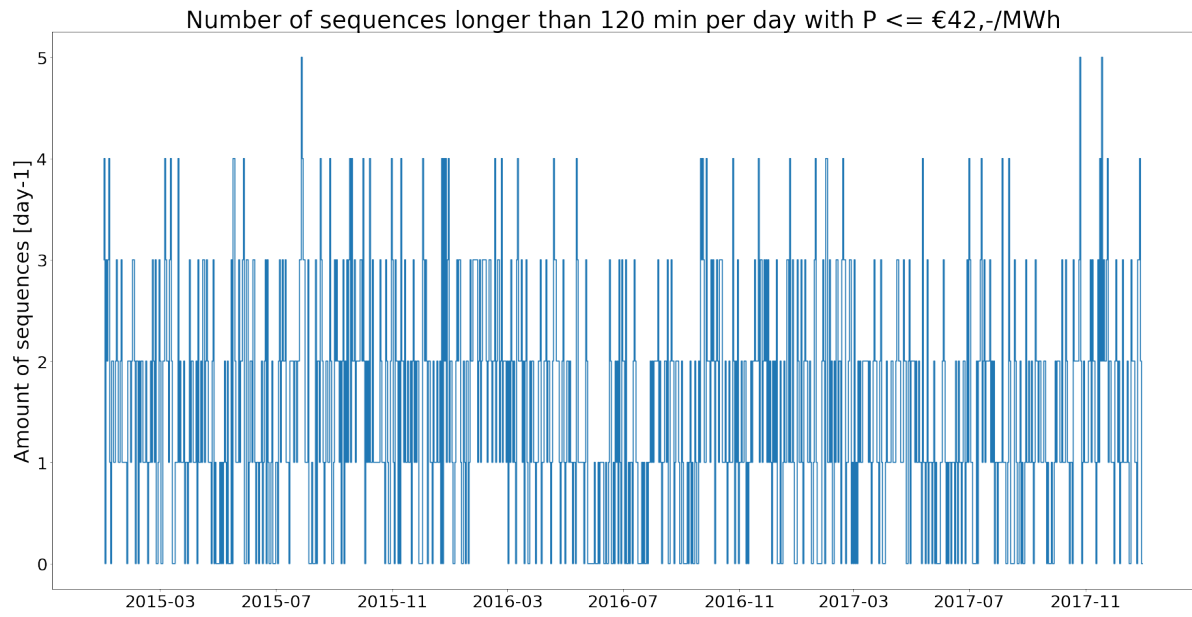


Figure B.18: Amount of times downward regulating occurred with $P \leq \text{€}42,-/\text{MWh}$ with an activation time of 120 minutes or longer

B.1.2.4. P = €31,50/MWh

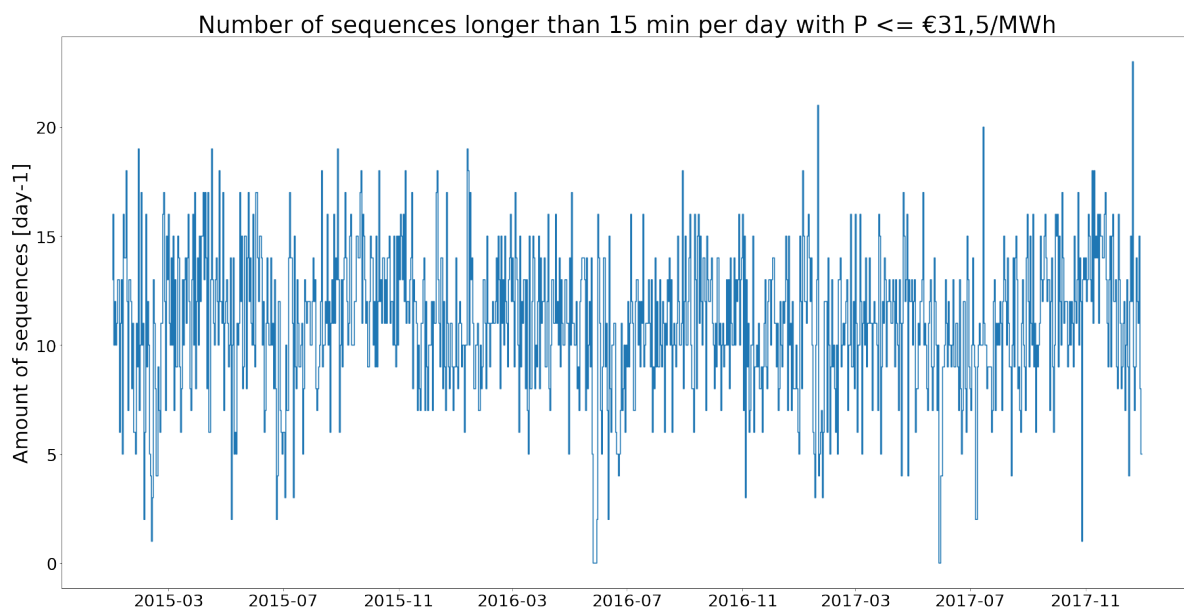


Figure B.19: Amount of times downward regulating occurred with $P \leq €31,50/\text{MWh}$ with an activation time of 15 minutes or longer

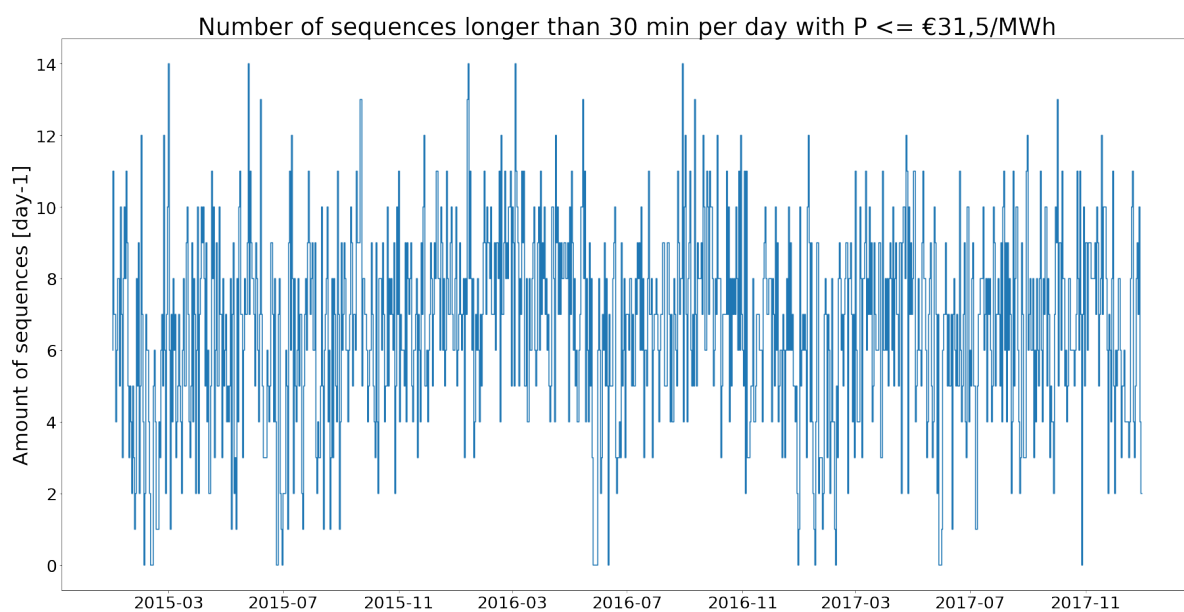


Figure B.20: Amount of times downward regulating occurred with $P \leq €31,50/\text{MWh}$ with an activation time of 30 minutes or longer

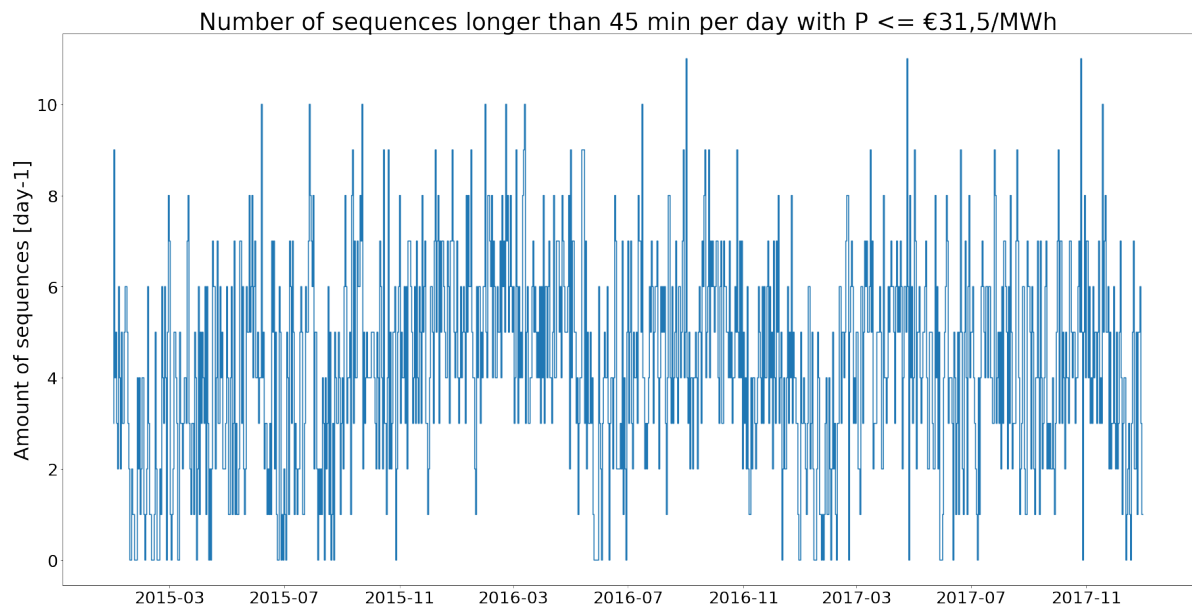


Figure B.21: Amount of times downward regulating occurred with $P \leq \text{€}31,50/\text{MWh}$ with an activation time of 45 minutes or longer

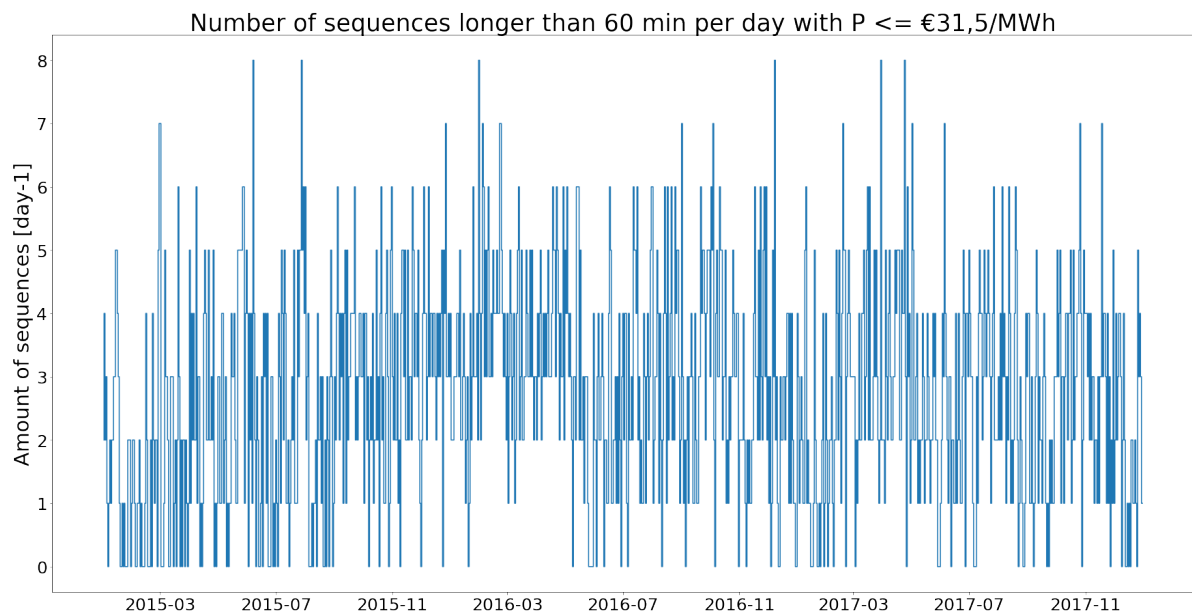


Figure B.22: Amount of times downward regulating occurred with $P \leq \text{€}31,50/\text{MWh}$ with an activation time of 60 minutes or longer

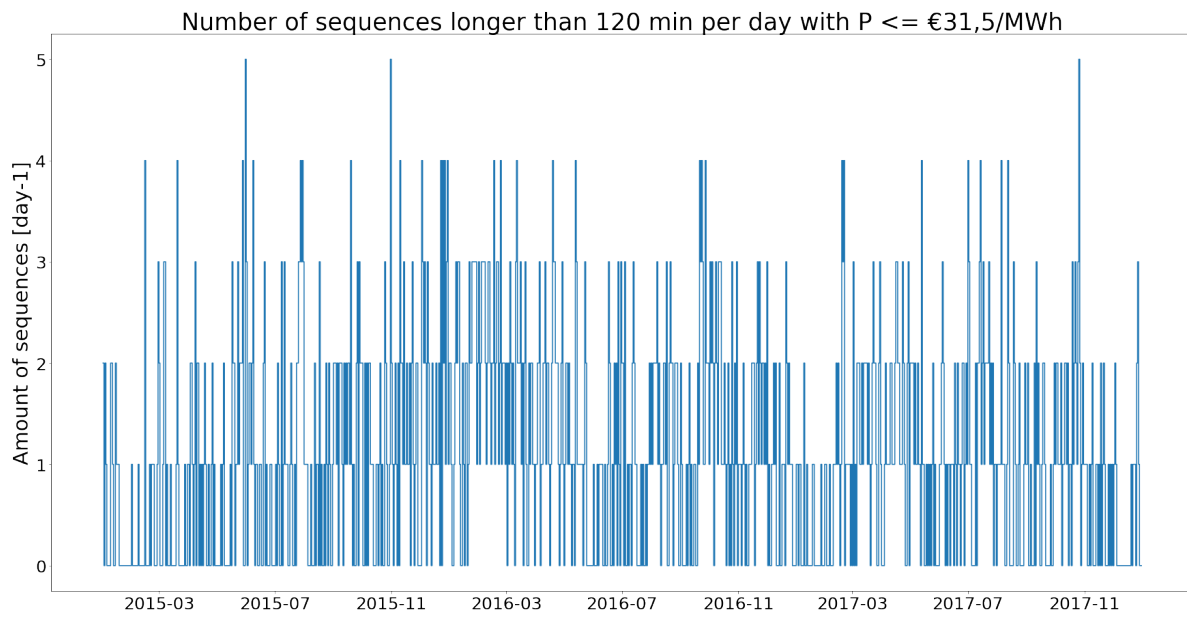


Figure B.23: Amount of times downward regulating occurred with $P \leq €31,50/\text{MWh}$ with an activation time of 120 minutes or longer

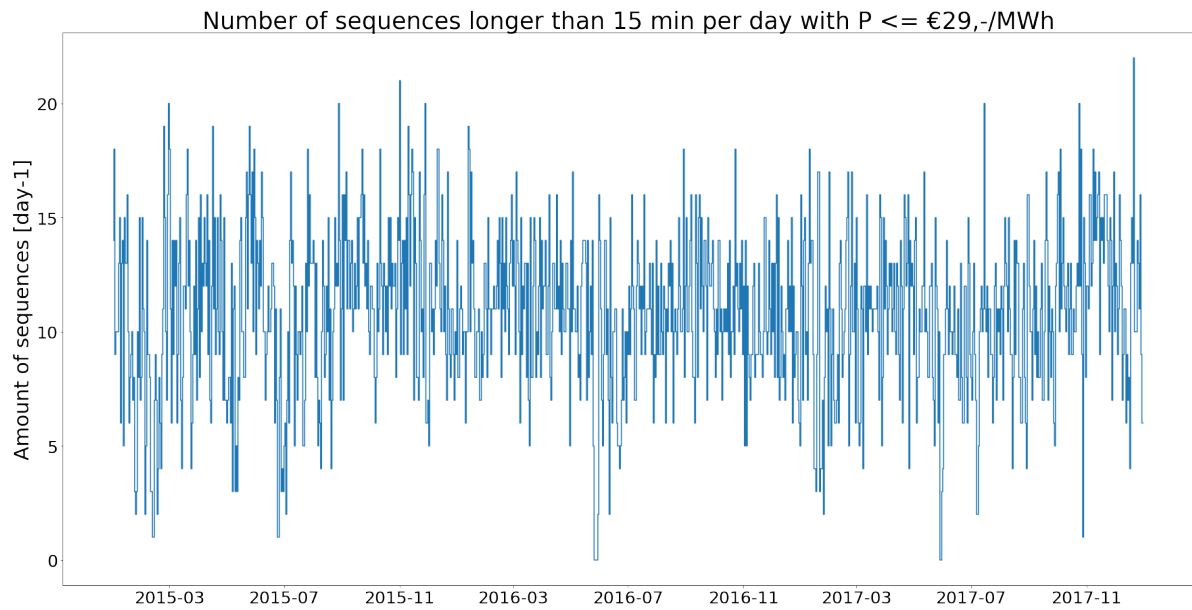
B.1.2.5. P = €29,-/MWh

Figure B.24: Amount of times downward regulating occurred with P ≤ €29,-/MWh with an activation time of 15 minutes or longer

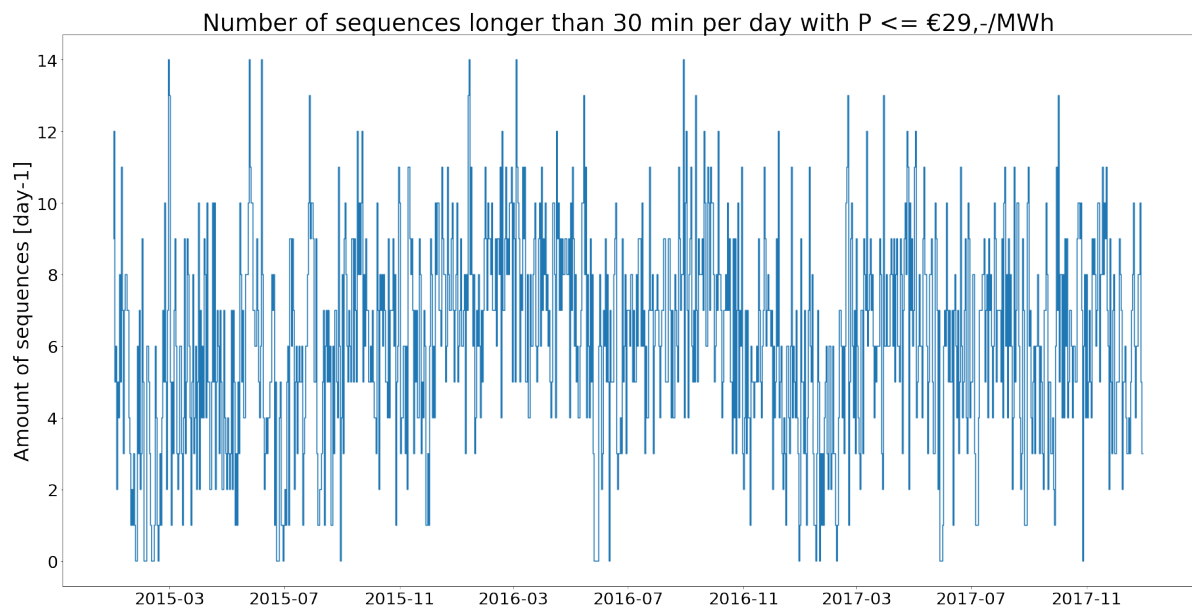


Figure B.25: Amount of times downward regulating occurred with P ≤ €29,-/MWh with an activation time of 30 minutes or longer

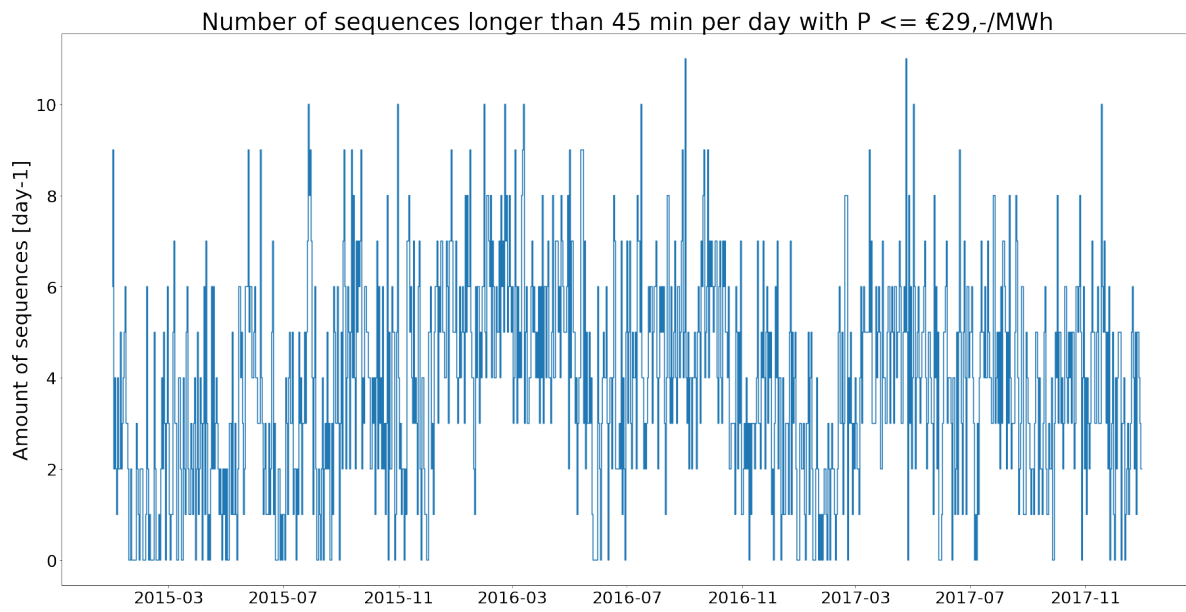


Figure B.26: Amount of times downward regulating occurred with $P \leq \text{€}29,-/\text{MWh}$ with an activation time of 45 minutes or longer

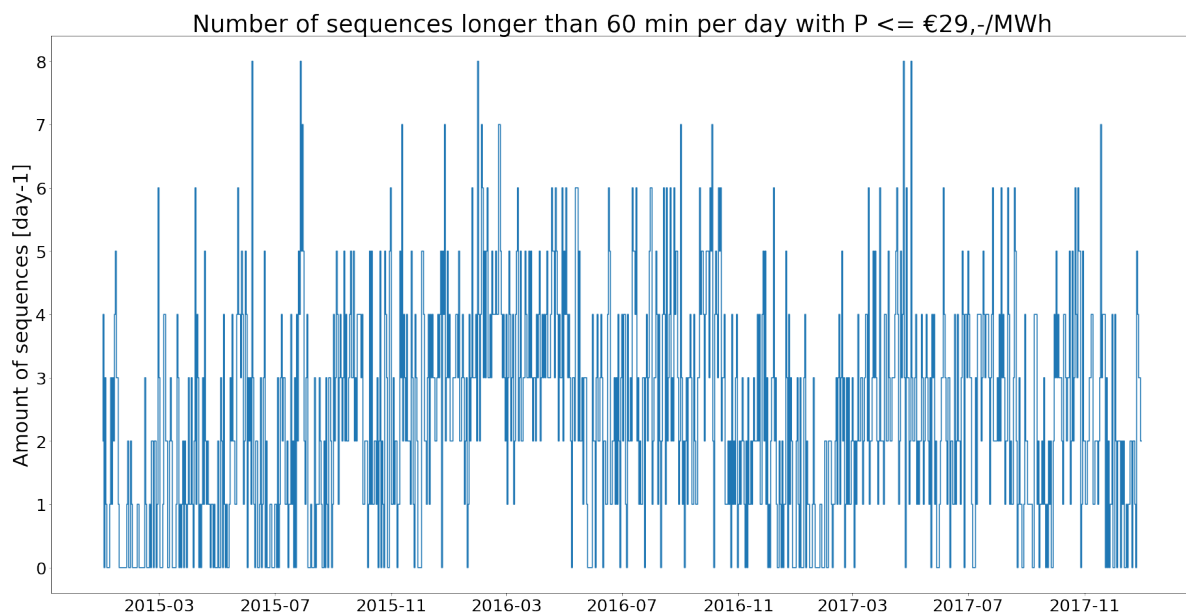


Figure B.27: Amount of times downward regulating occurred with $P \leq \text{€}29,-/\text{MWh}$ with an activation time of 60 minutes or longer

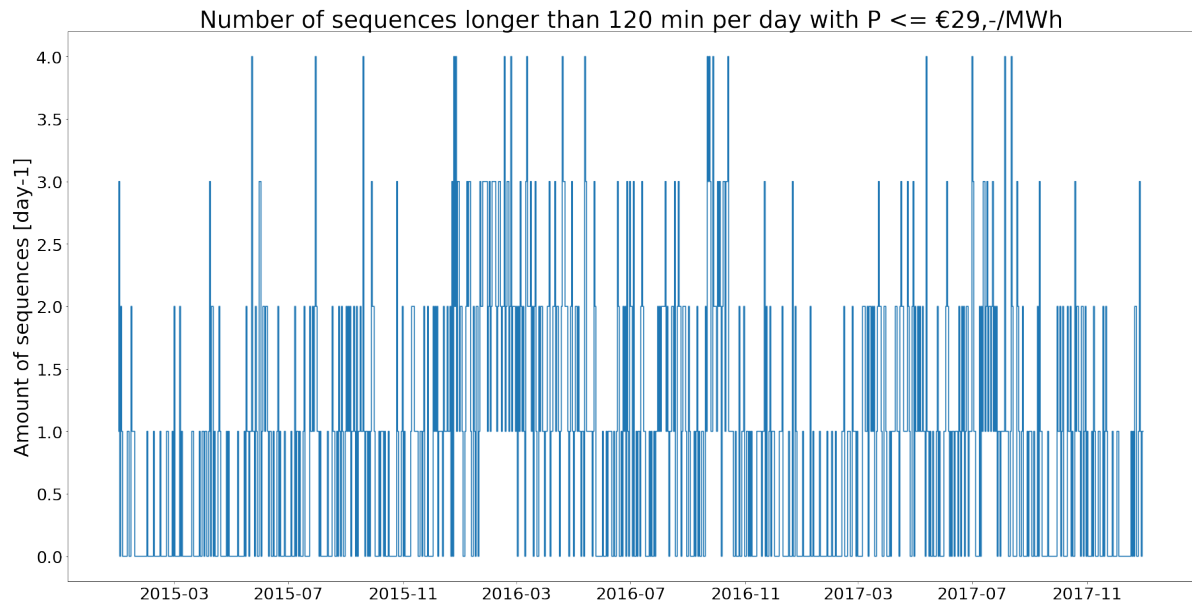


Figure B.28: Amount of times downward regulating occurred with $P \leq \text{€}29,-/\text{MWh}$ with an activation time of 120 minutes or longer

B.1.2.6. P = €21,-/MWh

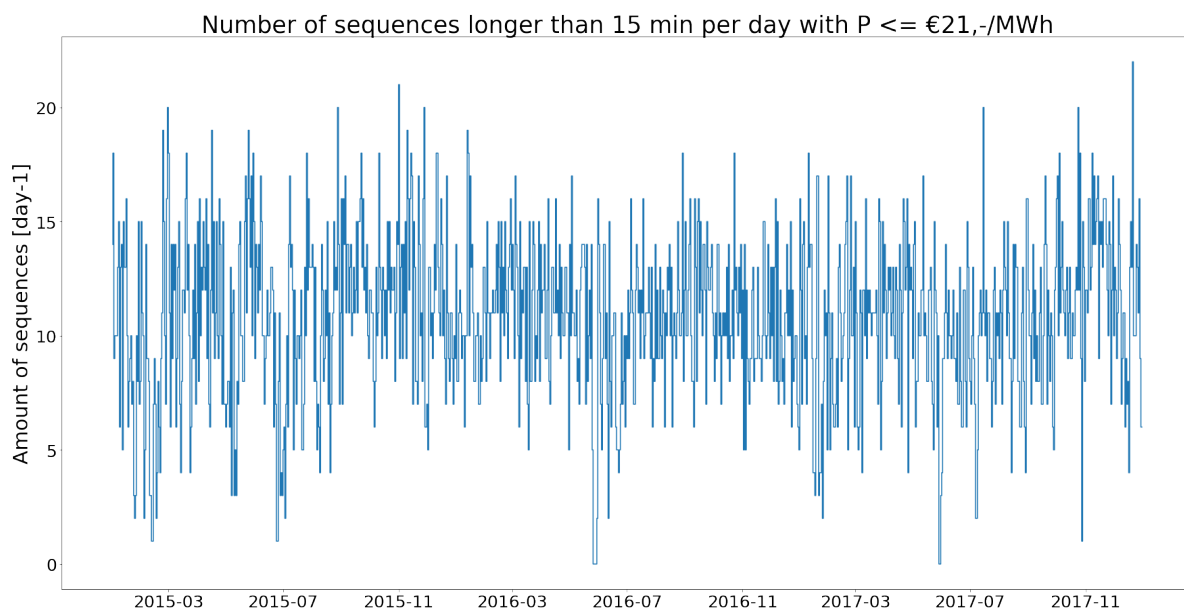


Figure B.29: Amount of times downward regulating occurred with $P \leq €21,-/MWh$ with an activation time of 15 minutes or longer

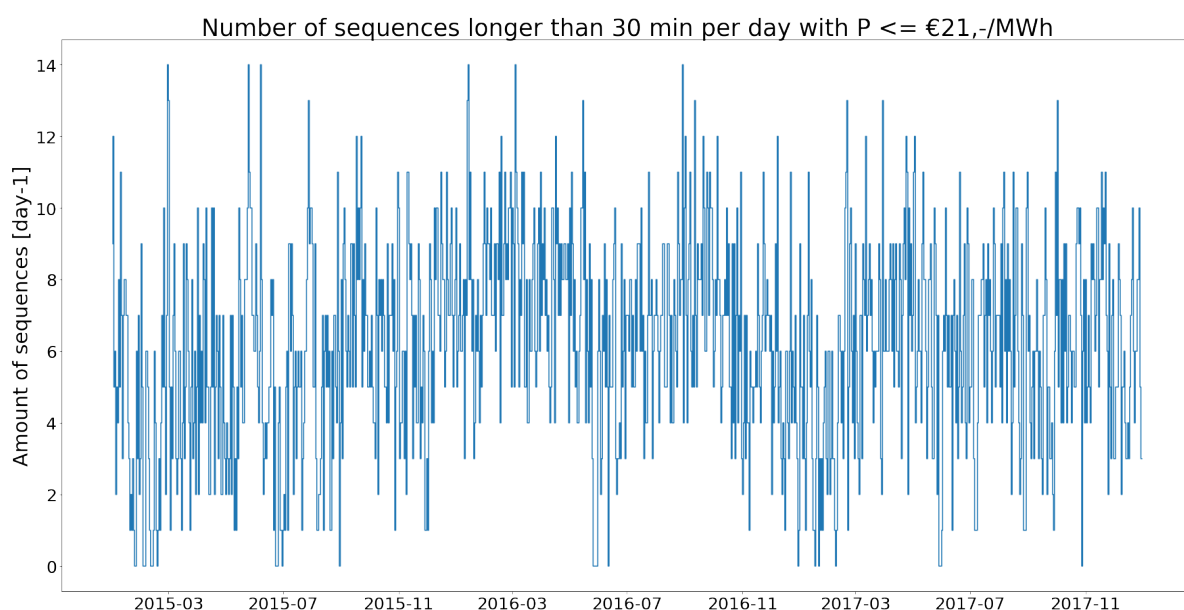


Figure B.30: Amount of times downward regulating occurred with $P \leq €21,-/MWh$ with an activation time of 30 minutes or longer

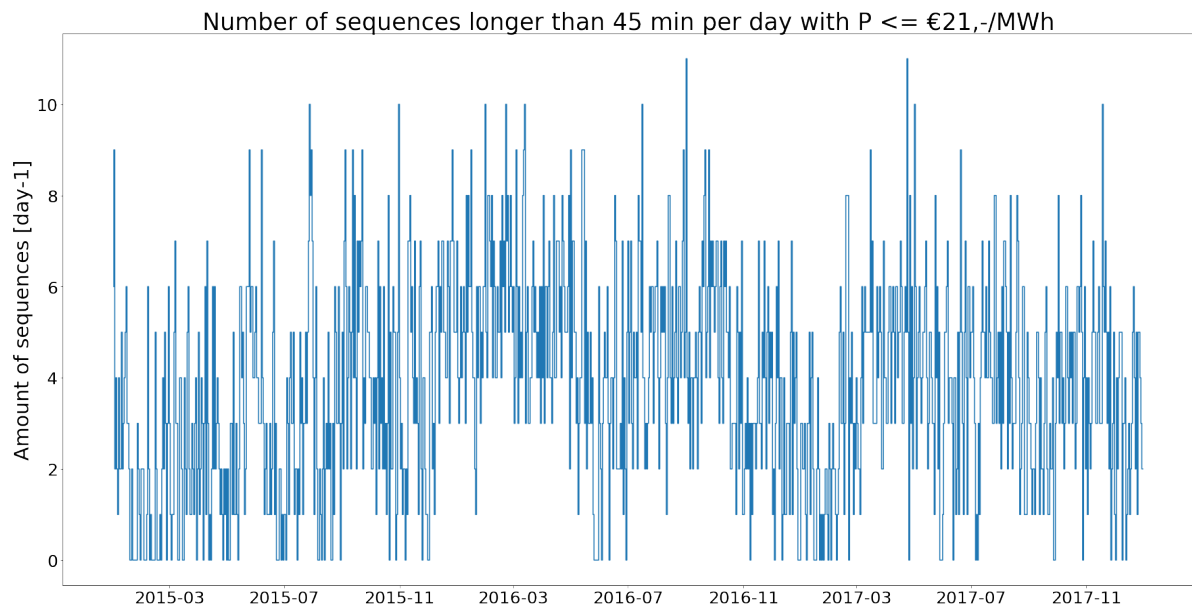


Figure B.31: Amount of times downward regulating occurred with $P \leq \text{€}21,-/\text{MWh}$ with an activation time of 45 minutes or longer

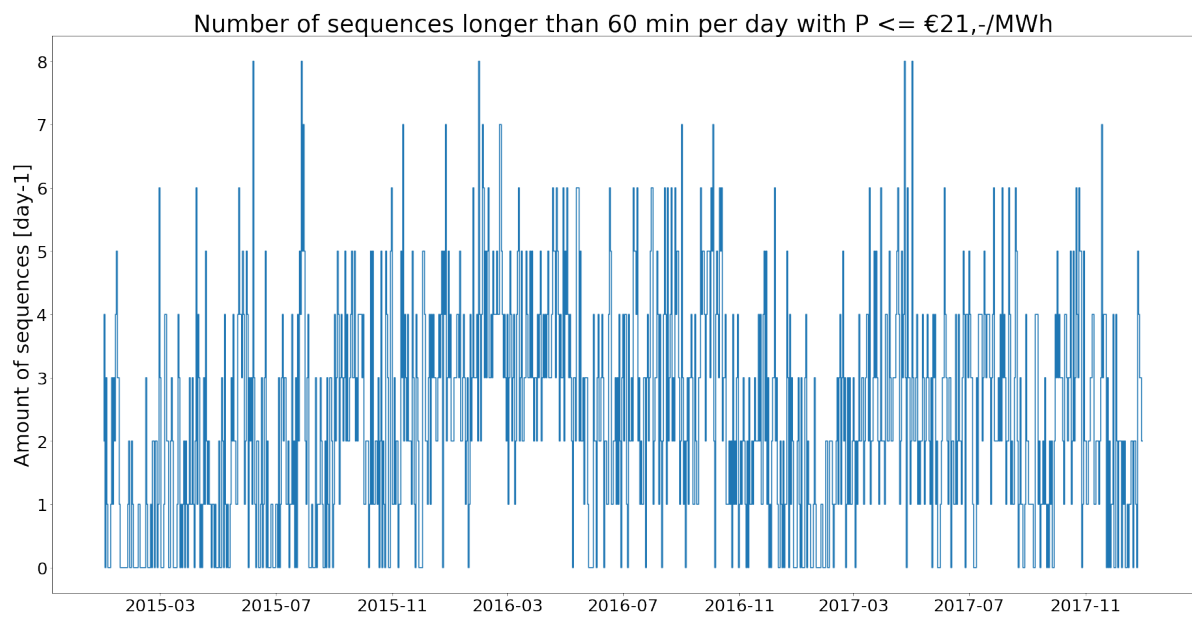


Figure B.32: Amount of times downward regulating occurred with $P \leq \text{€}21,-/\text{MWh}$ with an activation time of 60 minutes or longer

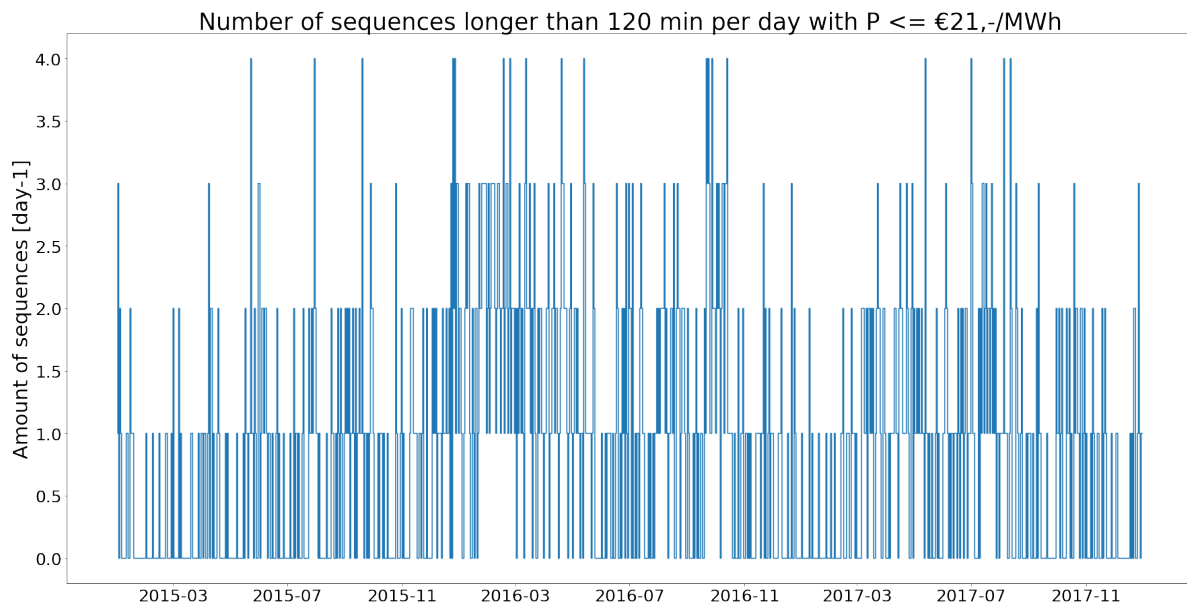


Figure B.33: Amount of times downward regulating occurred with $P \leq \text{€}21,-/\text{MWh}$ with an activation time of 120 minutes or longer

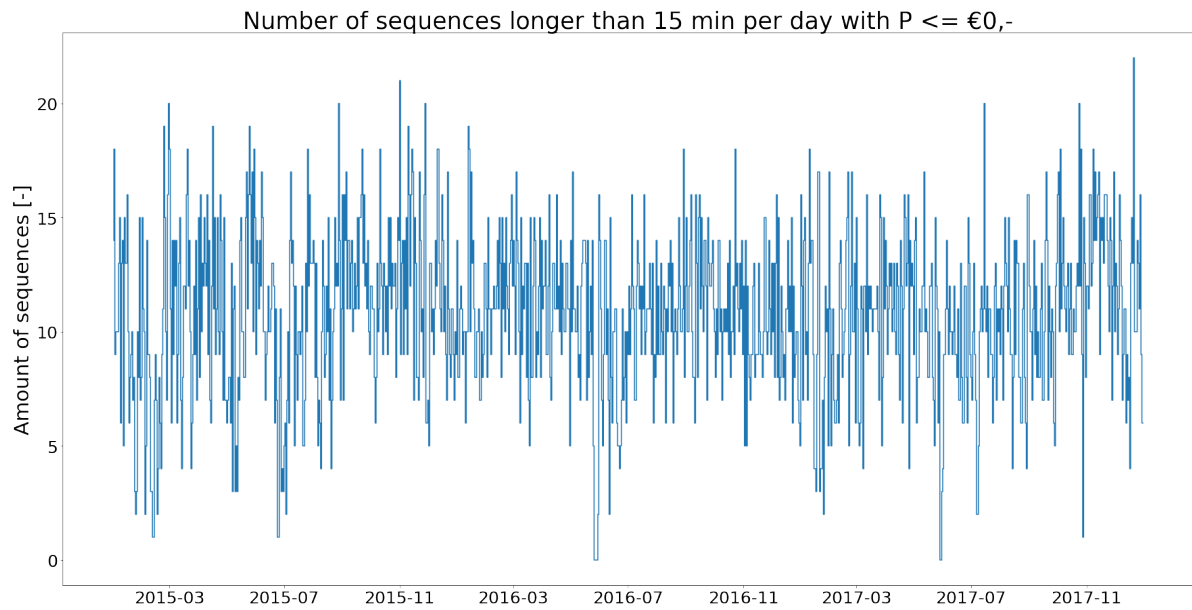
B.1.2.7. P = €0,-/MWh

Figure B.34: Amount of times downward regulating occurred with P ≤ €0,-/MWh with an activation time of 15 minutes or longer

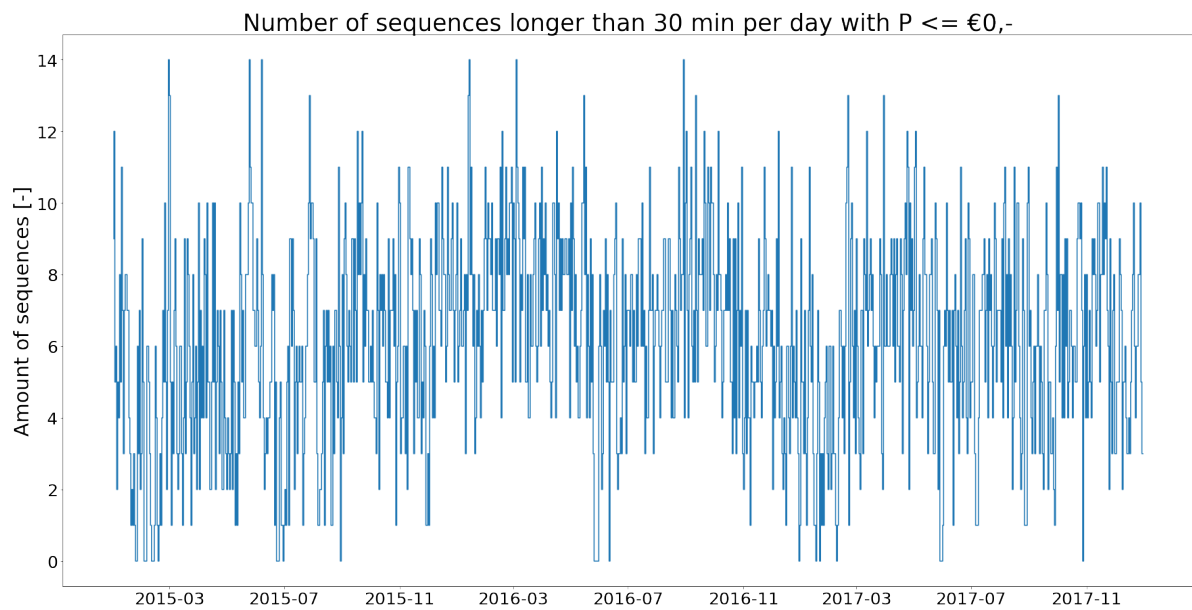


Figure B.35: Amount of times downward regulating occurred with P ≤ €0,-/MWh with an activation time of 30 minutes or longer

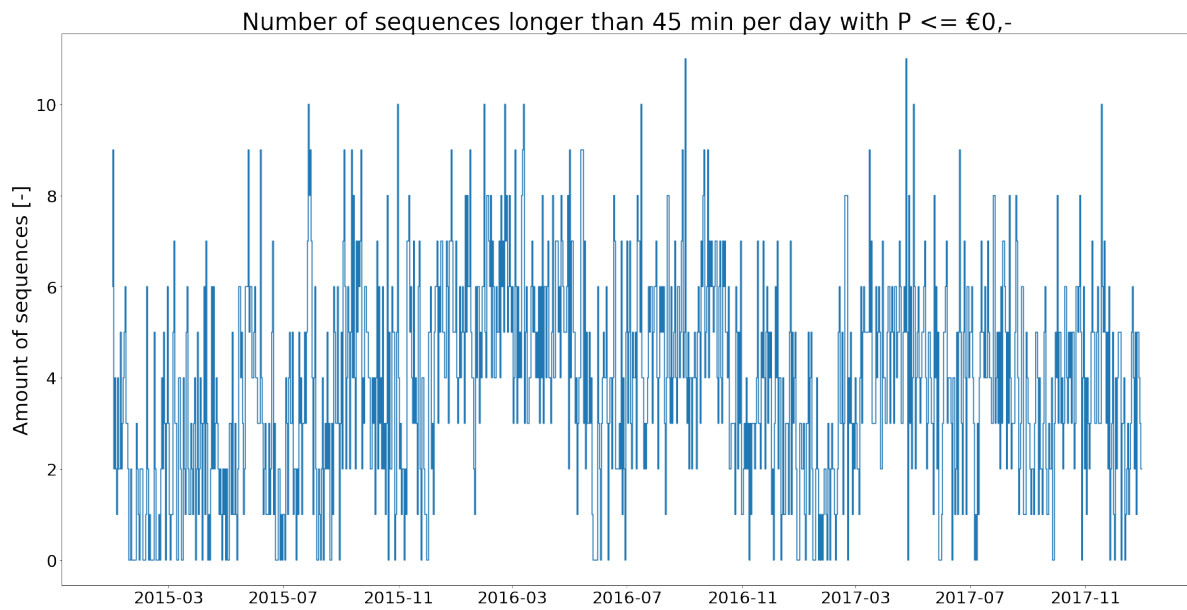


Figure B.36: Amount of times downward regulating occurred with $P \leq \text{€}0,-/\text{MWh}$ with an activation time of 45 minutes or longer

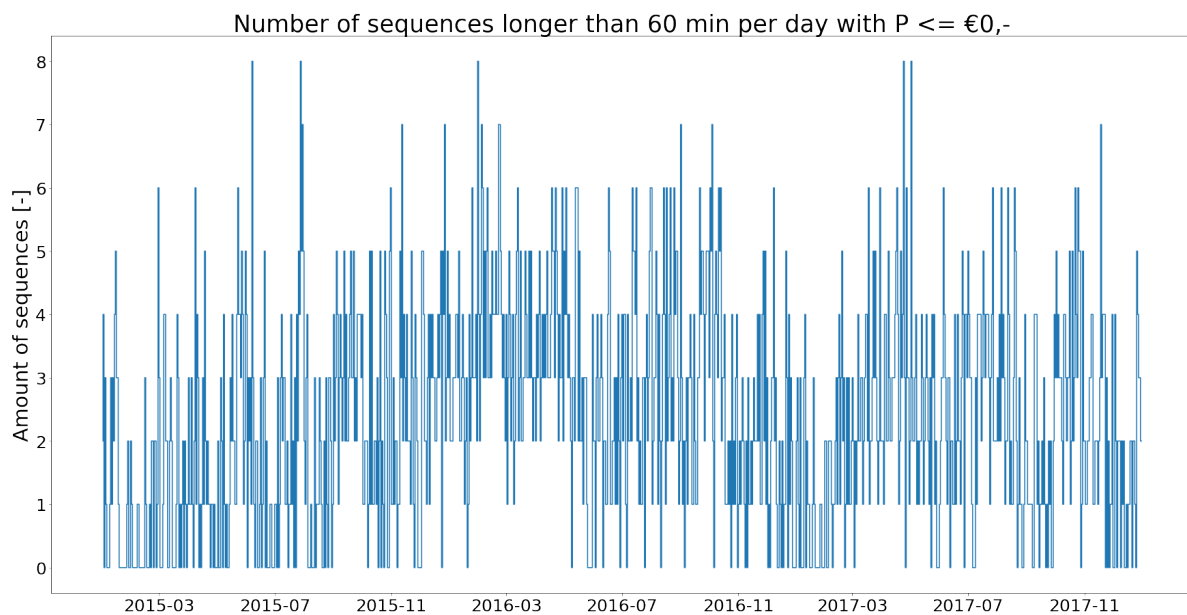


Figure B.37: Amount of times downward regulating occurred with $P \leq \text{€}0,-/\text{MWh}$ with an activation time of 60 minutes or longer

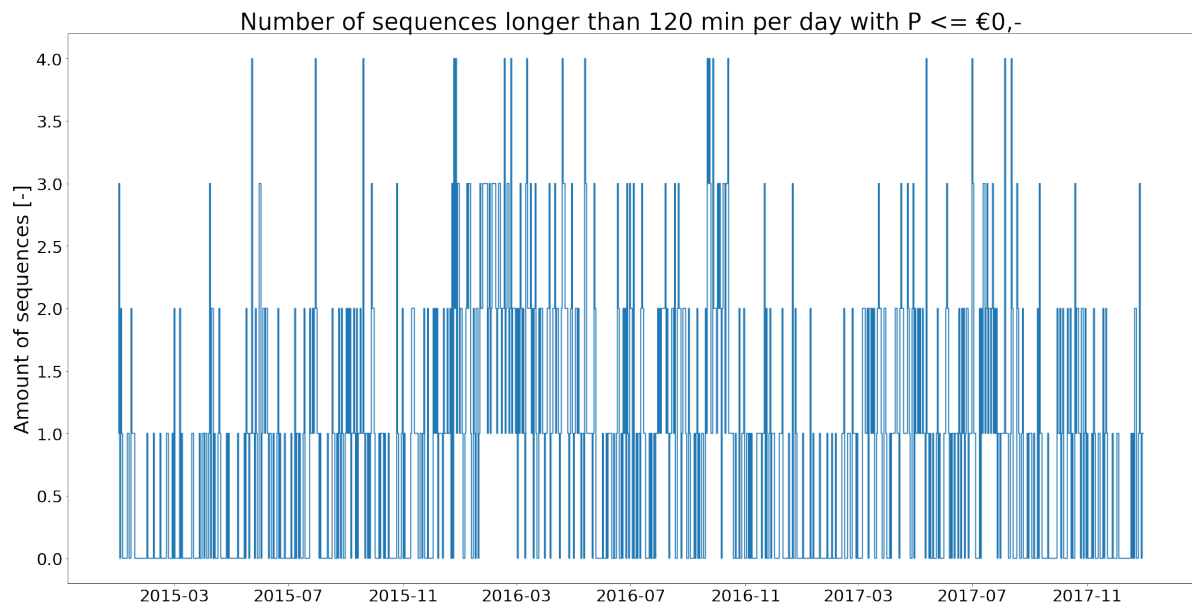


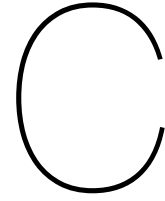
Figure B.38: Amount of times downward regulating occurred with $P \leq \text{€}0,-/\text{MWh}$ with an activation time of 120 minutes or longer

B.1.2.8. Conclusion

Downward Activation Sequence length [min]	Percentage of days occurred					
	$P [\text{€/MWh}] = 0$	$P = 21$	$P = 31.5$	$P = 42$	$P = 63$	$P = 84^*$
15 (+15) min	97.5%	99.3%	99.5%	99.5%	99.5%	99.5%
30 (+15) min	63.2%	89.8%	99.1%	99.1%	99.1%	99.1%
45 (+15) min	32.0%	71.5%	94.8%	97.9%	97.9%	97.9%
60 (+15) min	17.1%	55.4%	89.1%	95.4%	95.4%	95.4%
120 (+15) min	3.8%	22.5%	65.1%	79.0%	79.3%	79.3%

*RWS' current energy price

Table B.1: Percentage of days activated per sequence length and bid-price [ENTSO-E]



Appendix C

C.1. Piecewise linearization gate equations

C.1.1. Optimization

In order to solve the numerical issues that the gate-discharge equations gave, an optimization was performed to fit the curve with multiple linearizations. To get the "best approximation", the feasible region was maximized. The original equation looks the following way:

$$Q \leq C * \sqrt{2 * g * dH} \quad (C.1)$$

With Q being the discharge, C a collection of parameters and g the gravitational acceleration.

Constraints

The constraints implemented in the optimization are the following:

$$Q[m] = C * \sqrt{2 * g * dH[m]} \quad (C.2)$$

At which m is a range of 0 to 4, since a 4-piece linearization is wanted in this optimization (with 5 intersection points). The optimization is forced to let the linearization start at the minimal water level difference needed

$$dH_{min}$$

:

$$dH[0] = dH_{min} \quad (C.3)$$

Besides that, the last point (point 4) of intersect has to be at the maximum dH that occurs

$$dH_{max}$$

:

$$dH[4] = dH_{max} \quad (C.4)$$

The chosen intersection points has to be higher than the previous points, with a minimum difference of 1cm:

$$dH[n + 1] \geq dH[n] + 0.01 \quad (C.5)$$

Then it is defined what the value for a would be in a linear fit ($y = a*x + b$):

$$a[m] = \frac{Q[m + 1] - Q[m]}{dH[m + 1] - dH[m]} \quad (C.6)$$

And after that, the constant b of the linear fit is defined:

$$b[n] = Q[n] - a[n] * dH[n] \quad (C.7)$$

At which n is the set of lines that have to be fit.

Then the size of the feasible region, underneath a linearization, is defined:

$$A[n] = (dH[n + 1] - dH[n]) * (Q[n] + 0.5 * (Q[n + 1] - Q[n])) \quad (\text{C.8})$$

After which the objective is defined, which is to maximize the size of the feasible region:

$$\max \sum_{n=0}^N A[n] \quad (\text{C.9})$$

Results

The results of the optimization can be seen in the following graphs:

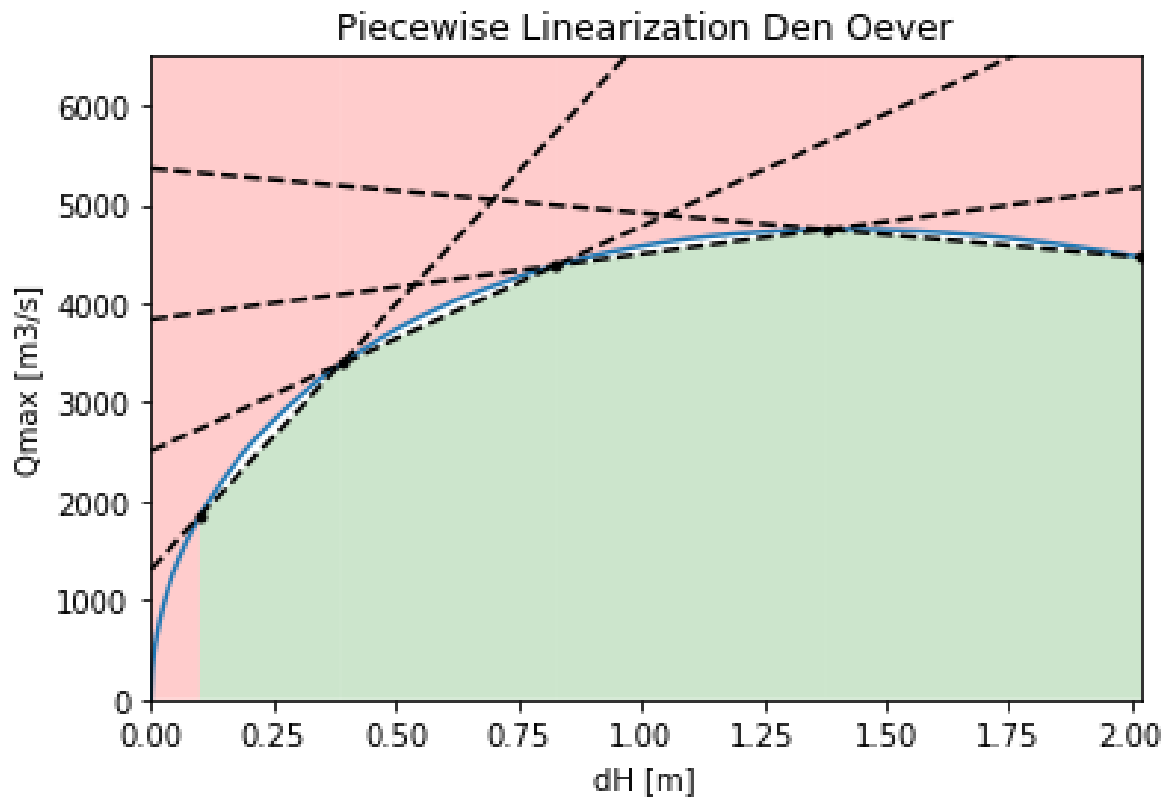


Figure C.1: Piecwise linearization Den Oever

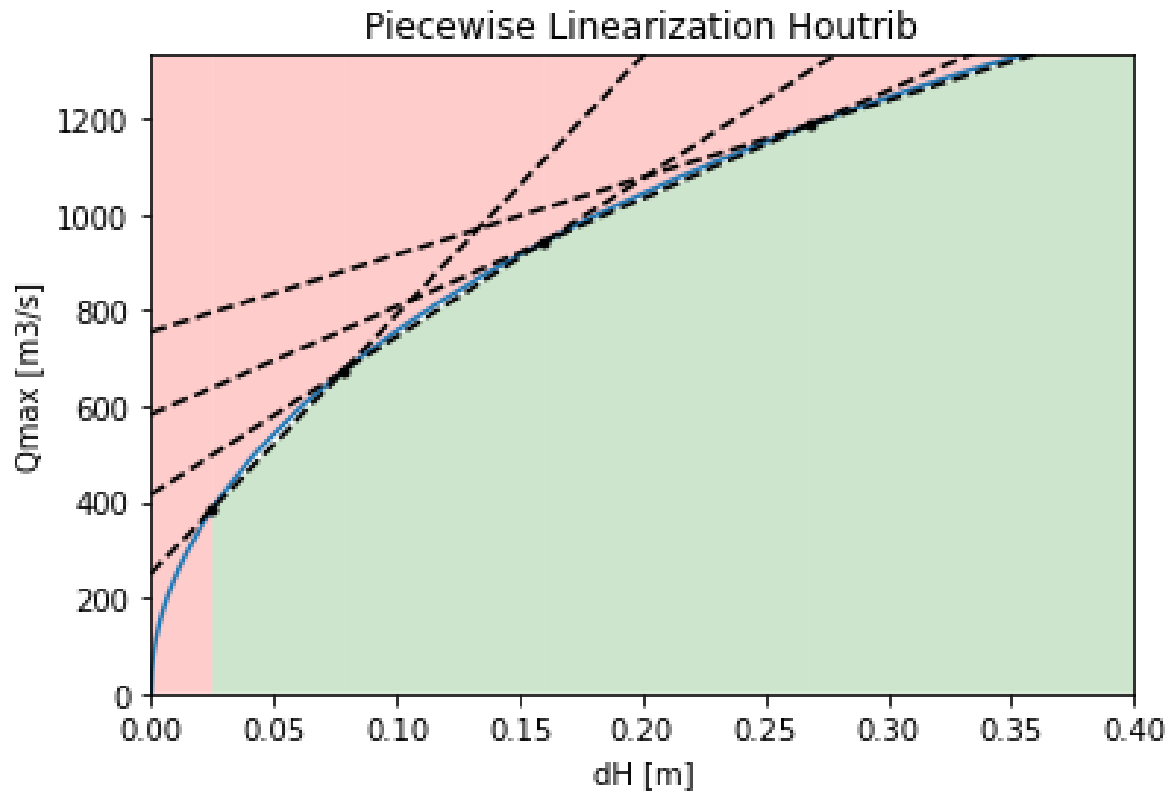


Figure C.2: Piecewise linearization Houtribsluis

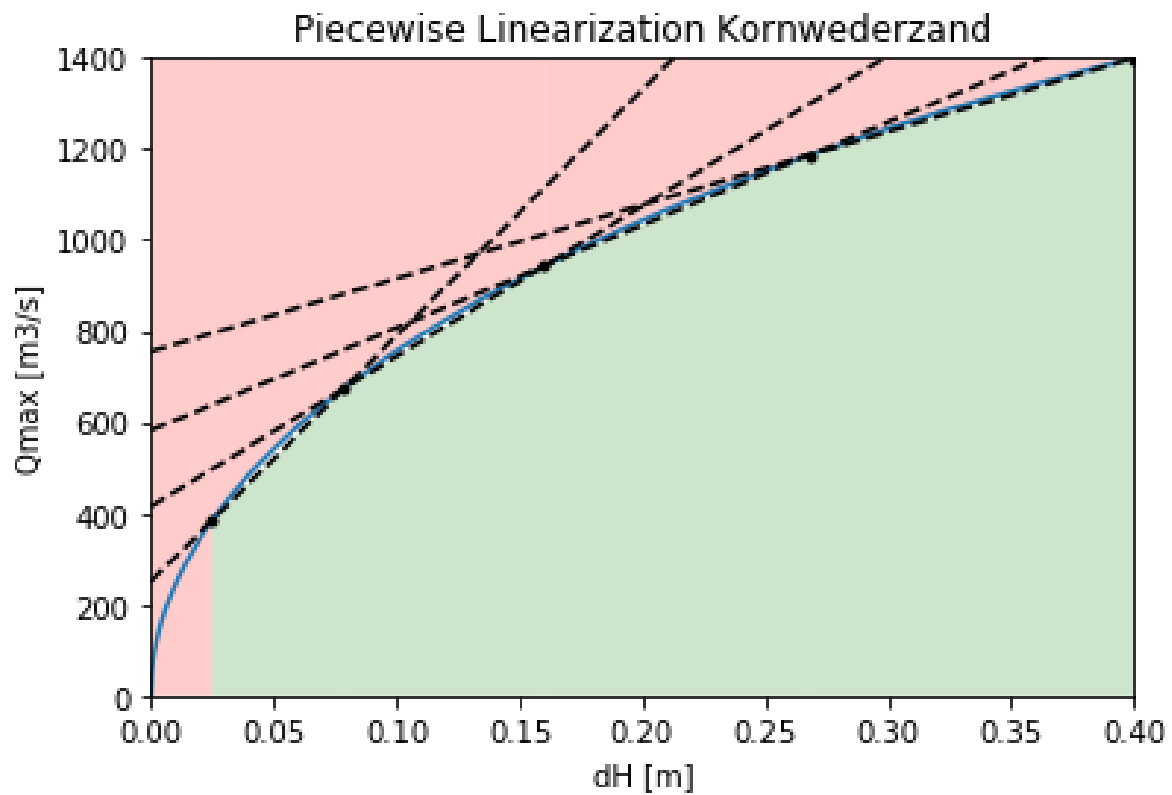


Figure C.3: Piecewise linearization Kornwederzand

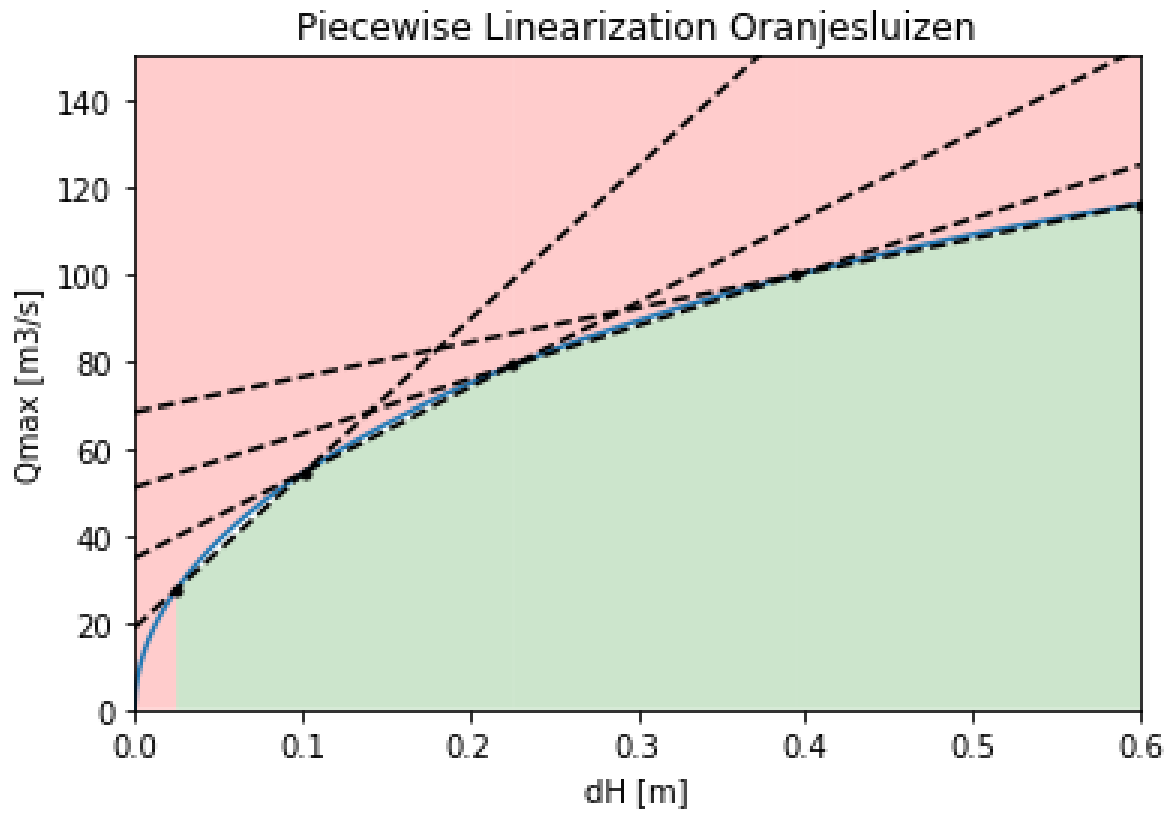


Figure C.4: Piecewise linearization Oranjesluizen

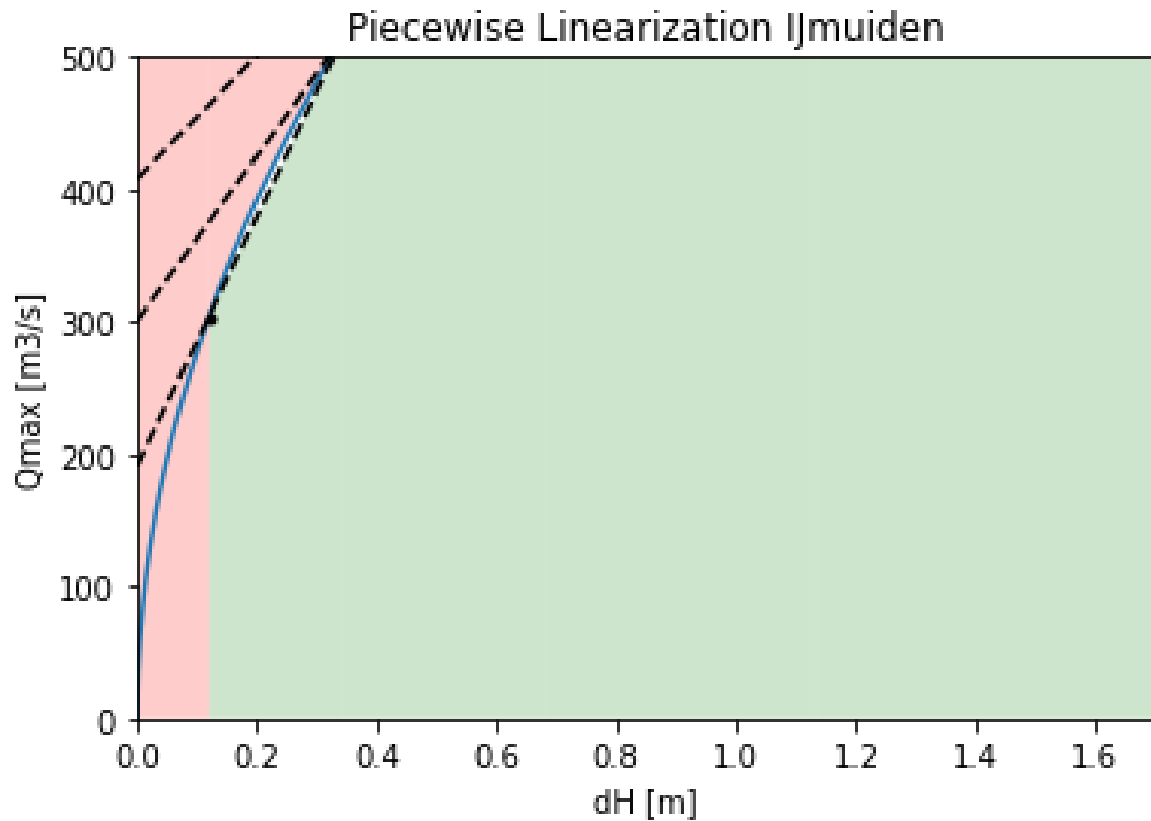


Figure C.5: Piecewise linearization IJmuiden

In IJmuiden it was found that the maximum discharge was more constraining than the actual gate discharge equation, given the water level differences that occur. The remaining linearizations are calculated, but only the first part of the linearization is implemented in the DR-optimization since the rest are not constraining.

C.2. Power curve optimization

To have the pumping station always operate at points of maximum efficiency, an optimization was performed to simplify the separate pump curves into one. This is done by implementing the Q-dH curves of each pump setting, and the power curve of each pump setting, and optimize the efficiency for combinations of Q and dH that occur. These curves are found in the research of Weisenburch [59].

C.2.1. Q-dH & P-dH curves

Pump 1 and 3

Pump 1 and 3 are pumps which have only one setting, so only one Q-dH and P-dH curve are implemented. Q is in m³/s, dH in m and P in kW.

$$Q = -5.4174 * dH + 44.93 \quad (C.10)$$

$$P = 208.08 * dH + 536.85 \quad (C.11)$$

Pump 2 and 4

Pump 2 and 4 have 2 settings, a high and low RPM setting:

$$Q1 = -6.4967 * dH + 33.149 \quad (C.12)$$

$$Q2 = -5.4171 * dH + 44.93 \quad (C.13)$$

$$P1 = 192.36 * dH + 217.26 \quad (C.14)$$

$$P2 = 208.08 * dH + 536.85 \quad (C.15)$$

Pump 5 and 6

Pump 5 and 6 are variable speed pumps, of which 3 Q-dH and power curves were given in Weisenburch's report.

$$Q1 = -7.1021 * dH + 48.164 \quad (C.16)$$

$$Q2 = 1.8544 * dH^2 - 7.774 * dH + 47.706 \quad (C.17)$$

$$Q3 = -1.9882 * dH^2 + 1.9726 * dH + 50.054 \quad (C.18)$$

$$P1 = 282.97 * dH + 417.32 \quad (C.19)$$

$$P2 = 379.09 * dH + 373.18 \quad (C.20)$$

$$P3 = 443.91 * dH + 476.3 \quad (C.21)$$

C.2.2. Optimization

In the optimization, the modes of pumps are indicated with binary variables. And every pump's curve is indicated with P or Q, the number of the pump, and the mode of the pump. Q63 means Q-dH curve of pump 6, mode 3. And every mode as a binary variable, in the previous case B63. For a given Q and dH, the following constraints are applied:

$$\begin{aligned} Q_{calc} = & B_1 * Q_1[dH] + B_{21} * Q_{21}[dH] + B_{22} * Q_{22}[dH] + B_3 * Q_3[dH] + B_{41} * Q_{41}[dH] \\ & + B_{42} * Q_{42}[dH] + B_{51} * Q_{51}[dH] + B_{52} * Q_{52}[dH] + B_{53} * Q_{53}[dH] + B_{61} * Q_{61}[dH] \\ & + B_{62} * Q_{62}[dH] + B_{63} * Q_{63}[dH] \end{aligned}$$

So the calculated pump discharge is equal to sum of the outcome of the Q-dH curves of the activated pump modes.

$$(Q_{calc} - Q)^2 \leq 5^2 \quad (C.22)$$

The calculated discharge cannot vary more than 5 m³/s from the wanted discharge. This is implemented because the pumping station might not be able to produce any discharge between 0 and its max, because of pump limitations. However, in this study this is assumed to be possible.

Complementary constraints were added to ensure that multiple modes of the same pump cannot be activated at the same time:

$$B_{21} * B_{22} \leq 10^{-4} \quad (C.23)$$

$$B_{41} * B_{42} \leq 10^{-4} \quad (C.24)$$

$$B_{51} * B_{52} \leq 10^{-4} \quad (C.25)$$

$$B_{51} * B_{53} \leq 10^{-4} \quad (C.26)$$

$$B_{53} * B_{52} \leq 10^{-4} \quad (C.27)$$

$$B_{61} * B_{62} \leq 10^{-4} \quad (C.28)$$

$$B_{61} * B_{63} \leq 10^{-4} \quad (C.29)$$

$$B_{62} * B_{63} \leq 10^{-4} \quad (C.30)$$

The the objective is defined, which is the minimize the power of the pumping station for the given Q and dH:

$$\begin{aligned} \min & B_1 * P_1[dH] + B_{21} * P_{21}[dH] + B_{22} * P_{22}[dH] + B_3 * P_3[dH] + B_{41} * P_{41}[dH] + B_{42} * P_{42}[dH] \\ & + B_{51} * P_{51}[dH] + B_{52} * P_{52}[dH] + B_{53} * P_{53}[dH] + B_{61} * P_{61}[dH] + B_{62} * P_{62}[dH] + B_{63} * P_{63}[dH] \end{aligned}$$

Similar to the Q-dH curves, the power consumption is equal to the sum of outcome of the activated power curves.

C.2.3. Results

GUROBI [28] was used to solve the problems for every Q from 0 to 260 in steps of 5 m³/s, in combination with every dH from 0m to 4m with steps of 5cm. The result can be seen in the following picture:

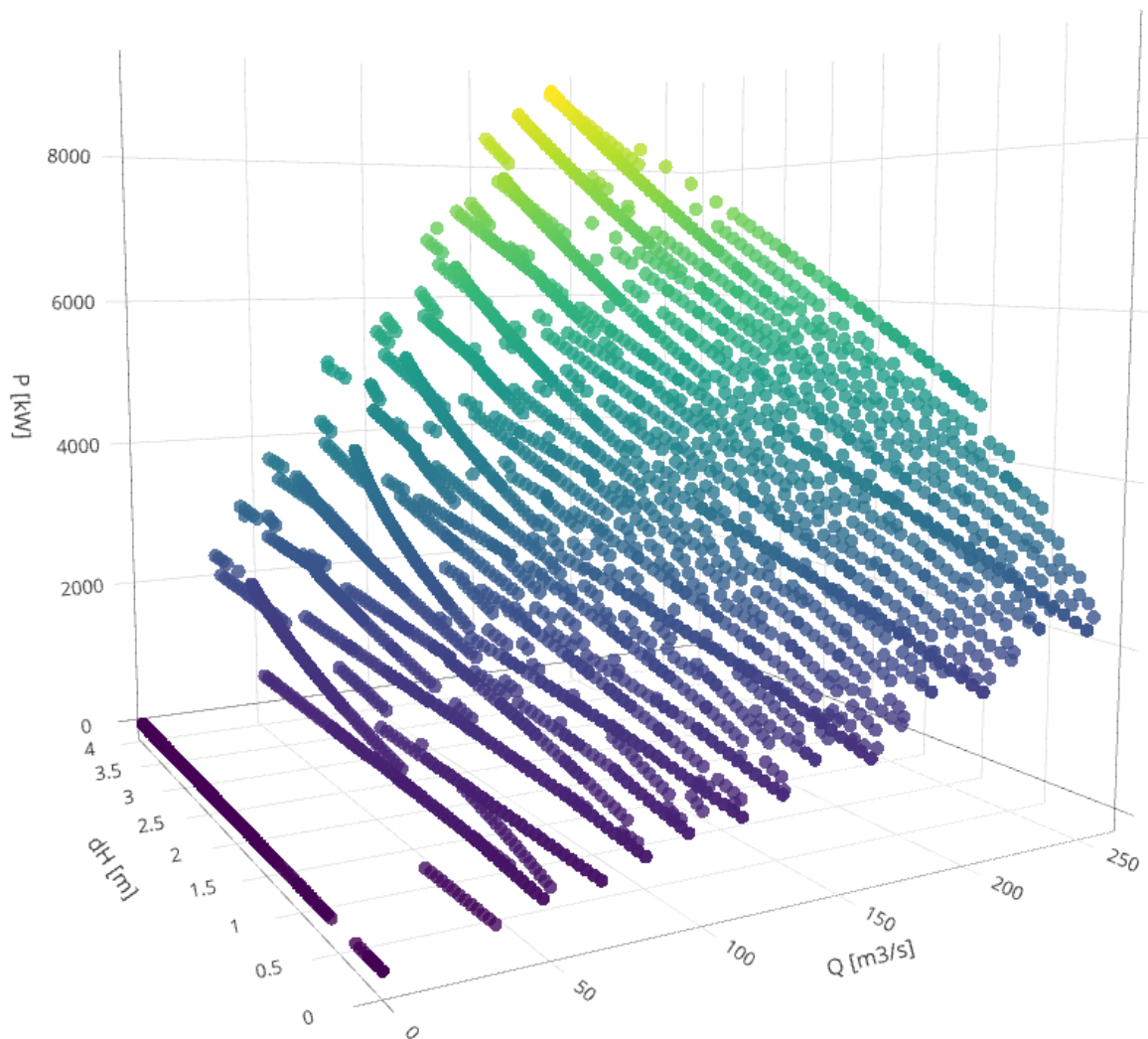
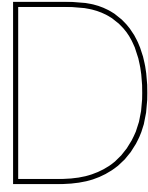


Figure C.6: Results optimization Gurobi

Not every exact combination of Q and dH were possible, which make sense that the pumping station cannot discharge at 260 m³/s with a pump-height of 4m. But also the very low discharges seem infeasible for the pumping station, which are assumed to be possible in the DR optimization.



Appendix D

D.1. Wind effects

Due to the effects of the wind, the water levels at the structures (and the whole system) change. The effect of wind on water level is well understood, and can be described by equation D.1.

$$W = \frac{0.5 * \kappa * U_w^2 * F * \cos(\theta)}{g * h} \quad (D.1)$$

D.1.1. Markermeer and IJsselmeer

For the Markermeer and IJsselmeer, a research [23] was already done on the effect of wind on the water level from different directions and speeds in the Markermeer and IJsselmeer. This is the method that is applied in SOBEK, a widely used flow-simulation software in the Netherlands. The following relationship was fitted through the observed wind effects, directions and speeds:

$$W = \frac{c * u_{wind}^a}{h_0^b} \quad (D.2)$$

Where a, b and c are fitted parameters depending on the wind direction,

$$u_{wind}$$

the wind speed and

$$h_0$$

the average water-depth. Multiple structures were evaluated, but in our case only the Houtribsluis has been taken into account in between the IJsselmeer and Markermeer, and Den Oever as only gate in the IJsselmeer. The following parameters were fitted per structure:

Direction	Den Oever IJsselmeer			Houtrib IJsselmeer			Houtrib Markermeer			Oranjesluizen Markermeer		
	a	b	c	a	b	c	a	b	c	a	b	c
0	1.89	1	-0.00490	2.24	1	0.00358	2.87	0.6	0.00003	2.27	0.6	0.00090
30	1.89	1	0.00033	2.24	1	0.00274	2.26	0.6	-0.00039	2.15	0.6	0.00185
60	1.89	1	0.00547	2.24	1	0.00116	2.37	0.6	-0.00050	2.14	0.6	0.00185
90	1.89	1	0.00914	2.24	1	-0.00072	2.60	0.6	-0.00026	2.25	0.6	0.00104
120	1.89	1	0.01037	2.24	1	-0.000241	2.54	0.6	-0.00027	2.38	0.6	0.00027
150	1.89	1	0.00882	2.24	1	-0.00346	2.49	0.6	-0.00022	1.71	0.6	-0.00243
180	1.89	1	0.00490	2.24	1	-0.00358	2.11	0.6	-0.00028	1.8	0.6	-0.00418
210	1.89	1	-0.00033	2.24	1	-0.00274	1.97	0.6	0.00140	1.89	0.6	-0.00593
240	1.89	1	-0.00547	2.24	1	-0.00116	2.08	0.6	0.00144	1.91	0.6	-0.00588
270	1.89	1	-0.00914	2.24	1	0.00072	2.19	0.6	0.00102	2.03	0.6	-0.00276
300	1.89	1	-0.01037	2.24	1	0.00241	2.23	0.6	0.00078	2.40	0.6	-0.00028
330	1.89	1	-0.00882	2.24	1	0.00346	2.39	0.6	0.00033	2.42	0.6	0.00025

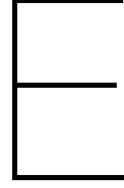
The wind effects were calculated with the downloaded wind data from KNMI station Houtribdijk, and then added as data. A constant average depth was assumed; 4.5m.

D.1.2. Noordzeekanaal

For the Noordzeekanaal, the general equation was used to calculate the wind effects. For multiple directions, the undisturbed length was measured using Google maps. The following lengths [m] were found per direction:

Direction	Oranjesluizen	IJmuiden
0	-2400	0
10	0	0
20	0	0
30	-500	0
40	-1000	0
50	-1200	0
60	-1200	0
70	-1500	0
80	-2000	0
90	-3750	0
100	-3750	2500
110	-4000	17500
120	-7100	7200
130	0	0
140	0	0
150	0	0
160	0	0
170	0	0
180	2400	0
190	0	0
200	0	0
210	500	0
220	1000	0
230	1200	0
240	1200	0
250	1500	0
260	2000	0
270	3750	0
280	3750	-2500
290	4000	-17500
300	7200	-7200
310	0	0
320	0	0
330	0	0
340	0	0
350	0	0

These values were used together with the wind data to create a dataset of the added wind effect, with a constant depth of 15m.



Appendix E

If Rijkswaterstaat would like to explore the possibility to optimize on sustainable energy use, they could use the day ahead predictions to optimize one. The day ahead predictions include a prediction of the sustainable energy generation, and the total energy generation. With average carbon intensities, the generation could be converted in CO₂ equivalents. The ratio of the two would be an indication of the carbon intensity of the grid. This is explained in the next section.

E.1. Optimize on CO₂/sustainable energy use

Another possibility is to optimize CO₂ emission. This would be based on the day-ahead predictions of renewable energy generation (REG), and total generation (TG). The fraction between predicted REG and TG would be implemented in a similar way as the day-ahead price. Bids would be done on the day ahead market based on these projections, and costs are calculated in hindsight.

During this study, it is assumed that energy is bought for the same price as the day ahead price and that bids are always accepted. The objective function for optimizing on predicted generation can be seen in (E.1).

$$\min_E \sum_{t=0}^N E[t] * TG[t]/REG[t] \quad (E.1)$$

Where E is the energy use [MWh], TG the total generation [MWh] and REG the renewable energy generation [MWh] This ensures that when REG is large, the fraction TG/REG is low. Which gives the optimization an incentive to choose times at which REG is relatively large compared to TG.

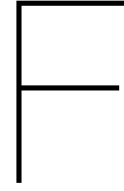
Another option is to estimate the amount of CO₂/MWh is present in the grid. This can be done by assuming a fixed CO₂/kWh for various sources of energy, and implementing these per estimated source of energy. The day ahead projections allow to differentiate between onshore wind, offshore wind and solar energy as REG types. These all have separate hourly projections. Besides that, the total generation is forecasted as well. The amount of CO₂/MWh in the total mix could be estimated by subtracting the REG and basing it on the average energy-mix of the Netherlands. This objective can be found in equation (E.2).

$$\min_E \sum_{t=0}^N E[t] * \frac{(TG[t]-REG[t])*CO_{2avg}+E_{solar}[t]*CO_{2solar}+E_{windonsh}[t]*CO_{2windonsh}+E_{windoffsh}[t]*CO_{2windoffsh}}{TG[t]} \quad (E.2)$$

Risk

This strategy basically brings the same risks as the day ahead market strategy, because energy is still bought on that market. However, this strategy could already be implemented

without changing the energy contract for the pumping station. However, this would not have any financial benefits for RWS.



Appendix F

To verify whether the effects of waves on the Sea water level are negligible on the discharge of the gates, the following analysis was performed.

For different wave heights (dH), the extra force on the water was calculated. Starting with the pressure at the top of the tube:

$$p_0 = (h_0 + dH) * \rho_{sea} \quad (F.1)$$

Where p_0 is the pressure [Pa] at the top of the tube the water flows through, h_0 the measured water level difference [m] between the surface and the top of the tube, dH the wave height [m] and ρ_{sea} the density of Sea water [1250 kg/m³].

Then the pressure at the bottom of the tube is calculated:

$$dp = h_{tube} * \rho_{sea} \quad (F.2)$$

$$p_{bot} = p_0 + dp \quad (F.3)$$

Where dp is the difference in pressure between the bottom and the top of the tube, h_{tube} the height of the tube and p_{bot} the pressure at the bottom of the tube.

The force on the water is then calculated by multiplying the pressure with the flow surface area:

$$F = (p_0 + 0.5 * dp) * A \quad (F.4)$$

Where F is the force on the water [N] and A the flow through surface area [m²].

The start force is also calculated, with which the gate was already in its equilibrium discharge:

$$F_0 = (h_0 * \rho_{sea} + 0.5 * dp) * A \quad (F.5)$$

Where F_0 is the force on the water, without a wave.

To estimate the time needed for a force (created by a wave on the water) to damp the discharge of the gate, an impulse balance was used:

$$F = \frac{dI}{dt} \quad (F.6)$$

Where F is the force, dI the difference in impulse and dt the time it takes for the difference in impulse to occur.

Where the difference in impulse is calculated the following way:

$$\frac{dI}{dt} = m * du = Q * \rho_{canal} * u \quad (F.7)$$

Where m is mass [kg], du difference in speed [m/s], Q discharge [m³/s], ρ_{canal} the density of fresh water [1000 kg/m³] and u the flow speed through the tube [m/s]. This makes it able

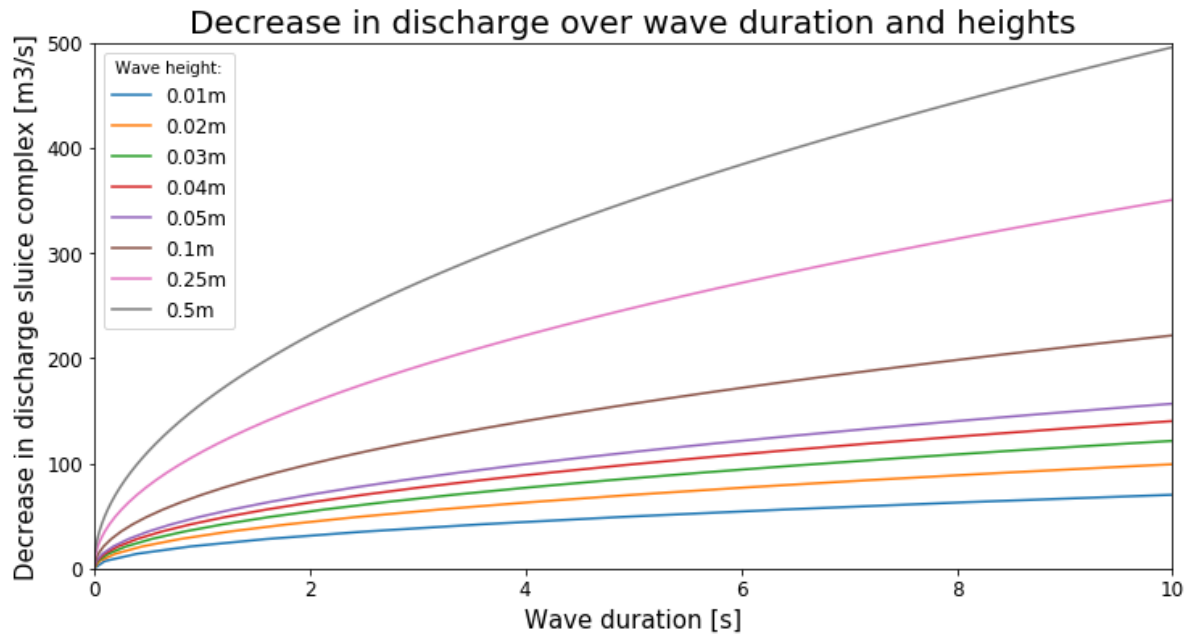


Figure F.1: Time needed for discharge to become 0, for different wave heights

to calculate the time needed for a force to fully stop the water from flowing.

$$dt = \frac{dl}{(F - F_0)} \quad (\text{F.8})$$

The result of this analysis can be seen in Figure F.1.

The figure shows that for short wave periods, the decrease in discharge is generally small. Taking into account that the decrease in discharge is only for the time of the wave period as well, and that the wave is now assumed to be at a fixed height for its entire duration, the effect of a wave on the water level in the canal is negligible.